UCAM
UNIVERSIDAD CATÓLICA DE MURCIA

ESCUELA INTERNACIONAL DE DOCTORADO
Programa de Doctorado en Ciencias de la Salud

Tendinopatía rotuliana: análisis termográfico y cuantificación de la señal Doppler intratendón.

Autor:
Francisco Javier Molina Payá

Directores:
Dr. D. José Ríos Díaz
Dr. D. Jacinto Javier Martínez Payá

Murcia, enero de 2022

UCAM
UNIVERSIDAD CATÓLICA
DE MURCIA

ESCUELA INTERNACIONAL DE DOCTORADO
Programa de Doctorado en Ciencias de la Salud

Tendinopatía rotuliana: análisis termográfico y cuantificación de la señal Doppler intratendón.

Autor:
Francisco Javier Molina Payá

Directores:
Dr. D. José Ríos Díaz
Dr. D. Jacinto Javier Martínez Payá

Murcia, enero de 2022

AUTORIZACIÓN DE LOS DIRECTORES DE LA TESIS

PARA SU PRESENTACIÓN

El Dr. D. JOSÉ RÍOS DÍAZ y el Dr. D. JACINTO JAVIER MARTÍNEZ PAYÁ como Directores de la Tesis Doctoral titulada **«Tendinopatía rotuliana: análisis termográfico y cuantificación de la señal Doppler intratendón»** realizada por D. Francisco Javier Molina Payá en el Programa de Doctorado de Ciencias de la Salud, **autorizan su presentación a trámite** dado que reúne las condiciones necesarias para su defensa.

Lo que firmo, para dar cumplimiento al Real Decreto 99/2011 de 28 de enero, en Murcia a 20 de enero de 2022.

Fdo. Dr. D. José Ríos Díaz.

Fdo. Dr. D. Jacinto Javier Martínez Payá.

DECLARACIÓN DE INTERESES

Esta tesis no contiene material que haya sido presentado para la obtención de ningún título o diploma en ninguna otra universidad o tercera institución y, hasta donde llega el conocimiento del autor, no contiene material previamente publicado y escrito por otras personas excepto en aquellas partes expresamente citadas.

Francisco Javier Molina Payá

Murcia, a 20 de enero de 2022

AGRADECIMIENTOS

Esta tesis viene firmada por una persona, pero no refleja la realidad. Se trata de un trabajo en el que ha participado, de forma directa o indirecta, mucha gente. De ahí el deseo de expresar mi agradecimiento a cada uno de ellos.

A mis directores, por haberme tendido la mano en este camino, por confiar en mis posibilidades y ser mi modelo a seguir. Un día despertaron la curiosidad en mí, y aquí estoy, intentando dar respuestas a las preguntas que vagan por mi cabeza. Jamás les podré agradecer suficientemente lo que han hecho por mí. Espero haber sido una buena bellota.

Al Dr. Paco Carrasco, sin su ayuda incondicional hubiese sido inimaginable poder hacer frente a este gigante.

A todas las personas que de forma desinteresada participaron en los estudios y dedicaron su tiempo para que este trabajo se pudiese desarrollar.

A mi familia, por todo el cariño, apoyo y educación que he recibido. Mamá, Papá, Hermi, Berta e Iñaki, disculpadme por todo el tiempo que os he robado.

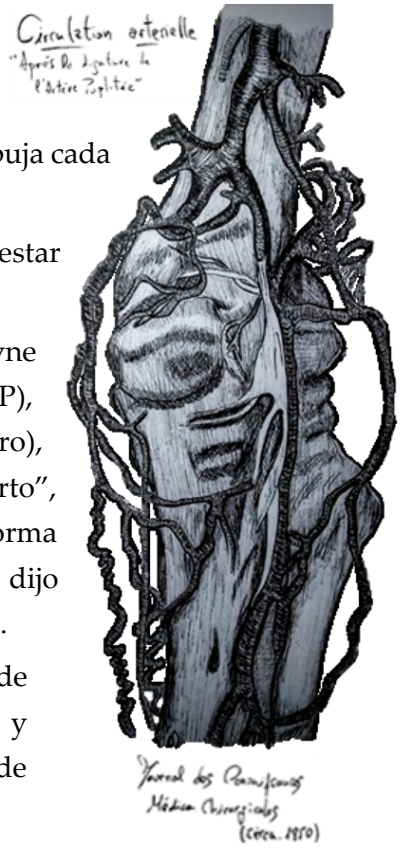

A Hermi, mi compañera de viaje, por vivir mis alegrías y sufrir mis penas, y ser quien me empuja cada día a ser mejor. Te admiro y te quiero.

A Pepe Quesada y Perrine Bertrand, por estar siempre dispuestos a prestar su ayuda e imagen.

A Alexandra Elbakyan (Sci-Hub), Wayne Rasband (ImageJ), Eric-Jan Wagenmakers (JASP), Dan Cohen, Josh Greenberg y Dan Stillman (Zotero), por su contribución al movimiento de "acceso abierto", a la difusión del conocimiento científico y, de forma indirecta, a la elaboración de este trabajo. Como dijo Din Djarin (The Mandalorian): "Este es el camino".

A mis compañeros del departamento de fisioterapia del CEU de Elche, por sus consejos y ánimos durante este largo proceso. Nunca dejo de aprender de ellos.

A mis padres, por absolutamente todo.

"Quien a buen árbol se arrima buena sombra
le cobija. Uno puede arrimarse a un tejo
centenario, incluso milenario lleno de musgo,
o bien a una encina de la dehesa salmantina,
más joven, que da flores y bellotas..."

DR. JOSÉ RÍOS DÍAZ.
XVII Congreso Nacional de Fisioterapia.
UCAM. 16 de abril 2015.

TABLA DE CONTENIDOS

SIGLAS Y ABREVIATURAS

Las abreviaturas de convenios de unidades no se incluyen en este listado al existir normas internacionalmente aceptadas sobre su uso universal, ni tampoco las del diccionario de la RAE. Se han reseñado por orden alfabético.

BF10. Factor Bayes.

CD. Color Doppler.

CrI. Intervalo de credibilidad.

EI. Ecointensidad.

EV. Ecovariación.

DS. Señal Doppler.

FOV. Campo de visión.

IC. Intervalo de confianza.

ICC. Coeficiente de correlación intraclase.

IRT. Termografía infrarroja.

LOA. Límite de acuerdo.

MoD. Diferencias medias.

PD. Power Doppler.

PRF. Frecuencia de repetición de pulsos.

RI. Índice de resistencia.

ROI. Región de interés.

SEm. Error estándar de medida.

SNS. Sistema nervioso simpático.

SRD. Menor diferencia real.

TR. Tendón rotuliano.

T1. Primer termograma.

T2. Segundo termograma.

VEGF. Factores de crecimiento endotelial vascular.

VISA-P. Victorian Institute of Sport Assessment—Patella.

VR. Resistencia vascular.

ÍNDICE DE FIGURAS

I. INTRODUCCIÓN Y JUSTIFICACIÓN

III. ESTUDIO I

IV. SOLICITUD DE PATENTE: DESARROLLO DE UN MÉTODO Y EQUIPO DE MEDICIÓN DE TEMPERATURA

V. ESTUDIO II

VI. ESTUDIO III

VII. ESTUDIO IV

VIII. SÍNTESIS DE LA TESIS

ÍNDICE DE TABLAS

III. ESTUDIO I

V. ESTUDIO II

VI. ESTUDIO III

VII. ESTUDIO IV

ÍNDICE DE ANEXOS

INTRODUCCIÓN Y JUSTIFICACIÓN

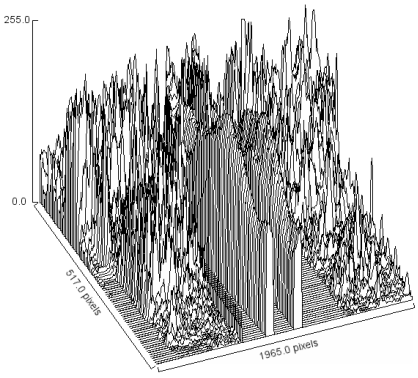

I. INTRODUCCIÓN Y JUSTIFICACIÓN

1.1. TENDINOPATÍA ROTULIANA

La tendinopatía es una lesión frecuente por sobreuso que incluye dolor al movimiento, sensibilidad a la palpación, aumento de la vascularización intratendón y cambios morfológicos en su estructura como la desorganización de las fibrillas y el aumento de grosor del tendón (Magnusson et al. 2010; Scott et al. 2013; Rio et al. 2014), que pueden llegar a afectar a la capacidad de carga y tolerancia del tendón (Cook et al. 2016). Las tendinopatías afectan más frecuentemente a los tendones de Aquiles y rotuliano (Maffulli et al. 2003), aunque también pueden aparecer en otras partes del cuerpo.

La tendinopatía rotuliana se caracteriza por un dolor en la zona anterior de la rodilla que aumenta con la palpación sobre el tendón rotuliano (TR), cerca de su inserción en la rótula (Blazina et al. 1973). Esta patología se suele asentar cerca de la inserción del tendón en el polo inferior de la rótula a nivel de sus fibras medias y posteriores, lo que provoca una función alterada de la rodilla (Basso et al. 2002).

A principios del siglo XX, la terminología empleada para referirse a la patología tendinosa empleaba el sufijo *-itis*, vinculando a la inflamación en el proceso fisiopatológico de las tendinopatías, aun cuando varios autores ya habían alertado de que los trastornos de los tendones eran degenerativos (Meyer 1922; Codman 1934). En la década de 1970 (Puddu et al. 1976), se propuso el término «tendinosis» para enfatizar la falta de evidencia de que la inflamación formase parte de la enfermedad crónica del tendón (Kraushaar y Nirschl 1999; Cook et al. 2000c; Khan et al. 2000). En la actualidad, gracias a estudios recientes, se sabe que la inflamación está presente en el desarrollo de la tendinopatía y las posibles funciones que puede desempeñar (Abate et al. 2009; Kjaer et al. 2013; Rees et al. 2014; Speed 2016). Estos hallazgos han generado una tendencia al consenso para denominar a este cuadro como «tendinopatía» (Peers y Lysens 2005).

1.2. EPIDEMIOLOGÍA

La tendinopatía rotuliana es una patología que afecta sobre todo a la población deportista y, mayoritariamente, a los deportistas de élite (Zwerver et al. 2011). Epidemiológicamente, se ha establecido un promedio de la duración del dolor y del déficit funcional de alrededor de tres años, por lo que este factor puede contribuir a que el deportista decida abandonar su carrera deportiva (Kettunen et al. 2002; Lian et al. 2005).

Determinar la prevalencia e incidencia de la tendinopatía rotuliana es difícil debido a que, a menudo, este tipo de lesiones por sobreuso no se registran (Clarsen et al. 2013). Algunos autores estiman alrededor del 14% la prevalencia general entre atletas de élite de diferentes deportes (Lian et al. 2005) y una incidencia de hasta un 20% en la población deportista (Järvinen 1992). Esta patología afecta a deportistas de multitud de deportes, pero especialmente a deportistas que incluyen el salto con impacto en sus entrenamientos o competiciones (Gisslén y Alfredson 2005); por ejemplo, se ha informado de una prevalencia en atletas amateurs del 14% en jugadores de voleibol y de solo un 2,5% en jugadores de fútbol (Zwerver et al. 2011).

Aunque la lesión del TR está más asociada a las edades adultas, en algunos estudios se han descrito frecuencias altas en atletas jóvenes (Cook et al. 2000b), con prevalencias en jugadores de baloncesto jóvenes de hasta el 7%, aunque el 26% presentaba una imagen patológica del tendón sin sintomatología (Cook et al. 2000a).

En relación al sexo, la evidencia sobre la prevalencia la asocia al tipo de deporte; así en balonmano, baloncesto, críquet y fútbol australiano se ha detectado una mayor prevalencia en los hombres (Lian et al. 2005), mientras que en el voleibol no existen diferencias significativas en relación al sexo, pero sí una mayor incidencia a favor de las mujeres (Ferretti et al. 1990).

1.3. FISIOPATOLOGÍA DE LA TENDINOPATÍA ROTULIANA

El modelo actual de patología del tendón se basa en el modelo continuo de tendinopatía de Cook y Purdam (2009) en el que se entrelazan tres estados tisulares en un proceso continuado: tendinopatía reactiva, tendón desestructurado y tendinopatía degenerativa (Cook y Purdam 2009; Cook et al. 2016) **(figura 1)**.

La tendinopatía reactiva se expone como una respuesta hiperactiva celular a la carga, con un aumento en el número de células y un crecimiento significativo del índice metabólico de los proteoglicanos de mayor tamaño que atraen agua al interior de la matriz extracelular, con lo que aumenta su tamaño y se altera su morfología (Cook et al. 2004a; Magnusson et al. 2010). Los cambios patológicos celulares y de la matriz no fibrilar proceden de la desorganización del colágeno (Cook et al. 2004a), esto justifica que en las imágenes diagnósticas se aprecie un aumento del diámetro del tendón sin signos de desorganización de la matriz celular (Freund et al. 2012).

La fase del tendón desestructurado es asintomática, se caracteriza por una mayor desorganización de la matriz celular en la que se produce un aumento del número de células y de la producción de proteoglicanos y colágeno. En esta fase se genera la reparación del colágeno y la desorganización de la matriz celular. Desde el punto de vista de la imagen ecográfica, se observa una desestructuración de la matriz con discontinuidad de las fibras de colágeno y pequeñas áreas hipoecoicas.

Finalmente, la fase degenerativa se corresponde con la progresión en la desorganización de la matriz de colágeno, con cambios en la celularidad, aparición de áreas de muerte celular e hipervascularización intratendón (Kraushaar y Nirschl 1999; Lian et al. 2007). En esta fase pueden encontrarse zonas del tendón sanas junto a zonas degeneradas, y a nivel ecográfico aparecen zonas hipoecoicas con señal Doppler (DS) intratendón. En este modelo fisiopatológico, se plantea que una tendinopatía presenta clínica cuando el tendón es sometido a sobrecarga y aparece un cuadro de reactividad de la parte sana del tendón degenerado (Cook et al. 2016).

En el modelo continuo de tendinopatía apenas se incluye información acerca de los mecanismos inflamatorios en la patología tendinosa, probablemente debido a los escasos estudios al respecto. Sin embargo, parece que la tendencia está cambiando y se dirige hacia una propuesta de convivencia del proceso inflamatorio junto al degenerativo (Abate et al. 2009; Rees et al. 2014; Dakin et al. 2015; Millar et al. 2015) puesto que existe una clara evidencia patológica y molecular de su desregulación en todo el proceso patológico, que incluso podría ayudar a explicar el desajuste entre la presencia de dolor y la estructura macroscópica del tendón (Dean et al. 2016).

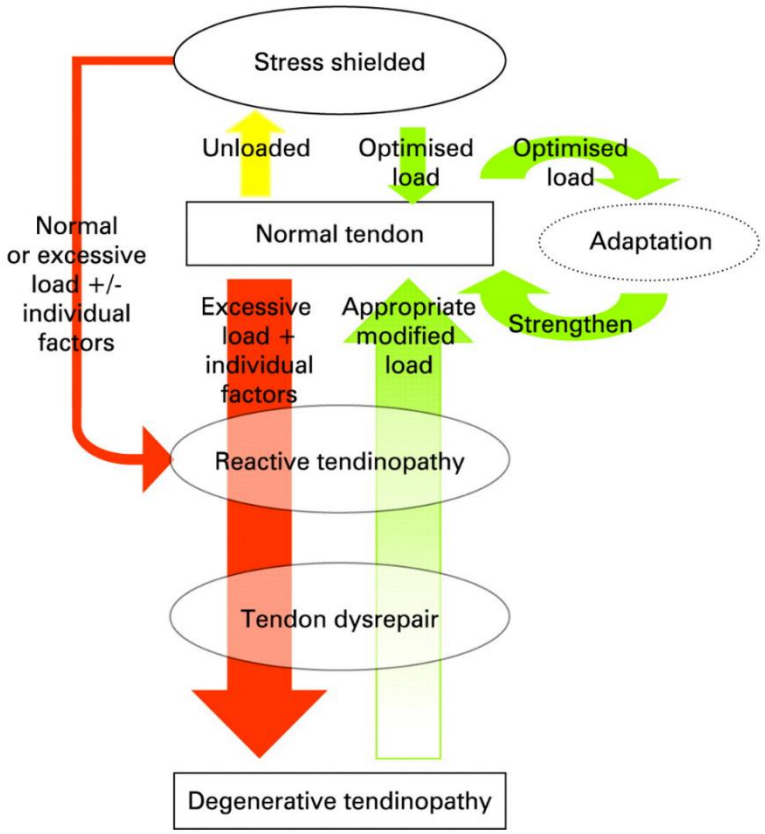

Figura 1. Esquema del modelo continuo de tendinopatía propuesto por Cook & Purdam en 2009. (Fuente: Tomado de Cook JL, Purdam CR. Is tendon pathology a continuum? A pathology model to explain the clinical presentation of load-induced tendinopathy. Br J Sports Med. junio de 2009;43(6):409-16).

Recientemente se han encontrado marcadores inflamatorios (cicloxigenasa-2 e interleuquina-6) en las primeras fases de la patología tendinosa (Millar et al. 2010; Dakin et al. 2014; Thorpe et al. 2015), que podrían provocar un aumento de las metaloproteinasas (MMP) responsables de la eliminación del colágeno tipo III y de los proteoglicanos en un intento de reparar el tendón (Manning et al. 2014; Thorpe et al. 2015). Además, se ha observado cierta respuesta inflamatoria junto a las respuestas regenerativa y degenerativa que sugiere la convivencia de estas respuestas en la tendinopatía crónica: mediadores inflamatorios como las prostaglandinas o las interleuquinas aparecen junto a la desorganización del colágeno, la infiltración grasa, la degeneración mixoide, la necrosis de los tenocitos

y a la respuesta regeneradora como la formación de nuevos vasos o la infiltración de tenocitos (Fredberg y Stengaard-Pedersen 2008; Abate et al. 2009).

Dentro del modelo continuo de tendinopatía, el dolor tendinoso se produce en el tendón sano y no en la parte degenerada, aunque el origen exacto de los conductores nociceptivos en la tendinopatía todavía plantea dudas. Se sugiere la posibilidad de que la célula tendinosa produzca sustancias nociceptivas (Rio et al. 2014) que podrían irritar receptores de nervios periféricos cercanos al peritendón (Danielson et al. 2006), pero no generar síntomas si se encuentran en zonas muy profundas del tendón alejadas de la inervación. Algunos tendones degenerados presentan anomalías en la matriz celular, pero sin producir sustancias nociceptivas ni actividad de señal nociceptiva, lo que daría explicación a la observación de tendones degenerados que se muestran asintomáticos. En el caso de que el estímulo nociceptivo se perpetúe sobre el tendón, como por ejemplo con una carga continua, es posible que se desencadene una respuesta de hiperalgesia secundaria a modo de sensibilización central (Plinsinga et al. 2015; Eckenrode et al. 2019).

Aunque los estudios disponibles sobre el tema son limitados y no muestran el verdadero significado de los cambios en los marcadores simpáticos de la tendinopatía (Jewson et al. 2015), parece ser que el sistema nervioso simpático (SNS) desempeña un papel importante debido a que puede influir en el dolor del tendón a través de mecanismos directos (Chabal et al. 1992; Torebjörk et al. 1995) e indirectos (Helme y Andrews 1985; Donnerer et al. 1991; Lam y Ferrell 1991), participando también en la proliferación y degeneración celular (Anesini y Borda 2002; Burniston et al. 2005). El SNS actúa principalmente sobre los tenocitos irregulares y el tejido paratendinoso (Jewson et al. 2015). Estos tenocitos forman parte de un circuito de retroalimentación local que activa el SNS, mientras que el tejido paratendinoso, que presenta una mayor inervación simpática (Andersson et al. 2007), proporciona una fuente de actividad simpática adicional (Danielson et al. 2008), al contrario que en el resto del tendón donde la inervación simpática no se altera. En los tendones patológicos, el SNS libera noradrenalina que actúa directamente sobre las fibras nerviosas aferentes de los tendones (Wong 1993; Ackermann 2014) e induce la liberación de catecolaminas que activan las fibras C y provocan nocicepción (Schlereth y Birklein 2008).

La proliferación del sistema nervioso, generalmente asociado a la aparición de vasos, podría generar una inflamación neurogénica (Green et al. 1993) con presencia de sustancia P y neuroquinina-1 y, en consecuencia, dolor (Andersson et al. 2008). Por otro lado, el SNS puede modificar el flujo sanguíneo local del tendón mediante la vasodilatación y vasoconstricción estimulada a través de la activación de los receptores adrenérgicos α-1 y α-2, con alteración de la temperatura cutánea a nivel del tendón doloroso (Koeppen y Stanton 2017).

1.4. HIPERVASCULARIZACIÓN INTRATENDÓN

Los tendones requieren un suministro de sangre al ser metabólicamente activos pero presentan una débil perfusión vascular en comparación con otros tejidos conectivos (Fenwick et al. 2002; Abate et al. 2009). La vascularización en los tendones sanos es muy limitada, con una pequeña cantidad de capilares localizados entre los haces de colágeno y que principalmente se ubican en la vaina, en la unión musculotendinosa y en la osteotendinosa (Fenwick et al. 2002).

La hipervascularización intratendón es uno de los hallazgos histológicos más comunes encontrados en las tendinopatías de carácter crónico (Pufe et al. 2005; Scott et al. 2008; Fu et al. 2010). La hipervascularización se describe como una proliferación en un tejido de vasos sanguíneos o redes microvasculares generalmente afuncionales y que, en los casos normales, no debería estar presente o solo en una pequeña cantidad (Risch et al. 2021). En el caso del tendón, el término se usa en relación con todo el flujo sanguíneo visible intratendón debido a una angiogénesis **(figura 2)** o a vasos nativos con flujo sanguíneo aumentado como, por ejemplo, durante un proceso de cicatrización o a la realización de ejercicio intenso (Alfredson y Ohberg 2006; Boesen et al. 2012; Tol et al. 2012).

En las tendinopatías crónicas se ha observado un aumento de la red microvascular intratendón (Yang et al. 2012; De Jonge et al. 2014), aunque no queda claro si el crecimiento de los vasos sanguíneos y el aumento de la expresión de factores de crecimiento endotelial vascular (VEGF) participan en el desarrollo de la tendinopatía o actúan como un intento de respuesta curativa (Merkel et al. 2021). Esta hipervacularización intratendón es una característica conocida durante el proceso degenerativo de la tendinopatía (Pufe et al. 2005; Andersson et al. 2011; De

Jonge et al. 2014; Malliaras y Purdam 2014), pero en la actualidad su papel en la tendinopatía es fuente de debate (Rees et al. 2006; Tol et al. 2012).

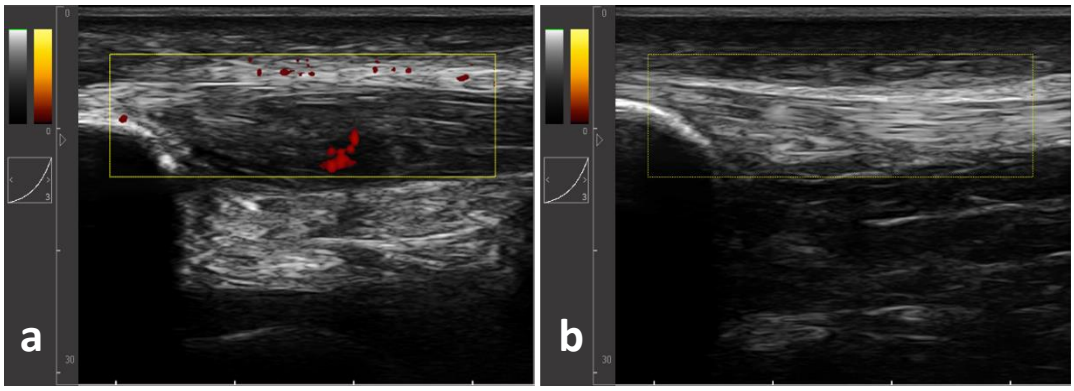

Figura 2. Imágenes ecográficas longitudinales del tendón rotuliano en modo Power Doppler. a) Con señal Doppler intratendón, b) sin señal Doppler. (Fuente: elaboración propia).

La degeneración del tendón se propicia con estímulos continuos de sobrecarga que rompen los enlaces cruzados del colágeno y una menor presencia en la matriz extracelular (Aström y Rausing 1995). Esta alteración induce cambios en la matriz extracelular como, por ejemplo, la producción de un colágeno de menor calidad (tipo III) (Riley et al. 1994; Cook et al. 2004a).

Para que se generen nuevos vasos es imprescindible que se produzca esta degradación de la matriz extracelular (Ferrara 1999), con un incremento de las inmunoreacciones (catecolaminas y receptores adrenérgicos) (Lian et al. 2007; Xu y Murrell 2008) y la presencia de VEGF, que inicia la respuesta de formación de nuevos vasos (Perry et al. 2005; Nakama et al. 2006), probablemente en un intento de instaurar la regeneración del tendón.

Las células endoteliales vasculares producen metaloproteinasa de matriz (MMP) como respuesta al estímulo de los VEGF (Wang y Keiser 1998; Sato et al. 2000). El aumento de la expresión de la MMP tipo 3 (MMP-3) aumenta la degradación de la matriz extracelular y debilitan el tendón (Kjaer et al. 2003), para que esto no ocurra, el inhibidor de la MMP tipo 3 (TIMP-3) bloquea la unión del

VEGF a su receptor (VEGFR-2) (Qi et al. 2003). Debido a que esta medida resulta ineficaz, se genera un desequilibrio entre las MMP y sus inhibidores que instaura un círculo vicioso provocando una alteración mayor de la matriz extracelular (Fu et al. 2002b, 2002a; Pufe et al. 2005). Finalmente, este proceso genera unos vasos inmaduros con una distribución irregular que no ayudan a reparar la zona dañada (Aström y Rausing 1995).

Se ha observado una relación entre los vasos intratendón de la tendinopatía rotuliana y algunos receptores neurológicos (mecanorreceptores y receptores NMDA del glutamato) (Bjur et al. 2005), y que estos vasos se acompañan de terminales nerviosos que participan en la transmisión nociceptiva en la tendinopatía (Danielson et al. 2008). En las tendinopatías se presenta una mayor concentración de glutamato (Alfredson et al. 1999), de sustancia P (Alfredson 2005; Tran et al. 2020) y de lactato (Alfredson et al. 2002) que en los tendones sanos, lo que puede hacer pensar que el aumento de estas sustancias inducido por el uso excesivo del tendón puedan estimular la angiogénesis y que, a su vez, derive en una respuesta neurovascular dolorosa (Ackermann 2013; Merkel et al. 2021), con lo que quedaría establecida una relación entre hipervascularización intratendón y sintomatología (Ohberg et al. 2001; Alfredson et al. 2003; Reiter et al. 2004; Yang et al. 2012). Por otro lado, y siguiendo una línea de pensamiento reciente, otros autores no han encontrado esta relación (Peers et al. 2003; Richards et al. 2005; Boesen et al. 2006; van Snellenberg et al. 2006; De Jonge et al. 2014). Además, esta falta de relación se ve reforzada por el hallazgo en el tendón de fibras nerviosas sensoriales que no acompañan a los vasos (Lian et al. 2006; Ackermann 2013; Spang et al. 2015) y que podrían estar implicadas en la señalización del dolor en los tendones afectos sin la presencia de vasos intratendón.

1.5. EVALUACIÓN ECO-DOPPLER EN LAS TENDINOPATÍAS

La hipervascularización intratendón se evalúa estimando el flujo sanguíneo, su presencia y el número de vasos intratendón, aunque su cuantificación no está exenta de dificultades, principalmente relacionadas con el tamaño y número de los vasos intratendón (Molina-Payá et al. 2021a).

La ecografía Doppler es una técnica de imagen que permite evaluar y clasificar los cambios en la perfusión del tendón (Cook et al. 2004b; Gisslén y

Alfredson 2005). Esta técnica de imagen basada en el efecto Doppler, descubierto por Christian Doppler en 1842, se basa en el cambio en la longitud de onda del sonido de una fuente de sonido, de un receptor o de un reflector en movimiento (Allan et al. 2008). En la exploración del cuerpo humano, se considera a la sonda ecográfica como la fuente y el receptor de las ondas de ultrasonido, mientras que la sangre que se encuentran en movimiento, es el reflector. Cuando el ultrasonido rebota en una estructura en movimiento cambia su longitud de onda, lo que permite detectar el movimiento del flujo sanguíneo de los vasos (Iriarte Posse 2020).

La ecografía Doppler proporciona diferentes modos de evaluación: *Colour Doppler* (CD), *Spectral Doppler* (SD) y *Power Doppler* (PD). El CD es un sistema de exploración en el que se superpone una imagen de color sobre una en escala de grises al detectar un cambio en la frecuencia Doppler, mostrando una representación del flujo de los vasos sanguíneos. La frecuencia Doppler se representa a través de una serie de píxeles de color cuya intensidad es proporcional a la frecuencia media detectada a ese nivel. El CD ofrece información sobre la presencia, dirección y velocidad del flujo detectado (Ventura 2010).

El SD es una representación gráfica en tiempo real de las velocidades sanguíneas relativas desde dentro de la puerta Doppler (área de medición) a lo largo del ciclo cardíaco (Rubin 1994).

Sin embargo, el PD es la técnica de imagen más utilizada en la investigación de la hipervascularización intratendón (Scott et al. 2013) puesto que informa sobre la amplitud de la DS, en lugar de la frecuencia media como en el CD. Esta característica le otorga al PD la ventaja de ser más sensible al flujo que el CD, aunque esta diferencia se ha visto reducida con la mejora tecnológica de los ecógrafos actuales (Torp-Pedersen y Terslev 2008). Además, esta modalidad de Doppler depende menos del ángulo de insonación, no presenta *aliasing* y le afecta menos el ruido, todo ello a expensas de perder la información sobre la dirección y velocidad del flujo (Rubin et al. 1994).

Por el momento no se ha establecido un umbral que delimite un flujo fisiológico de una hipervascularización patológica, esta circunstancia se ve agravada por la creciente mejora tecnológica de los ecógrafos actuales que ha permitido un aumento de la sensibilidad en la detección de la DS (Seo y Kim 2017). Esta sensibilidad además está afectada por factores fisiológicos o técnicos, como la

optimización de la imagen, la realización de actividad física previa a la medición (Boesen et al. 2006; Risch et al. 2018), el ciclo cardíaco (Yang et al. 2011b) o la posición de las articulaciones (Ohberg et al. 2001; Koenig et al. 2007b). Es decir, una variación de la hipervascularización puede no estar relacionada con la formación de neovasos sino con el aumento del flujo sanguíneo de los vasos ya existentes. Esta variabilidad hace imprescindible una estandarización de los parámetros y las recomendaciones previas a los sujetos a explorar para realizar una correcta evaluación ecográfica en modo Doppler intratendón (Fallows y Lumsden 2019).

Esta falta de relación se refuerza con la observación de la presencia de señal PD intratendón en tendones asintomáticos (Peers et al. 2003; Reiter et al. 2004) y su incremento ante la realización de determinados ejercicios físicos (Boesen et al. 2006, 2011; Malliaras et al. 2008; Koenig et al. 2010). Estos hallazgos indican que la presencia de flujo intratendinoso no siempre es un signo de un trastorno patológico, sino más bien una parte de una respuesta adaptativa a una carga fisiológica normal (Malliaras et al. 2008; Boesen et al. 2012; Tol et al. 2012). Esta variabilidad podría hacer pensar que el estudio de la presencia de DS intratendón no ofrece información relevante sobre la tendinopatía. En cambio, pueden analizarse otras variables Doppler que sí ofrezcan información sobre el estado del tejido, como es el caso de la resistencia vascular (VR) intratendón a través del índice de resistencia (RI) (Koenig et al. 2007b; Karzis et al. 2017).

1.5.1. Evaluación de la VR intratendón

En ecografía Doppler, para cuantificar el grado de VR periférica y obtener información objetiva sobre la calidad del flujo en el tejido se utiliza el RI (Terslev et al. 2003). Básicamente con este índice se evalúa el tipo de flujo en cuanto a que sea de baja o alta resistencia.

El RI es un valor relativo entre el flujo en la sístole y la diástole y puede tomar valores comprendidos entre 0 y 1, directamente proporcionales a la VR periférica, de tal forma que valores bajos se correlacionan con una baja resistencia periférica que indicaría una mayor perfusión tisular (Adamson 1999; Bude y Rubin 1999) y lo contrario ocurre con los valores altos. En reposo, los tejidos musculoesqueléticos normales tienen una alta resistencia periférica con poco o ningún flujo en la diástole (Koenig et al. 2007a), por lo que se establece un valor máximo de 1 como signo de

normalidad (Terslev et al. 2003). Esta condición se modifica en condiciones inflamatorias, en la que aparece una baja resistencia con flujo a lo largo del ciclo cardiaco (Sato et al. 2005; Torp-Pedersen et al. 2008; Terabayashi et al. 2014). A nivel técnico es destacable que, al igual que otros índices, el RI es matemáticamente independiente del ángulo de insonación, por lo que no requiere de su corrección, aunque si este ángulo es excesivo podría llegar a afectar a la precisión de la medida (Allan et al. 2008).

1.5.2. Cuantificación de la DS intratendón

Uno de los primeros estudios que cuantificó la DS intratendón se basó en el conteo del número de vasos en el interior del tendón de Aquiles trasladados a una escala ordinal de 4 puntos que dependía del número de señales halladas (Richards et al. 2001). Posteriormente, se propuso la utilización de la escala de Ohberg con 5 puntos que fue utilizada por varios autores, e incluso modificada (Ohberg y Alfredson 2002; De Jonge et al. 2014; Risch et al. 2016; Watson et al. 2018). En la actualidad, todavía se emplean estas escalas subjetivas de conteo debido a su facilidad de realización y aplicación clínica, a pesar de que el análisis de imagen es cada vez más utilizado al considerarse un método menos subjetivo.

El principal método empleado en la cuantificación de la DS intratendón es la de la fracción de color, donde se establece una relación entre el número de píxeles de color y los píxeles que se encuentran en una región de interés (ROI) intratendón (Koenig et al. 2004; Boesen et al. 2006). Para abordar la ubicación de la ROI intratendón, es necesario desarrollar reglas previas consensuadas que especifiquen la zona intratendón que se va a evaluar (Fallows y Lumsden 2019). En este método no debe olvidarse que, aunque el tamaño de la ROI esté estandarizado, su ubicación es dependiente del explorador y puede verse afectada por la presencia de señales que no lleguen a seleccionarse al encontrarse alejadas más allá del tamaño de la ROI. Además, hay que sumar la complejidad de la selección debido a la tridimensionalidad de la hipervascularización (Cook et al. 2005a).

Otro método empleado en la cuantificación de la vascularización intratendón es la medición de la longitud de los vasos que, aunque ha obtenido una buena fiabilidad intra e interobservador (Cook et al. 2005b), apenas se ha utilizado,

probablemente debido a que la información que aporta podría no ser útil para la práctica clínica (Cook et al. 2005b; Risch et al. 2016).

Generalmente, a la hora de cuantificar la DS no se tiene en cuenta la variable tiempo, lo que puede suponer un factor de confusión significativo por la naturaleza pulsátil y la variabilidad del flujo sanguíneo, que ofrecen una DS de potencia variable. Es decir, la cantidad de hipervascularización detectada dependerá de la fase del ciclo cardíaco en la que se registra la imagen (Yuan et al. 1994). Por un consenso tácito, suele utilizarse la imagen que ofrece una mayor DS, aunque esto suponga un procedimiento subjetivo. Para minimizar este efecto, la cuantificación de la DS debería promediarse en el tiempo (Fallows y Lumsden 2019), o bien utilizar imágenes Doppler tridimensionales (3D) que presentan la ventaja de poder reconstruir un volumen completo de la hipervascularización intratendón y obtener la máxima vascularización en toda una serie de imágenes en lugar de a partir solo una, como ocurre con la cuantificación mediante el modo Doppler convencional (Yang et al. 2011b, 2011a, 2012).

La cuantificación de la VR intratendón se realiza a través del RI de forma automática por el ecógrafo seleccionado el vaso intratendón con mayor DS (Karzis et al. 2017), o realizando la media de los tres vasos de mayor tamaño (Koenig et al. 2007b, 2007a). Actualmente, solo se conoce una alternativa a esta metodología de cuantificación de la VR intratendón que emplea el análisis de la intensidad de color de píxel de la DS propuesta en esta tesis (Molina-Payá et al. 2021a).

1.6. EVALUACIÓN TERMOGRÁFICA DEL TR

La termografía infrarroja (IRT) es una técnica que permite un registro seguro y no invasivo de la distribución de la temperatura de la superficie de la piel. Los termogramas o imágenes térmicas se crean con cámaras termográficas que registran la radiación infrarroja emitida por el cuerpo (Costello et al. 2013). Estas cámaras emplean detectores que operan en la longitud de onda del infrarrojo medio entre 0,9 y 14 μm (Grenn et al. 2013). Las imágenes obtenidas proporcionan información fisiológica sobre el flujo sanguíneo, la inflamación, la sudoración u otros procesos que pueden llegar a alterar la temperatura de la piel (Bouzida et al. 2009; Lee et al. 2014; Das et al. 2019). Esta técnica de imagen se ha mostrado útil en

la detección y seguimiento de afecciones vasculares, neurológicas, metabólicas y musculoesqueléticas (Lahiri et al. 2012; Ring y Ammer 2012), con una buena fiabilidad y reproducibilidad (Zaproudina et al. 2008; Choi et al. 2013; Rodrigues-Bigaton et al. 2013; Fernández-Cuevas et al. 2015b; Molina-Payá et al. 2019).

El ser humano es homeotérmico y su temperatura fisiológica es relativamente constante entorno a los 37ºC (Heikens et al. 2011; Childs 2018), y solo las partes distales del cuerpo presentan una mayor variabilidad de temperatura (Gatt et al. 2015). Además, la distribución de la temperatura entre áreas contralaterales debe ser simétrica en condiciones de normalidad (Uematsu et al. 1988; Niu et al. 2001). La medición de la asimetría térmica bilateral ha impulsado una de las modalidades más utilizadas en el análisis de la temperatura a nivel clínico, basada precisamente en diferencias térmicas bilaterales entre ROIs (Selfe et al. 2006; Sillero-Quintana et al. 2015; Gatt et al. 2018; Magas et al. 2019; Gizińska et al. 2021) **(figura 3)**.

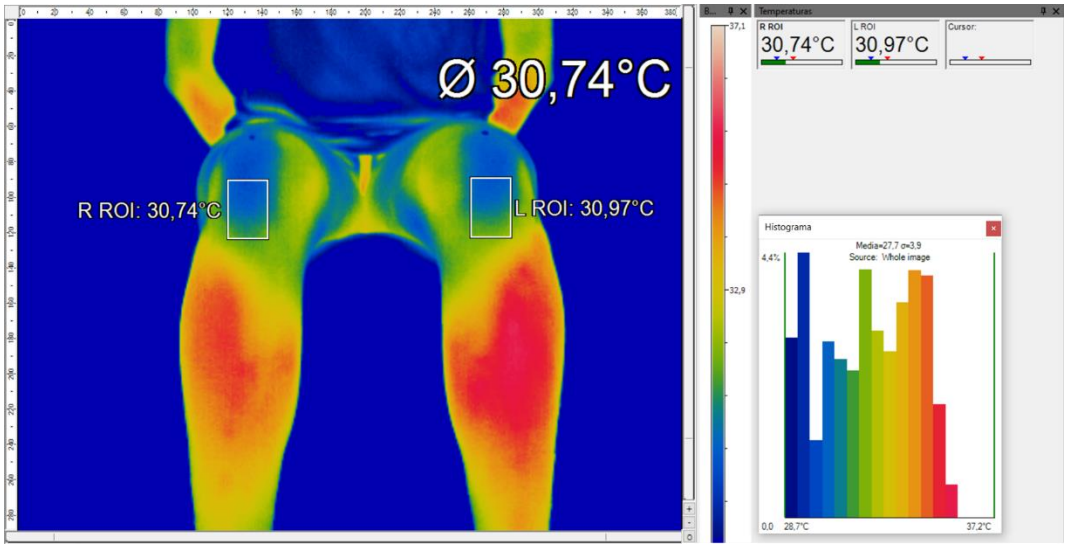

Figura 3. Imagen termográfica con ROIs ubicadas sobre el tendón rotuliano. (Fuente: elaboración propia).

Diferentes autores han intentado marcar un nivel mínimo de asimetría térmica entre la zona patológica y su contralateral sana, por encima del cual se podría sospechar de una patología. Esta diferencia de temperatura ha ido

descendiendo a lo largo de los años de los 2 o 3ºC en la década de 1970 (Watmough et al. 1970; Draper y Boag 1971), pasando por 1ºC en la década de 1980 (Uematsu 1985) hasta llegar a los 0,5ºC actuales (Uematsu et al. 1988; Sillero-Quintana et al. 2015). Probablemente, este descenso se deba a la mejora tecnológica de las cámaras y a un mayor conocimiento sobre el control de los factores de influencia y la metodología de evaluación que se ha experimentado con el paso de los años. Las diferencias térmicas por encima (hipertermia) o por debajo (hipotermia) de estos valores de referencia podrían estar indicando la presencia de patología (Uematsu 1985; Mangine et al. 1987; Ra et al. 2013; Gizińska et al. 2021).

1.6.1. Factores de influencia en la IRT clínica

El uso de la IRT no está exenta de complicaciones en su aplicación clínica debido a que existen una serie de factores de influencia que pueden afectar a los resultados. Estos factores de influencia se clasifican en tres grupos: factores ambientales, individuales y técnicos (Fernández-Cuevas et al. 2015a) **(figura 4)**.

Los factores ambientales están relacionados con las características del entorno donde se realiza la evaluación de la IRT. A diferencia de algunos factores individuales, los factores ambientales son más fáciles de controlar al poder ser modificados. Los factores individuales se pueden subdividir en factores intrínsecos que son propios del individuo y representan un estado a largo plazo, y extrínsecos que están relacionados con los hábitos del sujeto y, por lo tanto, son temporales y externos. Finalmente, los factores técnicos hacen referencia al propio equipo y a la metodología empleada para realizar la evaluación termográfica.

Uno de los factores técnicos más controvertidos es la selección de las ROIs. Muchos autores han desarrollado su propia metodología para crear y seleccionar las ROIs, lo que denota una falta de consenso en este campo. Se describen tres métodos principales para seleccionar las ROIs: **1)** Con la ubicación de las ROIs directamente sobre el termograma (Mangine et al. 1987; Ferreira et al. 2008), que depende de la destreza del evaluador al seleccionar la ROI sobre un termograma carente de referencias anatómicas y, en consecuencia, con un marcado carácter subjetivo. **2)** Mediante marcadores sobre la piel (Selfe et al. 2007; Denoble et al. 2010; Maniar et al. 2015) que, a pesar de ser una forma de selección específica de la estructura o región a evaluar, puede contaminar el termograma por conducción al

tener que contactar con el sujeto durante el emplazamiento de los marcadores. **3)** El empleo de programas informáticos que son capaces de segmentar el termograma generando ROIs sin contacto con el sujeto (Duarte et al. 2014; Gauci et al. 2018; Singh y Arora 2019; Requena-Bueno et al. 2020), pero con una especificidad a la hora de seleccionar una estructura condicionada por la propia automatización de la segmentación de las ROIs.

Para controlar la influencia de estos factores se han desarrollado diferentes protocolos y guías que minimizan los errores de la evaluación termográfica en busca de una medición de la temperatura lo más exacta y precisa posible (IACT 2002; Ammer, K. y Ring, F 2006; Ammer 2008).

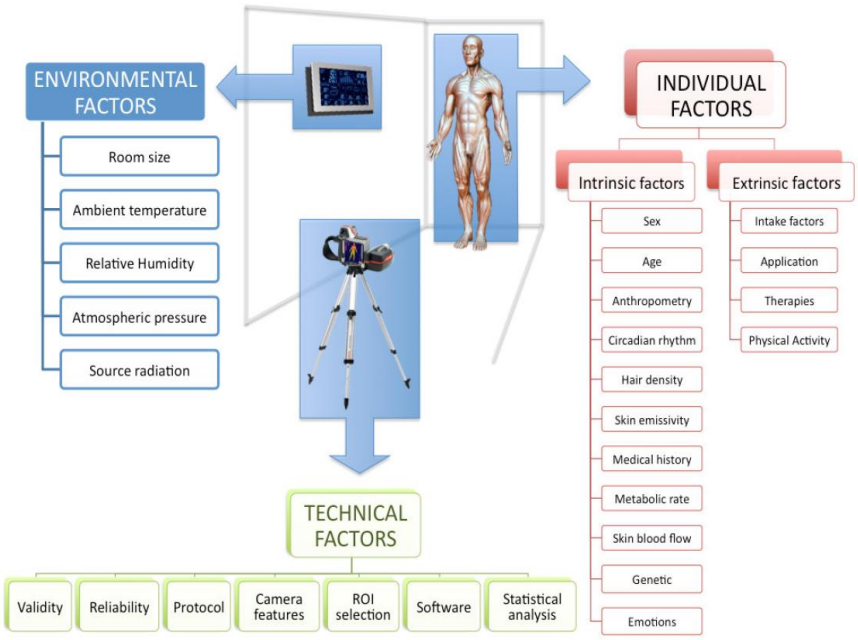

Figura 4. Esquema de la clasificación de los factores de influencia en la evaluación termográfica en humanos. (Fuente: Tomado de Fernández-Cuevas I, Bouzas Marins JC, Arnáiz Lastras J, Gómez Carmona PM, Piñonosa Cano S, García-Concepción MÁ, et al. Classification of factors influencing the use of infrared thermography in humans: A review. Infrared Physics & Technology. 1 de julio de 2015;71:28-55).

1.6.2. Evaluación termográfica de la tendinopatía rotuliana

Como ya se ha apuntado, el diagnóstico de la tendinopatía rotuliana es un desafío debido a que actualmente no existe una técnica diagnóstica estándar de oro (Scott et al. 2013; Malliaras et al. 2015). En la práctica clínica se diagnostica por antecedentes, exploración de la rodilla y palpación del tendón y sus inserciones (Cook et al. 2001). El diagnóstico se confirma con técnicas de imagen, generalmente mediante ecografía y resonancia magnética que permiten detectar anomalías en el TR y aportan información acerca de la gravedad de la patología (Khan et al. 1996; Cook et al. 2001), aunque en algunas ocasiones no se ha encontrado una correlación entre los resultados clínicos y las imágenes (Khan et al. 2003), por lo que este tipo de técnicas de imagen complementan a la evaluación clínica y nunca deberían considerarse la única vía de decisión diagnóstica.

Aunque existen pocos estudios que hayan evaluado la tendinopatía rotuliana mediante el uso de IRT, la han considerado como una técnica de imagen adecuada para su detección (Mangine et al. 1987; Seixas, A et al. 2013). Al igual que ocurre con el resto de patologías, la utilización de la IRT como técnica de imagen en la detección de afecciones musculoesqueléticas se basa fundamentalmente en la presencia de asimetrías térmicas que podrían ser un indicativo de anomalía (Uematsu et al. 1988; Vardasca et al. 2012; Sillero-Quintana et al. 2015).

Como se ha comentado anteriormente, la afectación del SNS se ha identificado como un componente de la tendinopatía, con influencia sobre el dolor y el flujo sanguíneo (Schlereth y Birklein 2008; Dean et al. 2013; Koeppen y Stanton 2017). Por lo tanto, las alteraciones del SNS, las vasculares y las metabólicas que se ven implicadas en las tendinopatías pueden modificar la temperatura cutánea, y esta variación podría medirse con relativa facilidad mediante IRT (Tumilty et al. 2019).

La IRT es capaz de detectar patrones térmicos alterados en la tendinopatía rotuliana generalmente asociados a una hipertemia de la rodilla del lado afecto (Mangine et al. 1987; Seixas, A et al. 2013). Además, según algunos autores, el dolor de la tendinopatía rotuliana presenta una correlación positiva con la diferencia térmica (Mangine et al. 1987; Seixas, A et al. 2013). Por el contrario, la observación de patrones fríos, se ha relacionado con la presencia de signos crónicos del tendón (Mangine et al. 1987; Hildebrandt et al. 2010), aunque en la actualidad este

concepto debería revisarse al incluirse elementos de la respuesta inflamatoria en el modelo fisiopatológico de la tendinopatía crónica (Abate et al. 2009; Rees et al. 2014).

1.7. ANÁLISIS DE LOS PARÁMETROS ECOTEXTURALES DE PRIMER ORDEN

Durante la evaluación ecográfica, la sonda emite un haz de ultrasonido que penetra en los diferentes tejidos con diferentes velocidades dependiendo de su impedancia acústica. Al travesar cada uno de los tejidos, el haz sufrirá fenómenos de reflexión que serán recogidos por la sonda y procesados para ofrecer una imagen digital (Strakowski 2016; Iriarte Posse 2020). Cada uno de los píxeles que forman la imagen digital viene representado por un nivel de intensidad de gris resultante de la reflexión de la estructura del tejido que esté representando (Ríos-Díaz et al. 2009).

En la práctica clínica y mediante la interpretación cualitativa, la ecografía nos permite discriminar algunos aspectos relacionados con la estructura y el grado de ecogenicidad que se alejan de la normalidad (del Baño Aledo et al. 2008). En cambio, el análisis de imagen permite la cuantificación de variables que pueden detectar patrones en la imagen, con una mayor sensibilidad que la interpretación visual del operador. Mediante el análisis de imagen es posible analizar variables morfológicas como perímetros, grosores o anchuras de diferentes estructuras o cuantificar la ecogenicidad de una determinada región (Ríos-Díaz et al. 2010), estas variables permiten una evaluación de la integridad del tejido, incluido el tendón (Malliaras et al. 2010; Auliffe et al. 2017).

Los parámetros ecográficos más utilizados son los de primer orden, que evalúan las intensidades de los píxeles ignorando las relaciones espaciales (Lalumiere et al. 2020). En este caso, la cuantificación se realiza a través del histograma de frecuencia de las intensidades de gris de los píxeles localizados en una ROI (Lalumiere et al. 2020) **(figura 5)**. La ecointensidad (EI) y la ecovariación (EV) son dos parámetros texturales de primer orden (Ríos-Díaz et al. 2010, 2015). La EI se calcula mediante el valor medio de nivel de gris, y la EV se determina mediante la relación entre la desviación estándar y la intensidad media de píxeles obtenida del histograma mediante la fórmula: $EV = \sigma / \mu \bullet 100$ donde σ es la desviación estándar de las intensidades de la imagen y μ es el valor medio de la intensidad en cada ROI (Gdynia et al. 2009; Ríos-Díaz et al. 2010).

Es importante resaltar que el análisis de los parámetros texturales de primer orden es fácil de implementar, pero no permite establecer relaciones espaciales entre píxeles, lo que puede limitar su capacidad para describir adecuadamente las características de textura y detectar diferentes patrones en la imagen de un tejido (Glasbey y Horgan 1995; Pratt 2007). En cambio, los parámetros ecotexturales de segundo orden basados en la matriz de co-ocurrencia de nivel de gris (GLCM) (Haralick et al. 1973) resultan más complicados de calcular e interpretar, pero permiten analizar, además de la intensidad de nivel de gris de los píxeles, la distribución espacial entre ellos (Haralick et al. 1973), lo que puede tener implicaciones importantes en la caracterización de la composición de los tejidos, como por ejemplo, en el tejido tendinoso.

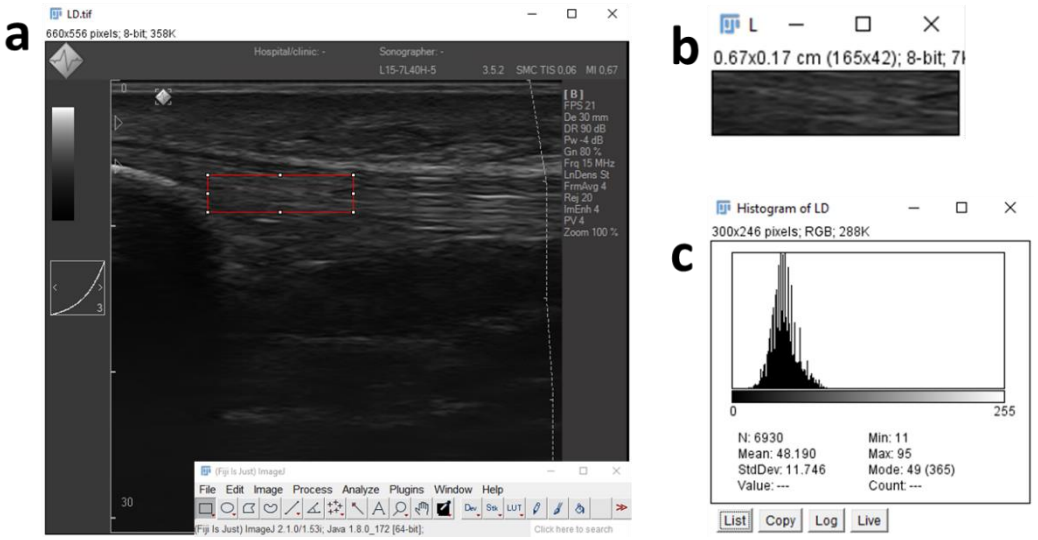

Figura 5. Histogramas de frecuencia de una ROI de un tendón rotuliano (ImageJ). Selección de la ROI (a), extracción de la ROI (b), histograma de frecuencia de la intensidad de gris (c). (Fuente: elaboración propia).

1.8. JUSTIFICACIÓN

Se estima que alrededor de 125 millones de ciudadanos europeos practican algún deporte (Rütten y Abu-Omar 2004). En las últimas décadas, el interés por la

práctica deportiva se ha incrementado debido al cambio de estilo de vida de la población (Bauman et al. 2009). Esta práctica conlleva un aumento de la demanda sobre el aparato locomotor asociado a un incremento de las lesiones, que a nivel tendinoso se asientan con más frecuencia en los tendones de Aquiles y rotuliano (Maffulli et al. 2003). En el caso de la tendinopatía rotuliana, su prevalencia en deportes con alta demanda de esta estructura, como el voleibol o el baloncesto, llegan a alcanzar una prevalencia del 15%-45% (Lian et al. 2005). Ante la carga , el tendón almacena y libera energía de forma repetitiva, que junto con la compresión, favorecen la aparición de la tendinopatía (Cook y Purdam 2012).

Las tendinopatías cursan con alteraciones estructurales y fisiológicas que se pueden valorar mediante técnicas de imagen como la ecografía, la resonancia magnética o la IRT, aunque en algunos estudios la correlación entre los resultados de las imágenes y los síntomas clínicos puede ser baja (Cook et al. 2000b, 2000a; Chaudhry et al. 2016). El papel de la inflamación en las tendinopatías ha suscitado un considerable debate durante décadas al abandonar la creencia de que la inflamación no forma parte del proceso fisiopatológico de las tendinopatías (Kraushaar y Nirschl 1999; Alfredson et al. 2000), y plantearse la convivencia del proceso degenerativo junto al inflamatorio en este proceso (Abate et al. 2009; Rees et al. 2014; Speed 2016).

En este sentido, en la búsqueda de nuevas variables basadas en técnicas de imagen que permitan reflejar este nuevo modelo de tendinopatía y aportar información sobre el estado del tejido, podría resultar de interés explorar la VR intratendón mediante ecografía PD (Bjordal et al. 2006; Torp-Pedersen et al. 2008; Terabayashi et al. 2014) junto a los cambios térmicos cutáneos mediante IRT (Mangine et al. 1987; Chaudhry et al. 2016), que permitirían obtener información respecto a patrón inflamatorio y, por otro lado, los análisis ecotexturales en modo B (Ríos-Díaz et al. 2010, 2015) para evaluar los cambios en la estructura tendinosa (Benítez-Martínez et al. 2020; López-Royo et al. 2021).

Sin embargo, y tal y como ya se ha apuntado, estas técnicas están influidas por diversos factores que pueden afectar a la obtención de resultados, por lo que previamente es necesario estudiar su fiabilidad y reproducibilidad en el contexto de la tendinopatía rotuliana. En esta tesis se propone un nuevo método de análisis

IRT que solventa los problemas de localización de las ROIs y su contaminación térmica por manipulación de los marcadores cutáneos (Molina-Payá et al. 2021b).

En segundo lugar, se propone un nuevo método para evaluar de manera fiable la VR intratendón basada en la cuantificación de la intensidad de color de píxel en la DS (Molina-Payá et al. 2021a).

En tercer lugar, se realiza una caracterización de pacientes con patología tendinosa en cuanto a la VR, los patrones térmicos y la ecotextura con el objeto de aportar nueva evidencia sobre el proceso fisiopatológico que permitiría la elección de tratamientos más eficaces (Bjordal et al. 2006; Torp-Pedersen et al. 2008) o la detección precoz y el desarrollo de nuevas intervenciones de prevención (Côrte et al. 2019; Gómez-Carmona et al. 2020).

En los siguientes capítulos se desarrollan los diferentes estudios.

OBJETIVOS

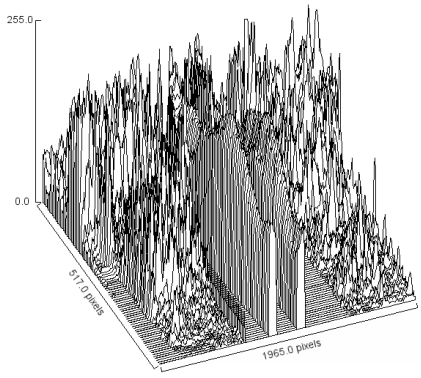

II. OBJETIVOS

1. Determinar la fiabilidad de un nuevo método de análisis termográfico del tendón rotuliano basado en la superposición de regiones de interés sobre una matriz de píxeles.

2. Analizar la fiabilidad de un nuevo método semiautomático basado en el análisis de imagen de la señal Power Doppler para evaluar la señal Doppler y la resistencia vascular intratendón en la tendinopatía rotuliana.

3. Examinar la correlación entre el índice de resistencia vascular y un nuevo método semiautomático basado en el análisis de imagen de la señal Power Doppler para evaluar la resistencia vascular intratendón.

4. Analizar las diferencias en las variables térmicas, vasculares y ecotexturales entre los tendones sintomáticos y asintomáticos de deportistas con tendinopatía rotuliana, así como con sujetos control asintomáticos.

ESTUDIO I:
FIABILIDAD INTER E INTRAOBSERVADOR DE UN NUEVO MÉTODO DE ANÁLISIS TERMOGRÁFICO INFRARROJO DEL TENDÓN ROTULIANO

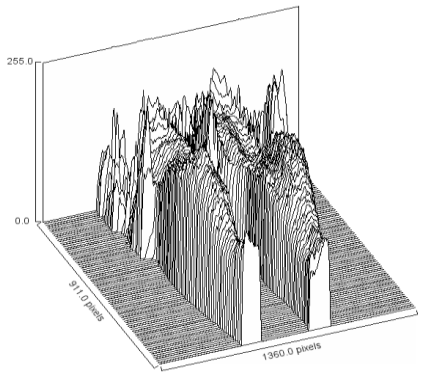

III. ESTUDIO I: FIABILIDAD INTER E INTRAOBSERVADOR DE UN NUEVO MÉTODO DE ANÁLISIS TERMOGRÁFICO INFRARROJO DEL TENDÓN ROTULIANO

QUANTITATIVE INFRARED THERMOGRAPHY JOURNAL
https://doi.org/10.1080/17686733.2019.1700697

Taylor & Francis
Taylor & Francis Group

Check for updates

Inter and intraexaminer reliability of a new method of infrared thermography analysis of patellar tendon

Javier Molina-Payá[a], José Ríos-Díaz[b] and Jacinto Martínez-Payá[c]

[a]Doctoral Program in Health Sciences, Universidad Católica San Antonio de Murcia, Murcia, Spain; [b]Centro de Ciencias de la Salud San Rafael. Fundación de San Juan de Dios, Universidad Antonio de Nebrija, Madrid, Spain; [c]Grupo de Investigación Discapacidad y Fisioterapia. Departamento de Fisioterapia, Facultad de Medicina, Universidad de Murcia, Murcia, Spain

3.1. INTRODUCTION

Thermoregulation of the skin is a complex system that is mainly linked to cutaneous vascularization and to the sympathetic nervous system as regulator (Kellog y Pérgola 2000; Charkoudian 2003), maintaining, in healthy subjects, a thermal symmetry between both sides of the body (Selfe y Whitaker 2008; Vardasca R 2008; Vardasca et al. 2012).

Infrared thermography (IRT) is an imaging technique that captures infrared radiation in a fast, safe and low-cost way for both the diagnosis and monitoring of various pathologies associated with temperature changes, making it the technique of choice for many authors (Ring y Ammer 2012). The extreme sensitivity of IRT permits the detection of temperature variations generated by metabolic changes in situations such as the regeneration of injured tissue (Mangine et al. 1987), alterations of the sympathetic nervous system (Schuhfried et al. 2000), inflammatory processes (Denoble et al. 2010), infections (Romanò et al. 2013), vascular disorders (Huang et al. 2011) or hormonal disorders (Costa et al. 2019).

Although some authors have reported good reproducibility (Zaproudina et al. 2008), a comprehensive methodology and protocol is required to accurately determine temperature (Joseph T Costello 2013). The study of factors that may influence thermal capture has allowed a protocol for obtaining thermographs to be normalized (2002; Ammer 2008). In this sense, the IRT of structures or areas determined on the body through the selection of regions of interest (ROI) can be considered as the most reliable method in static situations, whereas other methods are needed when the exploration is carried out in dynamic processes, involving the use averages of areas around hot spots within the area explored (Ludwig et al. 2014).

Unlike the protocol for IRT, there is no clear consensus for the determination of ROI (Choi et al. 2013). Thus, some authors delimit the ROI by means of markers on the skin (Denoble et al. 2010; Selfe et al. 2006, 2010; Costa et al. 2013), with the disadvantage that manipulation of the area during positioning can alter the temperature of the ROI (Ferreira et al. 2008). Other authors delimit the ROI on already captured thermographs (Varjú et al. 2004; George et al. 2008), although accurately interpreting anatomical references in this way is difficult (Herry y Frize 2004). Additionally, software is being developed that allows the automatic positioning of ROI (Fernández-Cuevas et al. 2012). Recently, a protocol has been developed by consensus to improve the acquisition of thermographic images (Moreira et al. 2017). However, the process of placing reference markers on the skin may introduce bias into the recorded temperature.

We propose an alternative method to select the ROI, while avoiding any modification of the original thermogram. The aim of this study was to assess the reliability and reproducibility of this IRT method to select ROIs by means of markers on the skin without manipulation of the region, which might alter the interpretation of the thermogram.

3.2. MATERIAL AND METHODS

3.2.1. Study subjects

A total of 17 participants (34 bilateral images) (7 women and 10 men) between 18 and 62 years old (mean: 32.2 years; S.D:10.9 years) were voluntarily recruited from a private Physical Therapy Centre (Murcia, Spain) in July and August 2018. All participants were informed and signed the informed consent document. The study was approved by the Ethical Committee of the Catholic University of Murcia (CE111803). As it is a study that compares the size, location and average temperature of the thermograms, the intrinsic influence factors of the subjects were not taken into account.

3.2.2. Sample size determination

Sample size was calculated by the data proposed by Walter et al. (Walter et al. 1998). For an expected intraclass correlation coefficient of 0.9 and a minimum acceptable value of 0.7, and two measurements per image, then the minimum required sample size is 19 participants with alpha=0.05 and beta=0.2.

3.2.3. IRT imaging

All images were recorded following the same standard protocol. The participant was acclimatized in an isolated room at a mean temperature of 22.7 ± 0.5ºC and a relative humidity of 43.4 ± 4% for 20 min without clothing on the lower limbs.

The participant was seated on a hydraulic stretcher with his/her feet on a step-in order to isolate contact with the ground. Then a point was marked bilaterally on the dorsal face of the metatarsophalangeal joint of the second toe and a vertical line on the Achilles tendon that was moved to the heel (Ribeiro et al. 2011). These two references were used to position the feet on two parallel lines (25 cm apart) drawn on the step. The knees were positioned at 90 degrees of flexion which allows a right angle of radiation while the skin that covers the patellar tendon a greater part of the patellar tendon (Zooker et al. 2013), than in the standing

position (Selfe y Whitaker 2008; Denoble et al. 2010). In addition, the sitting position improves perfusion and skin circulation by reducing the circulatory collapse of the area caused by gravity while standing, and also the influence on skin temperature (Ratovoson et al. 2013).

The IRT images were recorded with an OPTRIS PI 450 IRT camera coupled to Optris PI Connect Software (Germany). The IRT camera has a Noise Equivalent Temperature Difference <40 mK with 38º x 29º FOV, a wide range of temperature from −20°C to +100°C, spectrum range of 7.5–13 μm, focal plane array sensor size of 382 × 288 pixels, emissivity set at 0.98 and a measurement uncertainty of ± 2% of the overall temperature reading. The size of the capture frame was 55.4 × 40.63 cm (1.5 mm/px).

The most mid-cranial part of the patella was marked with metallic ink using a 0.7 mm marker so that it could be easily observed on the thermogram (reference points) and placed outside the ROI. The camera was positioned 80 cm from the knees and aligned on the three axes by means of a self-leveling laser with respect to the knee and step reference points (Tká et al. 2010) **(Figure 1(a,b))**. In this position a first thermogram (T1) was recorded without manipulation or modification (raw thermogram) **(Figure1(c))**.

In order to delimit the area of skin corresponding to the patellar tendon, metallic adhesives (Figure2(a)) were fixed on the skin with the following references: 1) midpoint: proximal distal midpoint of the patella; 2) lateral point: 1 cm lateral to the most lateral point of the patella (Veeramani 2010); 3) medial point: over the most medial point of the patella; and 4) distal point: 5 cm distal to the external femoro-tibial articular interline (Zooker et al. 2013). Contralateral knee ROI was symmetrically adjusted (Nahm 2013).

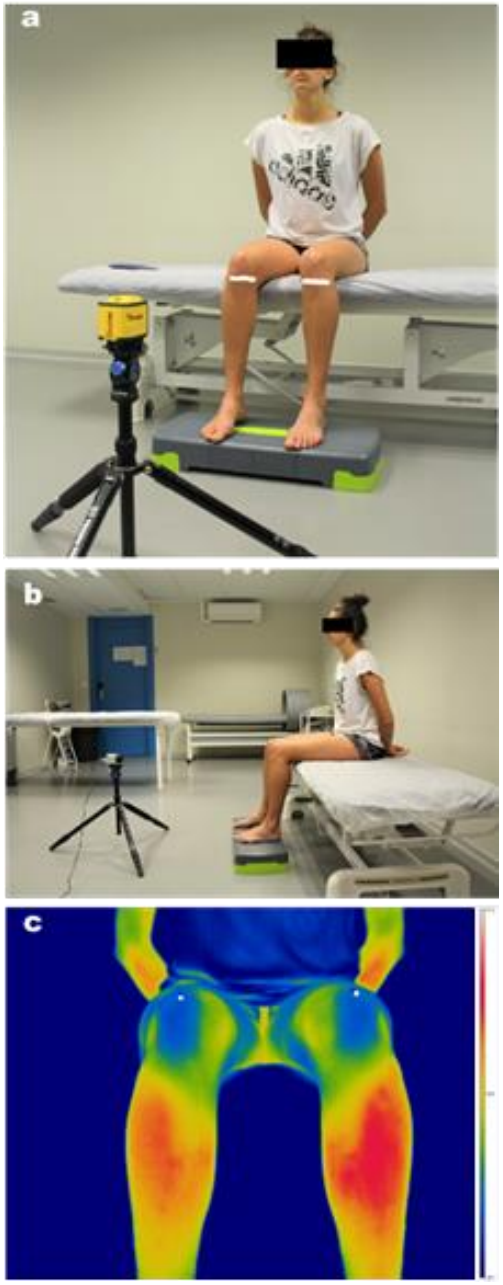

Figure 1. Participant and camera positioning (a,b) and the first thermogram with reference points (c).

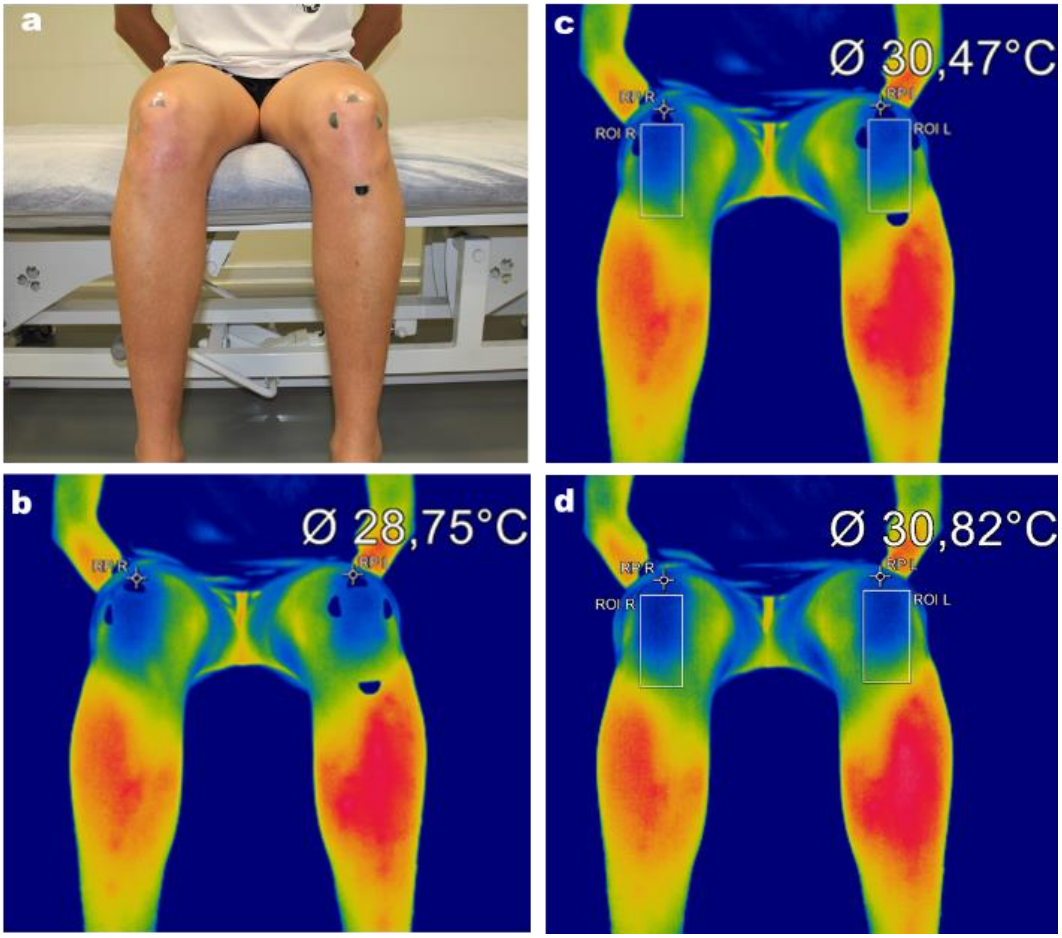

Figure 2. Metallic markers (a), thermogram with reference points (b), ROI boxes on the second thermogram (c) and superimposed over first thermogram (d).

A second thermogram (T2) was saved and ROI boxes were adjusted to the metal adhesives **(Figure 2(b,c))**. The size and position of ROI boxes on the pixel matrix (X and Y axis) of the image provided by the software was calculated. On the second thermogram (T2), the pixel distance between the ROI boxes and the reference points was calculated **(Figure 2(c))**. The ROI boxes from the second thermogram (T2) to the first (T1) **(Figure 2(d))** were transferred taking into account the size of the boxes and their distance (pixels) to the reference points **(Figures 1(c)**

and 2(b)). Thermogram 1 (T1) was re-recorded with the transferred of the ROI boxes of thermogram 2 (T2) and the average temperature, position and size data were extracted **(Figure 2(d))**.

The same first thermogram (T1) was used for both examiners as reference image. The reference points and ROI (T2) were located by the two examiners independently and blinded (interexaminer analysis) at two different times (one week) (intraexaminer analysis). The images were coded, and the order of analysis was random. The flowchart with the analysis phases is shown in **Figure 3**.

The main outcome was mean temperature of ROI (ºC) but the box size (width and height in pixels) and the position on the X and Y axis were also analyzed.

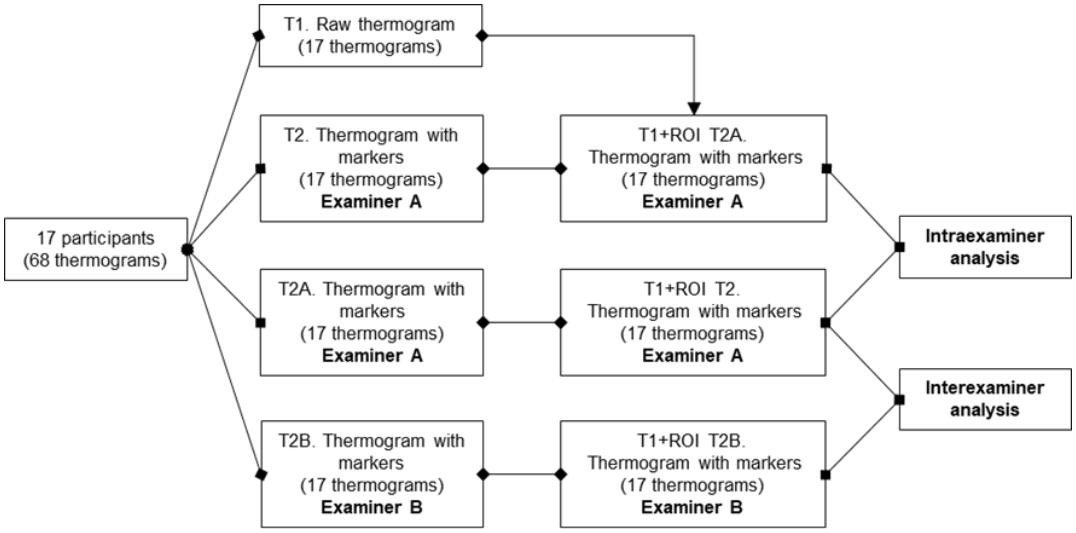

Figure 3. Flowchart of analysis method.

.

3.2.4. Statistical analysis

Descriptive statistics were calculated for ROI dimension variables: width, height, position on x-axis and y-axis, and mean temperature of the boxes in both knees corresponding to the different thermographs obtained by both observers. Although the sample size (n=34) allows the assumption of normality, it was

checked with the coefficients of asymmetry, kurtosis, the Q-Q normality plots and the Kolmogorov-Smirnov test. Parametric tests were applied to all variables. Descriptive statistics were used (mean, standard deviation, range and quartiles) to summarize the data for each examiner's assessment.

The intraclass correlation coefficient (ICC) was calculated in total agreement with a two-factor alpha model and mixed effects ($ICC_{2,1}$) for each of the variables of interest (McGraw y Wong 1996; Weir 2005). This coefficient offers values of between 0 and 1, where 0 would be a lack of agreement and 1 would be total agreement. Although the interpretation of these cut-off points is, to a certain extent, arbitrary, very good (ICC>0.8), good (ICC=0.61-0.80), moderate (0.41 to 0.6), low (0.21 to 0.4) and poor (<0.21) reproducibility will be considered (Shrout y Fleiss 1979).

Measurement precision (Atkinson y Nevill 1998; Lexell y Downham 2005) was evaluated using standard error of measurement (SEm) [$SEm=SD \bullet \sqrt{(1-ICC)}$] and its relative value with respect to the average of all measurements and the smallest real difference (SRD). SRD is useful for determining whether a change in the parameter is due to a real change or lies within the limits of error of the measuring method [$SRD=1.96 \bullet SEm \bullet \sqrt{2}$].

The limits of agreement (LOA) were calculated according to the method described by Bland and Altman (Atkinson y Nevill 2000) and the presence of summative or multiplicative biases with Passing-Bablock's linear regression method (Bablok y Passing 1985).

For a direct clinical interpretation, the graphical method proposed by Luiz et al. (Luiz et al. 2003), based on the Kaplan-Meier estimate representing the probability of survival as a function of the degree of disagreement, was applied.

Statistical analysis was performed using IBM SPSS Statistics 19.0 (SPSS Inc. IBM Company, 2010) and the *jmv package* (version 0.9) (Love, Jonathon et al.) for R (version 3.5.0; 2018). P-values of <0.05 were considered to indicate statistical significance.

3.3. RESULTS

A total of 68 thermograms were recorded from 17 participants. **Table 1** shows the descriptive data. The width-box variable showed no statistical differences in the intra-examiner ($F_{1,33}$=1.47; p=0.233) or inter-examiner ($F_{1,33}$=0.454; p=0.505) analysis. The intra-examiner differences in height-box were not significant ($F_{1,33}$=0.815; p=0.373) but statistical differences in the means were found for inter-examiner data ($F_{1,33}$=4.40; p=0.044). The X-axis did not show intra-examiner ($F_{1,33}$=0.045; p=0.833) or inter-examiner ($F_{1,33}$≈0; p≈1.0) differences. The means of the Y-axis were similar intra-examiner ($F_{1,33}$=2.65; p=0.133) but not inter-examiner ($F_{1,33}$=42.3; p=0.001). Finally, the skin temperature was similar intra-examiner ($F_{1,33}$=0.488; p=0.490) and inter-examiner ($F_{1,33}$=0.011; p=0.917).

The reliability results are shown in **Table 2** and **Figures 4 and 5**. Excellent reliability was observed both intra and inter-examiner in all parameters. No bias was found for the parameters analyzed. Only, as expected, in the X-axis parameter was a systematic bias detected, although it did not affect reproducibility.

For skin temperature, the difference between intra-examiner measurements was 0.006ºC (LOA: -0.10 to 0.10), and the differences between examiners were 0.001 ºC (LOA: -0.13 to 0.13).

Further information is provided in the supplementary material **(Suppl 1 and Suppl 2)**.

Table 1. Descriptive values for intra and inter-observer analysis.

Parameter	Mean (SD)	C.I. 95%	Minimum	Median (IQR)	Maximum
Width box A	34.1 (3.28)	33 to 35	26	34 (32 to 36)	40
Width box A2	33.9 (3.11)	33 to 35	26	35 (32 to 36)	40
Width box B	33.9 (3.64)	33 to 35	25	35 (31 to 36.3)	40
Height box A	56.6 (4.61)	55 to 58	47	56 (53.8 to 61)	63
Height box A2	56.3 (4.85)	55 to 50	47	57 (54 to 61)	61
Height box B	57.2 (4.45)	56 to 59	49	58 (54 to 61)	64
X-axis location A	192.5 (82.01)	164 to 221	106	193 (112 to 272)	279
X-axis location A2	192.4 (81.47)	164 to 221	107	194 (112 to 273)	278
X-axis location B	192.5 (80.99)	164 to 221	109	192 (112 to 272)	278
Y-axis location A	122.3 (7.99)	120 to 125	102	123 (119 to 124)	152
Y-axis location A2	121.7 (8.27)	119 to 125	98	122 (119 to 125)	147
Y-axis location B	120.3 (7.98)	118 to 123	98	121 (118 to 123)	147
Temperature A	32.9 (0.85)	32.6 to 33.2	31.2	32.9 (32.4 to 33.6)	34.6
Temperature A2	32.9 (0.85)	32.6 to 33.2	31.2	32.9 (32.4 to 33.6)	34.6
Temperature B	32.9 (0.84)	32.6 to 33.2	31.2	32.9 (32.5 to 33.6)	34.6

Box parameters units are pixels. Temperature in degrees Celsius. A: first evaluation for examiner A. A2: second evaluation for examiner A. B: evaluation for examiner B.

Table 2. Reliability for both intra and inter-observer analysis.

Parameter	ICC (95% CI)	Agreement	Mean difference (95% LOA)	% Change	SEm	SEm%	SRD (95% CI)	SRD%
Width box intra-observer	0.937 (0.878 to 0.968)	Excellent	-0.235 (-2.45 to 1.98)	-0.6	0.80	2.3%	2.21 (-1.5 to 2.92)	6.5%
Width box inter-observer	0.904 (0.818 to 0.951)	Excellent	-0.176 (-3.17 to 2.82)	-0.5	1.07	3.1%	2.96 (-1.72 to 4.19)	8.7%
Height box intra-observer	0.92 (0.846 to 0.959)	Excellent	-0.294 (-4.02 to 3.43)	-0.5	1.33	2.4%	3.68 (-2.80 to 4.56)	6.5%
Height box inter-observer	0.92 (0.846 to 0.959)	Excellent	0.588 (-2.62 to 3.79)	1.1	1.41	2.5%	3.91 (-2.50 to 5.32)	6.9%
X-axis location intra-observer	1 (1 to 1)	Excellent	-0.059 (-3.22 to 3.10)	0.1	0.00	0.00%	0 (-)	0.0%
X-axis location inter-observer	1 (0.999 to 1)	Excellent	0.00 (-4.97 to 4.97)	0.3	0.00	0.00%	0 (-)	0.0%
Y-axis location intra-observer	0.968 (0.937 to 0.984)	Excellent	-0.559 (-4.48 to 3.37)	-0.5	1.44	1.2%	4 (-2.56 to 5.45)	3.3%
Y-axis location inter-observer	0.946 (0.544 to 0.984)	Excellent	-2.0 (-5.51 to 1.51)	-1.6	1.43	1.2%	3.96 (-1.78 to 6.14)	3.3%
Temperature intra-observer	0.998 (0.997 to 0.999)	Excellent	0.0059 (-0.090 to 0.10)	0.0	-	-	-	-
Temperature inter-observer	0.997 (0.994 to 0.999)	Excellent	0.0012 (-0.127 to 0.129)	0.0	-	-	-	-

Box parameters units are pixels. Temperature in degrees Celsius. ICC: intraclass correlation coefficient. LOA: limits of agreement. %Change: mean difference respect total average of measures. SEm: standard error of measurement. SRD: smallest real difference. SEm and SRD for temperature are not shown because it is an interval variable.

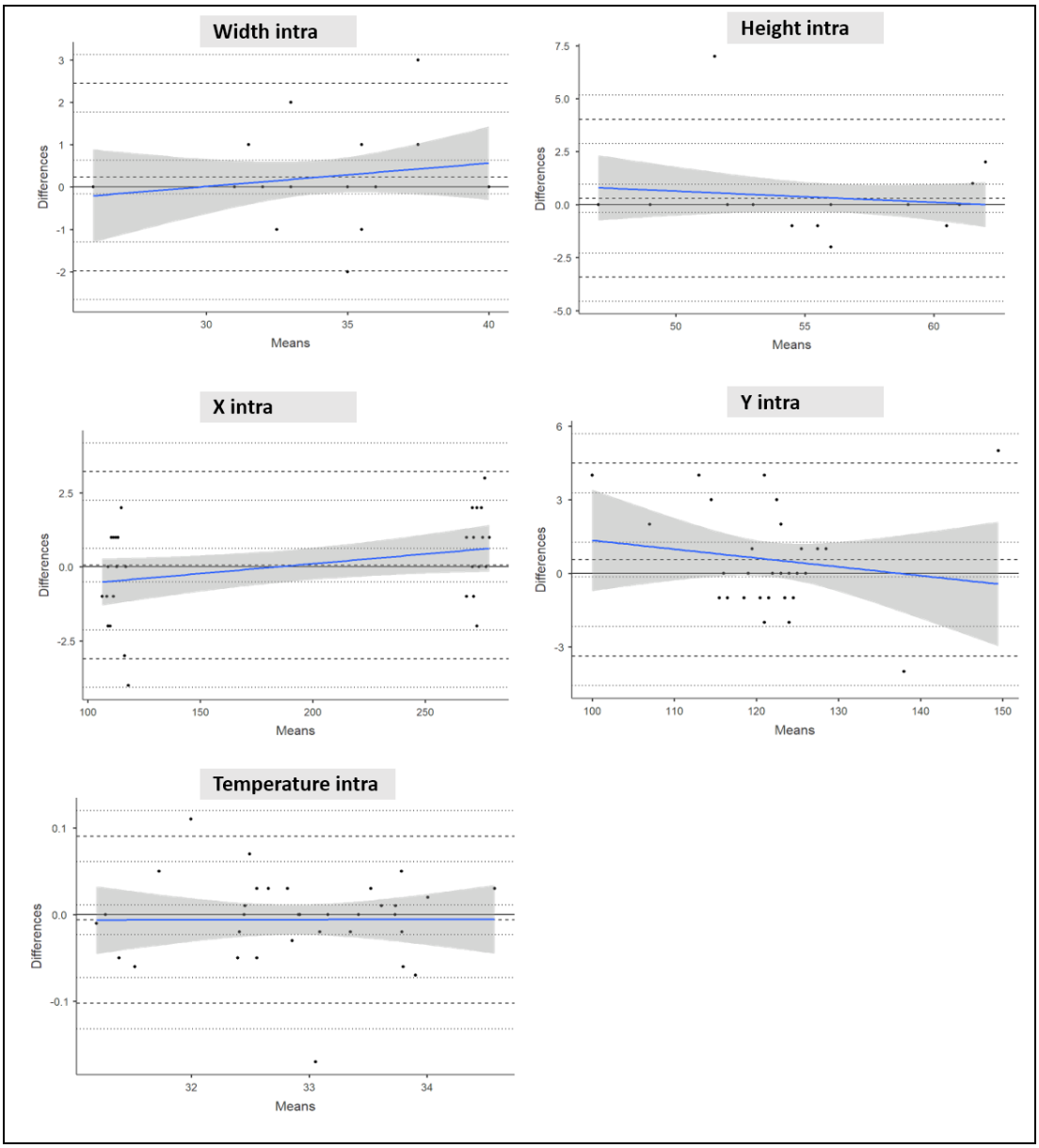

Figure 4. Intra-examiner reliability Bland–Altman's plots. Each pair of measurements is represented by a point determined by the mean value (x-axis) and by the difference between them (y-axis). Dotted lines represent the limits of agreement with the confidence intervals. Dark zone and blue line represent the proportional bias line with confidence intervals. The Width and Height are in millimetres (mm), X and Y are coordinates in pixels and Temperature is in Celsius grades (°C).

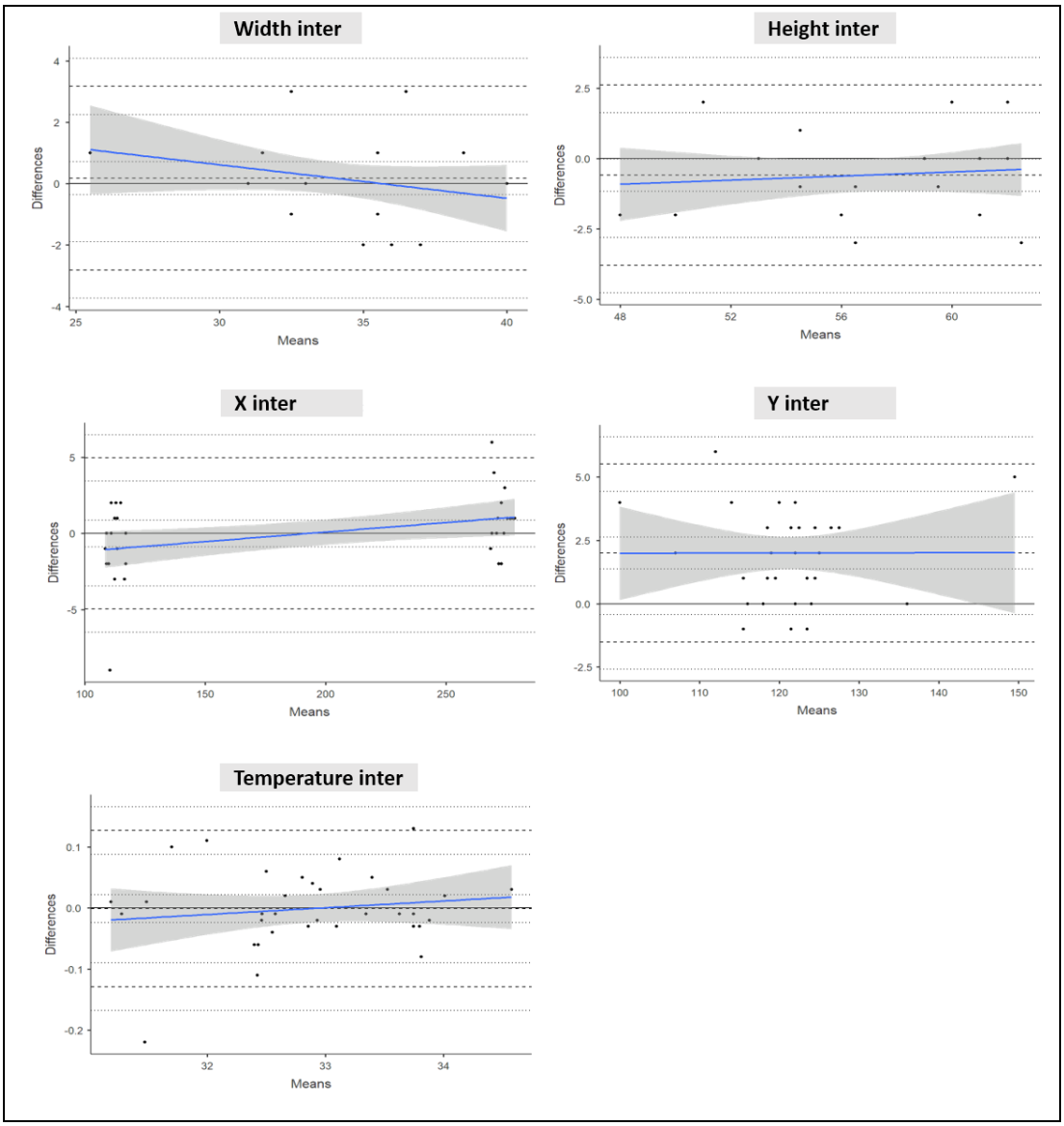

Figure 5. Inter-examiner reliability Bland–Altman's plots. Each pair of measurements is represented by a point determined by the mean value (x-axis) and by the difference between them (y-axis). Dotted lines represent the limits of agreement with the confidence intervals. Dark zone and blue line represent the proportional bias line with confidence intervals. The Width and Height are in millimetres (mm), X and Y are coordinates in pixels and Temperature is in Celsius grades (°C).

3.4. DISCUSSION

In this study, we analyzed the intra- and inter-observer reliability of a method of ROI determination for thermographic analysis that does not modify the original thermogram positioning through the positioning of markers.

The lower limits of the ICC confidence interval showed very close agreement for all variables (>0.85, except for Y-axis inter-examiner) and specifically superiors 0.99 for the intra- and inter-examiner temperature values. This finding may be due to several factors that are decisive for which extreme precautions were taken, such as the choice of easily locatable anatomical references, prior consensus by the observers and the meticulous positioning of the camera and the participant, which left little room for subjectivity on the part of the technicians.

Also facilitating the high degree of agreement in the size variables of the ROI was the use of symmetrical ROI boxes for both knees, which is an important factor when analyzing thermal asymmetry on both sides of the body (Nahm 2013). It should also be mentioned that the boxes are rectangular, which facilitates their positioning in relation to skin markers, whose inner edge is also rectilinear **(Figure 2)**.

From a practical point of view, mean differences were between 0 and 2 pixels, with R^2>82%, with a maximum relative SEm of 2.5% and a maximum relative SRD of 8.7%. All the differences were less than 10 px **(Figures 4 and 5)**.

As regards the temperature, the reliability was even higher, with mean differences in the order of the tenth degree, both in the intra-examiner and inter-examiner analysis. The total differences were below 0.20ºC.

It is possible that the close agreement found would be lower if, rather than using the same thermogram to determine the size, position and mean temperature of the ROI, different primary thermograms were used for each measurement and examiner. In this study it was decided to use a single primary thermogram to minimize the influence of both extrinsic and intrinsic factors that may affect the uptake of infrared radiation and thus analyze only the factors that influence the creation and positioning of ROI.

Inter-observer reliability has also been investigated in other studies with good results. Selfe et al. (Selfe et al. 2006) observed ICC values of between 0.82 to

0.97 in patients with knee pathologies. Similar results were obtained by Spalding et al. (Spalding et al. 2008) in patients with arthritis of the hands, by Costa et al. in cervical and facial musculature (Costa et al. 2013) with very good agreement (ICC between 0.852 to 0.998). By contrast, Mustacchi et al. (Mustacchi et al. 1990) found poor reliability in breast thermograms.

With regard to intra-examiner reliability, the good results of Varju et al. (Varjú et al. 2004) (ICC= 0.899) in hand measurements and Costa et al (Costa et al. 2013) (ICC= 0.879 to 0.998) in measurements of cervical and facial musculature should be highlighted. On the other hand, Denoble et al. (Denoble et al. 2010) obtained a much lower ICC (0.5 to 0.72) in the knee. Zaproudina et al. (Zaproudina et al. 2008) suggested that the relatively poor intra and inter-observer results obtained for ICC is because the selection of the ROI is essentially based on a manual procedure and therefore the skill of the technician to select the ROI.

In order to eliminate this subjective factor, different software have been developed to automate the ROI selection process (Plassmann P 2003). Fernandez et al. used a software with which they obtained very good results (inter-examiner ICC =0.989 and intra-examiner= 0.997) (Fernández-Cuevas et al. 2012). However, it should be borne in mind that ROI obtained automatically by software include more general location regions and do not allow measurements to be focused on specific structures because they cannot recognize determining anatomical references.

In recent years the technology and methodology of thermographic recordings have improved and different authors have analyzed the asymmetries in body temperature of different body regions to discriminate preventively areas susceptible to injury in football players (Plassmann P 2003) and in different pathologies (Schuhfried et al. 2000; Ferreira et al. 2008; Ludwig et al. 2014) so that it could become an imaging technique for preventive use and control of the evolution of both injuries and pathologies.

3.4.1. Limitations

The most important limitation of this study is that we located the ROI over only one raw thermogram for each participant. However, as discussed above, the

objective was to determine the reproducibility of the reference points to locate ROI, without the influence of other sources of variability.

The main strength of our study is the description of the method of anatomical localization of reference points without modifying skin temperature and the statistical analysis of the reliability from different perspectives and not only based on the ICC, which has several limitations (Atkinson y Nevill 1998, 2000; Lexell y Downham 2005; Weir 2005).

3.5. CONCLUSION

The results obtained confirm that the method used has a very good reliability and reproducibility, while any influence on the detected temperature is negligible.

In this sense, it will be of interest to extend the study in order to ascertain the reliability between different thermal cameras and software, which could increase the strength of the method.

3.6. REFERENCES

1. Ammer K. The Glamorgan Protocol for recording and evaluation of thermal images of the human body. Thermol Int. 2008;18(4):125-9.
2. Atkinson G, Nevill A. Measures of Reliability in Sports Medicine and Science: Correspondence. Sports Med. 2000;30(5):375-81.
3. Atkinson G, Nevill AM. Statistical Methods For Assessing Measurement Error (Reliability) in Variables Relevant to Sports Medicine: Sports Med. 1998;26(4):217-38.
4. Bablok W, Passing H. Application of statistical procedures in analytical instrument testing. J Autom Chem. 1985;7(2):74-9.
5. Charkoudian N. Skin Blood Flow in Adult Human Thermoregulation: How It Works, When It Does Not, and Why. Mayo Clin Proc. 1 de mayo de 2003;78(5):603-12.

6. Choi E, Lee P-B, Nahm FS. Interexaminer reliability of infrared thermography for the diagnosis of complex regional pain syndrome. Skin Res Technol Off J Int Soc Bioeng Skin ISBS Int Soc Digit Imaging Skin ISDIS Int Soc Skin Imaging ISSI. mayo de 2013;19(2):189-93.
7. Costa ACS, Dibai Filho AV, Packer AC, Rodrigues-Bigaton D. Intra and inter-rater reliability of infrared image analysis of masticatory and upper trapezius muscles in women with and without temporomandibular disorder. Braz J Phys Ther. febrero de 2013;17(1):24-31.
8. Costa APC, Maia JM, Brioschi ML, de Melo Mafra Machado JE. Thermography Evaluation in Patients with Hypothyroidism and Fibromyalgia by Analyzing the Temperatures of the Palms of Hands. En: Lhotska L, Sukupova L, Lacković I, Ibbott GS, editores. World Congress on Medical Physics and Biomedical Engineering 2018 [Internet]. Singapore: Springer Singapore; 2019 [citado 10 de octubre de 2019]. p. 15-9. Disponible en: http://link.springer.com/10.1007/978-981-10-9035-6_3
9. Denoble AE, Hall N, Pieper CF, Kraus VB. Patellar skin surface temperature by thermography reflects knee osteoarthritis severity. Clin Med Insights Arthritis Musculoskelet Disord. 2010;3:69-75.
10. Fernández-Cuevas I, Marins JC, Carmona PG, García MA, Lastras JA, Quintana MS. Reliability and Reproducibility of Skin Temperature of Overweight Subjects by an Infrared Thermography Software Designed for Human Beings. Thermol Int. 2012;22(Apendix1):130-7.
11. Ferreira JJA, Mendonça LCS, Nunes LAO, Andrade Filho ACC, Rebelatto JR, Salvini TF. Exercise-associated thermographic changes in young and elderly subjects. Ann Biomed Eng. agosto de 2008;36(8):1420-7.
12. George J, Bensafi A, Schmitt AM, Black D, Dahan S, Loche F, et al. Validation of a non-contact technique for local skin temperature measurements. Skin Res Technol Off J Int Soc Bioeng Skin ISBS Int Soc Digit Imaging Skin ISDIS Int Soc Skin Imaging ISSI. noviembre de 2008;14(4):381-4.
13. Herry CL, Frize M. Quantitative assessment of pain-related thermal dysfunction through clinical digital infrared thermal imaging. Biomed Eng OnLine. 28 de junio de 2004;3(1):19.

14. Huang C-L, Wu Y-W, Hwang C-L, Jong Y-S, Chao C-L, Chen W-J, et al. The application of infrared thermography in evaluation of patients at high risk for lower extremity peripheral arterial disease. J Vasc Surg. octubre de 2011;54(4):1074-80.

15. IACT. Standards and protocolos in Clinical Thermography Imaging. Thermology Guidelines [Electronic Version Internet]. 2002. [accessed 15 th April 2019]. Available from: http://www.iact-org.org/professionals/thermog-guidelines.html

16. 13. Costello JT, Stewart IB. Use of thermal imaging in sports medicine research: A short report. Int Sportmed J. 2013;14:94-8.

17. 2. Kellog D, Pérgola P. Skin responses to exercise and training. In: Garrett WE, Kirkendall DT, editors. Exerc Sport Sci. Lippincott Williams & Wilkins; 2000. p. 239-50.

18. Lexell JE, Downham DY. How to assess the reliability of measurements in rehabilitation. Am J Phys Med Rehabil. septiembre de 2005;84(9):719-23.

19. 43. Love J, Dropmann D, Selker R. jamovi project (2018) [Internet]. Available from: https://www.jamovi.org

20. Ludwig N, Formenti D, Gargano M, Alberti G. Skin temperature evaluation by infrared thermography: Comparison of image analysis methods. Infrared Phys Technol. enero de 2014;62:1-6.

21. Luiz RR, Costa AJL, Kale PL, Werneck GL. Assessment of agreement of a quantitative variable: a new graphical approach. J Clin Epidemiol. octubre de 2003;56(10):963-7.

22. Mangine RE, Siqueland KA, Noyes FR. The use of thermography for the diagnosis and management of patellar tendinitis. J Orthop Sports Phys Ther. 1987;9(4):132-40.

23. McGraw KO, Wong SP. Forming inferences about some intraclass correlation coefficients. Psychol Methods. 1996;1(1):30-46.

24. Moreira DG, Costello JT, Brito CJ, Adamczyk JG, Ammer K, Bach AJE, et al. Thermographic imaging in sports and exercise medicine: A Delphi study and consensus statement on the measurement of human skin temperature. J Therm Biol. octubre de 2017;69:155-62.

25. Mustacchi G, Milani S, Ciatto S, Del Turco MR, Luzzati G, Lattanzio V, et al. Observer variation in mammary thermography: results of a teaching file test carried out in four different centers. Tumori. 28 de febrero de 1990;76(1):29-31.

26. Nahm FS. Infrared Thermography in Pain Medicine. Korean J Pain. julio de 2013;26(3):219-22.

27. Plassmann P MP. CTHERM for standardised thermography. En Krako, Poland; 2003.

28. Ratovoson D, Jourdan F, Huon V. Influence of gravity on the skin thermal behavior: experimental study using dynamic infrared thermography. Skin Res Technol Off J Int Soc Bioeng Skin ISBS Int Soc Digit Imaging Skin ISDIS Int Soc Skin Imaging ISSI. febrero de 2013;19(1):e397-408.

29. Ribeiro AP, Trombini-Souza F, Tessutti V, Lima FR, de Camargo Neves Sacco I, João SMA. Rearfoot alignment and medial longitudinal arch configurations of runners with symptoms and histories of plantar fasciitis. Clinics. junio de 2011;66(6):1027-33.

30. Ring EFJ, Ammer K. Infrared thermal imaging in medicine. Physiol Meas. 1 de marzo de 2012;33(3):R33.

31. Romanò CL, D'Anchise R, Calamita M, Manzi G, Romanò D, Sansone V. Value of digital telethermography for the diagnosis of septic knee prosthesis: a prospective cohort study. BMC Musculoskelet Disord. 4 de enero de 2013;14(1):7.

32. Schuhfried O, Vacariu G, Lang T, Korpan M, Kiener HP, Fialka-Moser V. Thermographic parameters in the diagnosis of secondary Raynaud's phenomenon. Arch Phys Med Rehabil. abril de 2000;81(4):495-9.

33. Selfe J, Hardaker N, Thewlis D, Karki A. An accurate and reliable method of thermal data analysis in thermal imaging of the anterior knee for use in cryotherapy research. Arch Phys Med Rehabil. diciembre de 2006;87(12):1630-5.

34. Selfe J, Sutton C, Hardaker NJ, Greenhalgh S, Karki A, Dey P. Anterior knee pain and cold knees: a possible association in women. The Knee. octubre de 2010;17(5):319-23.

35. Selfe J, Whitaker J. A narrative literature review identifying the minimum clinically important difference for skin temperature asymmetry at the knee. Thermol Int. 2008;18:51-4.

36. Shrout PE, Fleiss JL. Intraclass correlations: uses in assessing rater reliability. Psychol Bull. marzo de 1979;86(2):420-8.

37. Spalding SJ, Kwoh CK, Boudreau R, Enama J, Lunich J, Huber D, et al. Three-dimensional and thermal surface imaging produces reliable measures of joint shape and temperature: a potential tool for quantifying arthritis. Arthritis Res Ther. 2008;10(1):R10.

38. Tká M, Hudák R, Foffová P, Živ J. An importance of camera subject distance and angle in musculoskeletal applications of medical thermography. Acta Electrotech Inf. 2010;10:57-60.

39. Vardasca R. Symmetry of temperature distribution in the upper and lower extremities. Thermol Int. 2008;18(4):154-5.

40. Vardasca R, Ring F, Plassmann P, Jones C. Thermal symmetry of the upper and lower extremities in healthy subjects. Thermol Int. 2012;22:53-60.

41. Varjú G, Pieper CF, Renner JB, Kraus VB. Assessment of hand osteoarthritis: correlation between thermographic and radiographic methods. Rheumatol Oxf Engl. julio de 2004;43(7):915-9.

42. Veeramani R. Gender differences in the mediolateral placement of the patella and tibial tuberosity: a geometric analysis. Anat Int J Exp Clin Anat. 2010;4:45-50.

43. Walter SD, Eliasziw M, Donner A. Sample size and optimal designs for reliability studies. Stat Med. 15 de enero de 1998;17(1):101-10.

44. Weir JP. Quantifying test-retest reliability using the intraclass correlation coefficient and the SEM. J Strength Cond Res. febrero de 2005;19(1):231-40.

45. Zaproudina N, Varmavuo V, Airaksinen O, Närhi M. Reproducibility of infrared thermography measurements in healthy individuals. Physiol Meas. abril de 2008;29(4):515-24.

46. Zooker C, Pandarinath R, Kraeutler MJ, Ciccotti MG, Cohen SB, DeLuca PF. Clinical measurement of patellar tendon: accuracy and relationship to surgical tendon dimensions. Am J Orthop Belle Mead NJ. julio de 2013;42(7):317-20.

3.7. SUPPLEMENTARY MATERIALS

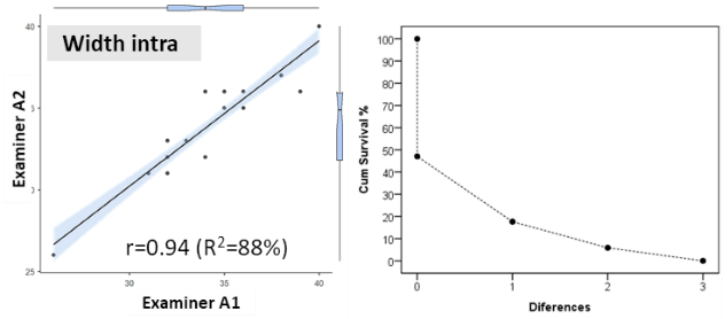

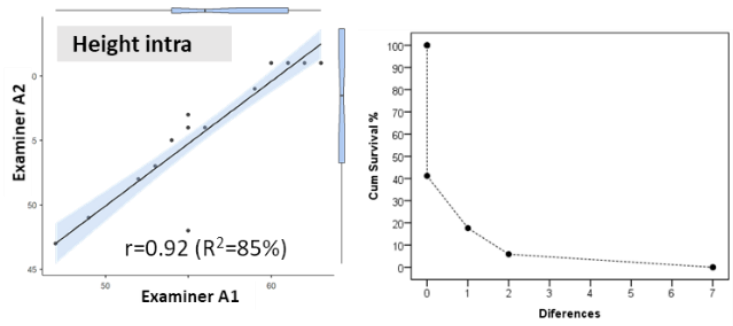

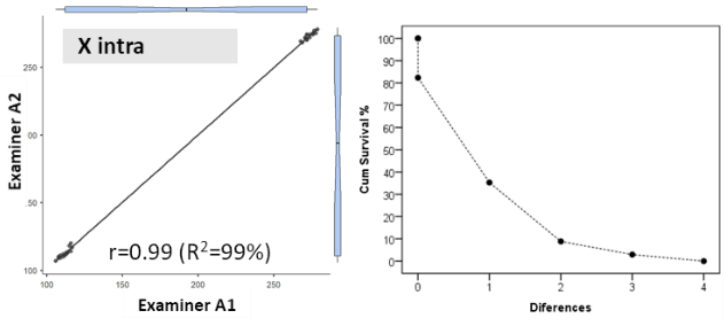

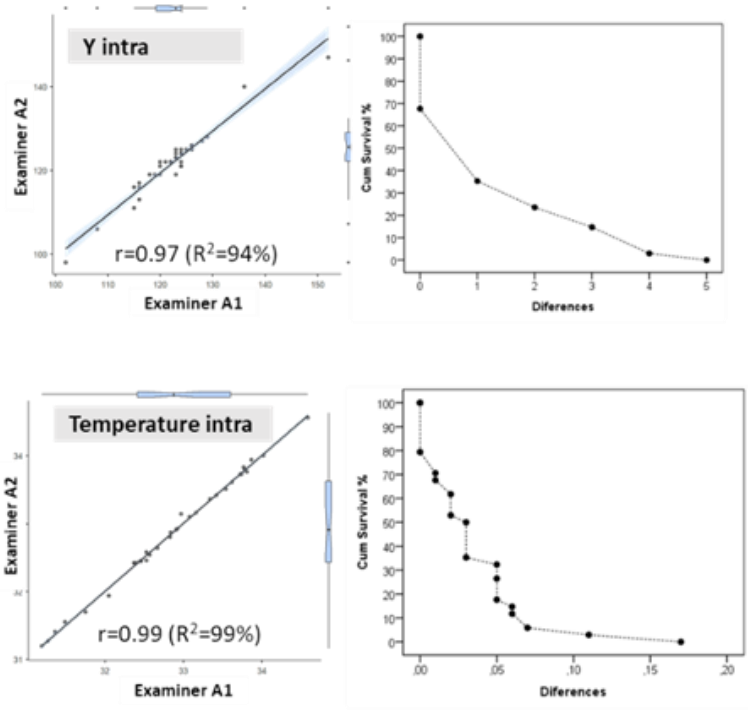

Figure suppl. 1. Intra-examiner reliability plots. Left: Linear regression with 95% CI. Right: Cumulative differences.

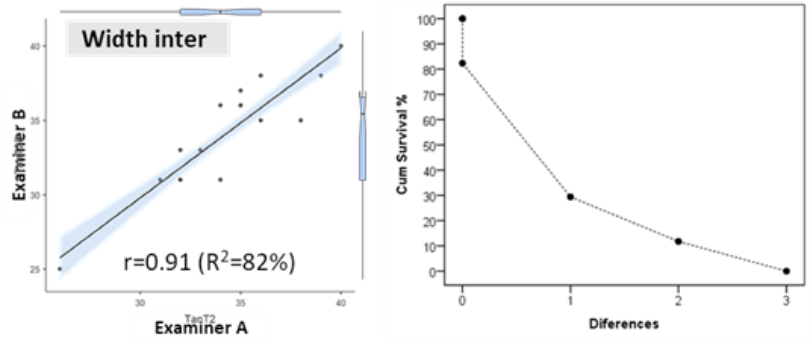
Width inter
Examiner B
Examiner A
r=0.91 (R²=82%)
Cum Survival %
Diferences

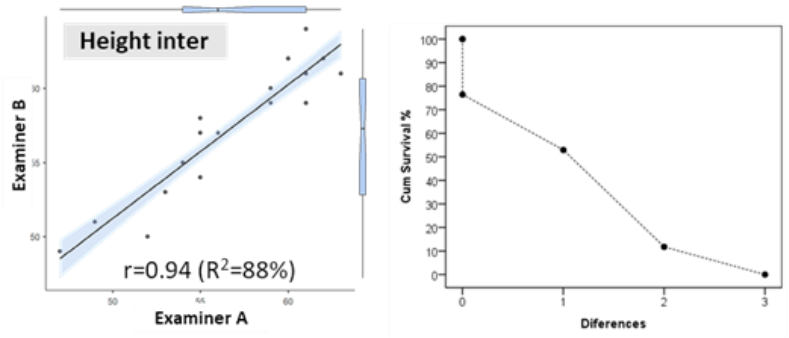
Height inter
Examiner B
Examiner A
r=0.94 (R²=88%)
Cum Survival %
Diferences

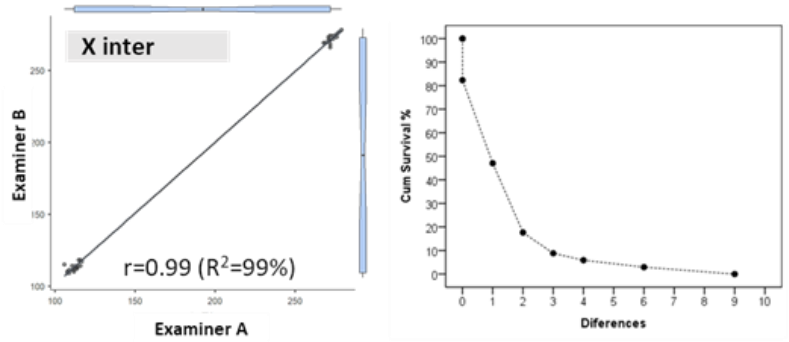
X inter
Examiner B
Examiner A
r=0.99 (R²=99%)
Cum Survival %
Diferences

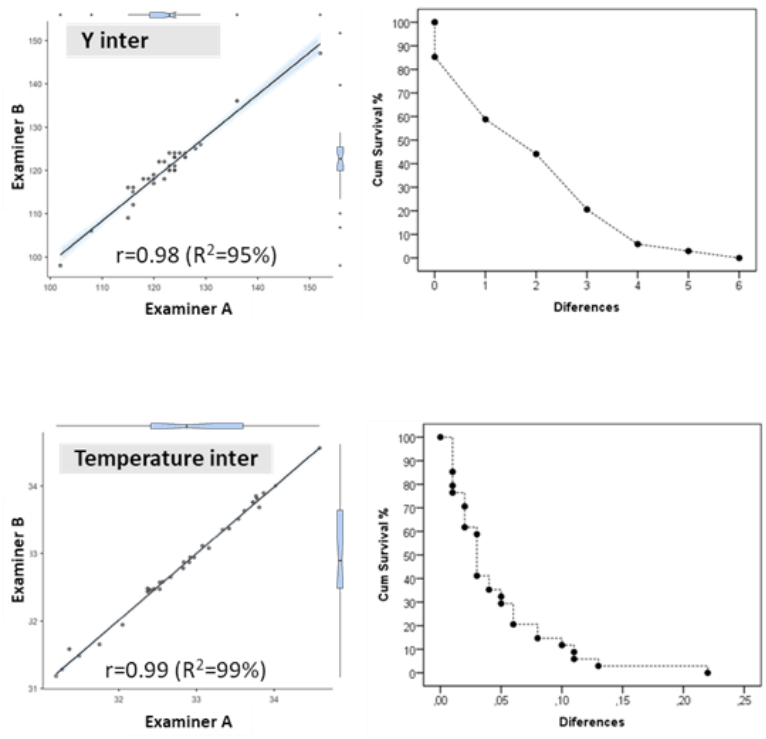

Figure suppl. 2. Inter-examiner reliability plots. Left: Linear regression with 95% CI. Right: Cumulative differences.

SOLICITUD DE PATENTE:

DESARROLLO DE UN MÉTODO Y EQUIPO DE MEDICIÓN DE LA TEMPERATURA

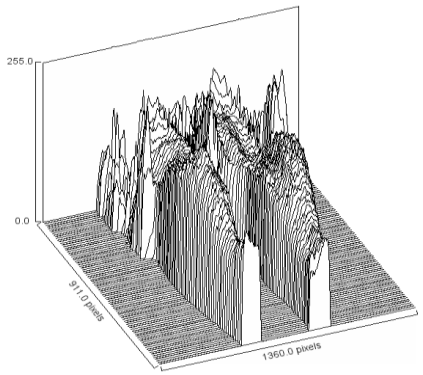

IV. SOLICITUD DE PATENTE: DESARROLLO DE UN MÉTODO Y EQUIPO DE MEDICIÓN DE TEMPERATURA

4.1. SOLICITUD DE PATENTE

El justificante de presentación electrónica de solicitud de patente con número P201830850 se puede consultar en el **anexo 1** y el expediente de la Oficina Española de Patentes y Marcas en el **anexo 2**.

4.2. MÉTODO Y EQUIPO DE MEDICIÓN DE TEMPERATURA

4.2.1. Descripción

4.2.1.1. Objeto de la invención

La invención, tal como expresa el enunciado de la presente memoria descriptiva, se refiere a un método y un equipo de medición de temperatura que aporta, a la función a que se destina, ventajas y características, que se describen en detalle más adelante, que suponen una destacable novedad en el estado actual de la técnica.

Más concretamente, el objeto de la invención se centra, por una parte, en un método de medición de la temperatura de una región de interés de la piel de un sujeto humano o animal, seleccionada previamente, mediante termografía infrarroja, la utilización de marcadores fijables a la piel del sujeto y medios informáticos de tratamiento de imágenes, pudiendo emplearse dicha información en cualquier ámbito relacionado con la salud o la actividad física, y por otra parte, a un equipo específicamente diseñado para llevar a cabo dicho método y que se basa, esencialmente, en un habitáculo móvil hecho de material específico y medios para controlar y monitorizar las condiciones ambientales del mismo, donde se sitúa al sujeto, y que está dotado con cámara de vídeo, láser de baja potencia y cámara termográfica, todo ello conectado a un ordenador con un programa informático

que permite obtener una imagen de la temperatura en las áreas de interés generadas por el evaluador mediante los marcadores fijados en la piel del sujeto.

4.2.1.2. Campo de aplicación de la invención

El campo de aplicación de la presente invención se enmarca dentro del sector de los sistemas metodológicos para aplicación de las cámaras de termografía infrarroja como medio de cuantificación de la temperatura de la piel humana o animal en áreas de interés clínico seleccionadas por el operador, abarcando al mismo tiempo el ámbito de la industria dedicada a la fabricación de aparatos y dispositivos para llevar a cabo dichos sistemas metodológicos.

4.2.1.3. Antecedentes de la invención

En la actualidad se utilizan diferentes técnicas de imagen médica para ayudar al diagnóstico de diferentes patologías. Estas técnicas comprenden diferentes técnicas como, por ejemplo, la radiología, la ecografía, la resonancia magnética, o la tomografía axial computerizada. La termografía infrarroja es una técnica de imagen que empieza a utilizarse en diferentes ámbitos relacionados con el diagnóstico de patologías, la prevención de lesiones, la optimización de cargas de trabajo en la realización de ejercicios terapéuticos, la evaluación del tratamiento o el seguimiento de lesiones entre otras.

Hace unas décadas, la baja sensibilidad de las cámaras infrarrojas y otras limitaciones técnicas representaban una fuente de error para la utilización de esta técnica en el ámbito médico, retrasando su aceptación hasta los años 1990. Actualmente, los equipos para adquisición de imágenes termográficas han evolucionado significativamente hasta proporcionar una tecnología que ofrece una información fiable, haciendo de la termografía un método de ayuda al diagnóstico seguro y preciso.

De una forma generalizada, la mayoría de las lesiones tisulares están relacionadas con variaciones del flujo sanguíneo, que alteran la temperatura de la piel. La termografía es un método no invasivo y sin contacto, que capta la radiación infrarroja de un cuerpo para determinar su temperatura, lo que le permite ser usada sin restricciones en humanos. Proporciona información sobre los procesos fisiológicos en curso, en tiempo real, evaluando las posibles anormalidades

fisiológicas representadas por el aumento o disminución de la temperatura en la superficie de la piel.

La invención que se presenta aquí se refiere, precisamente, a un procedimiento o método de cuantificación de la temperatura de áreas de interés con una localización específica en la piel, empleando una cámara termográfica. Por otro lado, también pretende minimizar la alteración de la medición por los factores de influencia con la introducción de un habitáculo diseñado para tal fin.

Como referencia al estado actual de la técnica, cabe señalar que, al menos por parte del solicitante, se desconoce la existencia de ningún otro método ni equipo de medición de temperatura o invención de aplicación similar que presente unas características técnicas, estructurales y constitutivas iguales o semejantes a las que presenta el que aquí se reivindica.

Ello se debe, principalmente, a que el uso de la termografía en el ámbito médico requiere la necesidad de crear un procedimiento o sistema que controle al máximo los factores de influencia que pueden alterar la correcta cuantificación de las áreas de interés y solucionar el problema de la ubicación selectiva de las áreas de interés, sin alterar su correcta medición de temperatura. Nuestra invención da solución a estos problemas planteados.

Existen patentes que utilizan la cuantificación de la temperatura en diferentes áreas de interés, que están sobre todo vinculadas a la determinación del posible riesgo cancerígeno en patología mamaria, estas invenciones se basan, principalmente, en la detección de áreas de temperatura máxima, en ellas no se realiza una delimitación manual con marcadores sobre la piel para la selección del área de interés, ni se aplica una superposición de imágenes termográficas para evitar la alteración de la medición al manipular al sujeto.

Otras invenciones, utilizan técnicas, incluida la termografía, para registrar alteraciones térmicas en diferentes partes del cuerpo y relacionarlas con posibles patologías, sin embargo, no cuantifican áreas de interés seleccionadas de forma específica, sino las zonas inespecíficas sobre la que se posiciona el instrumento.

Por otra parte, en la actualidad ha aumentado el interés por la utilización de programas informáticos para la aplicación de la termografía en la cuantificación de la asimilación de la carga de entrenamiento o actividad física. Estos sistemas delimitan áreas preestablecidas en el programa que se alejan de la especificidad

necesaria en el ámbito médico, pero su sencillez y rapidez de realización hacen de este sistema una opción interesante. Estos métodos distan de la presente invención al no permitir una selección manual específica de la áreas de interés, ni conseguir un registro de ubicación preciso del sujeto que permita realizar una superposición de las cajas que delimitan las ROI sobre imágenes termográficas sin manipular, para ello, la invención utiliza puntos de láser de baja potencia que se dirigen hacia puntos de referencia ubicados en la piel del paciente, o en su defecto, se utilizan puntos de referencia que se ubican en unas determinadas coordenadas dentro de la matriz de píxeles de la imagen.

Para un correcto procedimiento de medición, es necesario contar con una infraestructura y una metodología específica, que permitan realizar un protocolo estricto, que ya ha sido fijado por otros autores con anterioridad, y posteriormente adaptado al ámbito médico. La presente invención proporciona los medios para permitir adaptar estos protocolos de medición a las características de la misma, generando un método de cuantificación termográfico sencillo, fiable y preciso.

Algunos sistemas de cuantificación mediante termografía utilizan sensores para monitorizar algunos parámetros ambientales y poder controlarlos. Como se ha comentado anteriormente, existen protocolos reconocidos que describen la metodología a utilizar para minimizar, en la medida de lo posible, la influencia, no solo de estos factores ambientales, sino también de otros factores tanto extrínsecos como intrínsecos del sujeto. La presente invención, además de utilizar sensores para monitorizar algunas condiciones ambientales, utiliza un habitáculo móvil que minimiza la influencia de algunos de estos factores, como por ejemplo, posibles focos térmicos o el movimiento del aire circundante, permitiendo realizar una medición más precisa.

La aplicación de este método no se circunscribe exclusivamente al ámbito diagnóstico, puede utilizarse en cualquier ámbito que requiera de la cuantificación de la temperatura en áreas de interés específicas en la piel como, por ejemplo, el ámbito de la salud o de la actividad física.

4.2.1.4. Explicación de la invención

El método y un equipo de medición de temperatura que la invención propone se configuran, pues, como destacable novedad dentro de su campo de aplicación,

ya que a tenor de su implementación y de manera taxativa se alcanzan satisfactoriamente los objetivos anteriormente señalados, estando los detalles caracterizadores que lo hacen posible y que los distinguen convenientemente recogidos en las reivindicaciones finales que acompañan a la presente descripción.

Más concretamente, lo que la invención propone, tal como se ha apuntado anteriormente, es un método de medición de la temperatura de una región de interés con una localización específica en la piel de un sujeto, humano o animal, mediante termografía infrarroja, el uso de marcadores fijados en la piel del sujeto y medios informáticos de tratamiento de imágenes, aplicable en cualquier ámbito relacionado con la salud o la actividad física, y un equipo específicamente diseñado para llevar a cabo dicho método y que comprende, esencialmente, en un habitáculo móvil de material específico y con medios para controlar y monitorizar las condiciones ambientales de su interior, para minimizar al máximo la alteración de la medición por factores de influencia, donde se sitúa al sujeto o al menos una parte del mismo, y que está dotado con cámara de vídeo, láser de baja potencia y cámara termográfica, conectados a un ordenador con un programa informático que permite obtener una imagen de la temperatura en las áreas de interés generadas por el evaluador con ayuda de los antedichos marcadores fijados en la piel del sujeto.

Así pues, el método de la presente invención se basa en un protocolo de selección de ROI en la piel de un sujeto, extraídas de imágenes procedentes de una cámara termográfica para utilizarlas como técnica de imagen médica o relacionada con la actividad física. Este método permite cuantificar de forma selectiva la temperatura de las áreas de la piel que impliquen una relación de interés con respecto a una estructura, seleccionada por el evaluador, que esté sometida a cualquier alteración de origen físico, metabólico, nervioso o vascular, que originen cambios térmicos capaces de ser registrados por una cámara termográfica.

Aunque el término "sujeto", que se usa a lo largo de este documento, se debe apreciar que el sujeto sometido a evaluación termográfica puede ser diferente a un ser humano como, por ejemplo, un primate. Por lo tanto, el uso de tal término no se debe ver como una limitación del alcance de las reivindicaciones adjuntas a los humanos.

A la hora de realizar una imagen termográfica en un sujeto, surgen principalmente dos problemas. El primer problema es la gran cantidad de factores que influyen sobre la captación de la radiación infrarroja del sujeto, ya sean extrínsecos o intrínsecos del sujeto.

Este problema se ha intentado solucionar desde el comienzo del uso de la termografía en el ámbito de la salud, mediante el control y registro de estos factores mediante el uso y desarrollo de diferentes guías y protocolos utilizados e integrados en la actualidad. Esta invención añade a estos protocolos, un control más preciso de algunos factores ambientales que pueden influir en la correcta medición de la temperatura del sujeto. Este control queda ligado a la utilización de un habitáculo móvil que mejora algunos aspectos ambientales propuestos, como es la influencia de focos térmicos o el desplazamiento del aire.

El segundo problema es la selección de las áreas de interés, que resultan imprescindibles para cualquier estudio cuantitativo que se quiera realizar. La selección de las áreas de interés se puede realizar, básicamente, de dos formas, con una selección manual o una automática.

La selección manual utiliza marcadores en la piel para que puedan ser visualizados en la imagen termográfica y facilite la delimitación de la caja de medida sobre el área de interés. Esta selección, permite realizar una selección específica del área de interés, pero implica manipular al sujeto para poder ubicar los marcadores en la piel, alterando la correcta medición de la temperatura. La selección automática se realiza mediante programas informáticos específicos que permiten seleccionar áreas de interés sin manipular al sujeto, pero no permiten una selección específica de esas áreas.

La presente invención elimina los inconvenientes de ambos tipos de selección de las áreas de interés: permite realizar una selección específica de las áreas de interés de la piel del sujeto mediante marcadores en la piel sin alterar la correcta medición de su temperatura.

De manera más específica, el funcionamiento del método de la invención, que no debe ser interpretado con carácter limitativo, comprende las siguientes fases:

- El sujeto ha de vestirse, manteniendo la menor cantidad de ropa posible, al ser posible vestirá con ropa interior y siempre manteniendo descubierta la zona a evaluar.

- El sujeto se sitúa en el interior de un habitáculo, con sus paredes construidas con material que presente una alta emisividad, permitiendo crear un fondo de imagen termográfica que contraste con la imagen del sujeto. Una parte de su recubrimiento está realizada con material o tejido transpirable, permitiendo la regulación de la humedad relativa generada por el propio sujeto que se encuentra en el habitáculo. El interior está iluminado con luz de baja emisión térmica y presenta una temperatura y humedad relativa monitorizadas en un ordenador que se encuentra fuera del habitáculo, para controlar, constantemente, el rango de temperatura en el que se trabaja.

- Se coloca al sujeto en una posición que permita captar una imagen termográfica de la forma más perpendicular posible al área de interés. Para conseguir esta posición, se pueden utilizar instrumentos que permitan ajustar la altura de la cámara. Si en la posición apropiada, el sujeto se encuentra en contacto con el suelo, se añade una plataforma elevada que evite el contacto directo, evitando la transferencia térmica entre ambos.

- Se añaden, como mínimo, dos puntos de referencia, preferentemente elementos fijables en la piel compuestos por un material con alta reflexión, que facilite su visualización en la imagen termográfica. Estos puntos de referencia se ubican en sitios alejados del área de interés para evitar cualquier alteración térmica sobre la zona a evaluar.

- Con el uso de puntos procedentes de láseres de baja potencia, que se encuentran sujetos a una estructura estable, se fija la posición del sujeto haciendo coincidir los puntos láser con los puntos de referencia anteriormente descritos. Otra posibilidad, es ubicar los puntos de referencia en una matriz de píxeles de un programa informático de visión termográfica, se extraen las coordenadas exactas de su ubicación para poder reproducir, posteriormente, la misma posición de los puntos de referencia en posteriores capturas.

- Mediante la cámara termográfica, se captura una imagen y se almacena para su posterior procesado en el ordenador que se encuentra fuera del habitáculo de captación.

- Seguidamente, se aplican unos marcadores en la piel del sujeto, en este caso para delimitar el área de la piel de interés. Estos marcadores también consisten en elementos que están compuestos por un material con alta reflexión que permita su

visualización en la imagen termográfica. La ubicación de los marcadores viene dada por el interés del evaluador en un área de la piel determinada.

- Luego, se coloca al sujeto en la misma posición anterior, es decir, con los puntos láser colocados en la misma dirección que antes y en coincidencia con la posición de los puntos de referencia. Si se ha optado por la opción de ubicar los puntos de referencia en la matriz de píxeles, se posiciona al sujeto de tal forma que se hacen coincidir los puntos de referencia con las coordenadas de ubicación de estos puntos en la matriz de píxeles de la imagen termográfica, obtenidas en la primera captura de imagen. De esta forma, se garantiza la misma posición del sujeto en la captación de la primera y en la segunda imagen termográfica.

- Se capta una nueva imagen con la cámara termográfica y se almacena para su posterior procesado.

- Posteriormente, mediante el programa informático, se determina la posición y tamaño de la caja tomando como referencia la posición visual de los marcadores de la piel, que se traslada a la primera imagen capturada. Para un correcto traslado de la caja que contiene el área de la piel de interés, se tiene en cuenta el tamaño en número de píxeles y la distancia en el eje X e Y de la matriz de píxeles, desde el centro de la caja a uno de los puntos de referencia. De esta forma se garantiza la misma ubicación y tamaño de la caja sobre la primera imagen.

- La caja del área de interés superpuesta en la primera captura de imagen, muestra la medida de temperatura en el programa informático.

Con esta metodología se consigue una imagen termográfica que contiene una o varias cajas de selección del área de interés de la piel del sujeto, seleccionadas y delimitadas por el evaluador, y que quedan superpuestas a una imagen termográfica sin alteración térmica por su manipulación.

El descrito método y un equipo de medición de temperatura representa, pues, una innovación de características estructurales y constitutivas desconocidas hasta ahora, razones que unidas a su utilidad práctica, la dotan de fundamento suficiente para obtener el privilegio de exclusividad que se solicita.

4.2.1.5. Descripción de los dibujos

Para complementar la descripción que se está realizando y con objeto de ayudar a una mejor comprensión de las características de la invención, se

acompaña a la presente memoria descriptiva, como parte integrante de la misma, de un juego de planos en que con carácter ilustrativo y no limitativo se ha representado lo siguiente:

La figura número 1.- Muestra una vista esquemática en perspectiva de un ejemplo del equipo preconizado para llevar a cabo el método de medición de temperatura objeto de la invención, apreciándose las principales partes y elementos que comprende.

4.2.1.6. Realización preferente de la invención

A la vista de la descrita figura 1 y única, y de acuerdo con la numeración adoptada, se puede observar en ella un ejemplo de realización no limitativo del equipo de medición de temperatura de la invención, el cual comprende las partes y elementos que se indican y describen en detalle a continuación.

Así, tal como se observa en dichas figuras, el equipo (1) en cuestión comprende, esencialmente, un habitáculo móvil (100), debidamente iluminado con una luz (101) de baja emisión térmica, y compuesto por paredes (102) construidas con un material de alta emisividad e inserciones de material transpirable (103), por ejemplo, un tejido. Dentro del habitáculo se encuentran incorporados uno o más sensores de temperatura (104) y humedad relativa (105), además de, preferentemente, una cámara de vídeo (106) enfocada de modo que permite observar lo que ocurre en el interior del habitáculo (100), así como, en todo caso, una cámara termográfica (112) y, preferentemente, unos láseres de baja potencia (111), estando todos estos elementos conectados, con una conexión (108) que puede ser por cable o inalámbrica, a un ordenador (107) situado externamente al habitáculo móvil (100).

Este habitáculo móvil (100) tiene una configuración y dimensiones aptas para alojar en su interior al sujeto a evaluar (109), o al menos una parte del mismo que abarca la zona o miembro donde se encuentra el área de interés. El sujeto va marcado con unos puntos de referencia (110) y alejados del área de interés. El sujeto está posicionado haciendo coincidir unos puntos del láser de baja potencia (111) sobre los mencionados puntos de referencia (110). La cámara termográfica (112) realiza la primera toma de imágenes (113) con el área de interés sin manipular que

se visualiza en el programa informático (114) del ordenador (107) que se acopla a la cámara termográfica (112) con la conexión (108).

El equipo comprende asimismo unos marcadores (115) que se fijan en la piel del sujeto de modo que delimitan el área cutánea de interés generada por parte del evaluador para realizar, seguidamente, una segunda toma de imágenes (116).

Las dos capturas de imágenes (113, 116) son posteriormente procesadas con el programa informático (114) en el ordenador (107) para delimitar el área de interés con una caja alojada según la posición de los marcadores (115) de la piel y realizar una superposición de las áreas seleccionadas en la segunda toma sobre la imagen de la primera toma. Como resultado del proceso se obtiene una imagen (117) sin contaminar, que contiene la cuantificación de la temperatura en las áreas de interés generadas por parte del evaluador mediante los marcadores en la piel.

Preferentemente, tanto los puntos de referencia (110) como los marcadores (115) que se fijan en la piel del sujeto son elementos que están realizados con material de alta reflexión, ya que así facilitan la visualización en las imágenes de la cámara termográfica.

Opcionalmente, el habitáculo móvil (100) cuenta con una plataforma elevada (118) para que se sitúe sobre ella el sujeto (109) y evitar el contacto directo con el suelo, evitando la transferencia térmica entre ambos.

Con todo ello, el método comprende, esencialmente, la superposición de imágenes (116), que contienen cajas de áreas de interés específicas, seleccionadas y delimitadas por el evaluador con marcadores fijados en la piel (115) del sujeto, sobre imágenes termográficas sin manipular (113), sin influir sobre la temperatura de la piel.

Para la toma de dichas imágenes se contempla el uso de un habitáculo móvil (100) con las paredes (102) construidas con un material de alta emisividad, inserciones de tejido transpirable (103), iluminado con una luz (101) de baja emisión térmica y que contiene sensores de temperatura (104) y humedad relativa (105), para poder controlar y monitorizar las condiciones ambientales del habitáculo.

El posicionamiento del sujeto a evaluar se realiza mediante la utilización de puntos de referencia (110) y marcadores fijados en la piel (115) de material con alta reflexión, para poder visualizarlos en la imagen termográfica, haciendo coincidir unos puntos láser de baja potencia (111) con los puntos de referencia (110) para

poder reposicionar de la misma forma al sujeto en la segunda toma de imágenes (116).

Alternativamente, el posicionamiento del sujeto a evaluar se realiza mediante la utilización de puntos de referencia (110) y marcadores fijados en la piel (115) de material con alta reflexión, para poder visualizarlos en la imagen termográfica, extrayendo las coordenadas de los puntos de referencia (110) contenidas en la matriz de píxeles de la imagen termográfica de la primera toma (113) para poder posicionar, del mismo modo, al sujeto para realizar la segunda toma de imagen (116) termográfica, haciendo coincidir en la imagen, los puntos de referencia (110) marcados en la piel del sujeto con las coordenadas extraídas de la primera toma (113) termográfica.

En el segundo caso, se realiza un procesado de las imágenes en un programa informático (114) que comprende la determinación de las coordenadas de la caja del área de interés de la imagen (116) de la segunda toma, para poder reproducir la ubicación de la caja en la imagen de la primera toma (113), que se encuentra sin manipular.

El programa informático (114) está configurado para registrar unas variables ambientales de dentro del habitáculo móvil (100).

Descrita suficientemente la naturaleza de la presente invención, así como la manera de ponerla en práctica, no se considera necesario hacer más extensa su explicación para que cualquier experto en la materia comprenda su alcance y las ventajas que de ella se derivan, haciéndose constar que, dentro de su esencialidad, podrá ser llevada a la práctica en otras formas de realización que difieran en detalle de la indicada a título de ejemplo, y a las cuales alcanzará igualmente la protección que se recaba siempre que no se altere, cambie o modifique su principio fundamental.

4.3. REIVINDICACIONES

1.- MÉTODO DE MEDICIÓN DE TEMPERATURA, de una región de interés de la piel de un sujeto humano o animal, seleccionada previamente, mediante termografía infrarroja, aplicable en cualquier ámbito relacionado con la salud o la actividad física, caracterizado por comprender la superposición de imágenes (116)

termográficas que contienen cajas de áreas de interés específicas, seleccionadas y delimitadas por el evaluador con marcadores fijados en la piel (115) del sujeto, sobre imágenes termográficas sin manipular (113) del sujeto en la misma posición y tomadas sin influir sobre la temperatura de la piel, y un procesado de dichas imágenes (116, 113) en un programa informático (114) de ordenador (107) que comprende la determinación de las coordenadas de la caja del área de interés de la imagen (116) de la segunda toma, para poder reproducir la ubicación de la caja en la imagen de la primera toma (113) que se encuentra sin manipular.

2.- MÉTODO DE MEDICIÓN DE TEMPERATURA, según la reivindicación 1, caracterizado porque, para la toma de dichas imágenes se siguen los siguientes pasos:

- se sitúa al sujeto, manteniendo descubierta la zona a evaluar, en una posición que permita captar una imagen termográfica de la forma más perpendicular posible al área de interés;

- se le colocan al sujeto, como mínimo, dos puntos de referencia (110), ubicados en sitios alejados del área de interés, para evitar cualquier alteración térmica sobre la zona a evaluar, y que servirán para fijar la posición del sujeto posteriormente;

- mediante cámara termográfica (11), se captura, al menos, una imagen (113) y se almacena para su posterior procesado en el ordenador.

- se colocan marcadores (115) en la piel del sujeto, delimitando el área de la piel de interés, estando la ubicación de dichos marcadores (115) dada por el interés del evaluador en un área de la piel determinada;

- se coloca al sujeto en la misma posición que antes, con ayuda de los puntos de referencia (110);

- se capta una nueva imagen (116) con la cámara termográfica (112) y se almacena para su posterior procesado.

- mediante el programa informático (114), se determina la posición y tamaño de la caja tomando como referencia la posición visual de los marcadores (115) de la piel, que se traslada a la primera imagen (113) capturada;

- la caja del área de interés superpuesta en la primera captura de imagen (113), muestra la medida de temperatura en el programa informático.

3.- MÉTODO DE MEDICIÓN DE TEMPERATURA, según la reivindicación 2, caracterizado porque, para un correcto traslado de la caja que contiene el área de la piel de interés, se tiene en cuenta el tamaño en número de píxeles y la distancia en el eje X e Y de la matriz de píxeles, desde el centro de la caja a uno de los puntos de referencia (110), garantizando la misma ubicación y tamaño de la caja sobre la primera imagen.

4.- MÉTODO DE MEDICIÓN DE TEMPERATURA, según la reivindicación 2 ó 3, caracterizado porque, para fijar la posición del sujeto en la segunda captura de imagen, se utilizan unos láseres de baja potencia (111), haciendo coincidir los puntos láser con los puntos de referencia (110).

5.- MÉTODO DE MEDICIÓN DE TEMPERATURA, según la reivindicación 2 ó 3, caracterizado porque, para fijar la posición del sujeto en la segunda captura de imagen, se ubican los puntos de referencia (110) en una matriz de píxeles de un programa informático de visión termográfica, extrayendo las coordenadas exactas de su ubicación para poder reproducir, posteriormente, la misma posición de los puntos de referencia en posteriores capturas.

6.- MÉTODO DE MEDICIÓN DE TEMPERATURA, según cualquiera de las reivindicaciones 1 a 5, caracterizado porque los puntos de referencia (110) que se utilizan son elementos compuestos por material con alta reflexión, que facilitan su visualización en la imagen termográfica.

7.- MÉTODO DE MEDICIÓN DE TEMPERATURA, según cualquiera de las reivindicaciones 1 a 6, caracterizado porque los marcadores (115) que se utilizan son elementos compuestos por material con alta reflexión que facilitan su visualización en la imagen termográfica.

8.- MÉTODO DE MEDICIÓN DE TEMPERATURA, según cualquiera de las reivindicaciones 1 a 7, caracterizado porque para la captura de las imágenes, se sitúa al sujeto en un habitáculo móvil (100) que permite crear un fondo de imagen termográfica que contraste con la imagen del sujeto.

9.- MÉTODO DE MEDICIÓN DE TEMPERATURA, según la reivindicación 8, caracterizado porque el habitáculo móvil (100) cuenta con material transpirable y permite la regulación de la humedad relativa generada por el propio sujeto.

10.- MÉTODO DE MEDICIÓN DE TEMPERATURA, según cualquiera de las reivindicaciones 1 a 7, caracterizado porque el interior del habitáculo móvil (100)

está iluminado con luz de baja emisión térmica y presenta una temperatura y humedad relativa monitorizada en un ordenador (107) que se encuentra fuera del habitáculo, que controla constantemente el rango de temperatura en el que se trabaja.

11.- EQUIPO DE MEDICIÓN DE TEMPERATURA, aplicando el método descrito en las reivindicaciones 1 a 10, caracterizado por comprender un habitáculo móvil (100) con paredes (102) de material de alta emisividad e inserciones de material transpirable (103), con luz (101) de baja emisión térmica, sensores de temperatura (104) y humedad relativa (105), para controlar y monitorizar las condiciones ambientales del habitáculo, y cámara termográfica (112), todo ello conectado, mediante una conexión (108), a un ordenador (107) con un programa informático (114); y porque, además, comprende elementos fijables a la piel de un sujeto, aplicables como puntos de referencia (110) y/o marcadores (115).

12.- EQUIPO DE MEDICIÓN DE TEMPERATURA, según la reivindicación 11, caracterizado porque también comprende una cámara de vídeo (106) que permite observar el interior del habitáculo (100).

13.- EQUIPO DE MEDICIÓN DE TEMPERATURA, según la reivindicación 11 ó 12, caracterizado porque también comprende unos láseres de baja potencia (111).

14.- EQUIPO DE MEDICIÓN DE TEMPERATURA, según cualquiera de las reivindicaciones 11 a 13, caracterizado porque la conexión (108) al ordenador (107) es por cable.

15.- EQUIPO DE MEDICIÓN DE TEMPERATURA, según cualquiera de las reivindicaciones 11 a 13, caracterizado porque la conexión (108) al ordenador (107) es inalámbrica.

16.- EQUIPO DE MEDICIÓN DE TEMPERATURA, según cualquiera de las reivindicaciones 11 a 15, caracterizado porque el habitáculo móvil (100) comprende una plataforma elevada (118) que evite el contacto directo del sujeto con el suelo.

17.- EQUIPO DE MEDICIÓN DE TEMPERATURA, según cualquiera de las reivindicaciones 11 a 15, caracterizado porque los elementos fijables a la piel de un sujeto, aplicables como puntos de referencia (110) y/o marcadores (115), están compuestos por material con alta reflexión.

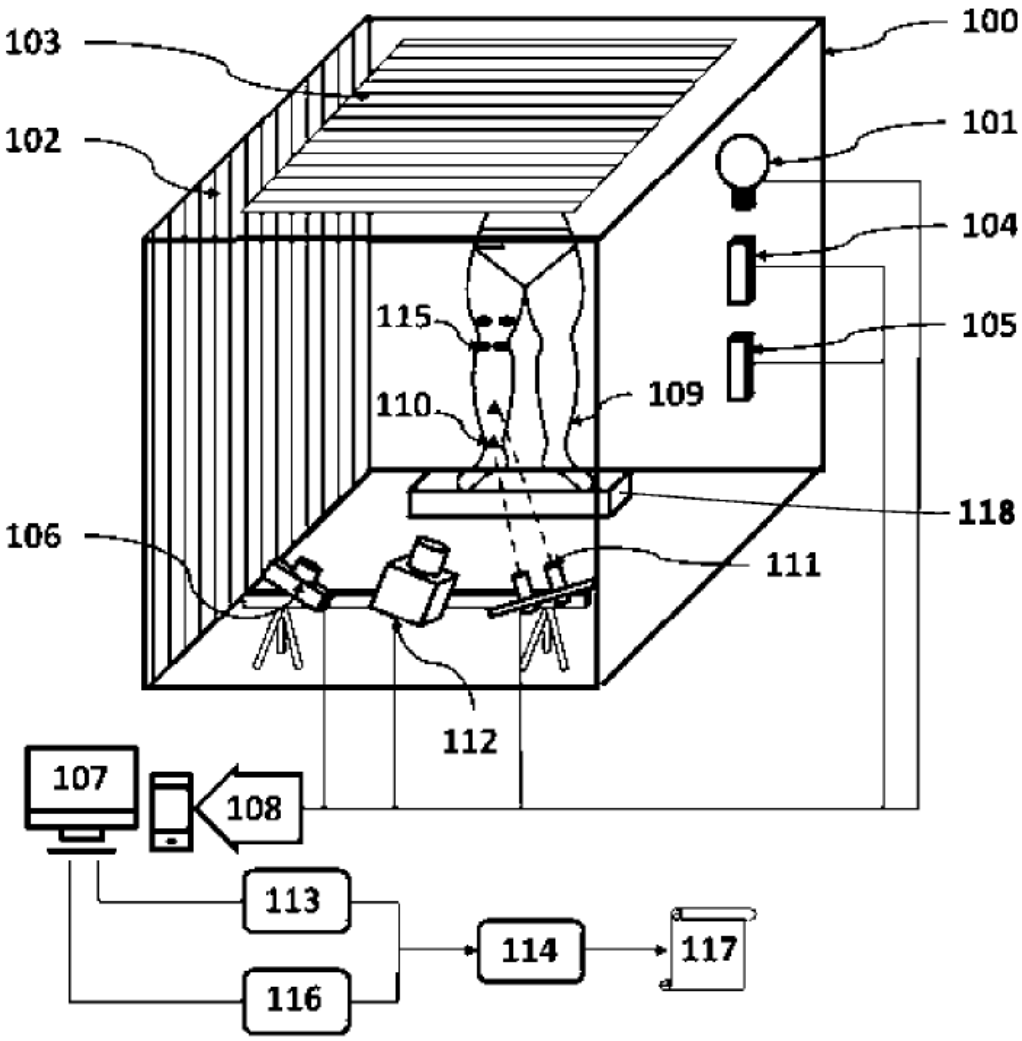

Fig. I

4.4. RESUMEN

MÉTODO DE MEDICIÓN DE TEMPERATURA, que comprende la superposición de imágenes (116) termográficas que contienen cajas de áreas de interés específicas, seleccionadas y delimitadas por el evaluador con marcadores

fijados en la piel (115) del sujeto, sobre imágenes termográficas sin manipular (113) del sujeto en la misma posición y tomadas sin influir sobre la temperatura de la piel, y un procesado de dichas imágenes (116, 113) en un programa informático (114) de ordenador (107). El equipo para llevarlo a cabo comprende un habitáculo móvil (100) con paredes (102) de alta emisividad material transpirable (103), luz (101) de baja emisión térmica, sensores de temperatura (104) y humedad relativa (105), cámara de vídeo (106), láseres de baja potencia (111) y cámara termográfica (112), todo con conexión (108) a un ordenador (107) con el programa informático (114).

ESTUDIO II:

FIABILIDAD DE UN NUEVO MÉTODO SEMIAUTOMÁTICO DE ANÁLISIS DE IMAGEN PARA EVALUAR LA SEÑAL DOPPLER Y LA RESISTENCIA VASCULAR INTRATENDÓN EN TENDINOPATÍA ROTULIANA

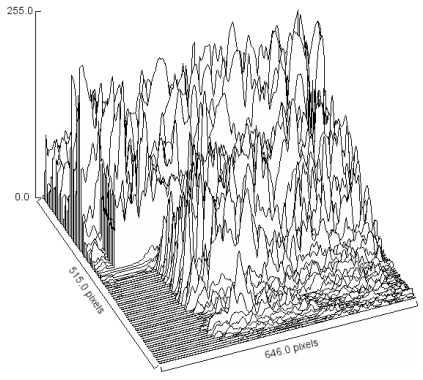

V. ESTUDIO II: FIABILIDAD DE UN NUEVO MÉTODO SEMIAUTOMÁTICO DE ANÁLISIS DE IMAGEN PARA EVALUAR LA SEÑAL DOPPLER Y LA RESISTENCIA VASCULAR INTRATENDÓN EN TENDINOPATÍA ROTULIANA

ARTICLE IN PRESS

ELSEVIER

Ultrasound in Med. & Biol., Vol. 00, No. 00, pp. 1–10, 2021

0301-5629/$ - see front matter

https://doi.org/10.1016/j.ultrasmedbio.2021.08.010

● *Original Contribution*

RELIABILITY OF A NEW SEMI-AUTOMATIC IMAGE ANALYSIS METHOD FOR EVALUATING THE DOPPLER SIGNAL AND INTRATENDINOUS VASCULAR RESISTANCE IN PATELLAR TENDINOPATHY

FRANCISCO J. MOLINA-PAYÁ,* JOSÉ RÍOS-DÍAZ,†
FRANCISCO CARRASCO-MARTÍNEZ,‡ and JACINTO J. MARTÍNEZ-PAYÁ§
* Doctoral Program in Health Sciences, Universidad Católica de Murcia, Murcia, Spain; † Fundación San Juan de Dios. Centro de Ciencias de la Salud San Rafael, Universidad Nebrija, Madrid, Spain; ‡ Private Practice, Clínica de fisioterapia F&C, Huelma, Spain; and § Physiotherapy Department, Facultad de Medicina, Universidad de Murcia, Murcia, Spain

(*Received* 12 *February* 2021; *revised* 9 *August* 2021; *in final form* 14 *August* 2021)

5.1. INTRODUCTION

The use of Doppler ultrasound is considered to be especially interesting in the evaluation of tendinopathies (de Vos et al. 2007; De Jonge et al. 2014) because it enables areas with increased blood flow to be observed, and even quantified (Roth et al. 2019; Vlist et al. 2020). Power Doppler facilitates visualisation of low velocity blood flow in very small vessels, representing an effective imaging modality to evaluate intratendinous vascularization (de Vos et al. 2007; Quack et al. 2020).

It is widely accepted that the presence of an intratendinous Doppler signal (DS) can be considered a sign of abnormality in the tendon (Alfredson y Ohberg

2005; Richards et al. 2005), while the absence of such a signal is a sign of healthy tendons (Ohberg et al. 2001; Alfredson et al. 2003). However, these findings contrast with those of other studies that suggest that intratendinous flow is not always a sign of a pathological disorder, but rather a part of an adaptive response to a normal physiological load (Malliaras et al. 2008; Boesen et al. 2012; Tol et al. 2012). Such variability can lead to the study of intratendinous vascularization to be unreliable.

In any case, to quantify a DS, semi-quantitative procedures are frequently used, based mainly on counting scales for grading the degree of DS presence (Vlist et al. 2020; Simon et al. 2021), these procedures have limited usefulness because only qualitative data can be obtained. By contrast, quantitative procedures involve mainly color pixel measurements (Terslev et al. 2003b; Koenig et al. 2007b; Boesen et al. 2012), vessel length (Cook et al. 2005) or, in the case of the resistance index (RI), on automatic ultrasound measurements (Koenig et al. 2007b; Albrecht et al. 2008; Karzis et al. 2017). In addition, the procedures permit the measurement of vascular resistance (VR), which could be useful in assessing the state of the tissue.

In this way it is possible to express numerically tissue resistance to the flow originated by the microvascular bed distal to the measurement site by reference to the RI (Pourcelot y Société parisienne d'expansion chimique 1982) defined as [peak systolic flow - end diastolic flow] / peak systolic velocity. A low RI is associated with low peripheral resistance and high perfusion of the distal bed and, therefore, with an inflammation situation (Terslev et al. 2003b; Bjordal et al. 2006; Koenig et al. 2007a; Torp-Pedersen et al. 2008; Terabayashi et al. 2014). The measurement of RI in intratendinous vessels is complicated because the DS that appear can be very small and numerous, making it difficult or impossible to use the traditional measurement methodology (Terslev et al. 2003a; Koenig et al. 2007a, 2007b).

Therefore, in the present study, our objective was to study the intra e inter-rater reliability of a new semi-automatic image analysis method for the quantification of the shape of the DS and the intratendinous VR, obtained from pixel intensities (Delorme et al. 1995), that allows quantification on regions of interest (ROI) with numerous and small DS.

5.2. MATERIALS AND METHODS

5.2.1. Study design and participants

A total of 30 athletes (8 women and 22 men) with patellar intratendinous vascularity were included in this cross-sectional observational study (42 tendons analyzed). Age ranged between 18 and 50 years (mean = 27.4 y, standard deviation [SD] = 8.57 y), and the participants were voluntarily recruited from a private physical therapy center (Clínica F&C Fisioterapia Avanzada y Neuro-Rehabilitación, Huelma, Spain) in July and August 2018. All participants were informed of the study's aims and signed an informed consent. The study was approved by the ethics committee of the Catholic University of Murcia, Murcia, Spain (CE111803).

5.2.2. Power Doppler parameters and scan method

The examination was performed with a Telemed SmartUS ultrasound system (Vilnius, Lithuania) and a 7-15 MHz linear probe (L15-7L40H-5). The intratendinous blood flow was assessed by Power Doppler set at a Doppler frequency of 6.7 MHz and a pulse repetition frequency of 0.7 kHz. The lowest wall filter and gain standardized to just below the level that produced random noise was applied. The adjustment parameters were the same for all patients, and pressure on the tendon from the probe was minimized to prevent vessel compression by placing the transducer on the skin without pressure.

The patient was positioned in a supine position with the knees extended to avoid occlusion of the vessels caused by the tension of the fibers of the patellar tendon (Koenig et al. 2007b); both knees were evaluated. The patellar tendon was scanned in power Doppler mode in the longitudinal plane at the location of maximum intratendinous Doppler activity, and a 4-s video was recorded for further analysis. All scans were performed by the same ultrasonographer with more than 20 y of experience in musculoskeletal ultrasonography.

5.2.3. Quantification of intratendinous DS shapes

Processing and analysis of the videos and images was carried out using ImageJ software (Version 1.50b, National Institutes of Health, Bethesda, MD, USA). After scaling the image, two observers manually selected and extracted the ROIs on the images with the highest and lowest signal corresponding to the systolic peak and the end of diastole for each patient. The image data were coded, anonymized and randomized thereafter to avoid possible bias or recall effects.

The observers, who were blinded to the patient's data, analysed the set of the images at two different times with at least a 15 days delay.

Because the DS appears in color on a gray-scale background, it is easy to segment and isolate the region for quantification. We used the color threshold plugin, which allows the cutoff point to be adjusted manually with slider bars.

To quantify the DS, the saved frame with the highest DS from each video was selected and the area of colour pixels was calculated. In addition, the number of signals, pixel intensity, area, perimeter, major diameter, minor diameter, circularity, and solidity were automatically calculated on the frames with the highest DS of each recording **(Fig. 1)**. Circularity and solidity are dimensionless parameters included in the so-called shape descriptors that evaluate the shape of a contour. When circularity is about 1, the contour is like a circle and when is about 0 is like a line. The solidity is a ratio that indicates the relation between the area of the shape and the convex area (theorical maximum =1).

5.2.4. Quantification of intratendinous VR

The flow pattern was evaluated by calculating the mean pixel color of the DS for each image. The pixel color mean of the image with the highest signal was considered the maximum systolic velocity, and that with the lowest signal, as the final diastolic velocity. These data were transferred to the RI formula, giving a value associated with the intratendinous VR **(Fig. 1)**.

In the images in which a DS was not detected, or did not present an intratendinous DS in diastole, the VR was considered 1, which represents normality in the musculoskeletal tissue (Terslev et al. 2003c; Koenig et al. 2007a).

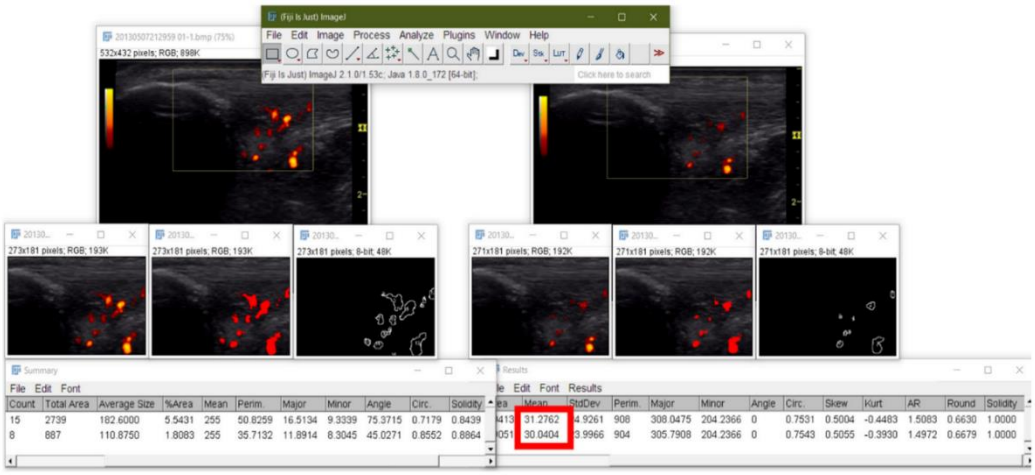

Fig. 1. Quantification of intratendinous Doppler signals and color pixel quantization. Left frame: Peak systolic flow. Right frame Diastolic flow. The analysis method reveals the number of Doppler signals and their morphology. The intensity of signals allows the VR to be obtained.

5.2.5. Statistical analysis

As the sample size allowed a normal distribution to be assumed, parametric tests were applied for all the variables, and the descriptive statistics used to summarize the data for each of the evaluators were mean, standard deviation, range and quartiles. The analyses were conducted for the number of DS, intensity of colour, total area (mm2) of active vessels, total perimeter (mm) of active vessels, major diameter, minor diameter, circularity (index between 0 and 1), solidity and VR.

The intraclass correlation coefficient (ICC) was calculated based on a total agreement and two-factor random-effects model (ICC2,1) for each of the variables of interest (McGraw y Wong 1996; Weir 2005). This coefficient offers values of between 0 and 1, where 0 would be a lack of agreement and 1 would be total agreement. Although the interpretation of these cut-off points is, to a certain extent, arbitrary, in our context an ICC above 0.90 was considered excellent, between 0.90

and 0.75 as good, between 0.75 and 0.50 as moderate and below 0.50 as poor (Portney y Watkins 2009).

Measurement precision (Atkinson y Nevill 1998; Lexell y Downham 2005) was evaluated using the standard error of measurement (SEm) [SEm=SD•√(1 ICC)] and its relative value with respect to the average of all measurements and the smallest real difference (SRD). SRD is useful for determining whether a change in the parameter is due to a real change or lies within the limits of error of the measuring method [SRD=1.96•SEm•√2] (Schuck y Zwingmann 2003).

The limits of agreement (LOA) were calculated according to the method described by Bland and Altman (Bland y Altman 1986; Hopkins 2000) and the presence of summative or multiplicative biases with Passing-Bablock's linear regression method (Passing y Bablok 1983; Bablok et al. 1988). For a direct clinical interpretation, the graphical method proposed by Luiz et al. (Luiz et al. 2003), based on the Kaplan-Meier estimate representing the probability of survival as a function of the degree of disagreement, was applied.

The analyses were conducted using IBM SPSS Statistics 19.0 (SPSS Inc. IBM Company, 2010) and the jmv package (version 0.9) for R (version 3.5.0; 2018).

5.3. RESULTS

5.3.1. Patient characteristics

Thirty participants aged between 18 and 50 y (mean = 27.4 y, SD = 8.57 y) took part in the study. All of them presented with intratendinous vascularity: 22 (73%) symptomatic and 8 (27%) asymptomatic. Twelve participants presented with bilateral and 18 with unilateral intratendinous vascularization, meaning that a total of 42 tendons were analyzed. In addition, each image was analyzed at maximum systolic speed and minimum diastolic speed so that finally all the parameters were calculated by both observers for a total of 84 images **(Table 1)**.

Table 1. Baseline characteristics (n=30).

Variable (n=30)	Mean (SD)	Min	Q1	Median	Q3	Max
Age	27.4 (8.57)	18	21	23	35.5	50
Time.Evol	21 (26.34)	0	0	12	36	120
VisaP	75.2 (22.18)	29	56.75	75.5	100	100
Tendinopathy; n(%)	22 (73%) Yes					
Side lession; n(%)	12 (40%) Right	10 (33%) Left				
Sex; n(%)	22 (73%) Male	8 (27%) Female				
Sport practice; n (%)	22 (73%) Yes	8 (27%) No				

SD = standard deviation. VisaP = Victorian Institute of Sport Assessment—Patella.

5.3.2. Reliability

Overall, both intra- and inter-rater reliability was very good, and no additive or multiplicative biases were detected **(Supplementary Figs. S1 and S2)**.

More specifically, the intra-rater ICC was maximum for area (ICC = 0.999; 95% confidence interval [CI]: 0.998-0.999) and minimum for solidity (ICC = 0.782, 95% CI: 0.682-0.853). The mean of differences (MoD) and 5% limits of agreement (95% LoA) **(Table 2 and Fig. 2)** were very low with respect to the magnitude of the measurement (at least one order), and the relatively SRDs were below 5.3%, and the relative SEM (%), below 2% (for VR). Supplementary Figure S3 contains the plot obtained with the Kaplan-Meier method. Although it cannot be taken as an indicator of reproducibility, no differences were found in t-tests for mean differences.

The agreement was also very good for inter-rater reliability, although, as expected, slightly lower than that for intra-rater reliability **(Table 3 and Fig. 3)**. Similarly, the maximum ICC was for area (ICC = 0.993; 95% CI: 0.989-0.996) and the minimum for circularity (ICC = 0.73, 95% CI: 0.611-0.817). The MoD and 95% LoA remained at least one order below the measurement, with a relative SEM (%) below of 2.2% and a relative SRD (%) below of 6% in the number of signals. **Supplementary Figures S3 and S4** are a practical interpretation of the magnitude of the differences.

Table 2. Intra-rater reproducibility and reliability.

Parameter (n=84)	Mean (SD) 1	Mean (SD) 2	t-value	p-value	Effect	MoD (LoA)	ICC (95%CI)	SEM	SEM%	SRD	SRD%
Number of signals	3.17 (2.281)	3.01 (2.209)	1.78	0.080	0.19	0.16 (-0.02 a 0.33)	0.935 (0.901-0.958)	0.028	0.90%	0.08	2.50%
Pixel intensity (0-255)	18.98 (5.449)	18.71 (5.806)	1.20	0.235	0.13	0.28 (-0.19 a 0.74)	0.928 (0.891-0.952)	0.053	0.28%	0.15	0.78%
Area (mm2)	2.05 (2.041)	2.04 (2.043)	1.71	0.090	0.19	0.02 (0 a 0.04)	0.999 (0.998-0.999)	0.000	0.02%	0.00	0.05%
Perimeter (mm)	3.04 (1.986)	3.09 (2.165)	-0.61	0.542	0.07	-0.05 (-0.21 a 0.11)	0.937 (0.904-0.958)	0.009	0.29%	0.02	0.80%
Major diameter (mm)	0.918 (0.8263)	0.916 (0.8524)	0.06	0.954	0.01	0 (-0.05 a 0.05)	0.966 (0.948-0.978)	0.000	0.02%	0.00	0.06%
Minor diameter (mm)	0.35 (0.2821)	0.354 (0.2892)	-0.48	0.633	0.05	0 (-0.02 a 0.01)	0.963 (0.944-0.976)	0.001	0.16%	0.00	0.44%
Circulatiry (0-1)	0.678 (0.2154)	0.665 (0.2393)	0.81	0.419	0.09	0.01 (-0.02 a 0.04)	0.803 (0.712-0.867)	0.004	0.59%	0.01	1.65%
Solidity (0-1)	0.836 (0.2154)	0.808 (0.2493)	1.64	0.105	0.18	0.03 (-0.01 a 0.06)	0.782 (0.682-0.853)	0.009	1.10%	0.03	3.04%
Vascular resistance (n=42)	0.198 (0.3362)	0.218 (0.3582)	-0.95	0.350	0.15	-0.02 (-0.06 a 0.02)	0.921 (0.859-0.957)	0.004	1.92%	0.01	5.31%

SD= standard deviation; MoD (95% LoA) = mean of differences (95% Limits of agreement); ICC (95% CI) = intraclass correlation coefficient (95% Confidence Interval); SEM = standard error of mean; SRD = smallest real difference.

Table 3. Inter-rater reproducibility and reliability.

Parameter (n=84)	Mean (SD) 1	Mean (SD) 2	t-value	p-value	Effect	MoD (LoA)	ICC (95%CI)	SEM	SEM%	SRD	SRD%
Number of signals	3.17 (2.281)	2.9 (2.408)	2.05	0.044	0.22	0.26 (0.01 a 0.52)	0.871 (0.806-0.915)	0.067	2.19%	0.18	6.08%
Pixel intensity (0-255)	18.98 (5.449)	18.69 (5.799)	1.27	0.208	0.14	0.02 (-0.08 a 0.11)	0.927 (0.889-0.952)	0.057	0.30%	0.16	0.84%
Area (mm^2)	2.05 (2.041)	1.99 (2.056)	2.81	0.006	0.31	0.05 (0 a 0.1)	0.993 (0.989-0.996)	0.004	0.20%	0.01	0.54%
Perimeter (mm)	3.04 (1.986)	3.22 (2.203)	-1.50	0.138	0.16	-0.14 (-0.39 a 0.11)	0.85 (0.777-0.9)	0.051	1.64%	0.14	4.54%
Major diameter (mm)	0.918 (0.8263)	0.97 (0.9077)	-1.32	0.190	0.14	-0.05 (-0.13 a 0.03)	0.912 (0.868-0.942)	0.011	1.16%	0.03	3.21%
Minor diameter (mm)	0.35 (0.2821)	0.362 (0.2898)	-0.81	0.422	0.09	-0.01 (-0.04 a 0.02)	0.895 (0.843-0.931)	0.003	0.74%	0.01	2.06%
Circularity (0-1)	0.678 (0.2154)	0.642 (0.2454)	1.97	0.053	0.21	0.04 (0 a 0.07)	0.73 (0.611-0.817)	0.013	2.00%	0.04	5.55%
Solidity (0-1)	0.836 (0.2154)	0.803 (0.2491)	1.91	0.060	0.21	0.03 (0 a 0.07)	0.772 (0.667-0.846)	0.011	1.34%	0.03	3.70%
Vascular resistance (n=42)	0.198 (0.3362)	0.217 (0.3593)	-0.88	0.386	0.14	-0.02 (-0.06 a 0.02)	0.921 (0.859-0.957)	0.004	1.78%	0.01	4.95%

SD= standard deviation; MoD (95% LoA) = mean of differences (95% Limits of agreement); ICC (95% CI) = intraclass correlation coefficient (95% Confidence Interval); SEM = standard error of mean; SRD = smallest real difference.

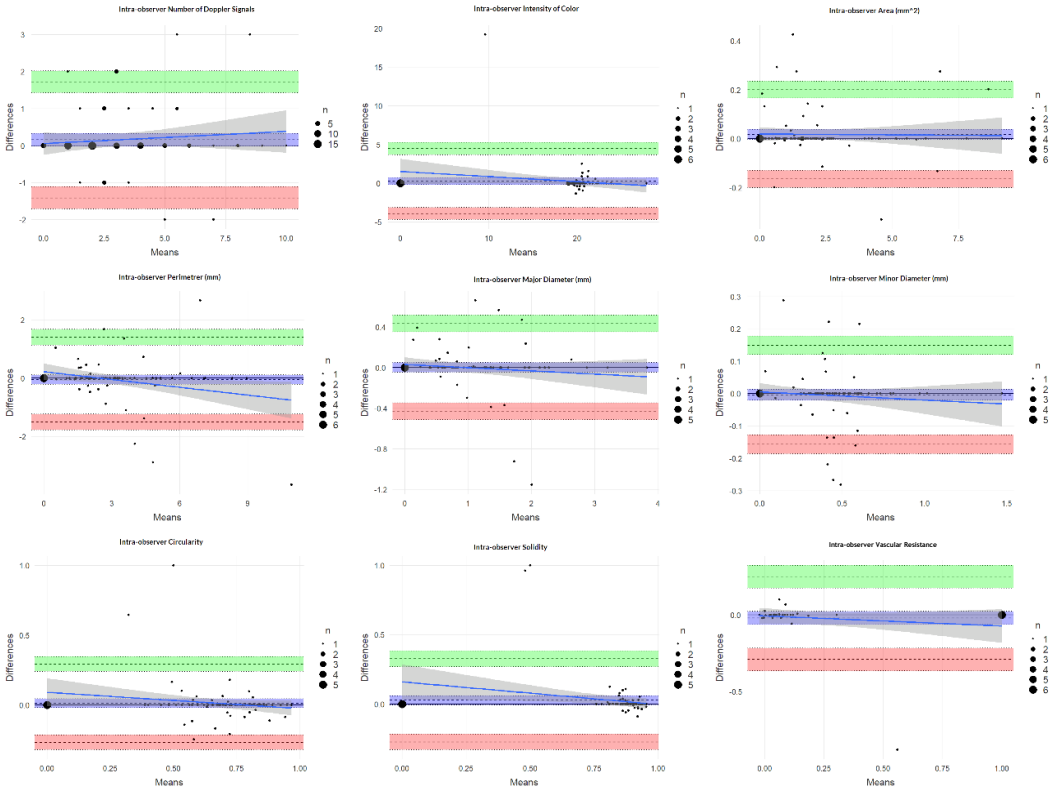

Figure 2. Bland-Altman plots of intra-observer (A1-A2) agreement. In order are the number of signals, pixel intensity mean, area, perimeter, major and minor diameter, circularity, solidity and vascular resistance.

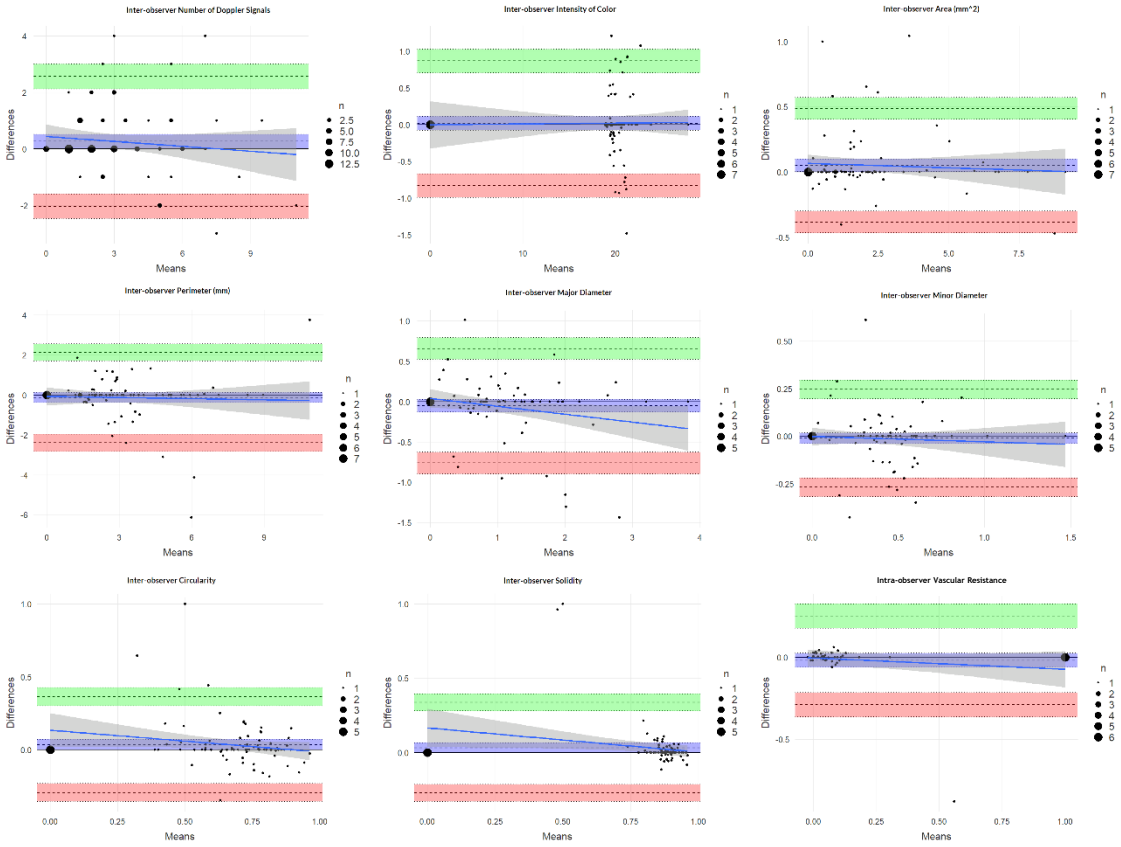

Figure 3. Bland-Altman plots of inter-observer (A1-A2) agreement. In order are the number of signals, pixel intensity mean, area, perimeter, major and minor diameter, circularity, solidity and vascular resistance.

5.4. DISCUSSION

Our results revealed very good intra- and interobserver reliability both for measurements of the DS and for the calculation of intra-tendon VR. These good results are probably owing to the semi-automatic nature of the measurement procedure, in which the dependence of the operator is involved only in selection of the location of the intratendinous ROI, in adjustment of the parameters of the computer program for the selection of the signal Doppler and in detection of images with higher and lower Doppler signal.

In comparing our results with those of other studies, we can only focus on the quantification of the DS area because VR can only be quantified using the RI. This is because the quantification methods that have been used were based mainly on the number of colored pixels (Strunk et al. 2007; Ellegaard et al. 2008) or on semi-quantitative scales corresponding to the count of the number of DS (D'agostino et al. 2009; Sunding et al. 2016; Risch et al. 2018), while RI measurements are made automatically through the ultrasound scanner (Qvistgaard et al. 2001; Terslev et al. 2003b; Albrecht et al. 2008).

The intra-rater and inter-rater reliability results for the remaining morphological and pixel intensity variables of the DS studied here were good, although we have not found studies that have examined the reliability of these variables, making it impossible to compare results.

In patients with rheumatoid arthritis (Qvistgaard et al. 2001), the area of the DS in the synovium has been quantified to determine the degree of joint inflammation of the fingers, the methodology used having excellent intra-rater (ICC = 0.82-0.97, $p < 0.0001$) and good inter-rater (ICC = 0.81, $p < 0.0001$) reliability. In the study of tumor vascularization in patients with gestational trophoblastic neoplasia, intra-rater reliability was also excellent (ICC = 0.94) (ICC = 0.94) (Li et al. 2018). These good results coincide with our study, in which quantification of the area revealed excellent agreement for intrarater and inter-rater reliability. Such good results are possible because it is a semi-automatic procedure whereby the influence of the operator is minimal.

Counting of the intratendinous DS by the investigator is essential for the different evaluation scales of the DS to be applied. Its use in the presence of abnormalities in the quadriceps tendon, patellar and Achilles tendons and plantar fascia (Bandinelli et al. 2011) led to excellent results for intra-rater (ICC = 0.97, 95% CI: 0.90-1) and inter-rater (ICC = 0.95; 95% CI: 0.89-1) reliability, using the classification of D´Agostino et al. (2009) (D'agostino et al. 2009). Poltawski et al. (2012) evaluated reliability to quantify hyperemia in the common extensor tendon in tennis elbow (Poltawski et al. 2012). To evaluate the DS, they used a PD scale that assigned five grades based on a subjective estimation of the extent of visible blood vessels. Inter-rater reliability was good (ICC = 0.89, 95% CI: 0.79-0.95) for DS graduation. Sunding et al. (2016) analyzed the intra and inter-rater reliability of

evaluating Achilles and patellar tendon neovascularization by means of color Doppler using a modified Ohberg score (Sunding et al. 2016). The intra-rater reliability results were good for neovascularization measured with this qualitative scale in the patellar tendon (k coefficient = 0.79-0.86) and the Achilles tendon (k coefficient = 0.64-0.78). However, the inter-rater reliability results were moderate for neovascularization in the patellar tendon (k coefficient = 0.45-0.76) and the Achilles tendon (k coefficient = 0.59-0.87).

Although in our method the intratendinous ROI must be selected manually to determine the number of DS, this is more sensitive than a visual inspection for detecting the signals, and both intra-rater and inter-rater reliability scores are good and clearly better than what can be achieved using qualitative methods. Qualitative methodology seems sensitive to slight changes in the number of vessels when complex vascularization is scored (Risch et al. 2018). However, this scoring procedure allows easy, immediate and absolute quantification of the intratendinous vessels and, therefore, may be suitable for application in clinical practice.

Another method to quantify the vascularization of the patellar tendon is that proposed by Cook et al. (2005) using colour Doppler and measuring the length of the vessels (Cook et al. 2005). The test-retest reliability of the measured vessel length was excellent (ICC = 0.94; 95% CI: 0.88-0.97), with good raters (ICC = 0.84, 95% CI: 0.51-0.94). However, unlike our quantification system, this classification system does not provide information on vascular diameter, and it remains debatable whether evaluation of the total vessel length is relevant to clinical practice (Cook et al. 2005; Risch et al. 2016).

In the few studies that have measured intratendinous VR, the most commonly used methods are based on the automatic measurement of RI using the pulsed Doppler mode, either as an average of three vessels (Koenig et al. 2007a, 2007b) or for a single vessel (Karzis et al. 2017). We have found no studies that have tested the reliability of intratendinous RI measurements, probably because many author believe it does not depend on the experience of the researcher, but on the ultrasound machine itself (Terslev et al. 2003b). However, the reliability of RI measurements has been tested in other tissues by measuring the RI of a single vessel. Albrecht et al. (2008) evaluated the inter-rater reliability of RI (ICC = 0.60) in

hand and wrist arthritis during anti-inflammatory treatment (Albrecht et al. 2008). Strunk et al. (2007) conducted a similar study, evaluating only the wrist; they found a weak correlation between observers (Pearson's r = 0.53) (Strunk et al. 2007).

The test-retest reliability of assessments of clitoral blood flow in healthy women using color Doppler in a pelvic floor muscle contraction task had moderate to good intra-rater reliability for the RI at rest (ICC = 0.67, 95% CI: 0.08-0.88, p = 0.018) and excellent reliability after a pelvic floor muscle contraction task (ICC = 0.81, 95% CI: 0.51-0.92, p < 0.001) (Mercier et al. 2018). These RI reliability results are poorer than the intratendon VR measurements used in our study (ICC = 0.921, 95% CI = 0.859-0.957), which may be due not only to the operator or the technical equipment, both of which influence the acquisition and interpretation of the images (Albrecht et al. 2007; Patil y Dasgupta 2012), but also to the difficult localization of the same intra-articular blood vessel (which can be very small) during the examinations, whereas our study used the mean of all SDs found in the ROI.

In the studies analyzed, the reliability results for the RI are worse than those obtained for quantification of the area of DS, perhaps because the results shown for the RI include those obtained during the exploration process of each researcher, and also because the RI is a relationship that depends on several measurements at different times. Intuitively, parameters that depend on several measurements are more likely to have lower reliability, compounded by the imperfect reliability of the individual measurements included in their equations (Mercier et al. 2018). This difference contrasts with our results, in which the VR had excellent intra and inter-rater reliability, and coincides with the results of most of the Doppler area quantification variables, probably because of the semi-automatic nature of the quantification procedure in both cases.

The main limitation of this study is that, although the reliability of the method is good, the analysis must be performed offline the ultrasound device and requires extra time for video export, image extraction and image analysis; therefore, its clinical application is not immediate. However, it can be considered a valid method for use in the investigation and quantification of tendon vascularization in this context.

The other limitation is related to the determination of RI, which, although it could be obtained from spectral analysis, in this study we calculated it indirectly

from the pixel intensity in systole and diastole. The advantage of this approach is that the intensity values are obtained using the same procedure used for other morphological parameters, thus saving time. However, it would be interesting in a future study to test the correlation between the RI obtained in this way and that obtained by spectral analysis.

In future studies, it would also be interesting to analyze the color Doppler mode, which is currently gaining momentum for evaluation of intratendon vascularization because of the improved sensitivity of ultrasound scanners (Torp-Pedersen et al. 2015).

Furthermore, including an examination of patients could give results more typical of clinical practice. Finally, the shape variables of the DS and the VR could be correlated with the symptoms of the patient, and their prognostic and monitoring capacity could be analyzed.

This quantification methodology exhibits very good reliability and reproducibility and is capable of combining the quantification of the number of signals, the magnitude and the VR of the tissue, which would allow a more precise evaluation of the state of the tissue, the improved monitoring of changes over time and the establishment of a threshold between pathological and physiological blood flow.

5.5. CONCLUSIONS

The results obtained confirm that the proposed method has very good reliability and reproducibility, while any influence on the detected DS is negligible. In this sense, it will be of interest to extend the study to ascertain the reliability between different ultrasound scanners and software, which could increase the robustness of the method.

5.6. REFERENCES

1. Albrecht K, Grob K, Lange U, Müller-Ladner U, Strunk J. Reliability of different Doppler ultrasound quantification methods and devices in the assessment of therapeutic response in arthritis. Rheumatology (Oxford). octubre de 2008;47(10):1521-6.

2. Albrecht K, Müller-Ladner U, Strunk J. Quantification of the synovial perfusion in rheumatoid arthritis using Doppler ultrasonography. Clin Exp Rheumatol. agosto de 2007;25(4):630-8.
3. Alfredson H, Ohberg L. Sclerosing injections to areas of neo-vascularisation reduce pain in chronic Achilles tendinopathy: a double-blind randomised controlled trial. Knee Surg Sports Traumatol Arthrosc. mayo de 2005;13(4):338-44.
4. Alfredson H, Ohberg L, Forsgren S. Is vasculo-neural ingrowth the cause of pain in chronic Achilles tendinosis? An investigation using ultrasonography and colour Doppler, immunohistochemistry, and diagnostic injections. Knee Surg Sports Traumatol Arthrosc. septiembre de 2003;11(5):334-8.
5. Atkinson G, Nevill AM. Statistical methods for assessing measurement error (reliability) in variables relevant to sports medicine. Sports Med. octubre de 1998;26(4):217-38.
6. Bablok W, Passing H, Bender R, Schneider B. A general regression procedure for method transformation. Application of linear regression procedures for method comparison studies in clinical chemistry, Part III. J Clin Chem Clin Biochem. noviembre de 1988;26(11):783-90.
7. Bandinelli F, Milla M, Genise S, Giovannini L, Bagnoli S, Candelieri A, et al. Ultrasound discloses entheseal involvement in inactive and low active inflammatory bowel disease without clinical signs and symptoms of spondyloarthropathy. Rheumatology (Oxford). julio de 2011;50(7):1275-9.
8. Bjordal JM, Lopes-Martins RAB, Iversen VV. A randomised, placebo controlled trial of low level laser therapy for activated Achilles tendinitis with microdialysis measurement of peritendinous prostaglandin E2 concentrations. Br J Sports Med. enero de 2006;40(1):76-80.
9. Bland JM, Altman DG. Statistical methods for assessing agreement between two methods of clinical measurement. Lancet. 8 de febrero de 1986;1(8476):307-10.
10. Boesen AP, Boesen MI, Torp-Pedersen S, Christensen R, Boesen L, Hölmich P, et al. Associations between abnormal ultrasound color Doppler measures and tendon pain symptoms in badminton players during a season: a prospective cohort study. Am J Sports Med. marzo de 2012;40(3):548-55.

11. Cook JL, Ptazsnik R, Kiss ZS, Malliaras P, Morris ME, De Luca J. High reproducibility of patellar tendon vascularity assessed by colour Doppler ultrasonography: a reliable measurement tool for quantifying tendon pathology. Br J Sports Med. octubre de 2005;39(10):700-3.
12. D'agostino MA, Aegerter P, Jousse-Joulin S, Chary-Valckenaere I, Lecoq B, Gaudin P, et al. How to evaluate and improve the reliability of power Doppler ultrasonography for assessing enthesitis in spondylarthritis. Arthritis Rheum. 15 de enero de 2009;61(1):61-9.
13. De Jonge S, Warnaars JLF, De Vos RJ, Weir A, van Schie HTM, Bierma-Zeinstra SMA, et al. Relationship between neovascularization and clinical severity in Achilles tendinopathy in 556 paired measurements. Scand J Med Sci Sports. octubre de 2014;24(5):773-8.
14. Delorme S, Weisser G, Zuna I, Fein M, Lorenz A, van Kaick G. Quantitative characterization of color Doppler images: reproducibility, accuracy, and limitations. J Clin Ultrasound. diciembre de 1995;23(9):537-50.
15. Ellegaard K, Torp-Pedersen S, Lund H, Henriksen M, Terslev L, Jensen PS, et al. Quantification of colour Doppler activity in the wrist in patients with rheumatoid arthritis--the reliability of different methods for image selection and evaluation. Ultraschall Med. agosto de 2008;29(4):393-8.
16. Hopkins WG. Measures of Reliability in Sports Medicine and Science. Sports Med. 1 de julio de 2000;30(1):1-15.
17. Karzis K, Kalogeris M, Mandalidis D, Geladas N, Karteroliotis K, Athanasopoulos S. The effect of foot overpronation on Achilles tendon blood supply in healthy male subjects. Scand J Med Sci Sports. octubre de 2017;27(10):1114-21.
18. Koenig MJ, Torp-Pedersen S, Holmich P, Terslev L, Nielsen MB, Boesen M, et al. Ultrasound Doppler of the Achilles tendon before and after injection of an ultrasound contrast agent--findings in asymptomatic subjects. Ultraschall Med. febrero de 2007a;28(1):52-6.
19. Koenig MJ, Torp-Pedersen ST, Christensen R, Boesen MI, Terslev L, Hartkopp A, et al. Effect of knee position on ultrasound Doppler findings in patients with patellar tendon hyperaemia (jumper's knee). Ultraschall Med. octubre de 2007b;28(5):479-83.

20. Lexell JE, Downham DY. How to assess the reliability of measurements in rehabilitation. Am J Phys Med Rehabil. septiembre de 2005;84(9):719-23.
21. Li Y, Tang MX, Agarwal R, Patel D, Eckersley RJ, Barrois G, et al. Power Doppler Quantification in Assessing Gestational Trophoblastic Neoplasia. Ultraschall Med. abril de 2018;39(2):206-12.
22. Luiz RR, Costa AJL, Kale PL, Werneck GL. Assessment of agreement of a quantitative variable: a new graphical approach. J Clin Epidemiol. octubre de 2003;56(10):963-7.
23. Malliaras P, Richards PJ, Garau G, Maffulli N. Achilles tendon Doppler flow may be associated with mechanical loading among active athletes. Am J Sports Med. noviembre de 2008;36(11):2210-5.
24. McGraw KO, Wong SP. Forming inferences about some intraclass correlation coefficients. Psychological Methods. 1996;1(1):30-46.
25. Mercier J, Tang A, Morin M, Khalifé S, Lemieux M-C, Reichetzer B, et al. Test-retest reliability of clitoral blood flow measurements using color Doppler ultrasonography at rest and after a pelvic floor contraction task in healthy adult women. Neurourology and Urodynamics. septiembre de 2018;37(7):2249-56.
26. Ohberg L, Lorentzon R, Alfredson H. Neovascularisation in Achilles tendons with painful tendinosis but not in normal tendons: an ultrasonographic investigation. Knee Surg Sports Traumatol Arthrosc. julio de 2001;9(4):233-8.
27. Passing H, Bablok null. A new biometrical procedure for testing the equality of measurements from two different analytical methods. Application of linear regression procedures for method comparison studies in clinical chemistry, Part I. J Clin Chem Clin Biochem. noviembre de 1983;21(11):709-20.
28. Patil P, Dasgupta B. Role of diagnostic ultrasound in the assessment of musculoskeletal diseases. Ther Adv Musculoskelet Dis. octubre de 2012;4(5):341-55.
29. Poltawski L, Ali S, Jayaram V, Watson T. Reliability of sonographic assessment of tendinopathy in tennis elbow. Skeletal Radiol. enero de 2012;41(1):83-9.
30. Portney LG, Watkins MP. Foundations of Clinical Research: Applications to Practice. Pearson/Prentice Hall; 2009.

31. Pourcelot L, Société parisienne d'expansion chimique. Application de l'examen Doppler à l'étude de la circulation périphérique. Paris (16, rue Clisson, 75646, cedex 13): SPECIA; 1982.
32. Quack V, Betsch M, Hellmann J, Eschweiler J, Schrading S, Gatz M, et al. Evaluation of Postoperative Changes in Patellar and Quadriceps Tendons after Total Knee Arthroplasty-A Comprehensive Analysis by Shear Wave Elastography, Power Doppler and B-mode Ultrasound. Acad Radiol. junio de 2020;27(6):e148-57.
33. Qvistgaard E, Røgind H, Torp-Pedersen S, Terslev L, Danneskiold-Samsøe B, Bliddal H. Quantitative ultrasonography in rheumatoid arthritis: evaluation of inflammation by Doppler technique. Ann Rheum Dis. julio de 2001;60(7):690-3.
34. Richards PJ, Win T, Jones PW. The distribution of microvascular response in Achilles tendonopathy assessed by colour and power Doppler. Skeletal Radiol. junio de 2005;34(6):336-42.
35. Risch L, Cassel M, Messerschmidt J, Intziegianni K, Fröhlich K, Kopinski S, et al. Is Sonographic Assessment of Intratendinous Blood Flow in Achilles Tendinopathy Patients Reliable? Ultrasound Int Open. marzo de 2016;2(1):E13-8.
36. Risch L, Wochatz M, Messerschmidt J, Engel T, Mayer F, Cassel M. Reliability of Evaluating Achilles Tendon Vascularization Assessed With Doppler Ultrasound Advanced Dynamic Flow. J Ultrasound Med. marzo de 2018;37(3):737-44.
37. Roth J, Stinson SE, Chan J, Barrowman N, Di Geso L. Differential pattern of Doppler signals at lower-extremity entheses of healthy children. Pediatr Radiol. septiembre de 2019;49(10):1335-43.
38. Schuck P, Zwingmann C. The «smallest real difference» as a measure of sensitivity to change: a critical analysis. Int J Rehabil Res. junio de 2003;26(2):85-91.
39. Simon D, Kleyer A, Bayat S, Knitza J, Valor-Mendez L, Schweiger M, et al. Biomechanical stress in the context of competitive sports training triggers enthesitis. Arthritis Res Ther. 21 de junio de 2021;23(1):172.
40. Strunk J, Strube K, Rumbaur C, Lange U, Müller-Ladner U. Interobserver agreement in two- and three-dimensional power Doppler sonographic

assessment of synovial vascularity during anti-inflammatory treatment in patients with rheumatoid arthritis. Ultraschall Med. agosto de 2007;28(4):409-15.

41. Sunding K, Fahlström M, Werner S, Forssblad M, Willberg L. Evaluation of Achilles and patellar tendinopathy with greyscale ultrasound and colour Doppler: using a four-grade scale. Knee Surg Sports Traumatol Arthrosc. junio de 2016;24(6):1988-96.
42. Terabayashi N, Watanabe T, Matsumoto K, Takigami I, Ito Y, Fukuta M, et al. Increased blood flow in the anterior humeral circumflex artery correlates with night pain in patients with rotator cuff tear. Journal of Orthopaedic Science. septiembre de 2014;19(5):744-9.
43. Terslev L, Torp-Pedersen S, Qvistgaard E, Bliddal H. Spectral Doppler and resistive index. A promising tool in ultrasonographic evaluation of inflammation in rheumatoid arthritis. Acta Radiol. noviembre de 2003a;44(6):645-52.
44. Terslev L, Torp-Pedersen S, Qvistgaard E, Danneskiold-Samso... B, Bliddal H. Estimation of inflammation by Doppler ultrasound: quantitative changes after intra-articular treatment in rheumatoid arthritis. Ann Rheum Dis. noviembre de 2003b;62(11):1049-53.
45. Terslev L, Torp-Pedersen S, Qvistgaard E, Kristoffersen H, Røgind H, Danneskiold-Samsøe B, et al. Effects of treatment with etanercept (Enbrel, TNRF:Fc) on rheumatoid arthritis evaluated by Doppler ultrasonography. Ann Rheum Dis. febrero de 2003c;62(2):178-81.
46. Tol JL, Spiezia F, Maffulli N. Neovascularization in Achilles tendinopathy: have we been chasing a red herring? Knee Surg Sports Traumatol Arthrosc. octubre de 2012;20(10):1891-4.
47. Torp-Pedersen S, Christensen R, Szkudlarek M, Ellegaard K, D'Agostino MA, Iagnocco A, et al. Power and color Doppler ultrasound settings for inflammatory flow: impact on scoring of disease activity in patients with rheumatoid arthritis. Arthritis & Rheumatology (Hoboken, NJ). febrero de 2015;67(2):386-95.
48. Torp-Pedersen TE, Torp-Pedersen ST, Qvistgaard E, Bliddal H. Effect of glucocorticosteroid injections in tennis elbow verified on colour Doppler

ultrasonography: evidence of inflammation. Br J Sports Med. diciembre de 2008;42(12):978-82.

49. Vlist AC, Veen JM, Oosterom RF, Veldhoven PLJ, Verhaar JAN, Vos R. Ultrasound Doppler Flow in Patients With Chronic Midportion Achilles Tendinopathy: Is Surface Area Quantification a Reliable Method? J Ultrasound Med. abril de 2020;39(4):731-9.
50. de Vos R-J, Weir A, Cobben LPJ, Tol JL. The value of power Doppler ultrasonography in Achilles tendinopathy: a prospective study. Am J Sports Med. octubre de 2007;35(10):1696-701.
51. Weir JP. Quantifying test-retest reliability using the intraclass correlation coefficient and the SEM. J Strength Cond Res. febrero de 2005;19(1):231-40.

5.7. SUPPLEMENTARY MATERIALS

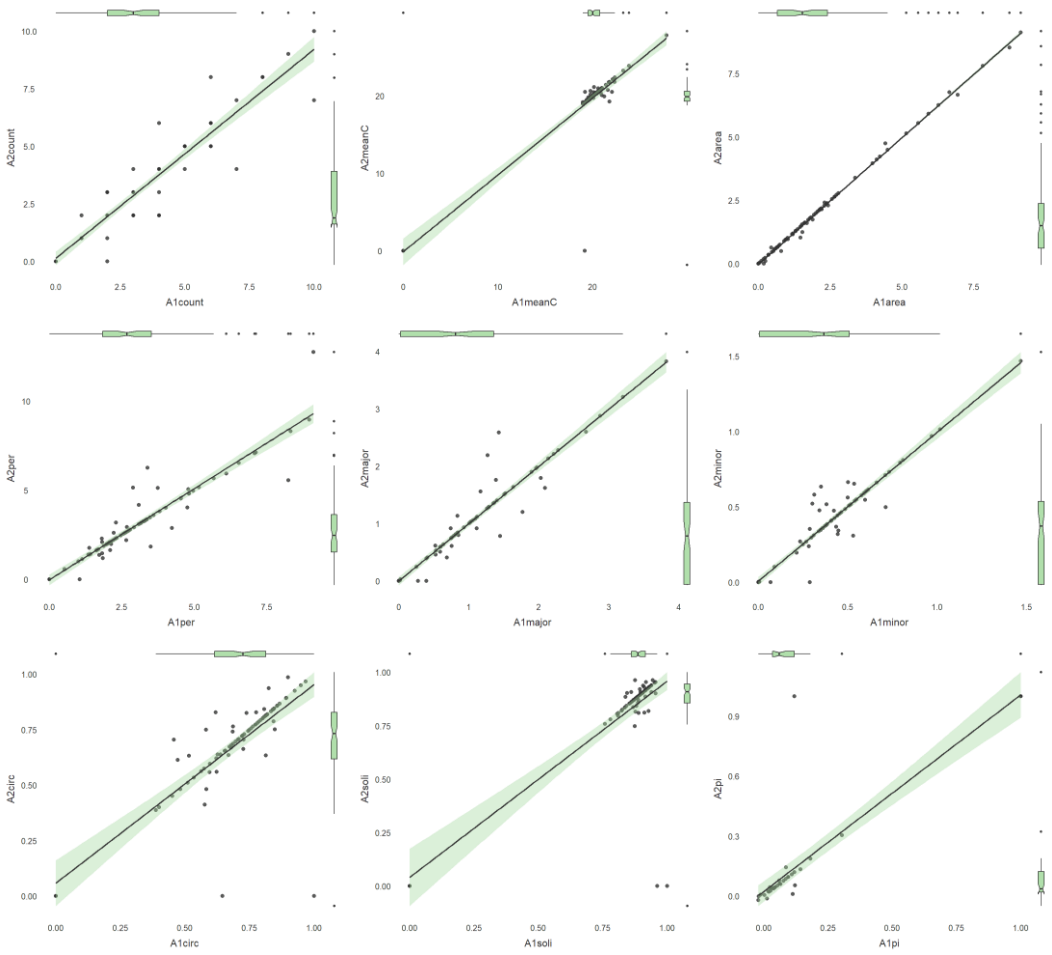

Figure 1 suppl. Scatterplots for the relation intra-rater (A1-A2) measurements. In order: Number of signals (count), pixel intensity mean (meanC), area, perimeter (per), major and minor diameter, circularity (circ), solidity (soli), and vascular resistance (pi).

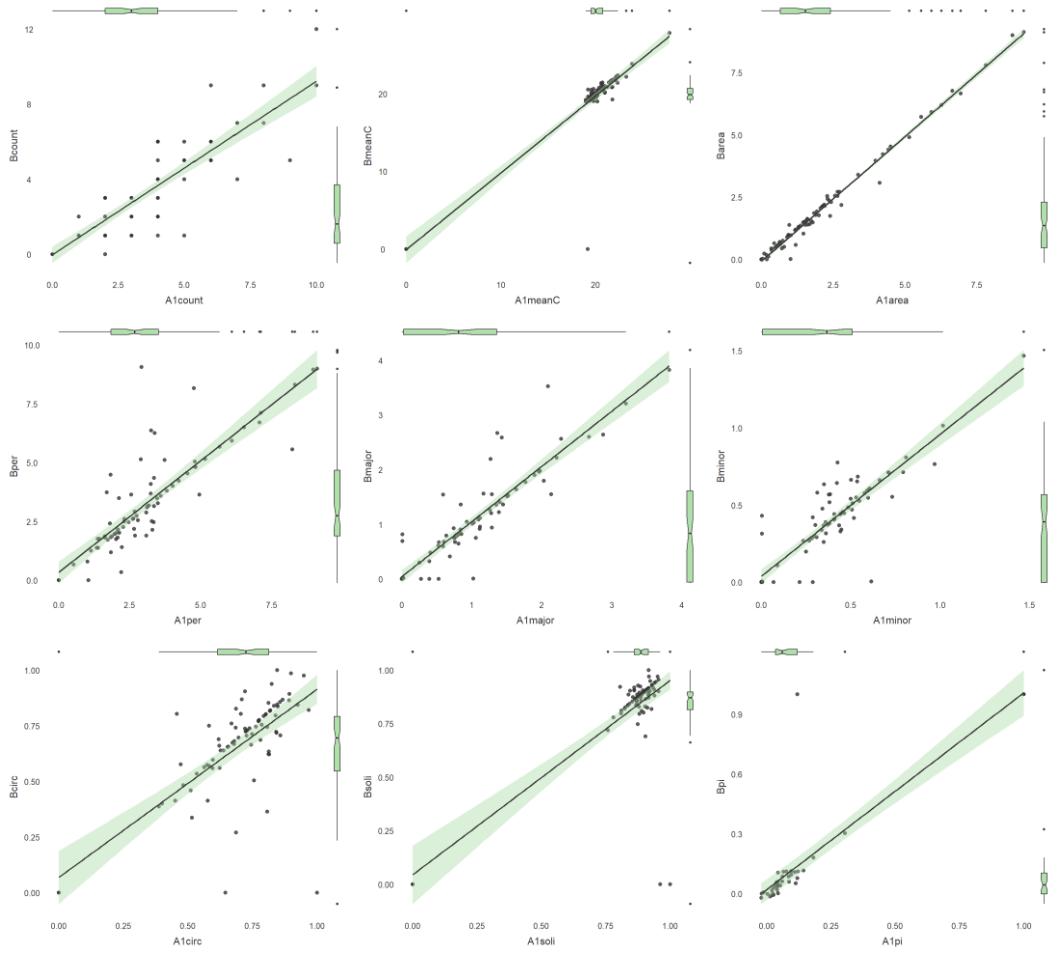

Figure 2 suppl. Scatterplots for the relation inter-rater (A1-B) measurements. In order: Number of signals (count), pixel intensity mean (meanC), area, perimeter (per), major and minor diameter, circularity (circ), solidity (soli), and vascular resistance (pi).

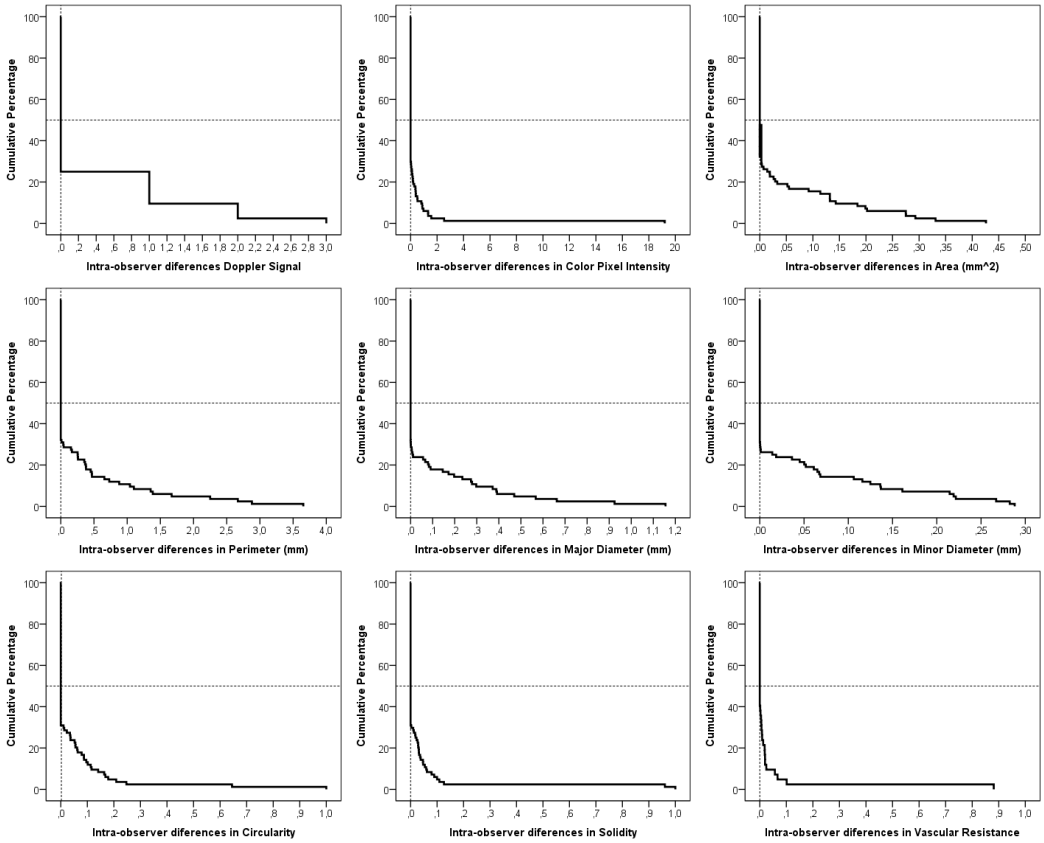

Figure 3 suppl. Intra-observer Kaplan-Meier estimate that represents the probability of survival as a function of the degree of disagreement. The dotted lines represent the minimum differences for 50% of the observations. In order: Number of signals, pixel intensity mean, area, perimeter, major and minor diameter, circularity, solidity, and vascular resistance.

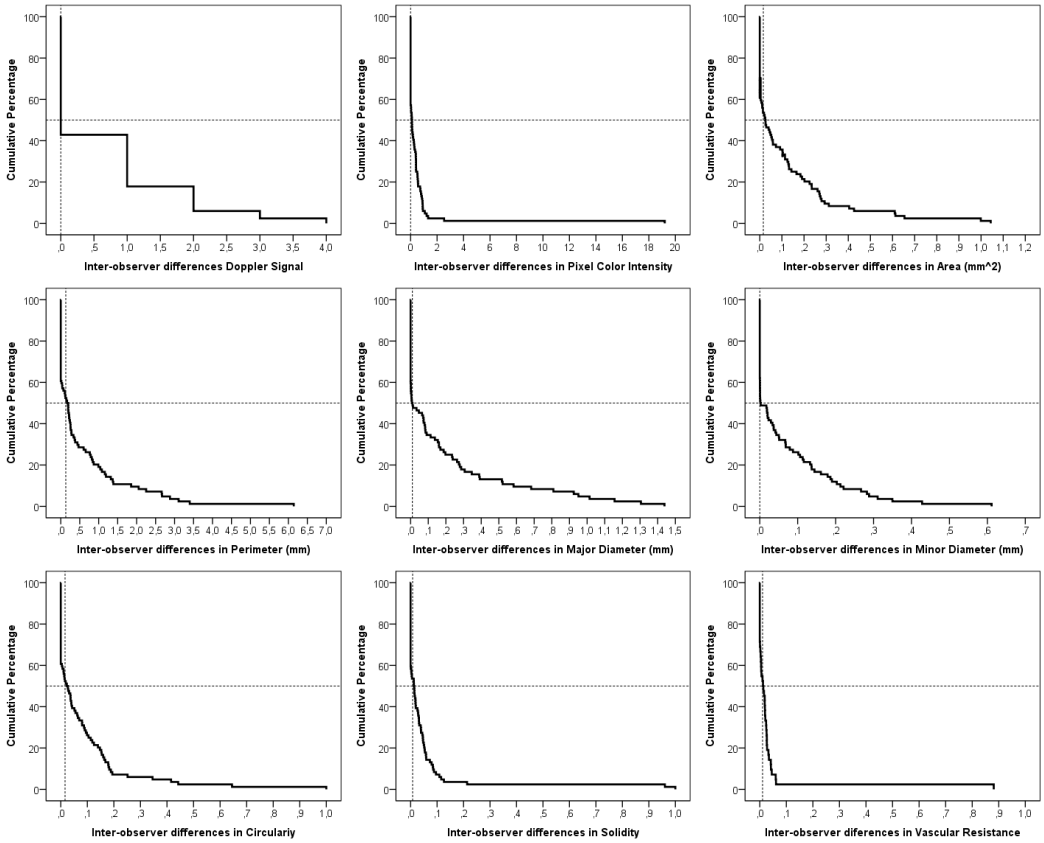

Figure 4 suppl. Inter-observer Kaplan-Meier estimate that represents the probability of survival as a function of the degree of disagreement. The dotted lines represent the minimum differences for 50% of the observations. In order: Number of signals, pixel intensity mean, area, perimeter, major and minor diameter, circularity, solidity, and vascular resistance.

ESTUDIO III:
CORRELACIÓN ENTRE EL ÍNDICE DE RESISTENCIA Y UN NUEVO MÉTODO SEMIAUTOMÁTICO DE ANÁLISIS DE IMAGEN PARA EVALUAR LA RESISTENCIA VASCULAR

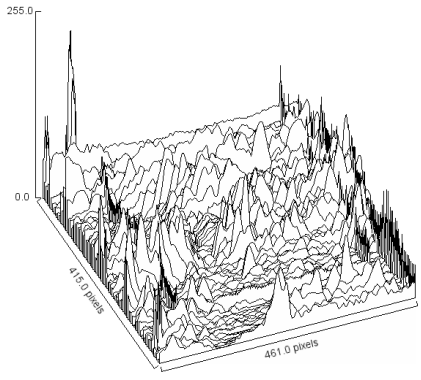

VI. ESTUDIO III: CORRELACIÓN ENTRE EL ÍNDICE DE RESISTENCIA Y UN NUEVO MÉTODO SEMIAUTOMÁTICO DE ANÁLISIS DE IMAGEN PARA EVALUAR LA RESISTENCIA VASCULAR

6.1. INTRODUCTION

The use of Doppler ultrasound in the evaluation of musculoskeletal pathologies is becoming increasingly common (Sunding et al. 2016; Mersmann et al. 2019; Risch et al. 2021). Doppler ultrasound can be used to localize areas of increased blood flow and quantify color pixels, which can provide clinically important information, more accurate diagnoses and assessments of response to treatment (Terslev et al. 2003; McCreesh et al. 2013). In tendinopathies, it allows locating areas with intratendinous Doppler signal (DS) (Gatz et al. 2020; Paantjens et al. 2020), although we must keep in mind that the presence of DS does not provide relevant data about the tendinopathy (Malliaras et al. 2008; Tol et al. 2012). However, the study of vascular resistance (VR) could provide more useful information on tissue status (Torp-Pedersen et al. 2008; Terabayashi et al. 2014).

Currently, the pathophysiological model of the continuous model of tendinopathy of Cook and Purdam (2009) is assumed, in which the degenerative and reactive process coexist (Cook y Purdam 2009; Cook et al. 2016), and although this model makes little reference to inflammation, some studies have observed a coexistence of inflammatory and degenerative processes in the development of tendinopathies (Bjordal et al. 2006; Torp-Pedersen et al. 2008; Millar et al. 2010).

Spectral Doppler allows evaluation of the type of blood flow, low or high resistance, through a velocity versus time curve that represents the variation of red blood cell flow velocity throughout the cardiac cycle. Through spectral Doppler can be measured the degree of resistance to arterial flow originating from the distal microvascular, expressed numerically with the resistance index (RI) (Pourcelot y Société parisienne d'expansion chimique 1982). At the musculoskeletal level, a RI equal to 1 is considered normal, while a lower value could be associated with

inflammatory processes (Bjordal et al. 2006; Koenig et al. 2007b, 2007a; Torp-Pedersen et al. 2008). The RI is provided directly by the ultrasound in spectral Doppler mode from the Pourcelot formula: *(peak systolic velocity - end-diastolic velocity) / peak systolic velocity* (Pourcelot y Société parisienne d'expansion chimique 1982).

For this purpose, the Doppler window is adjusted longitudinally, centered in the vessel lumen and occupying 2/3 of its section. Intratendon DS seen in tendinopathy may contain vessels with a smaller lumen than the Doppler window, so in many cases it is not possible to adjust the Doppler window to the size of these vessels. In addition, many intratendinous DS may appear, complicating and multiplying the measurement process in the attempt to obtain the mean RI of the intratendinous DS.

To avoid this problem, some authors have proposed measuring the RI in the three intratendinous vessels with the largest diameter and calculating the mean (Qvistgaard et al. 2001; Koenig et al. 2007b, 2007a; Torp-Pedersen et al. 2008) but the large number of intratendinous vessels that can be found suggests that this methodology is probably not robust enough to reproduce the entire intratendinous VR.

The analysis of the DS through the color pixels not only allows quantification of the area of the Spectral Doppler (Boesen et al. 2006, 2012; Rezaei et al. 2017), but also the establishment of a relationship between the pixel color intensity scale and the flow velocity (Delorme et al. 1995), so it could be used to measure the intratendinous VR through the RI formula. This procedure would allow its application on any number and size of DS found within the Doppler window.

However, there are no studies that have analyzed the relationship between the RI provided directly by the echograph and that estimated from the intensity of the color pixels. The consistent validity of the latter method would allow its application in tendon hypervascularization.

The aim of this study was to analyze the correlation between the RI obtained by spectral Doppler and VR calculated by quantifying the pixel color intensity of the power Doppler (PD) signal.

6.2. MATERIALS AND METHODS

6.2.1. Study design and participants

A total of 30 healthy participants with a systolic blood pressure less than 130 mmHg and less than 80 mmHg for diastolic and no medical history of pathologies or medication intake that could alter blood flow were included for this study. Participants were recruited voluntarily at a private Physiotherapy Center (Clínica F&C Fisioterapia Avanzada y Neuro-Rehabilitación, Huelma, Spain) in December 2018. All participants were informed about the study and signed an informed consent document. The study was approved by the Ethics Committee of the Catholic University of Murcia (CE111803).

6.2.2. PD and Spectral Doppler evaluation

The patient was placed in supine decubitus with the right upper limb in a comfortable position to obtain images of the brachial artery.

The brachial artery has been chosen to test the two methods because the measurement of the RI in the brachial artery does not offer difficulties as it is a single vessel with a considerable lumen diameter and allows the automatic acquisition of this index by the ultrasound scanner itself. In addition, the RI of the brachial artery is easily modified by vascular occlusion maintained for 5 min, which will generate hyperemia at 1 min after occlusion, with a decrease in RI (Takarada et al. 2000). In other words, vascular occlusion of the brachial artery allows alteration of the RI recordings, decreasing its value to test the two methods in different situations

The examination was performed with two Telemed SmartUS ultrasound scanners (Vilnius, Lithuania) with 7-15 MHz linear probes (L15-7L40H-5) and a Riester Minimus III pressure cuff (Jungingen, Germany) placed on the most distal part of the participant's arm (Frangi et al. 2003; Harris et al. 2010; Wray et al. 2013).

One of the probes was installed on an articulated arm to maintain its static position on the longitudinal plane of the brachial artery at midpoint between the antecubital and axillary regions. The ultrasound machine, in spectral Doppler

mode, identified the cardiac cycles, as well as the peak systolic velocity and end-diastolic velocity, automatically calculating the RI of the brachial artery.

The second probe was positioned distal to the first and transversally to the brachial artery to record the PD. A Doppler frequency of 6.7 MHz and a pulse repetition frequency of 1.5 kHz were used. The lowest wall filter and standardized gain were applied just below the level that produced random noise. The setting parameters were the same for all patients and minimal pressure was exerted with the probe on the arm to avoid vessel compression.

An occlusion of the brachial artery was applied for 5 min distal to the ultrasound slices with the pressure cuff, using a pressure calculated from the systolic arterial pressure + 50 mmHg (Corretti et al. 2002; Harris et al. 2010). In this way, endothelium-mediated, nitric oxide-dependent ischemia and subsequent reactive hyperemia were induced (Harris et al. 2010).

At 1 min post-occlusion and coinciding with the vasodilatation generated by the hyperemia and, therefore, with a decrease in the RI (Takarada et al. 2000; Betik et al. 2004; Rafati et al. 2009), the RI and a 4-s video of the transverse PD signal to the brachial artery were recorded by the two ultrasound scanners at the same time. The location of the ultrasound transducers and the pressure cuff can be seen in **figure 1**.

Three evaluations were performed on each participant, obtaining a total of 90 ultrasound evaluations of the brachial artery with their respective RI and 4-s videos of the PD signal after vascular occlusion. All scans were performed by the same sonographer (F.J.M.-P) with more than 10 years of experience in musculoskeletal ultrasound.

Figure 1. Location of ultrasound transducers and pressure cuff.

6.2.3. Processing and quantification of DS

Processing and analysis of the videos and images was performed by a second investigator using ImageJ software (Version 1.50b, National Institutes of Health, Bethesda, MD, USA). After image scaling, regions of interest (ROI) were manually selected and extracted on the brachial artery PD images with the highest and lowest signal corresponding to peak systolic and end diastole for each patient. Measurement and image data were coded and anonymized to avoid potential bias.

Since the DS appears in color on a grayscale background, it is easy to segment and isolate the region for further quantification. We use the color threshold plug-in, which allows the cutoff point to be manually adjusted with slider bars.

The flow pattern was assessed by calculating the mean pixel color intensity of the previously isolated PD signal for each image. The mean pixel color mean of

the image with the highest signal was considered as the peak systolic velocity and of the image with the lowest signal as the end-diastolic velocity. These data were transferred to the RI formula, giving a value associated with the RV of the brachial artery **(figure 2)**. The reproducibility and reliability of this procedure has been previously studied on intratendinous DS (Molina-Payá et al. 2021) with a very good intra- and interobserver agreement (ICC = 0.92 (95% IC = 0.86-0.96)).

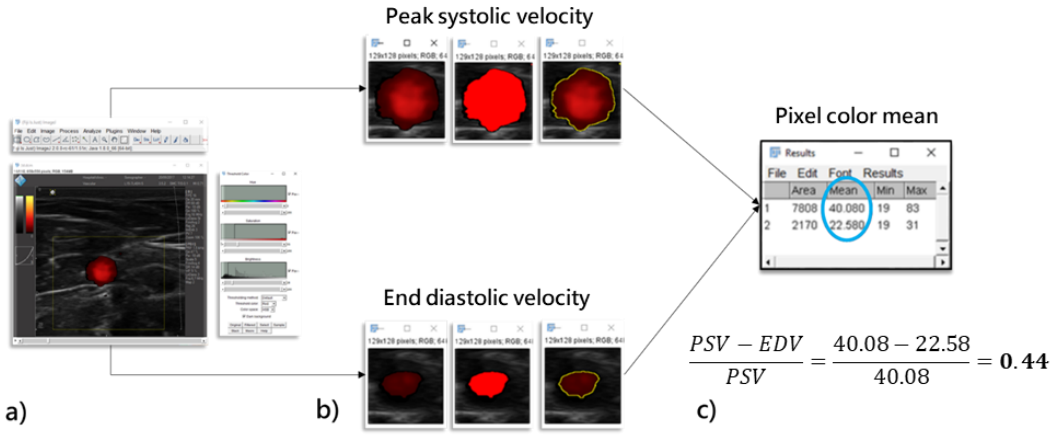

Figure 2. Quantification of vascular resistance by pixel color intensity (ImageJ). 4 s power Doppler video (a), Doppler signal processing (b), calculation of mean pixel color and vascular resistance (c).

6.2.4. Statistical analysis

Data analysis was conducted with the statistical package R v.3.6 and JASP Team (2020). JASP (Version 0.14.1) [Computer software], and Morey, R. D., & Rouder, J. N. (2015). BayesFactor (Version 0.9.11-3) [Computer software].

Data were summarized by mean and standard deviation and range and quartiles for continuous variables and absolute and relative frequencies for categorical variables.

Although the sample size allows the assumption of normality, multivariate and bivariate normality was explored with the Shapiro-Wilks test; in all contrasts

the *W* statistic was greater than .9, so the assumption of normality was finally assumed.

Correlation was evaluated with Pearson's correlation coefficient (95% CI) and the percentage of shared variability between variable pairs was determined with the coefficient of determination (r^2). In addition, the Vovk-Sellke Maximum *p*-Ratio was estimated, which provides the degree of plausibility evidence for the alternative hypothesis (presence of correlation), compared to the null hypothesis (no correlation), regardless of the *p*-values (Selke et al. 2001).

As a guideline, the following cut-off points will be considered for correlations: .0 to .19 - very weak correlation; .2 to .39 - weak correlation; .4 to .69 - moderate correlation; .7 to .89 - strong correlation; 0.9 to 1.0 - very strong correlation. In all cases, the significance level was set at $p \leq .05$.

6.3. RESULTS

Thirty participants (16 women [53%], mean age = 24.8 yrs; SD = 6.44 yrs) were included in this study. A descriptive summary of variables is showed in **table 1**.

Table 1. Descriptive summary of Doppler parameters.

Parameter	Mean	SD	VC%	Min	Q1	Median	Q3	Max
Area SPV	7520.1	1997.56	27%	3656.0	5980.5	7877.5	9037.0	11383.0
Area FDV	2328.4	1222.99	53%	268.0	1493.3	2152.0	3035.5	6356.0
Color pixel intensity SPV	40.1	9.18	23%	25.7	33.5	38.2	47.1	61.8
Color pixel intensity FDV	21.6	2.75	13%	19.0	19.5	20.8	22.7	31.7
Resistance index	0.82	0.073	9%	0.68	0.76	0.84	0.87	0.96
Vascular resistance	0.44	0.115	26%	0.23	0.35	0.44	0.50	0.69

SPV: Systolic Peak velocity. FDV: final diastolic velocity. SD: Standard deviation. VC%: variation coefficient. Q1: cuartile 1. Q2: cuartile 2. Min: minimum. Max: Maximum.

The correlations between interest variables obtained of DS, RI and VR are showed in **table 2**, and **figures 3-4**.

It was found a high correlation between RI and VR (*r*=.92; 95%CI= .88 to .95; *p*≤ .001) so there is a very strong concurrent validity between the two measures and they can be considered equivalents (common variability of 84%).

Table 2. Pairwise correlations between power Doppler, color variables and resistance index.

Pairwise correlation	Pearson's r (95%CI)	*p*-value	R^2%	VS-MPR
RI-VR	.92 (.88 to .95)	≤.001	84%	≥300
Systolic Area-SPV.px	.39 (.2 to .55)	≤.001	15%	262
Systolic Area-FDV.px	-.18 (-.37 to .03)	.09	3%	1.7
Systolic Area-RI	.53 (.36 to .67)	≤.001	28%	≥300
Systolic Area-VR	.57 (.41 to .69)	≤.001	32%	≥300
Diastolic Area-SPV.px	.27 (.07 to .45)	.010	7%	7.8
Diastolic Area-FDV.px	.61 (.47 to .73)	≤.001	38%	≥300
Diastolic Area-RI	-.04 (-.24 to .17)	.073	0%	1.0
Diastolic Area-VR	-.02 (-.23 to .19)	.85	0%	1.0
SPV.Px-RI	.72 (.61 to .81)	≤.001	52%	≥300
SPV.Px-VR	.85 (.78 to .9)	≤.001	72%	≥300
FDV.Px-RI	-.2 (-.39 to .01)	.06	4%	2.3
FDV.Px-VR	-.15 (-.34 to .06)	0.16	2%	1.2

RI: resistance index. VR: vascular resistance. SPV.px: mean color pixel intensity in systolic peak of velocity. FDV.px: mean color pixel intensity in final diastolic velocity. Vovk-Sellke Maximum *p*-Ratio: Based on the *p*-value, the maximum possible odds in favor of H_1 over H_0 equals 1/-e p (log(p)) for p ≤.37. Values about 1 indicates no favoured H_1.

In addition, we found interesting moderate correlations between the Doppler area at the sytolic peak with respect to IR (*r*=.53; 95%CI= .36 to .67; *p*≤ .001) and RV (*r*=.57; 95%CI= .41 to .69; *p*≤ .001) in a similar way, but no correlation with respect to the area in diastole.

Similarly, a strong correlation was found between the mean intensity of color pixels in systole with respect to RI (*r*=.72; 95%CI= .61 to .81; *p*≤ .001) and RV (*r*=.85; 95%CI= .78 to .90; *p*≤ .001) but not with respect to diastole.

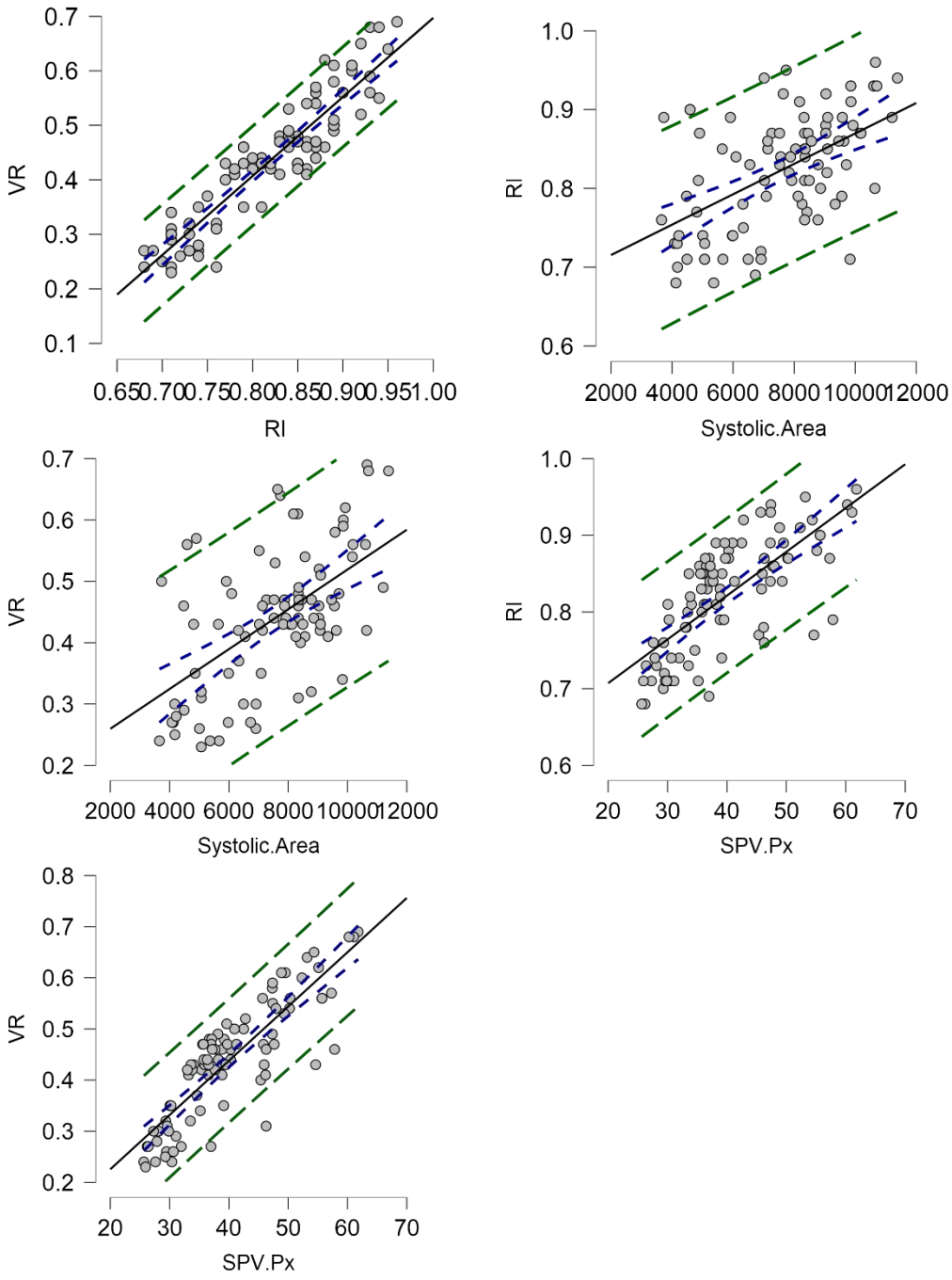

Figure 3. Regression lines between resistance index (RI), vascular resistance (VR) and systolic parameters. SPV.px: mean of color pixel in systolic peak velocity.

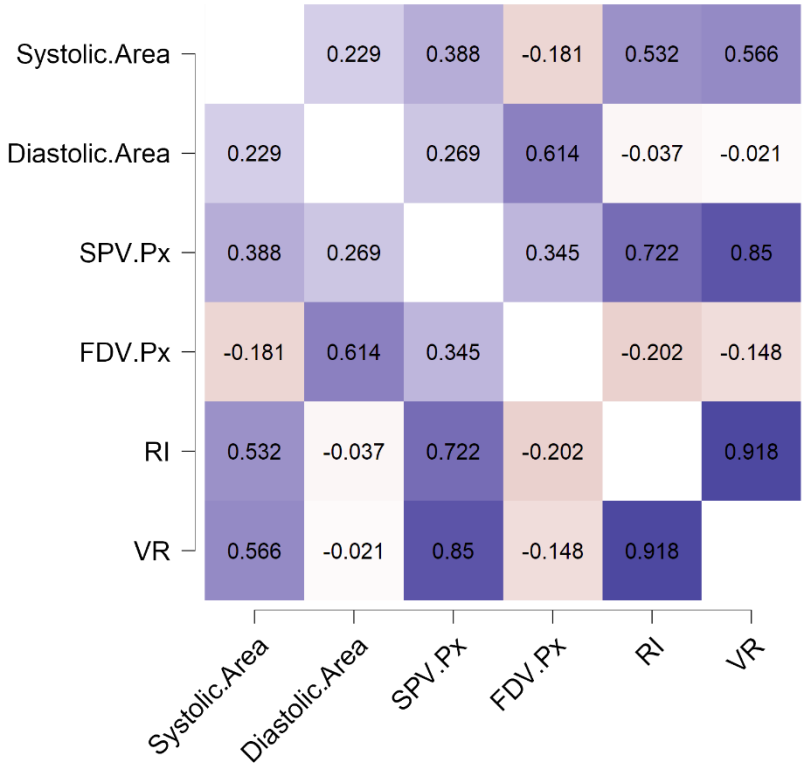

Figure 4. Pearson's *r* heatmap. The intensity of colors reflex the strong of correlations.

6.4. DISCUSSION

No other studies have been found that correlate RI with other methods of measuring VR, so the results obtained cannot be compared. Regarding the correlation between intratendinous VR calculated by quantifying the color intensity of the pixels of the PD signal and the RI measured at the same time and over the brachial artery, it was observed that there is a positive correlation, that is, the higher the value of intratendinous VR, the higher the RI.

It is difficult to think that the raw mean pixel color of the PD signal correlates with the flow velocity, because there are different filtering and interpolarization algorithms to represent the image that can distort the results. Moreover, in this

study we used the PD mode, which encodes the amplitude of the signal through the number of red blood cells moving, providing information about the amplitude of the DS, contrary to Colour Doppler which encodes the average of the velocities. This issue could further complicate this correlation because the RI is calculated with data on flow velocity and the PD provides information on intensity. Although the results obtained in this study have been very good, it would be interesting to study the correlation of this methodology applied on the color DS. However, in relation to the RI and given that it is a relative index, it seems that the two types of measures are equivalent.

In 1995, Delorme studied the relationship between the mean pixel color of the color Doppler and flow velocity (Delorme et al. 1995). The limitations of this modality of ultrasound are related with the interpolation algorithms used by the ultrasound machine itself when low levels of color Doppler are used, giving erroneous low values for the mean pixel color value (Delorme et al. 1995). The selection of an inadequate velocity scale and insonation angle in the color Doppler mode can generate the phenomenon of aliasing (Del Cura Rodríguez et al. 2021), altering the color representation of the signal pixel. Despite these limitations, the use of average pixel color analysis of the color Doppler is applicable in practice and provides additional information in the evaluation of DS (Delorme et al. 1995).

Although the quantification of the color DS has been extensively studied (Bell et al. 1995; Delorme et al. 1995; Fein et al. 1995), the quantification of PD signals has several advantages over color Doppler in the assessment of tissue vascularization and blood flow. In the case of this study, the PD mode has been used because it is less dependent on the Doppler angle, it is more sensitive in the representation of low flows in small vessels, the aliasing phenomenon does not appear (Pozniak y Allan 2013), and the codification in a single-color tone facilitates the quantification process and the results obtained correlate well with the perfusion rate (Sehgal et al. 2001).

6.4.1. Limitations

This quantification methodology presents some limitations, mainly related to standardization as it depends on the sensitivity and color tone of the PD signals,

which are altered by different parameters such as: the ultrasound model and probe used, the selection of the ultrasound slices, the selection of the images with higher and lower DS from the video sequence, the settings of the ultrasound Doppler parameters, the color scale used, the delimitation of the ROI of the DS in the image and the manual selection of the color thresholds of the image analysis software. However, in this study all these parameters have been optimized and kept constant in all scans.

6.5. CONCLUSION

This new method of analyzing DS by quantifying the color intensity of the PD signal pixel is a good predictor of RI and could be useful for VR analysis in tissues where RI measurement is complicated.

6.6. REFERENCES

1. Bell DS, Bamber JC, Eckersley RJ. Segmentation and analysis of colour Doppler images of tumour vasculature. Ultrasound Med Biol. 1995;21(5):635-47.
2. Betik AC, Luckham VB, Hughson RL. Flow-mediated dilation in human brachial artery after different circulatory occlusion conditions. Am J Physiol-Heart Circ Physiol. 1 de enero de 2004;286(1):H442-8.
3. Bjordal JM, Lopes-Martins RAB, Iversen VV. A randomised, placebo controlled trial of low level laser therapy for activated Achilles tendinitis with microdialysis measurement of peritendinous prostaglandin E2 concentrations. Br J Sports Med. enero de 2006;40(1):76-80.
4. Boesen AP, Boesen MI, Torp-Pedersen S, Christensen R, Boesen L, Hölmich P, et al. Associations between abnormal ultrasound color Doppler measures and tendon pain symptoms in badminton players during a season: a prospective cohort study. Am J Sports Med. marzo de 2012;40(3):548-55.
5. Boesen MI, Torp-Pedersen S, Koenig MJ, Christensen R, Langberg H, Hölmich P, et al. Ultrasound guided electrocoagulation in patients with chronic non-insertional Achilles tendinopathy: a pilot study. Br J Sports Med. septiembre de 2006;40(9):761-6.

6. Cook JL, Purdam CR. Is tendon pathology a continuum? A pathology model to explain the clinical presentation of load-induced tendinopathy. Br J Sports Med. junio de 2009;43(6):409-16.

7. Cook JL, Rio E, Purdam CR, Docking SI. Revisiting the continuum model of tendon pathology: what is its merit in clinical practice and research? Br J Sports Med. 1 de octubre de 2016;50(19):1187-91.

8. Corretti MC, Anderson TJ, Benjamin EJ, Celermajer D, Charbonneau F, Creager MA, et al. Guidelines for the ultrasound assessment of endothelial-dependent flow-mediated vasodilation of the brachial artery: a report of the International Brachial Artery Reactivity Task Force. J Am Coll Cardiol. 16 de enero de 2002;39(2):257-65.

9. Del Cura Rodríguez JL, Sánchez Guerrero A, Sociedad Española de Ultrasonografía diagnóstica. Ecografía Doppler esencial. Madrid: Editorial Médica Panamericana; 2021.

10. Delorme S, Weisser G, Zuna I, Fein M, Lorenz A, van Kaick G. Quantitative characterization of color Doppler images: reproducibility, accuracy, and limitations. J Clin Ultrasound JCU. diciembre de 1995;23(9):537-50.

11. Fein M, Delorme S, Weisser G, Zuna I, van Kaick G. Quantification of color Doppler for the evaluation of tissue vascularization. Ultrasound Med Biol. 1995;21(8):1013-9.

12. Frangi AF, Laclaustra M, Lamata P. A registration-based approach to quantify flow-mediated dilation (FMD) of the brachial artery in ultrasound image sequences. IEEE Trans Med Imaging. noviembre de 2003;22(11):1458-69.

13. Gatz M, Betsch M, Bode D, Schweda S, Dirrichs T, Migliorini F, et al. Intra individual comparison of unilateral Achilles tendinopathy using B-mode, power Doppler, ultrasound tissue characterization and shear wave elastography. J Sports Med Phys Fitness. noviembre de 2020;60(11):1462-9.

14. Harris RA, Nishiyama SK, Wray DW, Richardson RS. Ultrasound Assessment of Flow-Mediated Dilation. Hypertension. 1 de mayo de 2010;55(5):1075-85.

15. Koenig MJ, Torp-Pedersen S, Holmich P, Terslev L, Nielsen MB, Boesen M, et al. Ultrasound Doppler of the Achilles tendon before and after injection of an ultrasound contrast agent--findings in asymptomatic subjects. Ultraschall Med Stuttg Ger 1980. febrero de 2007a;28(1):52-6.

16. Koenig MJ, Torp-Pedersen ST, Christensen R, Boesen MI, Terslev L, Hartkopp A, et al. Effect of knee position on ultrasound Doppler findings in patients with patellar tendon hyperaemia (jumper's knee). Ultraschall Med Stuttg Ger 1980. octubre de 2007b;28(5):479-83.

17. Malliaras P, Richards PJ, Garau G, Maffulli N. Achilles tendon Doppler flow may be associated with mechanical loading among active athletes. Am J Sports Med. noviembre de 2008;36(11):2210-5.

18. McCreesh KM, Riley SJ, Crotty JM. Neovascularity in patellar tendinopathy and the response to eccentric training: a case report using Power Doppler ultrasound. Man Ther. diciembre de 2013;18(6):602-5.

19. Mersmann F, Pentidis N, Tsai M-S, Schroll A, Arampatzis A. Patellar Tendon Strain Associates to Tendon Structural Abnormalities in Adolescent Athletes. Front Physiol. 2019;10:963.

20. Millar NL, Hueber AJ, Reilly JH, Xu Y, Fazzi UG, Murrell GAC, et al. Inflammation is Present in Early Human Tendinopathy. Am J Sports Med. 1 de octubre de 2010;38(10):2085-91.

21. Molina-Payá FJ, Ríos-Díaz J, Carrasco-Martínez F, Martínez-Payá JJ. Reliability of a new semi-automatic image analysis method for evaluating the Doppler signal and intratendinous vascular resistance in patellar tendinopathy. Ultrasound Med Biol. 2021;In press.

22. Paantjens M, Leeuw M, Helmhout P, Isaac A, Maeseneer MD. The interrater reliability of ultrasonography for Achilles tendon structure. J Ultrason. 2020;20(80):e6-11.

23. Pourcelot L, Société parisienne d'expansion chimique. Application de l'examen Doppler à l'étude de la circulation périphérique. Paris (16, rue Clisson, 75646, cedex 13): SPECIA; 1982.

24. Pozniak MA, Allan PL. Clinical Doppler Ultrasound E-Book: Expert Consult: Online. Elsevier Health Sciences; 2013.

25. Qvistgaard E, Røgind H, Torp-Pedersen S, Terslev L, Danneskiold-Samsøe B, Bliddal H. Quantitative ultrasonography in rheumatoid arthritis: evaluation of inflammation by Doppler technique. Ann Rheum Dis. julio de 2001;60(7):690-3.

26. Rafati M, Mokhtari-Dizaji M, Saberi H. The Effect of Cuff Occlusion Protocols on Radial Strain and Arterial Haemodynamics. Ultrasound. agosto de 2009;17(3):144-9.

27. Rezaei H, af Klint E, Hammer HB, Terslev L, D'Agostino MA, Kisten Y, et al. Analysis of correlation and causes for discrepancy between quantitative and semi-quantitative Doppler scores in synovitis in rheumatoid arthritis. Rheumatol Oxf Engl. febrero de 2017;56(2):255-62.

28. Risch L, Stoll J, Schomöller A, Engel T, Mayer F, Cassel M. Intraindividual Doppler Flow Response to Exercise Differs Between Symptomatic and Asymptomatic Achilles Tendons. Front Physiol. 2021;12:617497.

29. Sehgal CM, Arger PH, Silver AC, Patton JA, Saunders HM, Bhattacharyya A, et al. Renal blood flow changes induced with endothelin-1 and fenoldopam mesylate at quantitative Doppler US: initial results in a canine study. Radiology. mayo de 2001;219(2):419-26.

30. Sellke T, Bayarri MJ, Berger O. Calibrarion of p-values for testin precise null hypotheses. Am Stat. 2001;55(1):62-71

31. Sunding K, Fahlström M, Werner S, Forssblad M, Willberg L. Evaluation of Achilles and patellar tendinopathy with greyscale ultrasound and colour Doppler: using a four-grade scale. Knee Surg Sports Traumatol Arthrosc Off J ESSKA. junio de 2016;24(6):1988-96.

32. Takarada Y, Takazawa H, Sato Y, Takebayashi S, Tanaka Y, Ishii N. Effects of resistance exercise combined with moderate vascular occlusion on muscular function in humans. J Appl Physiol Bethesda Md 1985. junio de 2000;88(6):2097-106.

33. Terabayashi N, Watanabe T, Matsumoto K, Takigami I, Ito Y, Fukuta M, et al. Increased blood flow in the anterior humeral circumflex artery correlates with night pain in patients with rotator cuff tear. J Orthop Sci. septiembre de 2014;19(5):744-9.

34. Terslev L, Torp-Pedersen S, Qvistgaard E, Danneskiold-Samso... B, Bliddal H. Estimation of inflammation by Doppler ultrasound: quantitative changes after intra-articular treatment in rheumatoid arthritis. Ann Rheum Dis. noviembre de 2003;62(11):1049-53.

35. Tol JL, Spiezia F, Maffulli N. Neovascularization in Achilles tendinopathy: have we been chasing a red herring? Knee Surg Sports Traumatol Arthrosc Off J ESSKA. octubre de 2012;20(10):1891-4.

36. Torp-Pedersen TE, Torp-Pedersen ST, Qvistgaard E, Bliddal H. Effect of glucocorticosteroid injections in tennis elbow verified on colour Doppler ultrasonography: evidence of inflammation. Br J Sports Med. diciembre de 2008;42(12):978-82.

37. Wray DW, Witman MAH, Ives SJ, McDaniel J, Trinity JD, Conklin JD, et al. Does brachial artery flow-mediated vasodilation provide a bioassay for NO? Hypertens Dallas Tex 1979. agosto de 2013;62(2):345-51.

ESTUDIO IV:
TERMOGRAFÍA INFRARROJA, RESISTENCIA VASCULAR INTRATENDÓN Y ECOTEXTURA EN DEPORTISTAS CON TENDINOPATÍA ROTULIANA: ESTUDIO TRANSVERSAL

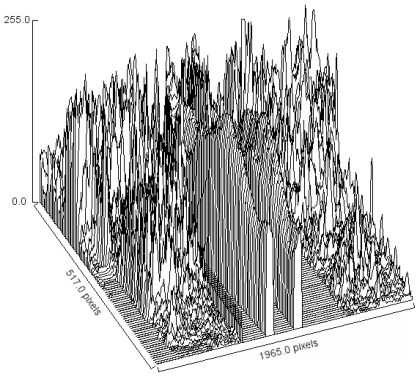

VII. ESTUDIO IV: TERMOGRAFÍA INFRARROJA, RESISTENCIA VASCULAR INTRATENDÓN Y ECOTEXTURA EN DEPORTISTAS CON TENDINOPATÍA ROTULIANA: ESTUDIO TRANSVERSAL

7.1. INTRODUCTION

Patellar tendinopathy (PT) is characterized by localized pain in the patellar tendon, related to load that increases with mechanical demand on the knee extensors, especially in activities that load and release energy in the patella (Ferretti et al. 1983). It is a common pathology in the knee with a high presence in both athlete (Frizziero et al. 2014) and non-athlete population (Toppi et al. 2015). Athletes with PT may suffer from uncomfortable symptoms accompanied by decreased function with a negative effect on their quality of life (Toppi et al. 2015), deterioration in physical performance (Lian et al. 2005), and even having to end their sporting career prematurely (Kettunen et al. 2002). It is difficult to determine the exact frequency of PT in athletes because these types of sports injuries are often underreported. Its incidence is higher in jumping sports and in sports where repetitive loading of the patellar tendon is required, and the prevalence among elite athletes from different sports has been estimated at around 14%. (Lian et al. 2005).

The diagnosis of PT is challenging, as there is currently no gold standard diagnostic technique (Scott et al. 2013; Malliaras et al. 2015). In clinical practice, it is diagnosed by antecedents, knee examination, and palpation of the tendon and its attachments (Cook et al. 2001b), however, the physiology of tendon pain is not yet fully understood (Rio et al. 2014).

Diagnosis can be confirmed by imaging tests, commonly ultrasonography and magnetic resonance imaging, which detect abnormalities in the structure of the patellar tendon such as increased thickness, loss of alignment of collagen fibers and presence of neovascularization (Khan et al. 1996; Cook et al. 2001b). More specifically, morphologic and echotextural analysis of the tendon using ultrasound image analysis has been shown to be reliability (Ríos-Díaz et al. 2010a) and useful in assessing changes in tendon structure (Benítez-Martínez et al. 2019; López-Royo et al. 2021). In addition, the possibility of assessing tendon vascular perfusion using

Doppler ultrasound image analysis and the resistance index (RI) formula has recently been demonstrated (Molina-Payá et al. 2021a). Low RI is associated with low peripheral resistance and high perfusion of the distal bed and therefore with a situation compatible with the presence of inflammation (Terslev et al. 2003a; Bjordal et al. 2006; Terabayashi et al. 2014). In musculoskeletal tissue, RI it is considered normal when is equal to one.

However, although it is generally considered that the presence of intratendinous Doppler signal (DS) is associated with a sign of tendon abnormality (Alfredson and Ohberg 2005; Richards et al. 2005) and its absence with healthy tendons (Ohberg et al. 2001; Alfredson et al. 2003), its presence has also been detected in asymptomatic subjects (Zanetti et al. 2003; Lind et al. 2006), which generates a debate about its usefulness.—Nevertheless, the analysis of the intratendinous vascular resistance (VR) can be more useful for the physiological state of the tissue (Molina-Payá et al. 2021a).

In this sense, some studies have also considered infrared thermography (IRT) as a suitable technique for the diagnosis of PT (Mangine et al. 1987; Seixas, A et al. 2013). IRT is an inexpensive, reliable, non-invasive and accurate imaging technique that provides information on thermal, metabolic, and vascular conditions of the human body that can be used to interpret pathophysiological changes (Hildebrandt et al. 2010). The use of IRT in musculoskeletal conditions is based on the thermal symmetry between both sides of the body, so that the presence of thermal asymmetry is indicative of some type of anomaly (Uematsu et al. 1988; Vardasca et al. 2012; Sillero-Quintana et al. 2015), specifically in the knee when the differences are greater than 0.5 ºC (James Selfe 2008; Liu et al. 2020). These temperature changes are attributed to an increased sympathetic innervation of the paratendinous tissue associated with tendinopathy (Andersson et al. 2007).

Even though, there are no studies that have evaluated and related tendon echotextural changes, intratendinous VR, thermal alterations, and functionality in athletes with PT. Therefore, the objectives of this study were 1) to show prevalence of abnormalities in thermal, vascular and echotextural parameters between athletes with PT and controls; 2) to analyze the differences in thermal, vascular and echotextural parameters within athletes with PT between symptomatic and

asymptomatic tendons, and 3) to explore the relationships between clinical parameters and thermal asymmetry respect vascular and echotextural parameters.

7.2. MATERIALS AND METHODS

7.2.1. Study design and participants

In this study there were 26 patients (athletes with PT) (mean age= 30.1 years; SD= 9.0 years; range= 18-50 years) of whom 21 were male (81%) and a control group of 27 asymptomatic participants (mean age= 23.3 years; SD= 5.38 years; range=19-42 years) of whom 12 (44%) were male. Of initial 27 patients, one participant with 120 months of pain evolution was excluded from analysis.

All the participants were voluntarily recruited from a private physical therapy center (Clínica F&C Fisioterapia Avanzada y Neuro-Rehabilitación, Huelma, Spain) in July and August 2018. All participants were informed of the study's aims and signed an informed consent. The study was approved by the ethics committee of the Catholic University of Murcia, Murcia, Spain (CE111803).

Demographical and clinical characteristics (sex, age, and time of evolution) were recorded. Knee functionality was assessed with Victorian Institute of Sport Patellar Tendon Assessment Questionnaire (VISA-P) (Visentini et al. 1998) that is simple and practical, with good clinimetric properties (Korakakis et al. 2021) and widely used in the investigation of PT.

The participants were divided in two groups: 1) Twenty-seven suffered from PT diagnosed with clinical criteria with an evolution time of more than three months and a VISA-P score of less than 100; 2) Twenty-seven healthy volunteers were recruited under the inclusion criteria of no previous PT and a VISA-P score of 100.

7.2.2. Data sources, measurements, and outcomes

7.2.2.1. Thermographic analysis of patellar tendon

To minimize the influence of extrinsic individual factors on vascular and thermographic recordings, all participants were asked not to exercise, not to drink

alcohol, coffee, or energy drinks in the previous 12 hours, and not to smoke in the previous 6 hours. They were asked not to apply creams or lotions on their legs to avoid alterations in skin emissivity, as well as to inform them about the use of drugs or treatments and to try to avoid the alteration of rest and mealtimes (Fernández-Cuevas et al. 2015).

The IRT images were recorded with an OPTRIS PI 450 IRT camera coupled to Optris PI Connect Software (Germany). The IRT camera has a Noise Equivalent Temperature Difference <40 mK with 38º x 29º FOV, a wide range of temperature from −20°C to +100°C, spectrum range of 7.5–13 μm, focal plane array sensor size of 382 × 288 pixels, emissivity set at 0.98 and a measurement uncertainty of ± 2% of the overall temperature reading. The size of the capture frame was 55.4 × 40.63 cm (1.5 mm/px).

The participant was acclimatized in an isolated room (3.86 x 3.47 m2), without temperature sources, and at a mean temperature of (23.7 ± 0.9ºC) and a relative humidity of (49 ± 5%) for 15 min without clothing on the lower limbs (Fernández-Cuevas et al. 2015; Ammer y Ring 2019). The participant was seated on a hydraulic stretcher with his/her feet on a step-in order to isolate contact with the ground and the camera was positioned perpendicular to subjects for a more accurate reading (Tkáčová et al. 2010; Fernández-Cuevas et al. 2015).

For the determination of the regions of interest of the patellar tendon, the method previously described by (Molina-Payá et al. 2021b) was used by superimposing region of interest (ROI) on thermal images using skin markers **(figure 1)**.

In this way the average temperature in each tendon was obtained and from both the temperature difference. A difference greater than 0.5 ºC between the affected side and the healthy side is compatible with tendon pathology.

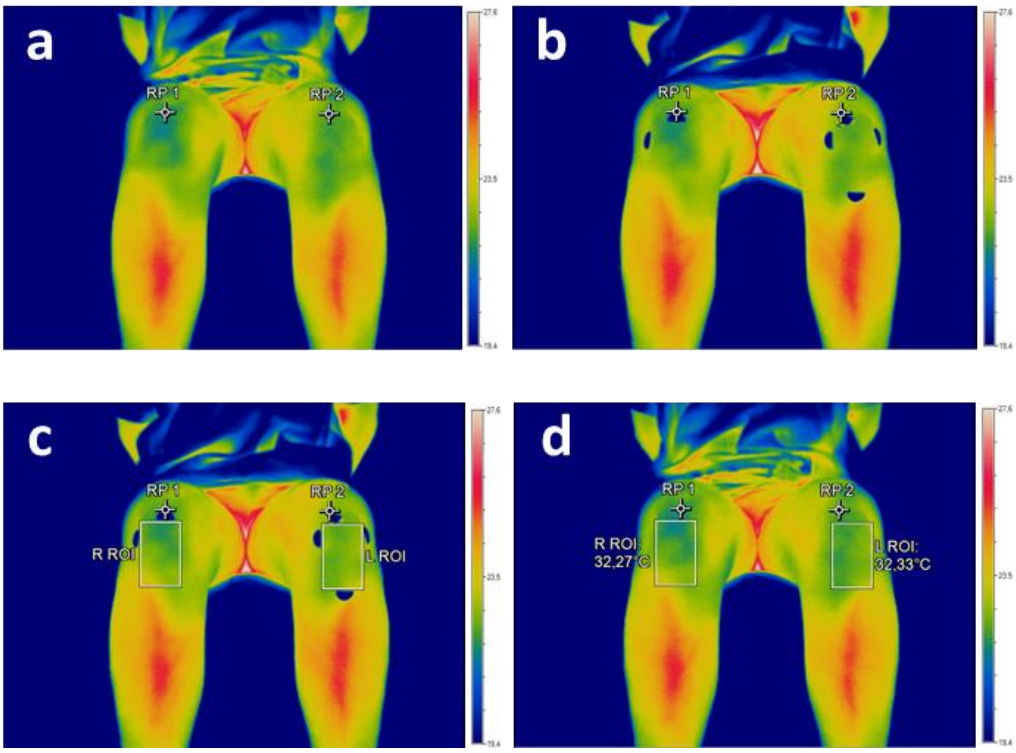

Figure 1. Temperature measurement methodology by infrared thermography. First thermogram with references points (a), location of the metallic markers in the second thermogram (b), location of the ROIs (c) and superposition of the ROIs on the first thermogram (d).

7.2.2.2. Quantification of intratendinous VR with Doppler Ultrasonography

Intratendinous VR was determined using the RI defined as (peak systolic velocity - end-diastolic velocity) / peak systolic velocity from power Doppler (PD) ultrasonography records.

The patient was placed in supine position and knees extended and both knees were evaluated. The scan was performed with a Telemed SmartUS ultrasound machine (Vilnius, Lithuania) with a 7-15 MHz linear transducer (L15-7L40H-5). The setting parameters were the same for all patients and care was taken not to apply pressure with the transducer. The PD settings were Doppler frequency of 6.7 MHz and a PRF of 0.7 kHz with the lowest wall filter and a Doppler gain just below the level of random noise production.

Since the use of spectral Doppler mode on intratendinous vessels quantification may be difficult by the high number and low diameter signals, the patellar tendon was scanned with PD mode in the longitudinal plane to localize the maximum intratendinous DS and 4-second video was stored for further processing and analysis. The image processing and analysis method to obtain RI was previously described (Molina-Payá et al. 2021a) **(figure 2)**. In the tendons where no DS was recorded the RI was equal to 1 which represents normality in the musculoskeletal tissue (Terslev et al. 2003b; Koenig et al. 2007a).

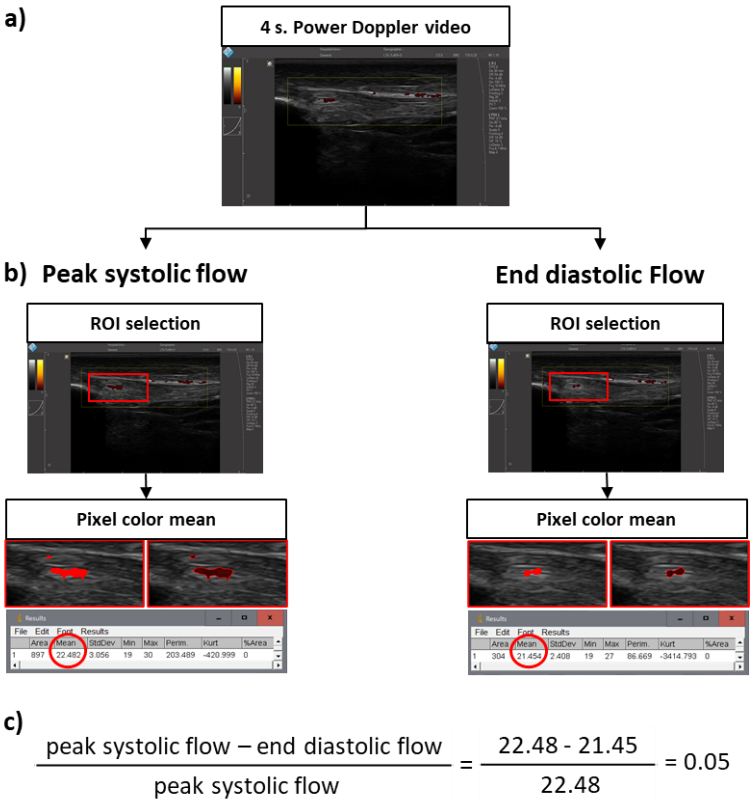

Figure 2. Quantification of intratendinous vascular resistance using color pixel quantization (ImageJ). 4 s. power Doppler video (a), Selection of the ROIs and signal intensity measurement (b), Calculation of vascular resistance through the resistance index formula (c).

7.2.2.3. Textural analysis of patellar tendon

The textural analysis of the tendon was performed on B-mode ultrasound images, both in longitudinal and transverse sections. The resulting bitmaps had a resolution of 660x 556 pixels (16.5 px/mm) with 256 gray levels and were stored as .TIFF files without compression or losses (Wiggins et al. 2001). Image processing and analysis were performed by the same researcher using ImageJ (v. 1.53) software. This researcher, who was blind to the diagnosis, selected the ROI using the ROI Manager application for ImageJ, which were 165 x 42 px for longitudinal section and 247 x 42 px for transverse section on an 8-bit gray scale. In the transverse section, the ROI was placed in the center of the tendon. In both cases the ROIs were prevented from crossing the paratendon as shown in **figure 3.**

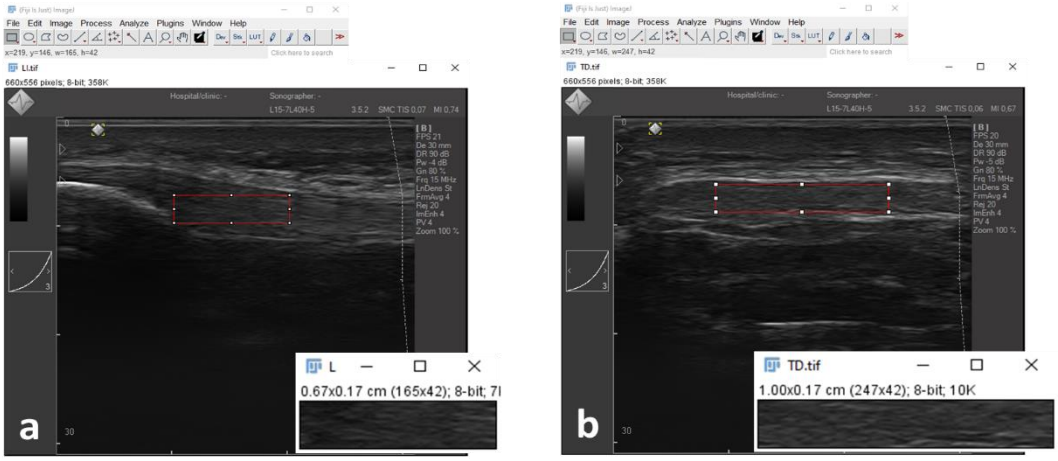

Figure 3. ROI selection in the patellar tendon. a) Longitudinal section; b) transverse section.

Echointensity (EI) and echovariation (EV), a variable that can be interpreted as a textural parameter (Ríos-Díaz et al. 2015), was determined by the relation between standard deviation and mean pixel intensity obtained from the histogram. This methodology has a good reliability and reproducibility (Ríos-Díaz et al. 2010b).

EV =σ/μ • 100 where σ is the standard deviation of the image intensities, and μ is the mean value of intensity in each ROI.

For convenience and henceforth we will refer to both EI and EV as echotextural parameters to differentiate them from other ultrasound variables.

7.2.3. Sample size

This study has an exploratory objective, so a sample of 27 subjects with chronic unilateral tendinopathy and a control group of asymptomatic subjects were recruited in a non-random, intentional, and consecutive manner.

7.2.4. Statistical methods

Data analysis was conducted with the statistical package R v.3.6 and JASP Team (2020). JASP (Version 0.14.1) [Computer software], and Morey, R. D., & Rouder, J. N. (2015). BayesFactor (Version 0.9.11-3) [Computer software].

Data were summarized by mean and standard deviation and range and quartiles for continuous variables and absolute and relative frequencies for categorical variables.

1) For the comparisons of presence of abnormal thermal asymmetry, presence of DS, presence of bilateral DS, presence of abnormal VR and presence of bilateral abnormal VR between control and tendinopathy group, odds ratio (95% interval of confidence) and p-values (level of significance ≤.05) were obtained with logistic regression analysis (Kleinbaum y Klein 2010; Field et al. 2012).

2) For the comparisons of thermographic, vascular, and textural ultrasonographic differences between patients and controls, independent sample means were compared by Bayesian statistics. We provide the Bayes factor (BF_{10}) interpreted as the number of times that the observations are more likely to support the hypothesis of interest than the null hypothesis (in this case no differences). It is a direct indicator of the degree of evidence provided by the observations and will be considered anecdotal (BF 1 to 3), moderate BF (3 to 10), strong (10 to 30), very strong (30 to 100) and extreme (>100). The median effect size and credibility intervals are also provided, and it will be assumed that if they contain 0, the differences between groups are no credible (Katki 2008; Rouder et al. 2009).

3) The comparisons for clinical variables, and thermographic, vascular and ultrasonographic parameters within the patient group were performed by paired sample means Bayesian analysis. In this case, two analysis were performed, the first one with all patients and the second one excluding the patients with bilateral intratendinous VR less than one.

4) Finally, to explore the relationship between VISA-P, time of evolution and thermal asymmetry with vascular and ultrasonographic parameter a Bayesian correlation analysis were performed. It was used Kendall's *tau-B* correlation coefficient for contrast with VISA-P (ordinal variable), time of evolution (no normal distribution) and Pearson's r coefficient for the contrasts between thermal asymmetry and vascular and ultrasonographic variables. In addition, the credibility interval for the coefficient, the effect size R^2%, and BF_{10} was showed (Ly et al. 2016, 2018).

7.3. RESULTS

7.3.1. Sample characterization and vascular assessment

Both age (mean dif.=6.8 years; 95%CI= 2.7 to 10.9 years; p-value= .001) and sex were significantly different (χ^2 =5.97; d.f=1; p-value=.0015) between the two groups and will therefore be entered as covariates in the models that require them.

The mean VISA-P score was 67.3 (S.D.=17.9) with a range from 29.0 to 94.0 points (median= 68.5; interquartile range= 56.3-81.5) and the mean time of evolution was 22.3 months (SD=16.9; range=3-60; median =13.5; IQR=12.0-34.5 months).

Table 1 shows the percentages between groups for the variables related to the presence of tendinopathy, DS, anomalous thermal differences, and anomalous intratendinous VR.

Sports practice was 3.2 times higher in the tendinopathy group than in the asymptomatic group (p-value= .055). About 90% of the participants in both groups had dominance in their right leg. Within the tendinopathy group, no relationship was found between the presence of tendinopathy and dominance (approximately 46% of the affected tendons were in the dominant leg).

In 73% of the cases the maximum temperature was recorded in the affected leg, although only 46% of the differences were abnormal (<0.5 ºC). However, an abnormal difference was found to be 7.3 times more likely among the tendinopathy group than among the asymptomatic group (p-value= .004).

In the tendinopathy group, DS were found in 85% of the affected tendons while DS also appeared in 50% of the unaffected tendons. DS also appeared in 30% of the tendons of asymptomatic subjects. However, the presence of DS in the tendons of patients (irrespective of whether it is the affected tendon or not) is 28.5 times more frequent (p-value <.001) than in asymptomatic subjects; and the presence of bilateral DS is 20.8 (p-value <.001) more likely in patients than in the control group.

Finally, in relation to the VR, it was found that abnormal RI was 25.3 times more likely in the tendinopathy group than in the asymptomatic group. In addition, bilateral RI was found in 33% of the patients.

7.3.2. Thermographic, vascular, and textural ultrasonographic differences between patients and controls

This section shows the analyses of the differences in absolute values between members for each of the groups **(table 2)**.

The absolute differences of temperature were greater (BF_{10}= 19) in patients than in controls with a strong evidence. The differences in area of DS also were greater (BF_{10}= 266 which is a extreme level of evidence.

The differences in maximum systolic velocity, final diastolic velocity, and VR show smaller values for patients than for controls, with a moderate to strong evidence (BF_{10}=17 for VR).

Respect to differences in echotextural parameters, only changes in EV (both longitudinal and transversal section) shows greater values in patients, especially in transversal section (BF_{10}=11). This means that EV between injury tendon and healthy tendon was greater than in controls (between both legs).

7.3.3. Thermographic, vascular, and textural ultrasonographic differences between injury and healthy tendons

In this section differences between injury and non-injury tendons (in patients' sample) are shown **(table 3)**.

For the temperature differences between the affected and healthy limb, strong evidence was found (BF_{10}= 14) in favor of the increase in temperature in the affected tendon (effect= 0.53 ºC; 95% CrI=0.15-0.95 ºC). Similarly, there is very strong evidence (BF_{10}= 71) in favor of a reduction in the VR in affected tendons compared to healthy tendons (effect=-0.67; 95% CrI=-1.10 - -0.25).

In relation to DS characteristics, there is moderate evidence (BF_{10}= 5.2) for increased DS area in the affected tendons (effect=0.44 mm^2; 95%ICr=0.09-0.84), and strong evidence for great maximum systolic velocity (BF_{10}= 17) and final diastolic velocity (BF_{10}= 18).

Since the presence of bilateral abnormal VR may affect the interpretation of thermal differences, a sensitivity analysis of these same variables was performed excluding cases with bilateral intratendinous VR (n=8), the results of which are shown in **table 4**.

In this case, the trends found are maintained, although the effect of the difference in temperatures and areas is slightly reduced. However, the VR (together with systolic and diastolic velocities), as expected, presents greater differences with extreme evidence (BF_{10}= 395) in favor of a decrease in the case of affected tendons (effect =-1.04; 95%ICr=-1.7 - -0.45).

The echotextural variables (EI and EV) also show no evidence of differences between pathological and healthy tendons in either longitudinal or cross-sectional ultrasound slices.

7.3.4. Relationships between clinic variables and thermographic, vascular, and textural ultrasonographic parameter

Finally, this section shows the relationships between the clinical variables VISA-P and time of evolution with the physiological parameters on the sample of injured tendons (note that in these cases only values of injury tendons was analyzed).

In addition, the correlations between the temperature differences between the affected and healthy limb with respect to the differences in vascular and ultrasound variables are shown in **table 5**.

VISA-P scores only showed a positive correlation (*tau-B*=.29; 95% CrI=.04-.51) with the thermal difference between members, although with a moderate degree of evidence.

The time of evolution was not related to any of the thermal, vascular or ultrasound variables.

The third point of interest was to determine the relationship between thermal asymmetry and the rest of the vascular and echotextural variables. In this regard, strong evidence of correlation was found between thermal asymmetry and the variables maximum systolic velocity (BF_{10}=128; r=.63; 95%CrI=.29 to .80), final diastolic velocity (BF_{10}=60; r=.59; 95%CrI=.24 to .78), and VR (BF_{10}=25; r=-.553; 95%CrI=-.75 to -.18). No correlations were found between thermal asymmetry and differences in EI and EV.

Table 1. Frequencies and Odds Ratios for sociodemographic variables and vascular parameters.

Variable	**Tendinopathy (n=26)**		**Healthy (n=27)**			
	n	**%**	**n**	**%**	**OR (95%IC)**	**p-value**
Sex (male)	21	80.8	12	44.4	5.4 (20.4 to 1.5)	**.006**
Sport practice	20	76.9	14	51.9	3.2 (0.87 to 11.2)	.055
Dominance leg (right)	24	92.3	24	88.9	1.5 (9.8 to 0.23)	.669
Injury leg (right)	12	46.2	--		--	--
Injury leg in dominant leg	12	46.2	--		--	--
Difference of temperature (abnormal)	12	46.2	3	11.1	7.3 (1.4 to 39.2)	**.004**
Knee with maximum temperature (injury)	19	73.1	--		--	--
Doppler Signal (tendons)	24	92.3	8	29.6	28.5 (5.4 to 150.2	**<.001**
Doppler Signal bilateral	11	42.3	1	3.7	19.1 (2.2 to 162.2)	**<.001**
Doppler Signal injury leg	22	84.6	--		--	--
Doppler Signal no-injury leg	13	50.0	--		--	--
Vascular resistance (abnormal)	22	84.6	5	18.5	28.9 (5.2 to 140.0)	**<.001**
Vascular resistance bilateral (abnormal)	8	30.8	0	0.0	--	--

The reference categories marked in parentheses have been used to calculate the odds ratios (OR).

Table 2. Thermographic, vascular and ultrasonographic differences between patients and controls.

Variable	Group	Mean	SD	Min	Q1	Median	Q3	Max	BF10	Efect size (median)	Lower 95% CrI	Upper 95% CrI	Evidence
Differences of temperature	Control	0.24	0.20	0.0	0.10	0.20	0.35	0.80	19	-0.72	-1.28	-0.19	Strong*
	Tendinopathy	0.49	0.36	0.0	0.20	0.40	0.78	1.5					
Differences of area Doppler	Control	0.42	0.85	0.0	0.00	0.00	0.30	3.40	266	-1.01	-1.56	-0.43	Extreme*
	Tendinopathy	2.1	1.91	0.0	0.83	1.7	2.7	9.2					
Differences of Maximum sistolic velocity	Control	5.6	9.52	0.0	0.0	0.00	11.1	23.2	4.3	-0.54	-1.08	-0.09	Moderate*
	Tendinopathy	12.0	11.08	0.0	1.0	12.7	22.9	25.5					
Differences of Final distolic velocity	Control	3.7	7.95	0.0	0.0	0.0	0.0	20.9	18	-0.71	-1.28	-0.19	Strong*
	Tendinopathy	11.1	10.18	0.0	0.4	19.2	20.3	23.5					
Differences of Vascular Resistance	Control	0.17	0.36	0.0	0.0	0.0	0.0	1.00	17	-0.71	-1.27	-0.19	Strong*
	Tendinopathy	0.49	0.42	0.0	0.0	0.8	0.9	1.0					
Differences of Echointensity longitudinal	Control	6.4	4.58	0.0	2.6	6.7	8.7	18.8	0.7	0.30	0.02	0.77	--
	Tendinopathy	5.1	4.29	0.3	1.6	4.0	7.4	15.5					
Differences of Echovariation longitudinal	Control	3.7	3.35	0.0	0.9	3.3	4.5	12.7	5.6	-0.569	-1.12	-0.10	Moderate*
	Tendinopathy	7.7	7.99	0.0	1.9	5.3	10.9	34.0					
Differences of Echointensity transversal	Control	3.8	2.54	0.1	1.9	3.2	5.4	10.1	0.3	-0.18	-0.60	-0.01	--
	Tendinopathy	4.0	3.64	0.3	1.6	2.4	5.9	15.6					
Differences of Echovariation transversal	Control	3.5	2.70	0.2	1.5	2.9	5.8	9.4	11	-0.657	-1.21	-0.15	Strong*
	Tendinopathy	7.2	6.38	0.0	2.6	6.0	8.5	25.8					

SD: standard deviation. Min: minimum. Q1: 1st quartile. Q3: 3rd quartile. Max: maximum. BF_{10}: Bayes factor as the number of times in favor of the evidence of the alternative hypothesis over the null hypothesis. 95% CrI: 95% credible interval. *: a priori unilateral contrast. **: a priori bilateral contrast

Table 3. Thermographic, vascular and ultrasonographic differences between injury tendons and healthy tendons.

Variables (n=26)	Mean	SD	Min	Q1	Median	Q3	Max	BF_{10}	Efect size (median)	Lower 95%CrI	Upper 95%CrI	Evidence
Temperature injury leg (°C)	31.1	1.66	27.9	30.1	31.3	32.7	33.8	14	0.53	0.15	0.95	Strong*
Temperature no-injury leg (°C)	30.8	1.71	27.7	29.9	31.1	32.0	33.9					
Area injury leg (mm^2)	2.57	2.41	0.00	1.03	1.95	3.55	9.20	5.2	0.44	0.09	0.84	Moderate*
Area no-injury leg (mm^2)	1.34	2.12	0.00	0.00	0.20	1.78	9.10					
Maximum sistolic velocity injury leg	19.6	8.62	0.0	21.9	22.4	23.7	26.9	17	0.55	0.16	0.97	Strong*
Maximum sistolic velocity no-injury leg	11.0	11.27	0.0	0.0	10.0	22.1	23.6					
Final distolic velocity injury leg	16.5	8.3	0.0	19.0	20.2	20.6	23.5	18	0.55	0.16	0.97	Strong*
Final distolic velocity no-injury leg	8.6	10.3	0.0	0.0	0.0	19.6	21.7					
Vascular Resistance injury leg	0.31	0.35	0.05	0.10	0.15	0.30	1.00	71	-0.67	-1.10	-0.25	Very strong*
Vascular Resistance no-injury leg	0.69	0.44	0.05	0.13	1.00	1.00	1.00					
Echointensity longitudinal injury leg	22.5	8.48	5.9	17.6	22.9	28.8	36.6	0.27	-0.13	-0.50	0.24	–
Echointensity longitudinal no-injury leg	23.4	6.67	10.2	18.4	24.2	27.7	34.7					
Echovariation longitudinal injury leg	34.1	10.28	19.4	26.1	31.9	41.6	53.5	0.23	0.085	-0.28	0.45	–
Echovariation longitudinal no-injury leg	33.1	9.32	17.8	28.3	30.8	36.6	52.3					
Echointensity transversal injury leg	35.5	7.70	13.6	31.7	36.6	42.1	45.3	0.21	-0.021	-0.38	0.34	–
Echointensity transversal no-injury leg	35.7	7.11	23.4	29.4	35.1	43.1	47.1					
Echovariation transversal injury leg	31.0	7.65	22.3	25.4	28.3	34.6	48.9	0.27	0.14	-0.23	0.51	–
Echovariation transversal no-injury leg	29.5	8.73	20.4	23.5	26.4	32.0	53.3					

SD: standard deviation. Min: minimum. Q1: 1st quartile. Q3: 3rd quartile. Max: maximum. BF_{10}: Bayes factor as the number of times in favor of the evidence of the alternative hypothesis over the null hypothesis. 95% CrI: 95% credible interval. *: a priori unilateral contrast. **: a priori bilateral contrast

Table 4. Thermographic, vascular and ultrasonographic differences between injury tendons and healthy tendons (excluded bilateral resistance index).

Variables (n=26)	Mean	SD	Min	Q1	Median	Q3	Max	BF_{10}	Efect size (median)	Lower 95%CrI	Upper 95%CrI	Evidence
Temperature injury leg (°C)	31.2	1.73	27.9	30.1	31.1	32.7	33.8	7.2	0.56	0.12	1.06	Moderate*
Temperature no-injury leg (°C)	30.8	1.84	27.7	29.9	30.9	31.9	33.9					
Area injury leg (mm^2)	1.81	2.16	0.00	0.50	1.45	2.30	9.20	8.1	0.57	0.12	1.08	Moderate*
Area no-injury leg (mm^2)	0.27	0.55	0.00	0.00	0.00	0.30	1.80					
Maximum sistolic velocity injury leg	17.7	9.82	0.0	20.4	22.2	23.6	25.5	16	0.66	0.17	1.18	Strong*
Maximum sistolic velocity no-injury leg	5.9	9.87	0.0	0.0	0.0	15.0	23.1					
Final distolic velocity injury leg	14.7	9.4	0.0	4.8	19.7	20.5	23.5	26	0.71	0.21	1.25	Strong*
Final distolic velocity no-injury leg	3.3	7.5	0.0	0.0	0.0	0.0	19.6					
Vascular Resistance injury leg	0.37	0.40	0.05	0.11	0.16	0.81	1.00	395	-1.04	-1.65	-0.45	Extrema*
Vascular Resistance no-injury leg	0.95	0.19	0.18	1.00	1.00	1.00	1.00					
Echointensity longitudinal injury leg	21.3	7.78	5.9	17.6	22.0	27.9	32.1	0.48	-0.29	-0.72	-0.02	–
chointensity longitudinal no-injury leg	23.4	6.66	10.2	20.4	24.2	27.6	34.7					
Echovariation longitudinal injury leg	34.8	9.72	22.7	28.1	32.9	40.6	53.0	0.24	0.02	-0.41	0.04	–
Echovariation longitudinal no-injury leg	34.5	9.12	19.0	28.3	33.9	38.1	52.3					
Echointensity transversal injury leg	35.6	5.83	25.0	31.7	36.0	40.2	45.0	0.25	0.05	-0.38	0.48	–
Echointensity transversal no-injury leg	35.4	7.28	23.4	29.4	35.5	43.1	46.1					
Echovariation transversal injury leg	30.5	7.39	22.3	25.1	27.7	34.6	48.9	0.25	0.06	-0.37	0.49	–
Echovariation transversal no-injury leg	29.7	8.78	21.5	24.3	26.8	30.4	53.3					

SD: standard deviation. Min: minimum. Q1: 1st quartile. Q3: 3rd quartile. Max: maximum. BF_{10}: Bayes factor as the number of times in favor of the evidence of the alternative hypothesis over the null hypothesis. 95% CrI: 95% credible interval. *: a priori unilateral contrast. **: a priori bilateral contrast

Table 5. Correlations between clinical variables and thermal asymmetry with vascular and ultrasonographic parameters.

Variables (for patients n=26)	R	Lower 95%CrI	Upper 95%CrI	R^2%	BF10	Evidence
VISA-P (for injury tendons) Kendall's tau-B						
Evolution Time	-.18	-.41	-.02	3%	1.0	Anecdotal*
Difference temperature	.29	.04	.51	8%	3.8	Moderate*
Area Doppler	-.15	-.39	-.01	2%	0.7	--
Maximum sistolic velocity	-.17	-.41	-.01	3%	0.9	--
Final distolic velocity	.00	-.29	-.01	0%	0.3	--
Vascular Resistance	-.13	-.38	-.01	2%	0.6	--
Echointensity longitudinal	.12	.01	.37	1%	0.6	--
Echovariation longitudinal	-.13	-.38	-.01	2%	0.6	--
Echointensity transversal	.02	.01	.30	0%	0.3	
Echovariation transversal	-.19	-.43	-.02	4%	1.1	Anecdotal*
Evolution Time (for injury tendons) Kendall's tau-B						
Difference temperature	-.14	-.38	-.01	2%	0.7	--
Area Doppler	.04	-.22	.29	0%	0.3	--
Maximum sistolic velocity	.11	-.16	.35	1%	0.3	--
Final distolic velocity	.18	-.09	.41	3%	0.6	--
Vascular Resistance	-.02	-.27	.23	.1%	0.3	--
Echointensity longitudinal	-.07	-.32	.19	.5%	0.3	--
Echovariation longitudinal	-.08	-.33	.18	.7%	0.3	--
Echointensity transversal	.08	-.18	.32	.7%	0.3	--
Echovariation transversal	.09	-.17	.33	.8%	0.3	--

(continua)

Variables (for patients n=26)	R	Lower 95%CrI	Upper 95%CrI	R^2%	BF10	Evidence
Difference of temperature (between injury and no-injury tendons) Pearson's r						
Diferences Area Doppler	.35	.04	.63	12%	1.9	Anecdotal*
Diferences Maximum sistolic velocity	.63	.29	.80	39%	128	Extreme*
Diferences Final distolic velocity	.59	.24	.78	35%	60	Very Strong*
Diferences Vascular Resistance	-.55	-.75	-.18	30%	25	Strong*
Diferences Echointensity longitudinal	.14	.01	.50	2%	0.5	--
Diferences Echovariation longitudinal	.04	-.34	.40	0%	0.2	--
Diferences Echointensity transversal	.07	-.31	.42	0%	0.3	--
Diferences Echovariation transversal	.15	-.24	.48	2%	0.3	--

R: coefficient of correlation (Pearson's r or Kendall's tau-B). R^2%: size effect. BF10: Bayes factor as the number of times in favor of the evidence of the alternative hypothesis over the null hypothesis. 95% CrI: 95% credible interval. *: a priori unilateral contrast; **: a priori bilateral contrast.

7.4. DISCUSION

7.4.1. Technical issues

Quantitative analysis on thermal imaging depends on the selection of the ROI (Ludwig et al. 2014; Molina-Payá et al. 2021b). Previous studies in which patellar tendons were analyzed included the entire knee area (Mangine et al. 1987; Seixas, A et al. 2013). By selecting a ROI of the entire knee, specificity is lost by including other structures that may alter the result. In this study, a previously designed protocol was used for the specific selection of the patellar tendon in which excellent intraobserver and interobserver reliability was found for both the variables of ROI position and size and mean temperature with all the lower limits of the intraclass correlation coefficient below 0.84 without biases (Molina-Payá et al. 2021b).

The quantification of DS is performed through the automatic calculation of the RI by the ultrasound scanner, measuring over a single vessel (Albrecht et al. 2008; Xu et al. 2020; Chen et al. 2021). At the intratendinous level, we can find a high number of vessels and of a small size that make it difficult to calculate the intratendinous RV. Some authors have tried to solve this problem by calculating the mean RI of the 3 largest vessels (Terslev et al. 2003a; Koenig et al. 2007a, 2007b). In this study, and with the aim of being able to average the RV of all the intratendinous vessels, a previously developed methodology based on pixel color intensity has been used, with excellent reliability (Molina-Payá et al. 2021a).

7.4.2. Differences between patients and controls

The skin temperature distribution of a healthy human body presents a contralateral symmetry (Houdas y Ring 1982) therefore, a thermal asymmetry may be an indicator of abnormality (Uematsu et al. 1988). When comparing the thermal difference between the knees of the patients and the control group, a greater thermal difference was observed in the patient group, these results are similar to those of Seixas et al. (2013) who analyzed the temperature of the knees of twenty male volleyball players suggesting that even mild tendinopathy can affect the skin

temperature of the affected knee when compared with control group with no history of tendon pathology.

Eighty-five percent of the affected tendons of the patients and 50% of the unaffected ones presented intratendinous DS, although it should be noted that 30% of the asymptomatic subjects also presented this finding. Other authors have also found similar percentages of presence of DS (29%) in asymptomatic athletes (Sengkerij et al. 2009). These data may suggest that the presence of intratendinous DS is not always a pathological sign (Peers et al. 2003; Reiter et al. 2004). This idea is reinforced by findings that intratendinous DS can increase with exercise, even in asymptomatic patients (Malliaras et al. 2008; Koenig et al. 2010; Boesen et al. 2011). In addition, intratendinous flow may appear as part of the normal adaptive physiological response to loading (Tol et al. 2012). In our study, the presence of DS in patients' tendons was found about 29 times more frequent than in asymptomatic subjects, so we cannot completely rule out this variable as one of the signs present in tendon pathology (Alfredson y Ohberg 2005; Pufe et al. 2005). The greater presence of DS bilaterally in patients reinforces the idea that this parameter is a sign to be considered, as there is a greater probability of finding similar deterioration in the contralateral tendon as well (Rabello et al. 2020).

In this study, intratendinous VR was calculated by image analysis of intratendinous DS and using the RI formula. As with the RI, a low value is associated with low peripheral resistance and high perfusion of the distal bed and therefore a situation compatible with the inflammatory process (Bjordal et al. 2006; Koenig et al. 2007a). A low VR was 25.3 times more likely to be found in patients than in the control group, and strong evidence (BF10 = 71) of finding a lower RV in affected tendons than in healthy ones, which added to the higher temperature observed in affected tendons, indicates to us a probable inflammatory process, in line with the current trend to consider tendinopathy as a pathophysiological process in which degenerative and inflammatory state coexist (Fredberg y Stengaard-Pedersen 2008; Tang et al. 2018).

In relation to echotextural parameters, echointensity has been extensively studied in the musculoskeletal system (Ríos-Díaz et al. 2010c; Suydam y Buchanan 2014; Kim et al. 2021), while very few authors have analyzed the variable of EV, focusing mainly on muscle and nervous tissue (Martínez-Payá et al. 2017a, 2017b;

Härtig et al. 2018), despite the fact that echogenicity could provide more information on the structural characteristics of the tissue than echogenicity, which provides only the mean intensity. When analyzing changes in EV among patients' tendons, higher values have been observed than in controls, reflecting changes in the ultrastructural pattern of the tendon, probably caused by a degenerative process. Although the presence of hypoechogenic regions and thickening in symptomatic tendons has been described (Malliaras et al. 2010), we have not found changes at the EI level between both groups, probably because we can find hypoechogenic regions in asymptomatic patellar tendons (Cook et al. 2001a).

7.4.3. Differences between injury and healthy tendons

In this study, symptomatic patellar tendons showed thermal asymmetry, as defined by other authors (Goodman et al. 1986; Mangine et al. 1987; Uematsu et al. 1988). This thermal asymmetry is shown as a warm pattern of the affected tendon (effect = 0.53 ºC; 95% CrI = 0.15-0.95 ºC), although only 46% of the differences were greater than 0.5ºC, which despite being a low percentage, is 7.3 times more likely to find this warm pattern in the patients than in the control group. This same warm pattern has also been observed in other studies (Mangine et al. 1987; Seixas, A et al. 2013) and in other types of tendinopathies (Binder et al. 1983; Meknas et al. 2008; Rodriguez-Sanz et al. 2018).

Of note, two patients presented an affected tendon with a cold pattern with respect to the contralateral one. Some authors have attributed this cold pattern to chronic PT (Mangine et al. 1987; Hildebrandt et al. 2010). In the results analyzed, we found no relationship between chronicity and temperature, vascular or echotexture variables, so we discard this hypothesis. Moreover, this association does not correspond with current studies that propose a coexistence of the inflammatory and degenerative process in tendinopathies (Abate et al. 2009; Rees et al. 2014; Millar et al. 2017). Along these lines, there is a possibility that the asymptomatic contralateral tendon presents an inflammatory process (Millar et al. 2017) with an increase in temperature, decreasing the thermal difference with the affected tendon or even showing a higher temperature, showing the symptomatic tendon hypothermic. This hypothesis is reinforced by observing that in the control group tendons with thermal asymmetry greater than 0.5 ºC appear despite being

asymptomatic, in this same line Liu et al. found 27.8% of asymptomatic collegiate athletes with thermal asymmetry greater than 0.5 ºC (Liu et al. 2020).

To avoid the possibility that an asymptomatic inflammatory process of the contralateral tendon could alter the thermal difference, a sensitivity analysis of the same variables was performed excluding cases with a bilateral anomalous VR, observing a similar trend in the results. Another hypothesis put forward is that this cold pattern is due to an activation of the sympathetic nervous system, which decreases microcirculation and local perfusion (Ackermann 2014; Tansey y Johnson 2015). The temperature of the skin overlying the patellar tendon may directly reflect underlying vascular disturbance and tissue metabolism, and thus could translate into a cold pattern, although it is unknown whether these effects occur before the tendon becomes painful and at what level they become clinically relevant (Tumilty et al. 2019).

We noted that, unlike between groups, there was only moderate evidence (BF10 = 5.2) of an increase in DS area in affected tendons. In contrast, there was strong evidence (BF10 = 71) of abnormal VR in affected tendons compared to healthy tendons, suggesting that analysis of intratendinous VR may provide more clinical information than Doppler area quantification.

Although higher values of EV were found in the tendons of the patients than in those of the control group, these changes were not reflected when comparing the affected tendons of the patients with the asymptomatic contralateral tendon, and no changes in EI or EV were evidenced. This finding is probably because the contralateral asymptomatic tendon may also be undergoing degenerative echotextural changes even though it is asymptomatic.

We should keep in mind that a direct relationship between pathological imaging and symptomatology cannot always be established (Kulig et al. 2014; McAuliffe et al. 2016; Splittgerber y Ihm 2019), since pathological images have been found in asymptomatic subjects, and symptomatic tendons in normal images (Lian et al. 1996; Cook et al. 1998), even some abnormality images may be due to different factors, such as an adaptation of the collagen fibers to the activity performed (Hagan et al. 2018).

7.4.4. Relationships between clinic variables and thermographic, vascular, and textural ultrasonographic parameter

The thermal difference between patients' knees has shown a correlation with the VISA-P score. This result is in line with the literature consulted, where a positive correlation was found between pain and thermal abnormalities (Mangine et al. 1987). Seixas et al. (2013) also reported that increased skin temperature in the knee of subjects affected by TR could be correlated with a decrease in the VISA-P scale score. In this study, and being a correlation with a moderate degree of evidence, we must make reference to the fact that not always symptomatology is accompanied by changes in physiological parameters or in the imaging techniques themselves (Vecchio et al. 1992; Splittgerber y Ihm 2019; Docking et al. 2021).

Currently, it has been revealed that the presence of intratendinous hypervascularization does not necessarily correspond with pain or patient's clinic (De Jonge et al. 2014; De Marchi et al. 2018; Zabrzyński et al. 2018; Järvinen 2019) in our study this relationship was also not found.

Contrary to what we have observed in the analysis of thermal asymmetry, the lack of an association between the analyzed variables of echotexture and knee pain and functionality (VISA-P), might suggest that the use of EI and EV as biomarkers may not be the best to characterize TR symptomatology.

Thermal asymmetry and abnormal intratendinous RV can be considered signs of an inflammatory process, and as expected, strong evidence of negative correlation between them has been found in this study. In contrast, no relationship has been found between these variables and the time of evolution, probably because during the evolution of the pathology the inflammatory process may be present to a greater or lesser extent (Millar et al. 2017). Nor has a correlation been found between thermal asymmetry and differences in EI and EV, although we must keep in mind that in the case of ultrasound structural changes are analyzed, and with IRT physiological changes are studied (Gabrhel et al. 2012).

7.4.5. Limitations of the study

The methodology used in this study is highly reliable. However, it has several limitations. First, both age and sex were significantly different between the two

groups. These variables can be considered as influencing factors in the thermographic recording performed in this study (Fernández-Cuevas et al. 2015). To minimize the influence of these variables, the analysis was performed on the thermal differences between knees and statistical analysis was adjusted by sex.

The type of sport practiced by the participants was also not considered, being able to affect, to a greater or lesser extent, the structural or physiological characteristics of the patellar tendon (Lian et al. 1996; Hagan et al. 2018; Florit et al. 2019). The analysis of the influence of the type of sport on the thermal, echotextural and vascular variables analyzed in this study could provide information about the impact of the type of sport on the patellar tendon.

Due to the complexity and time required in performing these image analyses, their application in daily clinical practice may be difficult. It would be interesting to conduct future research to incorporate these image analysis tools into ultrasound devices in collaboration with engineers and manufacturers.

7.5. CONCLUSION

Athletes with PT have shown a greater thermal difference, a larger area of DS, a lower intratendinous VR and a moderately higher EV than controls

In patients' group, the affected tendon presents with a higher temperature, a lower intratendinous VR, a moderately higher DS area and no differences between EI and EV parameters with respect to the contralateral asymptomatic tendon.

A relationship has been found between a greater temperature difference between patellar tendons and increased pain and decreased functionality of the patient's knee as measured by the VISA-P scale.

Athletes with tendinopathy have shown a correlation between thermal asymmetry and low intratendon VR, these inflammatory signs could be related to the coexistence of the degenerative and inflammatory process in PT.

7.6. REFERENCES

1. Abate M, Silbernagel KG, Siljeholm C, Di Iorio A, De Amicis D, Salini V, et al. Pathogenesis of tendinopathies: inflammation or degeneration? Arthritis Res Ther. 2009;11(3):235.
2. Ackermann P W. Neuronal pathways in tendon healing and tendinopathy - update. Front Biosci. 2014;19(8):1251.
3. Albrecht K, Grob K, Lange U, Müller-Ladner U, Strunk J. Reliability of different Doppler ultrasound quantification methods and devices in the assessment of therapeutic response in arthritis. Rheumatology (Oxford). octubre de 2008;47(10):1521-6.
4. Alfredson H, Ohberg L. Sclerosing injections to areas of neo-vascularisation reduce pain in chronic Achilles tendinopathy: a double-blind randomised controlled trial. Knee Surg Sports Traumatol Arthrosc. mayo de 2005;13(4):338-44.
5. Alfredson H, Ohberg L, Forsgren S. Is vasculo-neural ingrowth the cause of pain in chronic Achilles tendinosis? An investigation using ultrasonography and colour Doppler, immunohistochemistry, and diagnostic injections. Knee Surg Sports Traumatol Arthrosc. septiembre de 2003;11(5):334-8.
6. Ammer K, Ring F. Quality Assurance Procedures and Infrared Equipment Operation. En: The Thermal Human Body: A Practical Guide to Thermal Imaging. CRC Press; 2019. p. 177-90.
7. Andersson G, Danielson P, Alfredson H, Forsgren S. Nerve-related characteristics of ventral paratendinous tissue in chronic Achilles tendinosis. Knee Surg Sports Traumatol Arthr. 28 de septiembre de 2007;15(10):1272-9.
8. Benítez-Martínez JC, Valera-Garrido F, Martínez-Ramírez P, Ríos-Díaz J, Del Baño-Aledo ME, Medina-Mirapeix F. Lower Limb Dominance, Morphology, and Sonographic Abnormalities of the Patellar Tendon in Elite Basketball Players: A Cross-Sectional Study. J Athl Train. diciembre de 2019;54(12):1280-6.
9. Binder A, Parr G, Thomas RP, Hazleman B. A CLINICAL AND THERMOGRAPHIC STUDY OF LATERAL EPICONDYLITIS. Rheumatology. 1983;22(2):77-81.

10. Bjordal JM, Lopes-Martins RAB, Iversen VV. A randomised, placebo controlled trial of low level laser therapy for activated Achilles tendinitis with microdialysis measurement of peritendinous prostaglandin E2 concentrations. Br J Sports Med. enero de 2006;40(1):76-80.
11. Boesen AP, Boesen MI, Koenig MJ, Bliddal H, Torp-Pedersen S, Langberg H. Evidence of accumulated stress in Achilles and anterior knee tendons in elite badminton players. Knee Surg Sports Traumatol Arthrosc. enero de 2011;19(1):30-7.
12. Chen S-J, Liu R-R, Shang Y-R, Xie Y-J, Guo X-H, Huang M-J, et al. An Ultrasound Model to Predict the Short-Term Effects of Endovascular Stent Placement in the Treatment of Carotid Artery Stenosis. Front Cardiovasc Med. 22 de enero de 2021;7:607367.
13. Cook JL, Khan KM, Harcourt PR, Kiss ZS, Fehrmann MW, Griffiths L, et al. Patellar tendon ultrasonography in asymptomatic active athletes reveals hypoechoic regions: a study of 320 tendons. Victorian Institute of Sport Tendon Study Group. Clin J Sport Med. abril de 1998;8(2):73-7.
14. Cook JL, Khan KM, Kiss ZS, Coleman BD, Griffiths L. Asymptomatic hypoechoic regions on patellar tendon ultrasound: A 4-year clinical and ultrasound followup of 46 tendons. Scand J Med Sci Sports. diciembre de 2001a;11(6):321-7.
15. Cook JL, Khan KM, Kiss ZS, Purdam CR, Griffiths L. Reproducibility and clinical utility of tendon palpation to detect patellar tendinopathy in young basketball players. Victorian Institute of Sport tendon study group. Br J Sports Med. febrero de 2001b;35(1):65-9.
16. De Jonge S, Warnaars JLF, De Vos RJ, Weir A, van Schie HTM, Bierma-Zeinstra SMA, et al. Relationship between neovascularization and clinical severity in Achilles tendinopathy in 556 paired measurements. Scand J Med Sci Sports. octubre de 2014;24(5):773-8.
17. De Marchi A, Pozza S, Cenna E, Cavallo F, Gays G, Simbula L, et al. In Achilles tendinopathy, the neovascularization, detected by contrast-enhanced ultrasound (CEUS), is abundant but not related to symptoms. Knee Surg Sports Traumatol Arthrosc. julio de 2018;26(7):2051-8.

18. Docking SI, Rio E, Girdwood MA, Hannington MC, Cook JL, Culvenor AG. Physical Activity and Investigation With Magnetic Resonance Imaging Partly Explain Variability in the Prevalence of Patellar Tendon Abnormalities: A Systematic Review With Meta-analysis of Imaging Studies in Asymptomatic Individuals. J Orthop Sports Phys Ther. 1 de mayo de 2021;51(5):216-31.

19. Fernández-Cuevas I, Bouzas Marins JC, Arnáiz Lastras J, Gómez Carmona PM, Piñonosa Cano S, García-Concepción MÁ, et al. Classification of factors influencing the use of infrared thermography in humans: A review. Infrared Physics & Technology. 1 de julio de 2015;71:28-55.

20. Ferretti A, Ippolito E, Mariani P, Puddu G. Jumper's knee. Am J Sports Med. abril de 1983;11(2):58-62.

21. Field AP, Miles J, Field Z. Discovering statistics using R. London ; Thousand Oaks, Calif: Sage; 2012.

22. Florit D, Pedret C, Casals M, Malliaras P, Sugimoto D, Rodas G. Incidence of Tendinopathy in Team Sports in a Multidisciplinary Sports Club Over 8 Seasons. J Sports Sci Med. 19 de noviembre de 2019;18(4):780-8.

23. Fredberg U, Stengaard-Pedersen K. Chronic tendinopathy tissue pathology, pain mechanisms, and etiology with a special focus on inflammation. Scand J Med Sci Sports. febrero de 2008;18(1):3-15.

24. Frizziero A, Trainito S, Oliva F, Nicoli Aldini N, Masiero S, Maffulli N. The role of eccentric exercise in sport injuries rehabilitation. Br Med Bull. junio de 2014;110(1):47-75.

25. Gabrhel J, Popracová Z, Tauchmannová H, Chvojka Z. The Relationship Between Thermographic and Musculoskeletal Ultrasound Findings in the—Painful Knee Syndrome. Thermology international. 2012;12(2):43-52.

26. Goodman PH, Murphy MG, Siltanen GL, Kelley MP, Rucker L. Normal temperature asymmetry of the back and extremities by computer-assisted infrared imaging. Thermology. 1986;1(4):194-202.

27. Hagan KL, Hullfish TJ, Casey E, Baxter JR. Tendon Structure Quantified using Ultrasound Imaging Differs Based on Location and Training Type. J Appl Physiol (1985). 27 de septiembre de 2018;

28. Härtig F, Ross M, Dammeier NM, Fedtke N, Heiling B, Axer H, et al. Nerve Ultrasound Predicts Treatment Response in Chronic Inflammatory Demyelinating Polyradiculoneuropathy-a Prospective Follow-Up. Neurotherapeutics. abril de 2018;15(2):439-51.

29. Hildebrandt C, Raschner C, Ammer K. An Overview of Recent Application of Medical Infrared Thermography in Sports Medicine in Austria. Sensors (Basel). 7 de mayo de 2010;10(5):4700-15.

30. Houdas Y, Ring EFJ. Human Body Temperature: Its Measurement and Regulation [Internet]. Springer US; 1982 [citado 23 de agosto de 2021]. Disponible en: https://www.springer.com/gp/book/9780306408724

31. James Selfe JW. A narrative literature review identifying the minimum clinically important difference for skin temperature asymmetry at the knee. Thermology International. 2008;18:51-4.

32. Järvinen TA. Neovascularisation in tendinopathy: from eradication to stabilisation? Br J Sports Med. 8 de octubre de 2019;

33. Katki HA. Invited Commentary: Evidence-based Evaluation of p Values and Bayes Factors. American Journal of Epidemiology. 30 de junio de 2008;168(4):384-8.

34. Kettunen JA, Kvist M, Alanen E, Kujala UM. Long-term prognosis for jumper's knee in male athletes. A prospective follow-up study. Am J Sports Med. octubre de 2002;30(5):689-92.

35. Khan KM, Bonar F, Desmond PM, Cook JL, Young DA, Visentini PJ, et al. Patellar tendinosis (jumper's knee): findings at histopathologic examination, US, and MR imaging. Victorian Institute of Sport Tendon Study Group. Radiology. septiembre de 1996;200(3):821-7.

36. Kim D-H, Choi J-H, Park C-H, Park H-J, Yoon K-J, Lee Y-T. The Diagnostic Significance of Ultrasonographic Measurement of the Achilles Tendon Thickness for the Insertional Achilles Tendinopathy in Patients with Heel Pain. JCM. 17 de mayo de 2021;10(10):2165.

37. Kleinbaum DG, Klein M. Logistic Regression [Internet]. New York, NY: Springer New York; 2010 [citado 7 de enero de 2022]. (Statistics for Biology

and Health). Disponible en: http://link.springer.com/10.1007/978-1-4419-1742-3

38. Koenig MJ, Torp-Pedersen S, Boesen MI, Holm CC, Bliddal H. Doppler ultrasonography of the anterior knee tendons in elite badminton players: colour fraction before and after match. Br J Sports Med. febrero de 2010;44(2):134-9.

39. Koenig MJ, Torp-Pedersen S, Holmich P, Terslev L, Nielsen MB, Boesen M, et al. Ultrasound Doppler of the Achilles tendon before and after injection of an ultrasound contrast agent--findings in asymptomatic subjects. Ultraschall Med. febrero de 2007a;28(1):52-6.

40. Koenig MJ, Torp-Pedersen ST, Christensen R, Boesen MI, Terslev L, Hartkopp A, et al. Effect of knee position on ultrasound Doppler findings in patients with patellar tendon hyperaemia (jumper's knee). Ultraschall Med. octubre de 2007b;28(5):479-83.

41. Korakakis V, Whiteley R, Kotsifaki A, Stefanakis M, Sotiralis Y, Thorborg K. A systematic review evaluating the clinimetric properties of the Victorian Institute of Sport Assessment (VISA) questionnaires for lower limb tendinopathy shows moderate to high-quality evidence for sufficient reliability, validity and responsiveness—part II. Knee Surg Sports Traumatol Arthrosc [Internet]. 16 de abril de 2021 [citado 23 de agosto de 2021]; Disponible en: https://doi.org/10.1007/s00167-021-06557-0

42. Kulig K, Oki KC, Chang Y-J, Bashford GR. Achilles and patellar tendon morphology in dancers with and without tendon pain. Med Probl Perform Art. diciembre de 2014;29(4):221-8.

43. Lian O, Holen KJ, Engebretsen L, Bahr R. Relationship between symptoms of jumper's knee and the ultrasound characteristics of the patellar tendon among high level male volleyball players. Scand J Med Sci Sports. octubre de 1996;6(5):291-6.

44. Lian OB, Engebretsen L, Bahr R. Prevalence of jumper's knee among elite athletes from different sports: a cross-sectional study. Am J Sports Med. abril de 2005;33(4):561-7.

45. Lind B, Ohberg L, Alfredson H. Sclerosing polidocanol injections in mid-portion Achilles tendinosis: remaining good clinical results and decreased tendon thickness at 2-year follow-up. Knee Surg Sports Traumatol Arthrosc. diciembre de 2006;14(12):1327-32.

46. Liu L, Gisselman AS, Tumilty S. Thermal profiles over the Patella tendon in a cohort of non-injured collegiate athletes over the course of a cross-country season. Phys Ther Sport. julio de 2020;44:47-52.

47. López-Royo MP, Ríos-Díaz J, Galán-Díaz RM, Herrero P, Gómez-Trullén EM. A Comparative Study of Treatment Interventions for Patellar Tendinopathy: A Randomized Controlled Trial. Arch Phys Med Rehabil. mayo de 2021;102(5):967-75.

48. Ludwig N, Formenti D, Gargano M, Alberti G. Skin temperature evaluation by infrared thermography: Comparison of image analysis methods. Infrared Physics & Technology. enero de 2014;62:1-6.

49. Ly A, Marsman M, Wagenmakers E-J. Analytic posteriors for Pearson's correlation coefficient. Statistica Neerlandica. 2018;72(1):4-13.

50. Ly A, Verhagen J, Wagenmakers E-J. Harold Jeffreys's default Bayes factor hypothesis tests: Explanation, extension, and application in psychology. Journal of Mathematical Psychology. 1 de junio de 2016;72:19-32.

51. Malliaras P, Cook J, Purdam C, Rio E. Patellar Tendinopathy: Clinical Diagnosis, Load Management, and Advice for Challenging Case Presentations. J Orthop Sports Phys Ther. noviembre de 2015;45(11):887-98.

52. Malliaras P, Purdam C, Maffulli N, Cook J. Temporal sequence of greyscale ultrasound changes and their relationship with neovascularity and pain in the patellar tendon. Br J Sports Med. octubre de 2010;44(13):944-7.

53. Malliaras P, Richards PJ, Garau G, Maffulli N. Achilles tendon Doppler flow may be associated with mechanical loading among active athletes. Am J Sports Med. noviembre de 2008;36(11):2210-5.

54. Mangine RE, Siqueland KA, Noyes FR. The use of thermography for the diagnosis and management of patellar tendinitis. J Orthop Sports Phys Ther. 1987;9(4):132-40.

55. Martínez-Payá JJ, Del Baño-Aledo ME, Ríos-Díaz J, Tembl-Ferrairó JI, Vázquez-Costa JF, Medina-Mirapeix F. Muscular Echovariation: A New Biomarker in Amyotrophic Lateral Sclerosis. Ultrasound Med Biol. junio de 2017a;43(6):1153-62.

56. Martínez-Payá JJ, Ríos-Díaz J, del Baño-Aledo ME, Tembl-Ferrairó JI, Vazquez-Costa JF, Medina-Mirapeix F. Quantitative Muscle Ultrasonography Using Textural Analysis in Amyotrophic Lateral Sclerosis. Ultrason Imaging. noviembre de 2017b;39(6):357-68.

57. McAuliffe S, McCreesh K, Culloty F, Purtill H, O'Sullivan K. Can ultrasound imaging predict the development of Achilles and patellar tendinopathy? A systematic review and meta-analysis. Br J Sports Med. diciembre de 2016;50(24):1516-23.

58. Meknas K, Odden-Miland Å, Mercer JB, Castillejo M, Johansen O. Radiofrequency Microtenotomy: A Promising Method for Treatment of Recalcitrant Lateral Epicondylitis. Am J Sports Med. octubre de 2008;36(10):1960-5.

59. Millar NL, Murrell GAC, McInnes IB. Inflammatory mechanisms in tendinopathy - towards translation. Nat Rev Rheumatol. 25 de enero de 2017;13(2):110-22.

60. Molina-Payá FJ, Ríos-Díaz J, Carrasco-Martínez F, Martínez-Payá JJ. Reliability of a New Semi-automatic Image Analysis Method for Evaluating the Doppler Signal and Intratendinous Vascular Resistance in Patellar Tendinopathy. Ultrasound Med Biol. diciembre de 2021a;47(12):3491-500.

61. Molina-Payá J, Ríos-Díaz J, Martínez-Payá J. Inter and intraexaminer reliability of a new method of infrared thermography analysis of patellar tendon. Quantitative InfraRed Thermography Journal. 15 de marzo de 2021b;18(2):127-39.

62. Ohberg L, Lorentzon R, Alfredson H. Neovascularisation in Achilles tendons with painful tendinosis but not in normal tendons: an ultrasonographic investigation. Knee Surg Sports Traumatol Arthrosc. julio de 2001;9(4):233-8.

63. Peers KHE, Brys PPM, Lysens RJJ. Correlation between power Doppler ultrasonography and clinical severity in Achilles tendinopathy. Int Orthop. junio de 2003;27(3):180-3.

64. Pufe T, Petersen WJ, Mentlein R, Tillmann BN. The role of vasculature and angiogenesis for the pathogenesis of degenerative tendons disease. Scand J Med Sci Sports. agosto de 2005;15(4):211-22.

65. Rabello LM, van den Akker-Scheek I, Kuipers IF, Diercks RL, Brink MS, Zwerver J. Bilateral changes in tendon structure of patients diagnosed with unilateral insertional or midportion achilles tendinopathy or patellar tendinopathy. Knee Surg Sports Traumatol Arthrosc. mayo de 2020;28(5):1631-8.

66. Rees JD, Stride M, Scott A. Tendons--time to revisit inflammation. Br J Sports Med. noviembre de 2014;48(21):1553-7.

67. Reiter M, Ulreich N, Dirisamer A, Tscholakoff D, Bucek RA. Colour and power Doppler sonography in symptomatic Achilles tendon disease. Int J Sports Med. mayo de 2004;25(4):301-5.

68. Richards PJ, Win T, Jones PW. The distribution of microvascular response in Achilles tendonopathy assessed by colour and power Doppler. Skeletal Radiol. junio de 2005;34(6):336-42.

69. Rio E, Moseley L, Purdam C, Samiric T, Kidgell D, Pearce AJ, et al. The Pain of Tendinopathy: Physiological or Pathophysiological? Sports Med. 1 de enero de 2014;44(1):9-23.

70. Ríos-Díaz J, de Groot Ferrando A, Martínez-Payá JJ, del Baño Aledo ME. [Reliability and reproducibility of a morpho-textural image analysis method over a patellar ligament ultrasonography]. Reumatol Clin. diciembre de 2010a;6(6):278-84.

71. Ríos-Díaz J, de Groot Ferrando A, Martínez-Payá JJ, del Baño Aledo ME. Reliability and reproducibility of a morpho-textural image analysis method over a patellar ligament ultrasonography. Reumatología Clínica (English Edition). enero de 2010b;6(6):278-84.

72. Ríos-Díaz J, de Groot Ferrando A, Martínez-Payá JJ, del Baño Aledo ME. Reliability and reproducibility of a morpho-textural image analysis method

over a patellar ligament ultrasonography. Reumatología Clínica (English Edition). enero de 2010c;6(6):278-84.

73. Ríos-Díaz J, Martínez-Payá JJ, del Baño-Aledo ME, de Groot-Ferrando A, Botía-Castillo P, Fernández-Rodríguez D. Sonoelastography of Plantar Fascia: Reproducibility and Pattern Description in Healthy Subjects and Symptomatic Subjects. Ultrasound in Medicine & Biology. octubre de 2015;41(10):2605-13.

74. Rodriguez-Sanz D, Losa-Iglesias ME, Becerro de Bengoa-Vallejo R, Palomo-Lopez P, Beltran-Alacreu H, Calvo-Lobo C, et al. Skin temperature in youth soccer players with functional equinus and non-equinus condition after running. J Eur Acad Dermatol Venereol. noviembre de 2018;32(11):2020-4.

75. Rouder JN, Speckman PL, Sun D, Morey RD, Iverson G. Bayesian t tests for accepting and rejecting the null hypothesis. Psychonomic Bulletin & Review. 1 de abril de 2009;16(2):225-37.

76. Scott A, Docking S, Vicenzino B, Alfredson H, Zwerver J, Lundgreen K, et al. Sports and exercise-related tendinopathies: a review of selected topical issues by participants of the second International Scientific Tendinopathy Symposium (ISTS) Vancouver 2012. Br J Sports Med. junio de 2013;47(9):536-44.

77. Seixas, A, Gabriel, J, Vardasca, R. Thermographic evaluation in tendinopathies. En: Lecture notes of the ICB seminar: advances of infra-red thermal imaging in medicine. Warsaw: A. Nowakowski, James B. Mercer; 2013. p. 49-53.

78. Sengkerij PM, de Vos R-J, Weir A, van Weelde BJG, Tol JL. Interobserver reliability of neovascularization score using power Doppler ultrasonography in midportion achilles tendinopathy. Am J Sports Med. agosto de 2009;37(8):1627-31.

79. Sillero-Quintana M, Fernández-Jaén T, Fernández-Cuevas I, Gómez-Carmona PM, Arnaiz-Lastras J, Pérez M-D, et al. Infrared Thermography as a Support Tool for Screening and Early Diagnosis in Emergencies. Journal of Medical Imaging and Health Informatics. 1 de noviembre de 2015;5(6):1223-8.

80. Splittgerber LE, Ihm JM. Significance of Asymptomatic Tendon Pathology in Athletes. Current Sports Medicine Reports. junio de 2019;18(6):192-200.

81. Suydam SM, Buchanan TS. Is Echogenicity a Viable Metric for Evaluating Tendon Properties In Vivo? J Biomech. 3 de junio de 2014;47(8):1806-9.

82. Tang C, Chen Y, Huang J, Zhao K, Chen X, Yin Z, et al. The roles of inflammatory mediators and immunocytes in tendinopathy. Journal of Orthopaedic Translation. 1 de julio de 2018;14:23-33.

83. Tansey EA, Johnson CD. Recent advances in thermoregulation. Advances in Physiology Education. septiembre de 2015;39(3):139-48.

84. Terabayashi N, Watanabe T, Matsumoto K, Takigami I, Ito Y, Fukuta M, et al. Increased blood flow in the anterior humeral circumflex artery correlates with night pain in patients with rotator cuff tear. Journal of Orthopaedic Science. septiembre de 2014;19(5):744-9.

85. Terslev L, Torp-Pedersen S, Qvistgaard E, Danneskiold-Samso... B, Bliddal H. Estimation of inflammation by Doppler ultrasound: quantitative changes after intra-articular treatment in rheumatoid arthritis. Ann Rheum Dis. noviembre de 2003a;62(11):1049-53.

86. Terslev L, Torp-Pedersen S, Qvistgaard E, Kristoffersen H, Røgind H, Danneskiold-Samsøe B, et al. Effects of treatment with etanercept (Enbrel, TNRF:Fc) on rheumatoid arthritis evaluated by Doppler ultrasonography. Ann Rheum Dis. febrero de 2003b;62(2):178-81.

87. Tkáčová M, Hudák R, Foffová P, Živčák J. An importance of camera subject distance and angle in musculoskeletal applications of medical thermography. Acta Electrotech Inform. 2010;10:57-60.

88. Tol JL, Spiezia F, Maffulli N. Neovascularization in Achilles tendinopathy: have we been chasing a red herring? Knee Surg Sports Traumatol Arthrosc. octubre de 2012;20(10):1891-4.

89. Toppi J, Fairley J, Cicuttini FM, Cook J, Davis SR, Bell RJ, et al. Factors associated with magnetic resonance imaging defined patellar tendinopathy in community-based middle-aged women: a prospective cohort study. BMC Musculoskelet Disord. 5 de agosto de 2015;16:184.

90. Tumilty S, Adhia DB, Smoliga JM, Gisselman AS. Thermal profiles over the Achilles tendon in a cohort of non-injured collegiate athletes over the course of a cross country season. Phys Ther Sport. marzo de 2019;36:110-5.

91. Uematsu S, Edwin DH, Jankel WR, Kozikowski J, Trattner M. Quantification of thermal asymmetry. Part 1: Normal values and reproducibility. J Neurosurg. octubre de 1988;69(4):552-5.

92. Vardasca R, Ring F, Plassmann P, Jones C. Thermal symmetry of the upper and lower extremities in healthy subjects. Thermology International. 2012;22:53-60.

93. Vecchio PC, Adebajo AO, Chard MD, Thomas PP, Hazleman BL. Thermography of frozen shoulder and rotator cuff tendinitis. Clin Rheumatol. septiembre de 1992;11(3):382-4.

94. Visentini PJ, Khan KM, Cook JL, Kiss ZS, Harcourt PR, Wark JD. The VISA score: an index of severity of symptoms in patients with jumper's knee (patellar tendinosis). Victorian Institute of Sport Tendon Study Group. J Sci Med Sport. enero de 1998;1(1):22-8.

95. Wiggins RH, Davidson HC, Harnsberger HR, Lauman JR, Goede PA. Image file formats: past, present, and future. Radiographics. junio de 2001;21(3):789-98.

96. Xu R, Zhu Z, Tang W, Zhou Q, Zeng S. Zone-specific reference ranges of fetal adrenal artery Doppler indices: a longitudinal study. BMC Pregnancy Childbirth. diciembre de 2020;20(1):774.

97. Zabrzyński J, Paczesny Ł, Łapaj Ł, Grzanka D, Szukalski J. Process of neovascularisation compared with pain intensity in tendinopathy of the long head of the biceps brachii tendon associated with concomitant shoulder disorders, after arthroscopic treatment. Microscopic evaluation supported by immunohistochemical. Folia Morphol (Warsz). 2018;77(2):378-85.

98. Zanetti M, Metzdorf A, Kundert H-P, Zollinger H, Vienne P, Seifert B, et al. Achilles tendons: clinical relevance of neovascularization diagnosed with power Doppler US. Radiology. mayo de 2003;227(2):556-60.

SÍNTESIS DE LA TESIS

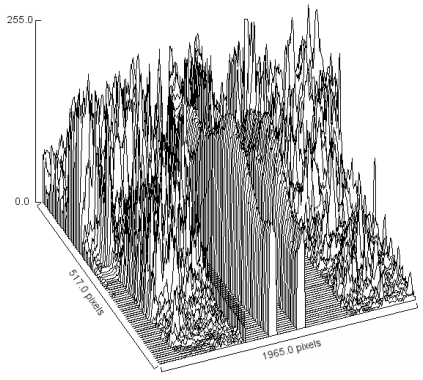

VIII. SÍNTESIS DE LA TESIS

En esta tesis se han desarrollado una secuencia de estudios para la consecución de los objetivos planteados **(anexo 3)** además del desarrollo de una solicitud de patente. Estos estudios se realizaron ante la necesidad de nuevas vías de evaluación de la tendinopatía rotuliana basadas en técnicas de imagen que permitiesen captar el nuevo modelo patológico del TR, en el que conviven el proceso degenerativo e inflamatorio **(figura 1)**.

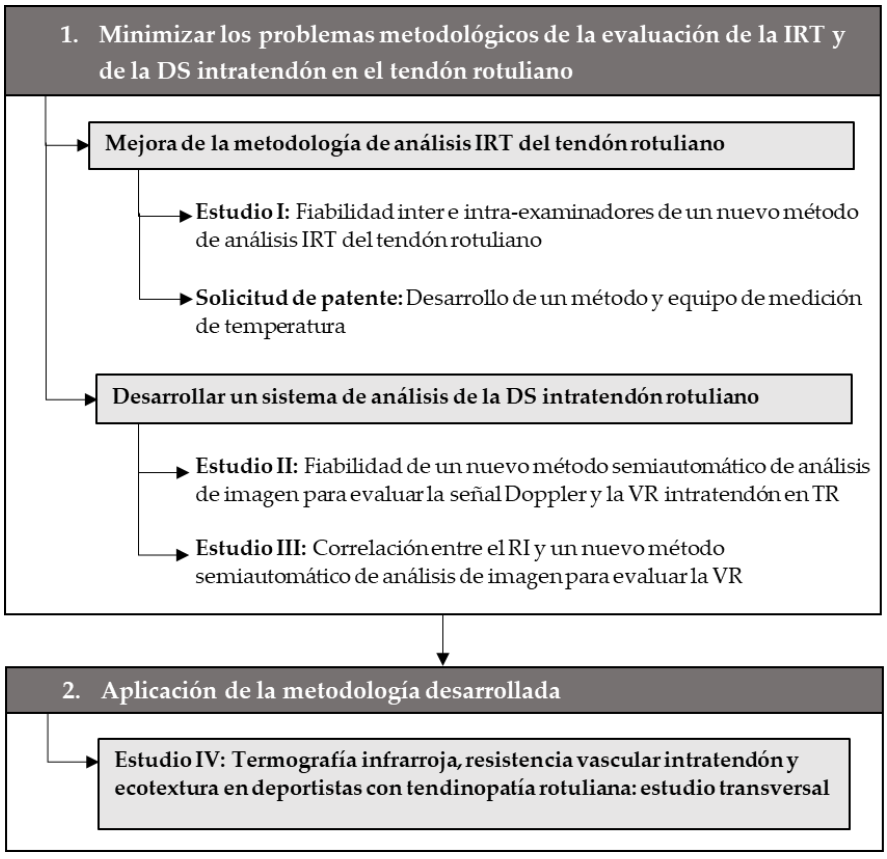

Figura 1. Diagrama de la metodología empleada. (Fuente: elaboración propia)

Todos los estudios realizados fueron aprobados por el Comité de Ética de la Universidad Católica de Murcia donde está inscrita la presente tesis.

Se ha descrito que en el diagnóstico y estudio de la tendinopatía rotuliana es cada vez más frecuente el uso de la ecografía Doppler y de la IRT como técnicas de imagen para complementar la exploración clínica, aunque en algunas ocasiones su utilización no siempre aporta una información relevante y, además, no está exenta de complicaciones.

8.1. FIABILIDAD TERMOGRÁFICA

Generalmente, la evaluación del cuerpo humano mediante IRT se realiza a través de una región de interés (ROI) pero no existe un consenso claro en la metodología de su selección. En el **estudio I** proponemos un método alternativo para seleccionar las áreas de análisis del TR, basado en la utilización de marcadores cutáneos y la superposición de las ROIs a través de las coordenadas en una matriz de píxeles. La fiabilidad de este método fue excelente para las variables estudiadas de tamaño (ancho y alto), posición (eje X e Y) y temperatura media de la ROI. Se debe tener en cuenta que en este estudio se emplearon las mismas imágenes para los dos observadores, lo que limita los resultados de fiabilidad a la creación y ubicación de las ROIs y excluye la parte operador-dependiente de la ubicación de los marcadores en la piel. Debido a los buenos resultados obtenidos, este estudio se ha materializado en una solicitud de patente que refleja la metodología desarrollada **(anexos 1 y 2)**.

En cuanto a la temperatura media de las ROIs, se han encontrado diferencias medias muy bajas, en torno a 0,10ºC y diferencias totales inferiores a 0,20ºC. Se ha observado una fiabilidad interobservador muy buena de la temperatura media de las ROIs en la evaluación de diferentes regiones del cuerpo como la rodilla, manos, musculatura cervical y a nivel facial (Selfe et al. 2006; Spalding et al. 2008; Costa et al. 2013), salvo en la región de la mama que es baja (Mustacchi et al. 1990). A pesar de estos buenos resultados en algunas de estas regiones, nuestro estudio ha mostrado una mayor fiabilidad interobservador que los estudios analizados. En relación con la fiabilidad intraobservador, las mediciones realizadas en la mano (Varjú et al. 2004), en la musculatura cervical y en la región facial son muy buenas (Costa et al. 2013), en cambio la rodilla presenta una fiabilidad más baja (Denoble

et al. 2010). Al igual que ocurre con la fiabilidad interobservador de nuestro estudio, la fiabilidad intraobservador sigue siendo superior a la del resto de estudios encontrados. En cambio, la utilización de programas informáticos para automatizar el proceso de selección de ROIs mediante la segmentación, han mostrado una fiabilidad intra e interobservador excelente (Fernández-Cuevas et al. 2012), similar a la aportada por nuestra metodología, pero a expensas de perder especificidad a la hora de poder seleccionar una estructura a través de una ROI.

8.2. FIABILIDAD DOPPLER

La evaluación mediante ecografía Doppler de las tendinopatías se basa principalmente en la presencia o recuento de las DS, a pesar de que la presencia de éstas no siempre es indicativo de anomalía (Malliaras et al. 2008; Tol et al. 2012). En cambio, la cuantificación de la VR a través del RI puede aportar información relacionada con el proceso fisiopatológico. Sin embargo, la determinación del RI directamente desde el ecógrafo cuando se evalúa la vascularización intratendinosa queda limitada por el pequeño tamaño y alto número de señales que pueden aparecer. En el **estudio II** se ha comprobado la fiabilidad intra e interobservador de un método de análisis semiautomático para la cuantificación de la morfología de la DS y de la VR intratendón basado en las intensidades de color de los píxeles. Este método permite la cuantificación de la DS sin importar su tamaño o número, a través de la selección de una ROI intratendón. Los resultados de fiabilidad intra e interobservador de esta metodología fueron muy buenos, tanto para las mediciones de número y forma de las DS, como para el cálculo de la VR.

No se han encontrado estudios que analicen la fiabilidad de la cuantificación del área de la DS a través del recuento de píxeles de color en el tejido tendinoso, pero si en otros tejidos como la membrana sinovial (Qvistgaard et al. 2001) o en la neoplasia trofoblástica gestacional (Li et al. 2018), que al igual que en nuestro estudio también ofrecen una muy buena fiabilidad en el análisis de la cuantificación del área de la DS. Generalmente, el recuento de los DS intratendón se realiza mediante diferentes escalas de evaluación del DS como la escala D´Agostino (D'agostino et al. 2009), la escala de Ohberg modificada (Sunding et al. 2016) o la escala de 5 grados (Poltawski et al. 2012). Si comparamos los resultados de estas escalas con los nuestros, observamos que el carácter cuantitativo de la metodología

desarrollada en esta tesis es más fiable que los métodos cualitativos utilizados en estos estudios, que precisan de una inspección visual para determinar el número de DS.

Por otro lado, la medición de la longitud del vaso podría ser un sistema interesante de cuantificación de las DS en el TR (Cook et al. 2005b), pero pese a presentar una excelente fiabilidad intraobservador y una buena interobservador, se cuestiona si este sistema es relevante para la práctica clínica (Cook et al. 2005b; Risch et al. 2016). En cualquier caso, con la metodología aquí presentada, es posible determinar el área y perímetro total de la DS registrada con una alta precisión.

8.3. VR INTRATENDÓN

Sin embargo, de las variables analizadas en el **estudio II**, probablemente el estudio de la VR sea una de las variables más interesantes en el análisis de la hipervascularización intratendón debido a la información que puede aportar sobre el estado del tendón (Torp-Pedersen et al. 2008; Terabayashi et al. 2014).

El método más utilizado para medir la VR intratendón es mediante el cálculo automático del RI a través del propio ecógrafo (Koenig et al. 2007a; Karzis et al. 2017). No se han encontrado estudios que hayan analizado la fiabilidad de las mediciones del RI intratendinosa, pero sí en otras regiones como el clítoris (Mercier et al. 2018) o la membrana sinovial de la muñeca y de la mano (Strunk et al. 2007; Albrecht et al. 2008). Si comparamos estos resultados de fiabilidad con los nuestros, observamos que son más débiles, probablemente se deba a que la adquisición e interpretación de las imágenes es una tarea operador-dependiente (Albrecht et al. 2007; Patil y Dasgupta 2012), y a la dificultad en la localización del vaso a medir al presentar un tamaño pequeño. En cambio, la metodología utilizada en nuestro estudio se basa en la media de las señales que se encuentran dentro de la ROI, resultando independiente de la localización y del tamaño de los vasos. El carácter semiautomático de esta metodología puede ser el responsable de los buenos resultados de fiabilidad puesto que el operador solo está involucrado en la selección de las imágenes con mayor y menor señal, la ubicación de las ROIs intratendón y en la parametrización del programa informático para la selección de las señales.

8.4. CORRESPONDENCIA ENTRE VR E RI

Podría aducirse que la VR determinada con esta metodología y el RI no son equivalentes puesto que la primera se basa en una intensidad media de color de píxel y la segunda se basa en la velocidad de flujo.

En el **estudio III** se analiza precisamente esta cuestión sobre un modelo con la arteria braquial que facilita el cálculo y la modificación del RI. La metodología empleada para calcular la VR intratendón a través de la cuantificación de la intensidad de color de los píxeles de la señal PD ha mostrado una correlación positiva y grande con el RI por lo que puede concluirse que, aunque no iguales, los dos parámetros son equivalentes. No se han encontrado estudios que cuantifiquen la VR mediante sistemas de análisis de imagen, por lo que no podemos comparar nuestros resultados con los de otros estudios.

8.5. TERMOGRAFÍA, ANÁLISIS VASCULAR INTRATENDÓN Y ECOTEXTURA EN PACIENTES CON TENDINOPATÍA ROTULIANA

Finalmente, en el **estudio IV** se aplicaron las metodologías desarrolladas en los estudios anteriores para analizar las variables de temperatura, ecotextura, DS y VR intratendón en la tendinopatía rotuliana en deportistas.

En relación a la IRT, al comparar la diferencia térmica entre las rodillas de los pacientes y las del grupo control, y al igual que ocurre en la bibliografía consultada, se observó una mayor diferencia térmica en el grupo de los pacientes. Los tendones rotulianos sintomáticos mostraron una asimetría térmica con el tendón asintomático contralateral, con un patrón con una temperatura más elevada que los tendones asintomáticos.

Aunque la presencia de DS intratendón se puede observar en tendones asintomáticos o como respuesta fisiológica adaptativa al ejercicio, en los pacientes del presente estudio se observó una fuerte evidencia en cuanto a la mayor probabilidad de presentar DS intratendón frente a los sujetos control, por lo que no podemos descartar por completo esta variable como un signo ecográfico de la tendinopatía rotuliana.

En cambio, si se comparan los tendones sintomáticos y los asintomáticos contralaterales, la diferencia entre el área de la DS ya no es tan evidente, probablemente debido a que se observó una mayor presencia de DS intratendón en los tendones contralaterales asintomáticos de los pacientes que en los controles.

Los tendones afectados mostraron una VR más baja que el grupo control y que los tendones contralaterales asintomáticos, que unido a la a la mayor temperatura observada en los tendones afectos, hace pensar en un probable proceso inflamatorio, reforzando la hipótesis de considerar la tendinopatía como un proceso fisiopatológico en el que conviven el estado degenerativo e inflamatorio (Fredberg y Stengaard-Pedersen 2008; Tang et al. 2018).

En cuanto al análisis estructural del tendón se encontró un cambio en el patrón ecotextural de los pacientes frente a los controles, que podría ser debido a una degradación estructural del tendón. Estos cambios no se han visto reflejados entre los tendones sintomáticos y asintomáticos de los pacientes, lo que sugiere una degradación similar en el lado contralateral. A pesar de que la disminución de la ecointensidad se ha considerado uno de los signos ecográficos de la tendinopatía (Malliaras et al. 2010), este parámetro no ha sido capaz de mostrar diferencias en nuestro estudio, aunque debemos tener en cuenta que en muchas ocasiones no existe una relación directa entre imagen patológica y la sintomatología (Kulig et al. 2014; McAuliffe et al. 2016; Splittgerber y Ihm 2019).

Tanto una temperatura elevada como una VR intratendón baja pueden reflejar un proceso inflamatorio, ambas variables han presentado una correlación fuerte entre los pacientes, lo que nuevamente puede reflejar que la evolución de la tendinopatía rotuliana puede contener un estado inflamatorio, más allá de la fase inicial (Millar et al. 2010; Rees et al. 2014; Tang et al. 2018).

8.6. APLICACIONES PRÁCTICAS

El nuevo método de análisis IRT del tendón rotuliano desarrollado en el **estudio I** y materializado en una solicitud de patente (**anexos 1 y 2**), se puede utilizar en la práctica por clínicos e investigadores que pretendan realizar una evaluación específica y fiable del TR sin contaminar el termograma, solventando el

problema de la selección de las ROIs en la evaluación clínica con IRT. Además, esta metodología es fácilmente extrapolable a otros tendones y tejidos.

El nuevo método semiautomático para evaluar la DS y la VR intratendón en la tendinopatía rotuliana (**estudios II y III**), permite calcular la VR a través del análisis de imagen de la señal PD, independientemente del número y tamaño de DS.

Como se manifiesta en el **estudio IV**, la utilización clínica de las variables de temperatura, DS intratendón, VR y el parámetro ecotextural de EV, permiten una caracterización del estado fisiológico y estructural del tendón, aportando información sobre el estado del tejido, lo que permite adoptar un mejor abordaje y seguimiento de los tratamientos sobre la tendinopatía rotuliana. Estos sistemas de análisis de imagen son fácilmente aplicables a cualquier tendón.

8.7. LIMITACIONES

Una de las limitaciones del estudio de fiabilidad inter e intraobservador de un nuevo método de análisis IRT del TR (**estudio I**) es que se realizó sobre los mismos termogramas de base debido a que el objetivo de este estudio fue determinar la fiabilidad de la metodología, eludiendo cualquier influencia de otras fuentes de variabilidad. Igual ocurrió con el estudio de fiabilidad del nuevo método semiautomático para evaluar la DS y la VR en el TR (**estudio II**), donde también se utilizaron los mismos vídeos de base para determinar la fiabilidad de la metodología, obviando el proceso operador dependiente de la evaluación ecográfica para la adquisición del vídeo con la DS.

El análisis de imagen propuesto en el nuevo método semiautomático para evaluar la DS y la VR (**estudio II**), debe realizarse una vez exportados los vídeos de PD y requiere un tiempo extra a la hora del procesado, segmentación y cuantificación de la DS, lo que plantea una limitación en su aplicación clínica al no ser inmediata. Sin embargo, puede considerarse un método válido para su uso en el contexto de la investigación, y en el caso de que se llegue a integrar en los programas informáticos de los ecógrafos, también podría utilizarse en la práctica clínica.

Las variables de edad y sexo que caracterizan a la muestra del **estudio IV**, fueron significativamente diferentes entre el grupo de pacientes y el control, por lo que los resultados termográficos pueden verse afectados por estas variables debido a que se consideran factores de influencia termográficos (Fernández-Cuevas et al. 2015a). Para minimizar la influencia de estas variables, el análisis se realizó sobre las diferencias térmicas entre rodillas y no sobre las medias de temperatura.

En el **estudio IV** no se consideró la modalidad deportiva practicada, cuestión que podría ser tenida en cuenta en futuros estudios.

8.8. FUTURAS LÍNEAS DE INVESTIGACIÓN

La fisiopatología de las tendinopatías sigue siendo una fuente de debate, con algunos giros en las últimas décadas provocados por la continua investigación sobre el tema. Esta tesis y las futuras líneas de investigación que derivarán de ella pretenden aportar luz para un mejor entendimiento de este proceso.

Debido a las características de la metodología empleada tanto en el análisis de la DS intratendón como en la evaluación IRT del TR, es relativamente sencillo trasladarlas a otros tendones o estructuras, aunque previamente sería recomendable realizar estudios de fiabilidad y validez para cada uno de ellos.

En esta tesis solo se ha analizado la fiabilidad intra e interobservador. En futuros estudios sería aconsejable analizar también la fiabilidad interecógrafos e intercámaras termográficas, debido a que utilizan diferentes algoritmos de interpolarización de la imagen que pueden afectar al resultado final, proporcionando informaciones diferentes.

Debido a la alta sensibilidad de las técnicas de imagen utilizadas y a la caracterización térmica y de la VR intratendón resultado de esta tesis, se podría estudiar su viabilidad como biomarcadores y analizar su capacidad pronóstica, de seguimiento y de prevención en la tendinopatía rotuliana mediante estudios longitudinales.

En relación a la ecotextura, sería interesante realizar un análisis de parámetros ecotexturales de segundo orden obtenidos a partir de matrices de co-ocurrencia del nivel de gris, que aportan mayor información estructural del tendón que las de primer orden analizadas en este estudio, e información fisiológica

resultante de las variables de IRT y del análisis de la DS empleadas en esta tesis. Esta relación podría ayudar a dar respuesta a la falta de correlación entre los hallazgos estructurales y la sintomatología del paciente.

Actualmente, se está trabajando en el desarrollo de una versión más automatizada a través de un programa informático que facilite el proceso y reduzca el tiempo de segmentación y cuantificación de la DS, lo cual puede contribuir a su aplicación y a aumentar su interés en la práctica clínica.

La aplicabilidad de las técnicas de imagen desarrolladas en esta tesis nos dirige hacia la realización de diferentes ensayos clínicos con el objetivo de analizar el comportamiento de las variables utilizadas bajo las intervenciones de diferentes técnicas de fisioterapia, así como explorar los factores que actúan como potenciales barreras o facilitadores de su uso en la práctica clínica diaria, con la intención de mejorar este recurso.

Nuestras investigaciones futuras deben ir ligadas a la constante adaptación de las variables analizadas en esta tesis, a la mejora tecnológica de los equipos de imagen médica y a continuar con la búsqueda de nuevas variables que, a modo de biomarcadores, nos permitan entender mejor el proceso fisiopatológico de la tendinopatía rotuliana con el fin de mejorar el abordaje y seguimiento de esta patología.

CONCLUSIONES

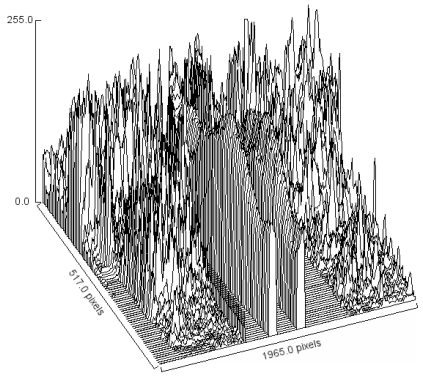

IX. CONCLUSIONES

I. La fiabilidad y reproducibilidad del nuevo método de análisis termográfico del tendón rotuliano es muy buena, por lo que la variabilidad introducida por los exploradores no es significativa y el método es potencialmente válido para el análisis termográfico de regiones simétricas del tendón rotuliano.

II. La fiabilidad y reproducibilidad del nuevo método semicuantitativo de evaluación de la señal Doppler y la resistencia vascular intratendón en la tendinopatía rotuliana mediante el análisis de imagen de la señal Power Doppler son muy buenas.

III. El nuevo método semiautomático de evaluación de la resistencia vascular basado en la cuantificación de la intensidad del color del píxel de la señal Power Doppler es una buena variable predictora del índice de resistencia vascular, y podría resultar de utilidad en aquellos tejidos donde resulte complicada su medición.

IV. El nuevo método semiautomático de evaluación de la resistencia vascular basado en la cuantificación de la intensidad del color del píxel de la señal Power Doppler puede ser utilizado en el análisis de la resistencia vascular intratendón, la perfusión y el estado del tejido en la tendinopatía rotuliana al presentar una metodología fiable y una muy buena correlación con el índice de resistencia vascular.

V. Los deportistas con tendinopatía rotuliana unilateral han mostrado una mayor diferencia térmica entre tendones rotulianos, una mayor área de señales Doppler intratendón, una resistencia vascular intratendón más baja y una ecovariación moderadamente más alta que los sujetos sanos.

VI. En la tendinopatía rotuliana unilateral, el tendón afecto de los deportistas cursa con un aumento de la temperatura, una resistencia vascular intratendón más baja, un área de señal Doppler moderadamente mayor y no presenta diferencias en los parámetros ecotexturales de ecointensidad y ecovariación con respecto al tendón asintomático contralateral.

VII. El dolor y la disminución de la funcionalidad de la rodilla medidas con la escala VISA-P de los deportistas con tendinopatía rotuliana unilateral, se correlacionan con una asimetría térmica y una resistencia vascular intratendón más baja.

VIII. Los deportistas con tendinopatía rotuliana unilateral han mostrado una correlación entre una mayor diferencia de temperatura entre tendones rotulianos y una resistencia vascular intratendón más baja, que concuerdan con la hipótesis de convivencia de proceso degenerativos e inflamatorios en la tendinopatía rotuliana.

REFERENCIAS BIBLIOGRÁFICAS

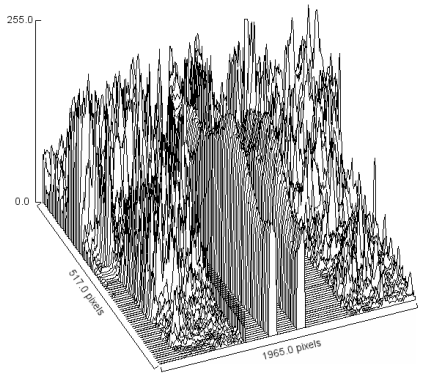

X. REFERENCIAS BIBLIOGRÁFICAS.

1. Abate M, Silbernagel KG, Siljeholm C, Di Iorio A, De Amicis D, Salini V, et al. Pathogenesis of tendinopathies: inflammation or degeneration? Arthritis Res Ther. 2009;11(3):235.
2. Ackermann PW. Neuronal regulation of tendon homoeostasis. Int J Exp Path. agosto de 2013;94(4):271-86.
3. Adamson SL. Arterial pressure, vascular input impedance, and resistance as determinants of pulsatile blood flow in the umbilical artery. Eur J Obstet Gynecol Reprod Biol. junio de 1999;84(2):119-25.
4. Albrecht K, Grob K, Lange U, Müller-Ladner U, Strunk J. Reliability of different Doppler ultrasound quantification methods and devices in the assessment of therapeutic response in arthritis. Rheumatology (Oxford). octubre de 2008;47(10):1521-6.
5. Albrecht K, Müller-Ladner U, Strunk J. Quantification of the synovial perfusion in rheumatoid arthritis using Doppler ultrasonography. Clin Exp Rheumatol. agosto de 2007;25(4):630-8.
6. Alfredson H. The chronic painful Achilles and patellar tendon: research on basic biology and treatment. Scand J Med Sci Sports. agosto de 2005;15(4):252-9.
7. Alfredson H, Bjur D, Thorsen K, Lorentzon R, Sandström P. High intratendinous lactate levels in painful chronic Achilles tendinosis. An investigation using microdialysis technique. J Orthop Res. septiembre de 2002;20(5):934-8.
8. Alfredson H, Ljung BO, Thorsen K, Lorentzon R. In vivo investigation of ECRB tendons with microdialysis technique--no signs of inflammation but high amounts of glutamate in tennis elbow. Acta Orthop Scand. octubre de 2000;71(5):475-9.

9. Alfredson H, Ohberg L. Increased intratendinous vascularity in the early period after sclerosing injection treatment in Achilles tendinosis : a healing response? Knee Surg Sports Traumatol Arthrosc. abril de 2006;14(4):399-401.

10. Alfredson H, Ohberg L, Forsgren S. Is vasculo-neural ingrowth the cause of pain in chronic Achilles tendinosis? An investigation using ultrasonography and colour Doppler, immunohistochemistry, and diagnostic injections. Knee Surg Sports Traumatol Arthrosc. septiembre de 2003;11(5):334-8.

11. Alfredson H, Thorsen K, Lorentzon R. In situ microdialysis in tendon tissue: high levels of glutamate, but not prostaglandin E2 in chronic Achilles tendon pain. Knee Surg Sports Traumatol Arthrosc. 1999;7(6):378-81.

12. Allan PL, McDicken WN, Pozniak MA, Dubbins PA. Ecografía Doppler clínica. Elsevier España; 2008.

13. Andersson G, Backman LJ, Scott A, Lorentzon R, Forsgren S, Danielson P. Substance P accelerates hypercellularity and angiogenesis in tendon tissue and enhances paratendinitis in response to Achilles tendon overuse in a tendinopathy model. Br J Sports Med. octubre de 2011;45(13):1017-22.

14. Andersson G, Danielson P, Alfredson H, Forsgren S. Presence of substance P and the neurokinin-1 receptor in tenocytes of the human Achilles tendon. Regul Pept. 9 de octubre de 2008;150(1-3):81-7.

15. Aström M, Rausing A. Chronic Achilles tendinopathy. A survey of surgical and histopathologic findings. Clin Orthop Relat Res. julio de 1995;(316):151-64.

16. Auliffe SM, Creesh KM, O'Sullivan K, Purtill H, Culloty F. Can Ultrasound Imaging Predict the Development of Achilles and Patellar Tendinopathy? A Systematic Review and Meta-Analysis. Br J Sports Med. 1 de febrero de 2017;51(4):359-60.

17. del Baño Aledo M ae, Martínez Payá JJ, Ríos Díaz J, Palomino Cortés MA. Aplicación en fisioterapia de la valoración cuantitativa de las características morfoecogénicas del tendón de Aquiles. Fisioterapia. 1 de abril de 2008;30(2):61-8.

18. Basso O, Amis AA, Race A, Johnson DP. Patellar tendon fiber strains: their differential responses to quadriceps tension. Clin Orthop Relat Res. julio de 2002;(400):246-53.

19. Bauman A, Bull F, Chey T, Craig CL, Ainsworth BE, Sallis JF, et al. The International Prevalence Study on Physical Activity: results from 20 countries. Int J Behav Nutr Phys Act. 31 de marzo de 2009;6:21.

20. Benítez-Martínez JC, Martínez-Ramírez P, Valera-Garrido F, Casaña-Granell J, Medina-Mirapeix F. Comparison of Pain Measures Between Tendons of Elite Basketball Players With Different Sonographic Patterns. Journal of Sport Rehabilitation. 1 de febrero de 2020;29(2):142-7.

21. Bjordal JM, Lopes-Martins RAB, Iversen VV. A randomised, placebo controlled trial of low level laser therapy for activated Achilles tendinitis with microdialysis measurement of peritendinous prostaglandin E2 concentrations. Br J Sports Med. enero de 2006;40(1):76-80.

22. Bjur D, Alfredson H, Forsgren S. The innervation pattern of the human Achilles tendon: studies of the normal and tendinosis tendon with markers for general and sensory innervation. Cell Tissue Res. abril de 2005;320(1):201-6.

23. Blazina ME, Kerlan RK, Jobe FW, Carter VS, Carlson GJ. Jumper's knee. Orthop Clin North Am. julio de 1973;4(3):665-78.

24. Boesen AP, Boesen MI, Koenig MJ, Bliddal H, Torp-Pedersen S, Langberg H. Evidence of accumulated stress in Achilles and anterior knee tendons in elite badminton players. Knee Surg Sports Traumatol Arthrosc. enero de 2011;19(1):30-7.

25. Boesen AP, Boesen MI, Torp-Pedersen S, Christensen R, Boesen L, Hölmich P, et al. Associations between abnormal ultrasound color Doppler measures and tendon pain symptoms in badminton players during a season: a prospective cohort study. Am J Sports Med. marzo de 2012;40(3):548-55.

26. Boesen MI, Koenig MJ, Torp-Pedersen S, Bliddal H, Langberg H. Tendinopathy and Doppler activity: the vascular response of the Achilles tendon to exercise. Scand J Med Sci Sports. diciembre de 2006;16(6):463-9.

27. Bouzida N, Bendada A, Maldague XP. Visualization of body thermoregulation by infrared imaging. Journal of Thermal Biology. abril de 2009;34(3):120-6.

28. Bude RO, Rubin JM. Effect of downstream cross-sectional area of an arterial bed on the resistive index and the early systolic acceleration. Radiology. septiembre de 1999;212(3):732-8.

29. Chaudhry S, Fernando R, Screen H, Waugh C, Tucker A, Morrissey D. The use of medical infrared thermography in the detection of tendinopathy: a systematic review. Physical Therapy Reviews. 3 de marzo de 2016;21(2):75-82.

30. Childs C. Body temperature and clinical thermometry. En: Handbook of Clinical Neurology [Internet]. Elsevier; 2018 [citado 20 de octubre de 2021]. p. 467-82. Disponible en: https://linkinghub.elsevier.com/retrieve/pii/B978044464074100029X

31. Choi E, Lee P-B, Nahm FS. Interexaminer reliability of infrared thermography for the diagnosis of complex regional pain syndrome. Skin Res Technol. mayo de 2013;19(2):189-93.

32. Clarsen B, Myklebust G, Bahr R. Development and validation of a new method for the registration of overuse injuries in sports injury epidemiology: the Oslo Sports Trauma Research Centre (OSTRC) overuse injury questionnaire. Br J Sports Med. mayo de 2013;47(8):495-502.

33. Codman EA. The shoulder;: Rupture of the supraspinatus tendon and other lesions in or about the subacromial bursa. 1934.

34. Cook J, Malliaras P, De Luca J, Ptasznik R, Morris M, Khan K. Vascularity and pain in the patellar tendon of adult jumping athletes: a 5 month longitudinal study. Br J Sports Med. julio de 2005a;39(7):458-61.

35. Cook JL, Feller JA, Bonar SF, Khan KM. Abnormal tenocyte morphology is more prevalent than collagen disruption in asymptomatic athletes' patellar tendons. J Orthop Res. marzo de 2004a;22(2):334-8.

36. Cook JL, Khan KM, Kiss ZS, Griffiths L. Patellar tendinopathy in junior basketball players: a controlled clinical and ultrasonographic study of 268

patellar tendons in players aged 14-18 years. Scand J Med Sci Sports. agosto de 2000a;10(4):216-20.

37. Cook JL, Khan KM, Kiss ZS, Purdam CR, Griffiths L. Prospective imaging study of asymptomatic patellar tendinopathy in elite junior basketball players. J Ultrasound Med. julio de 2000b;19(7):473-9.
38. Cook JL, Khan KM, Kiss ZS, Purdam CR, Griffiths L. Reproducibility and clinical utility of tendon palpation to detect patellar tendinopathy in young basketball players. Victorian Institute of Sport tendon study group. Br J Sports Med. febrero de 2001;35(1):65-9.
39. Cook JL, Khan KM, Maffulli N, Purdam C. Overuse tendinosis, not tendinitis part 2: applying the new approach to patellar tendinopathy. Phys Sportsmed. junio de 2000c;28(6):31-46.
40. Cook JL, Malliaras P, De Luca J, Ptasznik R, Morris ME, Goldie P. Neovascularization and pain in abnormal patellar tendons of active jumping athletes. Clin J Sport Med. septiembre de 2004b;14(5):296-9.
41. Cook JL, Ptazsnik R, Kiss ZS, Malliaras P, Morris ME, De Luca J. High reproducibility of patellar tendon vascularity assessed by colour Doppler ultrasonography: a reliable measurement tool for quantifying tendon pathology. Br J Sports Med. octubre de 2005b;39(10):700-3.
42. Cook JL, Purdam C. Is compressive load a factor in the development of tendinopathy? Br J Sports Med. 1 de marzo de 2012;46(3):163-8.
43. Cook JL, Purdam CR. Is tendon pathology a continuum? A pathology model to explain the clinical presentation of load-induced tendinopathy. Br J Sports Med. junio de 2009;43(6):409-16.
44. Cook JL, Rio E, Purdam CR, Docking SI. Revisiting the continuum model of tendon pathology: what is its merit in clinical practice and research? Br J Sports Med. 1 de octubre de 2016;50(19):1187-91.
45. Côrte AC, Pedrinelli A, Marttos A, Souza IFG, Grava J, José Hernandez A. Infrared thermography study as a complementary method of screening and prevention of muscle injuries: pilot study. BMJ Open Sport Exerc Med. 2019;5(1):e000431.

46. Costa ACS, Dibai Filho AV, Packer AC, Rodrigues-Bigaton D. Intra and inter-rater reliability of infrared image analysis of masticatory and upper trapezius muscles in women with and without temporomandibular disorder. Braz J Phys Ther. febrero de 2013;17(1):24-31.

47. Costello J, Stewart I, Selfe J, Karki A, Donnelly A. Use of thermal imaging in sports medicine research: A short report. International SportMed Journal. 2013;14(2):94-8.

48. D'agostino MA, Aegerter P, Jousse-Joulin S, Chary-Valckenaere I, Lecoq B, Gaudin P, et al. How to evaluate and improve the reliability of power Doppler ultrasonography for assessing enthesitis in spondylarthritis. Arthritis Rheum. 15 de enero de 2009;61(1):61-9.

49. Dakin SG, Dudhia J, Smith RKW. Resolving an inflammatory concept: the importance of inflammation and resolution in tendinopathy. Vet Immunol Immunopathol. 15 de abril de 2014;158(3-4):121-7.

50. Dakin SG, Martinez FO, Yapp C, Wells G, Oppermann U, Dean BJ, et al. Inflammation activation and resolution in human tendon disease. Sci Transl Med. 28 de octubre de 2015;7(311):311ra173.

51. Danielson P, Andersson G, Alfredson H, Forsgren S. Marked sympathetic component in the perivascular innervation of the dorsal paratendinous tissue of the patellar tendon in arthroscopically treated tendinosis patients. Knee Surg Sports Traumatol Arthrosc. junio de 2008;16(6):621-6.

52. Das K, Bhowmik MK, Chowdhuary O, Bhattacharjee D, De BK. Accurate segmentation of inflammatory and abnormal regions using medical thermal imagery. Australas Phys Eng Sci Med. junio de 2019;42(2):647-57.

53. De Jonge S, Warnaars JLF, De Vos RJ, Weir A, van Schie HTM, Bierma-Zeinstra SMA, et al. Relationship between neovascularization and clinical severity in Achilles tendinopathy in 556 paired measurements. Scand J Med Sci Sports. octubre de 2014;24(5):773-8.

54. Dean BJF, Franklin SL, Carr AJ. The Peripheral Neuronal Phenotype is Important in the Pathogenesis of Painful Human Tendinopathy: A Systematic Review. Clinical Orthopaedics & Related Research. septiembre de 2013;471(9):3036-46.

55. Dean BJF, Gettings P, Dakin SG, Carr AJ. Are inflammatory cells increased in painful human tendinopathy? A systematic review. Br J Sports Med. febrero de 2016;50(4):216-20.

56. Denoble AE, Hall N, Pieper CF, Kraus VB. Patellar skin surface temperature by thermography reflects knee osteoarthritis severity. Clin Med Insights Arthritis Musculoskelet Disord. 2010;3:69-75.

57. Draper JW, Boag JW. The calculation of skin temperature distributions in thermography. Phys Med Biol. abril de 1971;16(2):201-11.

58. Fallows R, Lumsden G. Pitfalls in the study of neovascularisation in achilles and patellar tendinopathy: a review of important factors for clinicians to consider and the need for greater standardisation. Physical Therapy Reviews. 2 de noviembre de 2019;24(6):346-57.

59. Fenwick SA, Hazleman BL, Riley GP. The vasculature and its role in the damaged and healing tendon. Arthritis Res. 2002;4(4):252-60.

60. Fernández-Cuevas I, Bouzas Marins JC, Arnáiz Lastras J, Gómez Carmona PM, Piñonosa Cano S, García-Concepción MÁ, et al. Classification of factors influencing the use of infrared thermography in humans: A review. Infrared Physics & Technology. 1 de julio de 2015a;71:28-55.

61. Fernández-Cuevas I, Marins JC, Carmona PG, García MA, Lastras JA, Quintana MS. Reliability and Reproducibility of Skin Temperature of Overweight Subjects by an Infrared Thermography Software Designed for Human Beings. Thermol Int. 2012;22(3 (Appendix)):130-7.

62. Fernández-Cuevas I, Marins JC, Lastras JA, Carmona PG, Quintana MS. Validity, Reliability, and Reproducibility of Skin Temperature in Healthy Subjects Using Infrared Thermography. En: Humbert P, Maibach H, Fanian F, Agache P, editores. Agache's Measuring the Skin [Internet]. Springer International Publishing; 2015b [citado 27 de diciembre de 2016]. p. 1-9. Disponible en: http://link.springer.com/referenceworkentry/10.1007/978-3-319-26594-0_74-1

63. Ferrara N. Molecular and biological properties of vascular endothelial growth factor. J Mol Med. julio de 1999;77(7):527-43.

64. Ferretti A, Papandrea P, Conteduca F. Knee injuries in volleyball. Sports Med. agosto de 1990;10(2):132-8.

65. Fredberg U, Stengaard-Pedersen K. Chronic tendinopathy tissue pathology, pain mechanisms, and etiology with a special focus on inflammation. Scand J Med Sci Sports. febrero de 2008;18(1):3-15.

66. Freund W, Weber F, Billich C, Schuetz UH. The foot in multistage ultra-marathon runners: experience in a cohort study of 22 participants of the Trans Europe Footrace Project with mobile MRI. BMJ Open. 2012;2(3):e001118.

67. Fu SC, Chan BP, Wang W, Pau HM, Chan KM, Rolf CG. Increased expression of matrix metalloproteinase 1 (MMP1) in 11 patients with patellar tendinosis. Acta Orthop Scand. diciembre de 2002a;73(6):658-62.

68. Fu S-C, Rolf C, Cheuk Y-C, Lui PP, Chan K-M. Deciphering the pathogenesis of tendinopathy: a three-stages process. Sports Med Arthrosc Rehabil Ther Technol. 13 de diciembre de 2010;2:30.

69. Fu SC, Wang W, Pau HM, Wong YP, Chan KM, Rolf CG. Increased expression of transforming growth factor-beta1 in patellar tendinosis. Clin Orthop Relat Res. julio de 2002b;(400):174-83.

70. Gatt A, Falzon O, Cassar K, Ellul C, Camilleri KP, Gauci J, et al. Establishing Differences in Thermographic Patterns between the Various Complications in Diabetic Foot Disease. Int J Endocrinol. 2018;2018:9808295.

71. Gatt A, Formosa C, Cassar K, Camilleri KP, De Raffaele C, Mizzi A, et al. Thermographic patterns of the upper and lower limbs: baseline data. Int J Vasc Med. 2015;2015:831369.

72. Gdynia H-J, Müller H-P, Ludolph AC, Köninger H, Huber R. Quantitative muscle ultrasound in neuromuscular disorders using the parameters «intensity», «entropy», and «fractal dimension». Eur J Neurol. octubre de 2009;16(10):1151-8.

73. Gisslén K, Alfredson H. Neovascularisation and pain in jumper's knee: a prospective clinical and sonographic study in elite junior volleyball players. Br J Sports Med. julio de 2005;39(7):423-8; discussion 423-428.

74. Gizińska M, Rutkowski R, Szymczak-Bartz L, Romanowski W, Straburzyńska-Lupa A. Thermal imaging for detecting temperature changes

within the rheumatoid foot. J Therm Anal Calorim. 1 de julio de 2021;145(1):77-85.

75. Glasbey CA, Horgan GW. Image Analysis for the Biological Sciences. Wiley; 1995.

76. Gómez-Carmona P, Fernández-Cuevas I, Sillero-Quintana M, Arnaiz-Lastras J, Navandar A. Infrared Thermography Protocol on Reducing the Incidence of Soccer Injuries. Journal of Sport Rehabilitation. 1 de noviembre de 2020;29(8):1222-7.

77. Green PG, Luo J, Heller PH, Levine JD. Further substantiation of a significant role for the sympathetic nervous system in inflammation. Neuroscience. agosto de 1993;55(4):1037-43.

78. Grenn M, Vizgaitis J, Pellegrino J, Percont P. Infrared camera and optics for medical applications. En: Medical Infrared Imaging: Principles and Practices. Diakides M, Bronzino JD, Peterson DR. Boca Raton: CRC Press; 2013. p. 5.1-5.15.

79. Haralick RM, Shanmugam K, Dinstein I. Textural Features for Image Classification. IEEE Transactions on Systems, Man and Cybernetics. noviembre de 1973;SMC-3(6):610-21.

80. Heikens MJ, Gorbach AM, Eden HS, Savastano DM, Chen KY, Skarulis MC, et al. Core body temperature in obesity. Am J Clin Nutr. mayo de 2011;93(5):963-7.

81. Hildebrandt C, Raschner C, Ammer K. An Overview of Recent Application of Medical Infrared Thermography in Sports Medicine in Austria. Sensors (Basel). 7 de mayo de 2010;10(5):4700-15.

82. Iriarte Posse Í. Ecografía musculoesquelética: exploración anatómica y patología. Madrid: Panamericana; 2020.

83. Järvinen M. Epidemiology of tendon injuries in sports. Clin Sports Med. julio de 1992;11(3):493-504.

84. Karzis K, Kalogeris M, Mandalidis D, Geladas N, Karteroliotis K, Athanasopoulos S. The effect of foot overpronation on Achilles tendon blood supply in healthy male subjects. Scand J Med Sci Sports. octubre de 2017;27(10):1114-21.

85. Kettunen JA, Kvist M, Alanen E, Kujala UM. Long-term prognosis for jumper's knee in male athletes. A prospective follow-up study. Am J Sports Med. octubre de 2002;30(5):689-92.

86. Khan K, Forster B, Robinson J, Cheong Y, Louis L, Maclean L, et al. Are ultrasound and magnetic resonance imaging of value in assessment of Achilles tendon disorders? A two year prospective study. Br J Sports Med. abril de 2003;37(2):149-53.

87. Khan KM, Bonar F, Desmond PM, Cook JL, Young DA, Visentini PJ, et al. Patellar tendinosis (jumper's knee): findings at histopathologic examination, US, and MR imaging. Victorian Institute of Sport Tendon Study Group. Radiology. septiembre de 1996;200(3):821-7.

88. Khan KM, Cook JL, Taunton JE, Bonar F. Overuse tendinosis, not tendinitis part 1: a new paradigm for a difficult clinical problem. Phys Sportsmed. mayo de 2000;28(5):38-48.

89. Kjaer M, Bayer ML, Eliasson P, Heinemeier KM. What is the impact of inflammation on the critical interplay between mechanical signaling and biochemical changes in tendon matrix? Journal of Applied Physiology. 15 de septiembre de 2013;115(6):879-83.

90. Kjaer M, Langberg H, Magnusson P. [Overuse injuries in tendon tissue: insight into adaptation mechanisms]. Ugeskr Laeg. 31 de marzo de 2003;165(14):1438-43.

91. Koenig MJ, Torp-Pedersen S, Boesen MI, Holm CC, Bliddal H. Doppler ultrasonography of the anterior knee tendons in elite badminton players: colour fraction before and after match. Br J Sports Med. febrero de 2010;44(2):134-9.

92. Koenig MJ, Torp-Pedersen S, Holmich P, Terslev L, Nielsen MB, Boesen M, et al. Ultrasound Doppler of the Achilles tendon before and after injection of an ultrasound contrast agent--findings in asymptomatic subjects. Ultraschall Med. febrero de 2007a;28(1):52-6.

93. Koenig MJ, Torp-Pedersen S, Qvistgaard E, Terslev L, Bliddal H. Preliminary results of colour Doppler-guided intratendinous glucocorticoid injection for

Achilles tendonitis in five patients. Scand J Med Sci Sports. abril de 2004;14(2):100-6.

94. Koenig MJ, Torp-Pedersen ST, Christensen R, Boesen MI, Terslev L, Hartkopp A, et al. Effect of knee position on ultrasound Doppler findings in patients with patellar tendon hyperaemia (jumper's knee). Ultraschall Med. octubre de 2007b;28(5):479-83.

95. Koeppen BM, Stanton BA. Berne & Levy Physiology. Elsevier; 2017.

96. Kraushaar BS, Nirschl RP. Tendinosis of the elbow (tennis elbow). Clinical features and findings of histological, immunohistochemical, and electron microscopy studies. J Bone Joint Surg Am. febrero de 1999;81(2):259-78.

97. Kulig K, Oki KC, Chang Y-J, Bashford GR. Achilles and patellar tendon morphology in dancers with and without tendon pain. Med Probl Perform Art. diciembre de 2014;29(4):221-8.

98. Lahiri BB, Bagavathiappan S, Jayakumar T, Philip J. Medical applications of infrared thermography: A review. Infrared Physics & Technology. julio de 2012;55(4):221-35.

99. Lalumiere M, Larivière C, Nadeau M-J, Paquette P, Lamontagne M, Desmeules F, et al. Proposing a Minimal Data Set of Musculoskeletal Ultrasound Imaging Biomarkers to Inform Clinical Practice: An Analysis Founded on the Achilles Tendon. Ultrasound in Medicine & Biology. septiembre de 2020;46(9):2222-35.

100. Lee H, Petrofsky J, Shah N, Awali A, Shah K, Alotaibi M, et al. Higher sweating rate and skin blood flow during the luteal phase of the menstrual cycle. Tohoku J Exp Med. octubre de 2014;234(2):117-22.

101. Li Y, Tang MX, Agarwal R, Patel D, Eckersley RJ, Barrois G, et al. Power Doppler Quantification in Assessing Gestational Trophoblastic Neoplasia. Ultraschall Med. abril de 2018;39(2):206-12.

102. Lian Ø, Dahl J, Ackermann PW, Frihagen F, Engebretsen L, Bahr R. Pronociceptive and antinociceptive neuromediators in patellar tendinopathy. Am J Sports Med. noviembre de 2006;34(11):1801-8.

103. Lian Ø, Scott A, Engebretsen L, Bahr R, Duronio V, Khan K. Excessive apoptosis in patellar tendinopathy in athletes. Am J Sports Med. abril de 2007;35(4):605-11.

104. Lian OB, Engebretsen L, Bahr R. Prevalence of jumper's knee among elite athletes from different sports: a cross-sectional study. Am J Sports Med. abril de 2005;33(4):561-7.

105. López-Royo MP, Ríos-Díaz J, Galán-Díaz RM, Herrero P, Gómez-Trullén EM. A Comparative Study of Treatment Interventions for Patellar Tendinopathy: A Randomized Controlled Trial. Archives of Physical Medicine and Rehabilitation. mayo de 2021;102(5):967-75.

106. Maffulli N, Wong J, Almekinders LC. Types and epidemiology of tendinopathy. Clinics in Sports Medicine. 1 de octubre de 2003;22(4):675-92.

107. Magas V, Abreu de Souza M, Borba Neves E, Nohama P. Evaluation of thermal imaging for the diagnosis of repetitive strain injuries of the wrist and hand joints. Res Biomed Eng. 1 de marzo de 2019;35(1):57-64.

108. Magnusson SP, Langberg H, Kjaer M. The pathogenesis of tendinopathy: balancing the response to loading. Nat Rev Rheumatol. 2010;6(5):262-8.

109. Malliaras P, Cook J, Purdam C, Rio E. Patellar Tendinopathy: Clinical Diagnosis, Load Management, and Advice for Challenging Case Presentations. J Orthop Sports Phys Ther. noviembre de 2015;45(11):887-98.

110. Malliaras P, Purdam C. Proximal hamstring tendinopathy assessment and management. Sport Health. mayo de 2014;32(1):21.

111. Malliaras P, Purdam C, Maffulli N, Cook J. Temporal sequence of greyscale ultrasound changes and their relationship with neovascularity and pain in the patellar tendon. Br J Sports Med. octubre de 2010;44(13):944-7.

112. Malliaras P, Richards PJ, Garau G, Maffulli N. Achilles tendon Doppler flow may be associated with mechanical loading among active athletes. Am J Sports Med. noviembre de 2008;36(11):2210-5.

113. Mangine RE, Siqueland KA, Noyes FR. The use of thermography for the diagnosis and management of patellar tendinitis. J Orthop Sports Phys Ther. 1987;9(4):132-40.

114. Manning CN, Havlioglu N, Knutsen E, Sakiyama-Elbert SE, Silva MJ, Thomopoulos S, et al. The early inflammatory response after flexor tendon healing: a gene expression and histological analysis. J Orthop Res. mayo de 2014;32(5):645-52.

115. McAuliffe S, McCreesh K, Culloty F, Purtill H, O'Sullivan K. Can ultrasound imaging predict the development of Achilles and patellar tendinopathy? A systematic review and meta-analysis. Br J Sports Med. diciembre de 2016;50(24):1516-23.

116. Mercier J, Tang A, Morin M, Khalifé S, Lemieux M-C, Reichetzer B, et al. Test-retest reliability of clitoral blood flow measurements using color Doppler ultrasonography at rest and after a pelvic floor contraction task in healthy adult women. Neurourology and Urodynamics. septiembre de 2018;37(7):2249-56.

117. Merkel MFR, Hellsten Y, Magnusson SP, Kjaer M. Tendon blood flow, angiogenesis, and tendinopathy pathogenesis. Translational Sports Med. noviembre de 2021;4(6):756-71.

118. Meyer AW. FURTHER OBSERVATIONS UPON USE-DESTRUCTION IN JOINTS. JBJS. julio de 1922;4(3):491-511.

119. Millar NL, Gilchrist DS, Akbar M, Reilly JH, Kerr SC, Campbell AL, et al. MicroRNA29a regulates IL-33-mediated tissue remodelling in tendon disease. Nat Commun. 10 de abril de 2015;6:6774.

120. Millar NL, Hueber AJ, Reilly JH, Xu Y, Fazzi UG, Murrell GAC, et al. Inflammation is Present in Early Human Tendinopathy. Am J Sports Med. 1 de octubre de 2010;38(10):2085-91.

121. Molina-Payá FJ, Ríos-Díaz J, Carrasco-Martínez F, Martínez-Payá JJ. Reliability of a new semi-automatic image analysis method for evaluating the Doppler signal and intratendinous vascular resistance in patellar tendinopathy. Ultrasound in Med & Biol. 2021a;In press.

122. Molina-Payá J, Ríos-Díaz J, Martínez-Payá J. Inter and intraexaminer reliability of a new method of infrared thermography analysis of patellar tendon. Quantitative InfraRed Thermography Journal. 17 de diciembre de 2019;0(0):1-13.

123. Molina-Payá J, Ríos-Díaz J, Martínez-Payá J. Inter and intraexaminer reliability of a new method of infrared thermography analysis of patellar tendon. Quantitative InfraRed Thermography Journal. 15 de marzo de 2021b;18(2):127-39.

124. Mustacchi G, Milani S, Ciatto S, Del Turco MR, Luzzati G, Lattanzio V, et al. Observer variation in mammary thermography: results of a teaching file test carried out in four different centers. Tumori. 28 de febrero de 1990;76(1):29-31.

125. Nakama LH, King KB, Abrahamsson S, Rempel DM. VEGF, VEGFR-1, and CTGF cell densities in tendon are increased with cyclical loading: An in vivo tendinopathy model. J Orthop Res. marzo de 2006;24(3):393-400.

126. Niu HH, Lui PW, Hu JS, Ting CK, Yin YC, Lo YL, et al. Thermal symmetry of skin temperature: normative data of normal subjects in Taiwan. Zhonghua Yi Xue Za Zhi (Taipei). agosto de 2001;64(8):459-68.

127. Ohberg L, Alfredson H. Ultrasound guided sclerosis of neovessels in painful chronic Achilles tendinosis: pilot study of a new treatment. Br J Sports Med. junio de 2002;36(3):173-5; discussion 176-177.

128. Ohberg L, Lorentzon R, Alfredson H. Neovascularisation in Achilles tendons with painful tendinosis but not in normal tendons: an ultrasonographic investigation. Knee Surg Sports Traumatol Arthrosc. julio de 2001;9(4):233-8.

129. Patil P, Dasgupta B. Role of diagnostic ultrasound in the assessment of musculoskeletal diseases. Ther Adv Musculoskelet Dis. octubre de 2012;4(5):341-55.

130. Peers KHE, Brys PPM, Lysens RJJ. Correlation between power Doppler ultrasonography and clinical severity in Achilles tendinopathy. Int Orthop. junio de 2003;27(3):180-3.

131. Peers KHE, Lysens RJJ. Patellar tendinopathy in athletes: current diagnostic and therapeutic recommendations. Sports Med. 2005;35(1):71-87.

132. Perry SM, McIlhenny SE, Hoffman MC, Soslowsky LJ. Inflammatory and angiogenic mRNA levels are altered in a supraspinatus tendon overuse animal model. J Shoulder Elbow Surg. febrero de 2005;14(1 Suppl S):79S-83S.

133. Poltawski L, Ali S, Jayaram V, Watson T. Reliability of sonographic assessment of tendinopathy in tennis elbow. Skeletal Radiol. enero de 2012;41(1):83-9.

134. Pratt WK. Digital Image Processing: PIKS Scientific Inside. Wiley; 2007.

135. Puddu G, Ippolito E, Postacchini F. A classification of Achilles tendon disease. Am J Sports Med. agosto de 1976;4(4):145-50.

136. Pufe T, Petersen WJ, Mentlein R, Tillmann BN. The role of vasculature and angiogenesis for the pathogenesis of degenerative tendons disease. Scand J Med Sci Sports. agosto de 2005;15(4):211-22.

137. Qi JH, Ebrahem Q, Moore N, Murphy G, Claesson-Welsh L, Bond M, et al. A novel function for tissue inhibitor of metalloproteinases-3 (TIMP3): inhibition of angiogenesis by blockage of VEGF binding to VEGF receptor-2. Nat Med. abril de 2003;9(4):407-15.

138. Qvistgaard E, Røgind H, Torp-Pedersen S, Terslev L, Danneskiold-Samsøe B, Bliddal H. Quantitative ultrasonography in rheumatoid arthritis: evaluation of inflammation by Doppler technique. Ann Rheum Dis. julio de 2001;60(7):690-3.

139. Ra JY, An S, Lee G-H, Kim TU, Lee SJ, Hyun JK. Skin Temperature Changes in Patients With Unilateral Lumbosacral Radiculopathy. Ann Rehabil Med. 2013;37(3):355.

140. Rees JD, Stride M, Scott A. Tendons--time to revisit inflammation. Br J Sports Med. noviembre de 2014;48(21):1553-7.

141. Rees JD, Wilson AM, Wolman RL. Current concepts in the management of tendon disorders. Rheumatology (Oxford). mayo de 2006;45(5):508-21.

142. Reiter M, Ulreich N, Dirisamer A, Tscholakoff D, Bucek RA. Colour and power Doppler sonography in symptomatic Achilles tendon disease. Int J Sports Med. mayo de 2004;25(4):301-5.

143. Richards PJ, Dheer AK, McCall IM. Achilles tendon (TA) size and power Doppler ultrasound (PD) changes compared to MRI: a preliminary observational study. Clin Radiol. octubre de 2001;56(10):843-50.

144. Richards PJ, Win T, Jones PW. The distribution of microvascular response in Achilles tendonopathy assessed by colour and power Doppler. Skeletal Radiol. junio de 2005;34(6):336-42.

145. Riley GP, Harrall RL, Constant CR, Chard MD, Cawston TE, Hazleman BL. Tendon degeneration and chronic shoulder pain: changes in the collagen composition of the human rotator cuff tendons in rotator cuff tendinitis. Ann Rheum Dis. junio de 1994;53(6):359-66.

146. Ring EFJ, Ammer K. Infrared thermal imaging in medicine. Physiol Meas. 1 de marzo de 2012;33(3):R33.

147. Rio E, Moseley L, Purdam C, Samiric T, Kidgell D, Pearce AJ, et al. The Pain of Tendinopathy: Physiological or Pathophysiological? Sports Med. 1 de enero de 2014;44(1):9-23.

148. Ríos-Díaz J, Groot Ferrando A de, Martínez-Payá JJ, Baño Aledo ME del. Fiabilidad y reproducibilidad de un nuevo método de análisis morfotextural de imágenes ecográficas del tendón rotuliano. Reumatol Clin. 1 de noviembre de 2010;6(6):278-84.

149. Ríos-Díaz J, Martínez-Payá JJ, delBaño-Aledo ME. El análisis textural mediante las matrices de co-ocurrencia (GLCM) sobre la imagen ecográfica del tendón rotuliano es de utilidad para la detección de cambios histológicos tras un entrenamiento con plataforma de vibración. Cultura, ciencia y deporte. 2009;4(11):91-102.

150. Ríos-Díaz J, Martínez-Payá JJ, del Baño-Aledo ME, de Groot-Ferrando A, Botía-Castillo P, Fernández-Rodríguez D. Sonoelastography of Plantar Fascia: Reproducibility and Pattern Description in Healthy Subjects and Symptomatic Subjects. Ultrasound in Medicine & Biology. octubre de 2015;41(10):2605-13.

151. Risch L, Cassel M, Mayer F. Acute effect of running exercise on physiological Achilles tendon blood flow. Scand J Med Sci Sports. enero de 2018;28(1):138-43.

152. Risch L, Cassel M, Messerschmidt J, Intziegianni K, Fröhlich K, Kopinski S, et al. Is Sonographic Assessment of Intratendinous Blood Flow in Achilles

Tendinopathy Patients Reliable? Ultrasound Int Open. marzo de 2016;2(1):E13-8.

153. Risch L, Stoll J, Schomöller A, Engel T, Mayer F, Cassel M. Intraindividual Doppler Flow Response to Exercise Differs Between Symptomatic and Asymptomatic Achilles Tendons. Front Physiol. 2021;12:617497.
154. Rodrigues-Bigaton D, Dibai Filho AV, Costa AC de S, Packer AC, de Castro EM. Accuracy and reliability of infrared thermography in the diagnosis of arthralgia in women with temporomandibular disorder. J Manipulative Physiol Ther. mayo de 2013;36(4):253-8.
155. Rubin JM. Spectral Doppler US. Radiographics. enero de 1994;14(1):139-50.
156. Rubin JM, Bude RO, Carson PL, Bree RL, Adler RS. Power Doppler US: a potentially useful alternative to mean frequency-based color Doppler US. Radiology. marzo de 1994;190(3):853-6.
157. Rütten A, Abu-Omar K. Prevalence of physical activity in the European Union. Soz Praventivmed. 2004;49(4):281-9.
158. Sato A, Takahashi A, Yamadera Y, Takeda I, Kanno T, Ohguchi Y, et al. Doppler sonographic analysis of synovial vascularization in knee joints of patients with rheumatoid arthritis: increased color flow signals and reduced vascular resistance. Mod Rheumatol. 2005;15(1):33-6.
159. Sato Y, Abe M, Tanaka K, Iwasaka C, Oda N, Kanno S, et al. Signal transduction and transcriptional regulation of angiogenesis. Adv Exp Med Biol. 2000;476:109-15.
160. Schlereth T, Birklein F. The Sympathetic Nervous System and Pain. Neuromol Med. septiembre de 2008;10(3):141-7.
161. Scott A, Docking S, Vicenzino B, Alfredson H, Zwerver J, Lundgreen K, et al. Sports and exercise-related tendinopathies: a review of selected topical issues by participants of the second International Scientific Tendinopathy Symposium (ISTS) Vancouver 2012. Br J Sports Med. junio de 2013;47(9):536-44.
162. Scott A, Lian Ø, Bahr R, Hart DA, Duronio V. VEGF expression in patellar tendinopathy: a preliminary study. Clin Orthop Relat Res. julio de 2008;466(7):1598-604.

163. Seixas, A, Gabriel, J, Vardasca, R. Thermographic evaluation in tendinopathies. En: Lecture notes of the ICB seminar: advances of infra-red thermal imaging in medicine. Warsaw: A. Nowakowski, James B. Mercer; 2013. p. 49-53.

164. Selfe J, Hardaker N, Thewlis D, Karki A. An accurate and reliable method of thermal data analysis in thermal imaging of the anterior knee for use in cryotherapy research. Arch Phys Med Rehabil. diciembre de 2006;87(12):1630-5.

165. Seo J, Kim Y. Ultrasound imaging and beyond: recent advances in medical ultrasound. Biomed Eng Lett. mayo de 2017;7(2):57-8.

166. Sillero-Quintana M, Fernández-Jaén T, Fernández-Cuevas I, Gómez-Carmona PM, Arnaiz-Lastras J, Pérez M-D, et al. Infrared Thermography as a Support Tool for Screening and Early Diagnosis in Emergencies. Journal of Medical Imaging and Health Informatics. 1 de noviembre de 2015;5(6):1223-8.

167. van Snellenberg W, Wiley JP, Brunet G. Achilles tendon pain intensity and level of neovascularization in athletes as determined by color Doppler ultrasound. Scand J Med Sci Sports. noviembre de 2006;0(0):061120070736011-???

168. Spalding SJ, Kwoh CK, Boudreau R, Enama J, Lunich J, Huber D, et al. Three-dimensional and thermal surface imaging produces reliable measures of joint shape and temperature: a potential tool for quantifying arthritis. Arthritis Res Ther. 2008;10(1):R10.

169. Spang C, Harandi VM, Alfredson H, Forsgren S. Marked innervation but also signs of nerve degeneration in between the Achilles and plantaris tendons and presence of innervation within the plantaris tendon in midportion Achilles tendinopathy. J Musculoskelet Neuronal Interact. junio de 2015;15(2):197-206.

170. Speed C. Inflammation in Tendon Disorders. En: Ackermann PW, Hart DA, editores. Metabolic Influences on Risk for Tendon Disorders [Internet]. Cham: Springer International Publishing; 2016 [citado 21 de octubre de 2021]. p. 209-20. (Advances in Experimental Medicine and Biology; vol. 920). Disponible en: http://link.springer.com/10.1007/978-3-319-33943-6_20

171. Splittgerber LE, Ihm JM. Significance of Asymptomatic Tendon Pathology in Athletes. Current Sports Medicine Reports. junio de 2019;18(6):192-200.

172. Strakowski JA. Introduction to musculoskeletal ultrasound: getting started. New York: Demos Medical; 2016.

173. Strunk J, Strube K, Rumbaur C, Lange U, Müller-Ladner U. Interobserver agreement in two- and three-dimensional power Doppler sonographic assessment of synovial vascularity during anti-inflammatory treatment in patients with rheumatoid arthritis. Ultraschall Med. agosto de 2007;28(4):409-15.

174. Sunding K, Fahlström M, Werner S, Forssblad M, Willberg L. Evaluation of Achilles and patellar tendinopathy with greyscale ultrasound and colour Doppler: using a four-grade scale. Knee Surg Sports Traumatol Arthrosc. junio de 2016;24(6):1988-96.

175. Tang C, Chen Y, Huang J, Zhao K, Chen X, Yin Z, et al. The roles of inflammatory mediators and immunocytes in tendinopathy. Journal of Orthopaedic Translation. 1 de julio de 2018;14:23-33.

176. Terabayashi N, Watanabe T, Matsumoto K, Takigami I, Ito Y, Fukuta M, et al. Increased blood flow in the anterior humeral circumflex artery correlates with night pain in patients with rotator cuff tear. Journal of Orthopaedic Science. septiembre de 2014;19(5):744-9.

177. Terslev L, Torp-Pedersen S, Qvistgaard E, Bliddal H. Spectral Doppler and resistive index. A promising tool in ultrasonographic evaluation of inflammation in rheumatoid arthritis. Acta Radiol. noviembre de 2003;44(6):645-52.

178. Thorpe CT, Chaudhry S, Lei II, Varone A, Riley GP, Birch HL, et al. Tendon overload results in alterations in cell shape and increased markers of inflammation and matrix degradation. Scand J Med Sci Sports. agosto de 2015;25(4):e381-391.

179. Tol JL, Spiezia F, Maffulli N. Neovascularization in Achilles tendinopathy: have we been chasing a red herring? Knee Surg Sports Traumatol Arthrosc. octubre de 2012;20(10):1891-4.

180. Torp-Pedersen ST, Terslev L. Settings and artefacts relevant in colour/power Doppler ultrasound in rheumatology. Ann Rheum Dis. febrero de 2008;67(2):143-9.

181. Torp-Pedersen TE, Torp-Pedersen ST, Qvistgaard E, Bliddal H. Effect of glucocorticosteroid injections in tennis elbow verified on colour Doppler ultrasonography: evidence of inflammation. Br J Sports Med. diciembre de 2008;42(12):978-82.

182. Tran PHT, Malmgaard-Clausen NM, Puggaard RS, Svensson RB, Nybing JD, Hansen P, et al. Early development of tendinopathy in humans: Sequence of pathological changes in structure and tissue turnover signaling. FASEB j. enero de 2020;34(1):776-88.

183. Tumilty S, Adhia DB, Smoliga JM, Gisselman AS. Thermal profiles over the Achilles tendon in a cohort of non-injured collegiate athletes over the course of a cross country season. Phys Ther Sport. marzo de 2019;36:110-5.

184. Uematsu S. Thermographic imaging of cutaneous sensory segment in patients with peripheral nerve injury. Skin-temperature stability between sides of the body. J Neurosurg. mayo de 1985;62(5):716-20.

185. Uematsu S, Edwin DH, Jankel WR, Kozikowski J, Trattner M. Quantification of thermal asymmetry. Part 1: Normal values and reproducibility. J Neurosurg. octubre de 1988;69(4):552-5.

186. Vardasca R, Ring F, Plassmann P, Jones C. Thermal symmetry of the upper and lower extremities in healthy subjects. Thermology International. 2012;22:53-60.

187. Varjú G, Pieper CF, Renner JB, Kraus VB. Assessment of hand osteoarthritis: correlation between thermographic and radiographic methods. Rheumatology (Oxford). julio de 2004;43(7):915-9.

188. Ventura L. Manual de ecografía musculoesqulética. México: Editorial Médica Panamericana; 2010.

189. Wang H, Keiser JA. Vascular endothelial growth factor upregulates the expression of matrix metalloproteinases in vascular smooth muscle cells: role of flt-1. Circ Res. 19 de octubre de 1998;83(8):832-40.

190. Watmough DJ, Fowler PW, Oliver R. The thermal scanning of a curved isothermal surface: implications for clinical thermography. Phys Med Biol. enero de 1970;15(1):1-8.

191. Watson J, Barker-Davies RM, Bennett AN, Fong DTP, Wheeler PC, Lewis M, et al. Sport and exercise medicine consultants are reliable in assessing tendon neovascularity using ultrasound Doppler. BMJ Open Sport Exerc Med. 2018;4(1):e000298.

192. Xu Y, Murrell GAC. The basic science of tendinopathy. Clin Orthop Relat Res. julio de 2008;466(7):1528-38.

193. Yang X, Coleman DP, Pugh ND, Liu W, Nokes L. Quantitative assessment of intra-vascular volume in human Achilles tendinopathy. J Med Eng Technol. mayo de 2011a;35(3-4):172-8.

194. Yang X, Coleman DP, Pugh ND, Nokes LDM. A Novel 3-D Power Doppler Ultrasound Approach to the Quantification of Achilles Tendon Neovascularity. Ultrasound in Medicine & Biology. julio de 2011b;37(7):1046-55.

195. Yang X, Coleman DP, Pugh ND, Nokes LDM. The volume of the neovascularity and its clinical implications in achilles tendinopathy. Ultrasound Med Biol. noviembre de 2012;38(11):1887-95.

196. Yuan A, Chang DB, Yu CJ, Kuo SH, Luh KT, Yang PC. Color Doppler sonography of benign and malignant pulmonary masses. AJR Am J Roentgenol. septiembre de 1994;163(3):545-9.

197. Zaproudina N, Varmavuo V, Airaksinen O, Närhi M. Reproducibility of infrared thermography measurements in healthy individuals. Physiol Meas. abril de 2008;29(4):515-24.

198. Zwerver J, Bredeweg SW, van den Akker-Scheek I. Prevalence of Jumper's knee among nonelite athletes from different sports: a cross-sectional survey. Am J Sports Med. septiembre de 2011;39(9):1984-8.

ANEXOS

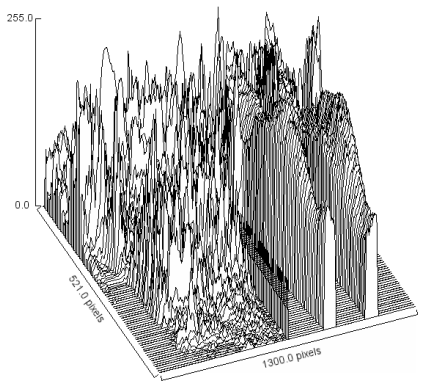

XI. ANEXOS

11.1. ANEXO 1. JUSTIFICANTE DE PRESENTACIÓN ELECTRÓNICA DE SOLICITUD DE PATENTE

Justificante de presentación electrónica de solicitud de patente

Este documento es un justificante de que se ha recibido una solicitud española de patente por vía electrónica utilizando la conexión segura de la O.E.P.M. De acuerdo con lo dispuesto en el art. 16.1 del Reglamento de ejecución de la Ley 24/2015 de Patentes, se han asignado a su solicitud un número de expediente y una fecha de recepción de forma automática. La fecha de presentación de la solicitud a la que se refiere el art. 24 de la Ley le será comunicada posteriormente.

Número de solicitud:	P201830950	
Fecha de recepción:	02 October 2018, 11:17 (CEST)	
Oficina receptora:	OEPM Madrid	
Su referencia:	1	
Solicitante:	Francisco Javier Molina Paya	
Número de solicitantes:	1	
País:	ES	
Título:	MÉTODO Y EQUIPO DE MEDICIÓN DE TEMPERATURA.	
Documentos enviados:	Descripcion.pdf (11 p.) Reivindicaciones.pdf (4 p.) Resumen.pdf (1 p.) Dibujos.pdf (1 p.) OLF-ARCHIVE.zip POWATT.pdf (1 p.)	package-data.xml es-request.xml application-body.xml es-fee-sheet.xml feesheet.pdf request.pdf
Enviados por:	CN=MUÑOZ FERNANDEZ FRANCISCO JAVIER - 00836408J,givenName=FRANCISCO JAVIER,SN=MUÑOZ FERNANDEZ,serialNumber=00836408J,C=ES	
Fecha y hora de recepción:	02 October 2018, 11:17 (CEST)	
Codificación del envío:	2A:57:61:89:CC:A4:76:EF:6D:1C:C7:5F:57:41:E8:39:65:58:D9:2F	

AVISO IMPORTANTE
Las tasas pagaderas al solicitar y durante la tramitación de una patente o un modelo de utilidad son las que se recogen en el Apartado "Tasas y precios públicos" de la página web de la OEPM (http://www.oepm.es/es/propiedad_industrial/tasas/). Consecuentemente, si recibe una comunicación informándole de la necesidad de hacer un pago por la inscripción de su patente o su modelo de utilidad en un "registro central" o en un "registro de internet" posiblemente se trate de un fraude.
La anotación en este tipo de autodenominados "registros" no despliega ningún tipo de eficacia jurídica ni tiene carácter oficial.
En estos casos le aconsejamos que se ponga en contacto con la Oficina Española de Patentes y Marcas en el correo electrónico informacion@oepm.es.

ADVERTENCIA: POR DISPOSICIÓN LEGAL LOS DATOS CONTENIDOS EN ESTA SOLICITUD PODRÁN SER PUBLICADOS EN EL BOLETÍN OFICIAL DE LA PROPIEDAD INDUSTRIAL E INSCRITOS EN EL REGISTRO DE PATENTES DE LA OEPM, SIENDO AMBAS BASES DE DATOS DE CARÁCTER PÚBLICO Y ACCESIBLES VÍA REDES MUNDIALES DE INFORMÁTICA.
Para cualquier aclaración puede contactar con la O.E.P.M.

/Madrid, Oficina Receptora/

MINISTERIO DE INDUSTRIA, ENERGÍA Y TURISMO

Oficina Española de Patentes y Marcas

(1) MODALIDAD: **PATENTE DE INVENCIÓN** **MODELO DE UTILIDAD**	[✓] [ ]
(2) TIPO DE SOLICITUD: PRIMERA PRESENTACIÓN SOLICITUD DIVISIONAL CAMBIO DE MODALIDAD TRANSFORMACION SOLICITUD PATENTE EUROPEA PCT: ENTRADA FASE NACIONAL	[✓] [ ] [ ] [ ] [ ]
(3) EXP. PRINCIPAL O DE ORIGEN: MODALIDAD: N.º SOLICITUD: FECHA SOLICITUD:	
4) LUGAR DE PRESENTACIÓN:	OEPM, Presentación Electrónica
(5-1) SOLICITANTE 1: APELLIDOS: NOMBRE: NACIONALIDAD: CÓDIGO PAÍS: NIF/NIE/PASAPORTE: DOMICILIO: LOCALIDAD: PROVINCIA: CÓDIGO POSTAL: PAÍS RESIDENCIA: CÓDIGO PAÍS: TELÉFONO: FAX: CORREO ELECTRÓNICO: EMPRENDEDOR: EL SOLICITANTE ES INVENTOR EL SOLICITANTE NO ES INVENTOR PORCENTAJE DE TITULARIDAD:	 Molina Paya Francisco Javier España ES 44751322-S C/ Joaquin Turina, 3 MONOVAR 03 Alicante 03640 España ES [ ] [✓] [ ] 100,00 %
(6-1) INVENTOR 1: APELLIDOS: NOMBRE: NACIONALIDAD: CÓDIGO PAÍS:	 Molina Paya Francisco Javier España ES
(7) TÍTULO DE LA INVENCIÓN:	MÉTODO Y EQUIPO DE MEDICIÓN DE TEMPERATURA.
(8) NÚMERO DE INFORME TECNOLÓGICO DE PATENTES (ITP):	P
(9) SOLICITA LA INCLUSIÓN EN EL PROCEDIMIENTO ACELERADO DE CONCESIÓN SI NO	 [ ] [✓]
(10) EFECTUADO DEPÓSITO DE MATERÍA BIOLÓGICA: SI NO	 [ ] [✓]

(11) DEPÓSITO: REFERENCIA DE IDENTIFICACIÓN: INSTITUCIÓN DE DEPÓSITO: NÚMERO DE DEPÓSITO: ORÍGEN BIOLÓGICO:	
(12) RECURSO GENÉTICO: NÚMERO DE REGISTRO: NÚMERO DE CERTIFICADO DE ACCESO AL RECURSO: UTILIZACIÓN DEL RECURSO GENÉTICO: CONOCIMIENTO TRADICIONAL ASOCIADO A UN RECURSO GENÉTICO:	
(13) DECLARACIONES RELATIVAS A LA LISTA DE SECUENCIAS: LA LISTA DE SECUENCIAS NO VA MÁS ALLÁ DEL CONTENIDO DE LA SOLICITUD LA LISTA DE SECUENCIAS EN FORMATO PDF Y ASCII SON IDENTICOS	 [ ] [ ]
(14) EXPOSICIONES OFICIALES: NOMBRE: LUGAR: FECHA:	
(15) DECLARACIONES DE PRIORIDAD: PAÍS DE ORIGEN: CÓDIGO PAÍS: NÚMERO: FECHA:	
(16) REMISION A UNA SOLICITUD ANTERIOR: PAÍS DE ORIGEN: CÓDIGO PAÍS: NÚMERO: FECHA:	
(17) AGENTE DE PROPIEDAD INDUSTRIAL: APELLIDOS: NOMBRE: CÓDIGO DE AGENTE: NÚMERO DE PODER:	 DE PABLOS RIBA JUAN RAMON 0512/6
(18) DIRECCIÓN A EFECTOS DE COMUNICACIONES: SÓLO EN CASO DE DIRECCIÓN DIFERENTE DE LA INDICADA PARA EL PRIMER SOLICITANTE DOMICILIO: LOCALIDAD: PROVINCIA: CÓDIGO POSTAL: PAÍS RESIDENCIA: CÓDIGO PAÍS: TELÉFONO: FAX: CORREO ELECTRÓNICO: MEDIO PREFERENTE DE COMUNICACIÓN	
(19) RELACIÓN DE DOCUMENTOS QUE SE ACOMPAÑAN: DESCRIPCIÓN: REIVINDICACIONES: DIBUJOS: RESUMEN: FIGURA(S) A PUBLICAR CON EL RESUMEN: ARCHIVO DE PRECONVERSION: DOCUMENTO DE REPRESENTACION: LISTA DE SECUENCIAS PDF: ARCHIVO PARA LA BUSQUEDA DE LS: OTROS (Aparecerán detallados):	 [✓] N.º de páginas: 11 [✓] N.º de reivindicaciones: 17 [✓] N.º de dibujos: 1 [✓] N.º de páginas: 1 [✓] N.º de figura(s): 1 [✓] [✓] N.º de páginas: 1 [ ] N.º de páginas: [ ]

(20) EL SOLICITANTE SE ACOGE A LA REDUCCIÓN DE TASAS PARA EMPRENDEDORES PREVISTA EN EL ART. 186 DE LA LEY 24/2015 DE PATENTES Y, A TAL EFECTO, APORTA LA SIGUIENTE DOCUMENTACIÓN ADJUNTA:	[ ]
(21) NOTAS:	
(22) FIRMA: FIRMA DEL SOLICITANTE O REPRESENTANTE: LUGAR DE FIRMA: FECHA DE FIRMA:	

11.2. ANEXO 2. EXPEDIENTE DE LA OFICINA ESPAÑOLA DE PATENTES Y MARCAS

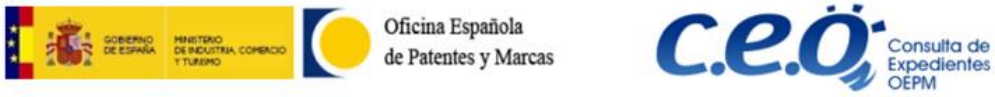

Fecha consulta: 22/11/2021 10:25:41

Patente nacional P201830950(1) - MÉTODO Y EQUIPO DE MEDICIÓN DE TEMPERATURA.

Nº Solicitud: P201830950 **Fecha presentación:** 02/10/2018

Nº publicación: ES2752084 **Fecha publicación:** 02/04/2020

Título: MÉTODO Y EQUIPO DE MEDICIÓN DE TEMPERATURA.

Estado: Solicitud publicada **Actualizado el:** 17/07/2020

Solicitante / Titular:

Nombre:	Francisco Javier Molina Paya (100,00%)
Dirección:	C/ Joaquin Turina, 3
Localidad:	MONOVAR
Provincia:	Alicante
Código Postal:	03640
País de residencia:	ES ESPAÑA

Inventor/es:

Francisco Javier Molina Paya

Agente:

Código del agente:	0512
Nombre:	Juan Ramón de Pablos Riba
Dirección:	C/ Los Madrazo, 24
Localidad:	Madrid
Código postal:	28014

Clasificaciones:

CIP invención publicación: *A61B 5/01*

Publicación:

Nº Publicación	País de publicación	Fecha publicación	Tipo documento
ES2752084	ES	02/04/2020	A1 Solicitud de patente con informe sobre el estado de la técnica

Tramitado según Ley 24/2015

Actos de tramitación:

Fecha	Acto de tramitación
02/10/2018	Registro Instancia de Solicitud
02/10/2018	Admisión a Trámite
02/10/2018	1001P_Comunicación Admisión a Trámite
04/10/2018	Superado examen de oficio
21/11/2019	Realizado IET
22/11/2019	Revisión Calidad IET AA (Conforme)
22/11/2019	1109P_Comunicación Traslado del IET
02/04/2020	Publicación Solicitud
02/04/2020	Publicación Folleto Solicitud con IET (A1)
20/04/2020	PETEX_Petición de examen sustantivo
17/07/2020	Validación petición y/o pago de examen sustantivo conforme

Anotaciones de pagos:

Fecha	Texto
02/10/2018	Pago Tasas IET

11.3. ANEXO 3. COMPENDIO DE PUBLICACIONES

Esta tesis se presenta en formato de estudios individuales a modo de artículos que representan algunos de los apartados de la investigación. Los dos primeros estudios están publicados en revistas científicas, y los dos posteriores en proceso de envío. A este compendio de publicaciones se añade una solicitud de patente derivaba de esta tesis.

ESTUDIO I.

Molina-Payá J, Ríos-Díaz J, Martínez-Payá J. Inter and intraexaminer reliability of a new method of infrared thermography analysis of patellar tendon. Quant InfraRed Thermogr J. 15 de marzo de 2021;18(2):127-39.

DOI: 10.1080/17686733.2019.1700697.

DATOS INDEX ISI WEB OF SCIENCE: ISSN: 1768-6733. RANKING (2020): MATERIALS SCIENCE, CHARACTERIZATION & TESTING 18/32; INSTRUMENTS & INSTRUMENTATION 42/64.

IMPACT FACTOR JCR (2020): 1.667.

ESTUDIO II.

Molina-Payá FJ, Ríos-Díaz J, Carrasco-Martínez F, Martínez-Payá JJ. Reliability of a New Semi-automatic Image Analysis Method for Evaluating the Doppler Signal and Intratendinous Vascular Resistance in Patellar Tendinopathy. Ultrasound Med Biol. 15 de septiembre de 2021;S0301-5629(21)00365-3.

DOI: 10.1016/j.ultrasmedbio.2021.08.010.

DATOS INDEX ISI WEB OF SCIENCE: ISSN: 0301-5629. RANKING (2020): RADIOLOGY, NUCLEAR MEDICINE & MEDICAL IMAGIND 64/133; ACOUSTICS 7/31.

IMPACT FACTOR JCR (2020): 2.998.

ESTUDIO III.

Molina-Payá J, Ríos-Díaz J, Martínez-Payá J. Correlación entre el índice de resistencia y un nuevo método semiautomático de análisis de imagen para evaluar la resistencia vascular. (en proceso de publicación).

ESTUDIO IV.

Molina-Payá FJ, Ríos-Díaz J, Carrasco-Martínez F, Martínez-Payá JJ. Termografía infrarroja, resistencia vascular intratendón y ecotextura en deportistas con tendinopatía rotuliana: estudio transversal. (en proceso de publicación).

SOLICITUD DE PATENTE.

Número de solicitud: P201830950

Título: Método y equipo de medición de temperatura

CIP invención publicación: A61B 5/01

Solicitante: Francisco Javier Molina Payá

Fecha de recepción: 02 de octubre del 2018

Fecha de publicación: 02 de abril del 2020

COMUNICACIÓN 1

Título: "Fiabilidad y reproducibilidad de un método de análisis termográfico del tendón rotuliano".

Autores: Molina J, Ríos-Díaz J.

En: II Jornadas Internacionales de prevención de lesiones deportivas y XXIII Jornadas Nacionales de Traumatología del Deporte.

Lugar: UCAM.

Fecha: del 5 al 7 de marzo del 2015.

- **Primer premio a la mejor comunicación.**

COMUNICACIÓN 2

Título: "Sensibilidad de los parámetros de optimización ecográfica en la ecogenicidad y ecotextura del tendón".

Autores: Molina-Payá J, Ríos-Díaz J, Martínez-Payá J J, delBaño-Aledo M E.

En: XVII Congreso Nacional de Fisioterapia UCAM.

Lugar: UCAM.

Fecha: del 15 al 17 de abril del 2015.

- **Primer premio a la mejor comunicación.**

COMUNICACIÓN 3

Título: "Influencia de los parámetros de optimización en ecografía cuantitativa del tendón".

Autores: Molina-Payá J, Ríos-Díaz J.

En: I Jornadas de Investigación y doctorado UCAM".

Lugar: UCAM.

Fecha: 26 de junio del 2015.

- **Primer premio a la mejor comunicación.**

COMUNICACIÓN 4

Título: "Cuantificación de la perfusión tisular en patología tendinosa".

Autores: Molina-Payá J.

En: II Jornadas de Fisioterapia San Rafael-Nebrija".

Lugar: Universidad San Rafael-Nebrija.

Fecha: 24 de noviembre del 2017.

COMUNICACIÓN TIPO PÓSTER 5

Título: "Fiabilidad y reproducibilidad de marcadores termográficos en el tendón rotuliano".

Autores: Molina-Payá J, Ríos-Díaz J.

En: I Encuentro de Investigación en Fisioterapia Neuromusculoesquelética".

Lugar: Universidad de Alcalá.

Fecha: 5, 6 y 7 de abril del 2019.

COMUNICACIÓN 6

Título: "Análisis de la perfusión tisular mediante cuantificación Doppler".

Autores: Molina-Payá J.

En: I International Online Congress Physiotherapy Musculoskeletal Ultrasound (PhyMU).

Lugar: On-line.

Fecha: 9 de enero del 2021.

COMUNICACIÓN 7

Título: "Termografía como herramienta de valoración e investigación en fisioterapia".

Autores: Molina-Payá J.

En: I Congreso Internacional de Investigación Biosanitaria para Jóvenes Investigadores.

Lugar: Universidad de Murcia.

Fecha: Del 24 al 25 de junio del 2021.

11.4. ANEXO 4. ARTÍCULO I

QUANTITATIVE INFRARED THERMOGRAPHY JOURNAL
https://doi.org/10.1080/17686733.2019.1700697

Taylor & Francis
Taylor & Francis Group

Check for updates

Inter and intraexaminer reliability of a new method of infrared thermography analysis of patellar tendon

Javier Molina-Payá[a], José Ríos-Díaz[b] and Jacinto Martínez-Payá[c]

[a]Doctoral Program in Health Sciences, Universidad Católica San Antonio de Murcia, Murcia, Spain; [b]Centro de Ciencias de la Salud San Rafael. Fundación de San Juan de Dios, Universidad Antonio de Nebrija, Madrid, Spain; [c]Grupo de Investigación Discapacidad y Fisioterapia. Departamento de Fisioterapia, Facultad de Medicina, Universidad de Murcia, Murcia, Spain

ABSTRACT

Thermography is an imaging technique that records the infrared radiation of the skin with a potential to detect asymmetries in body temperature and relating them to pathologies or risk of injury. However, the location of landmarks and region of interest (ROI) can influence the recording process. In this study we describe the reliability of a method to select the ROI without modifying the original thermogram over 68 thermograms (17 participants) of patellar tendon with an infrared camera (softwareOptris 450PI). The width-height, X-Y axis and mean temperature of the ROI was measured by two examiners.All the lower limits of the Intraclass Correlation Coeficiente (CCI) were over 0.84 without biases. The skin temperature was similar for both intra-examiner ($F_{1,33}$=0.488; p=0.490) and inter-examiner ($F_{1,33}$=0.011; p=0.917). The mean differences were 0.006ºC (Limit of agreement (LoA): -0.10 to 0.10), The differences between examiners were 0.001 ºC (LoA: -0.13 to 0.13). All temperature differences were <0.25ºC. The method used has very good intra and inter-examiner reliability and reproducibility and the influence on the skin temperature is negligible. It will be of interest to extend the study to ascertain the reliability using different thermal cameras and software, which could increase the strength of the method.

ARTICLE HISTORY
Received 7 May 2019
Accepted 2 December 2019

KEYWORDS
Thermography; reliability; patellar tendon; infrared; interexaminer; intraexaminer

1. Introduction

Thermoregulation of the skin is a complex system that is mainly linked to cutaneous vascularisation and to the sympathetic nervous system as a regulator [1,2], maintaining, in healthy subjects, a thermal symmetry between both sides of the body [3–5].

Infrared thermography (IRT) is an imaging technique that captures infrared radiation in a fast, safe and low-cost way for both the diagnosis and monitoring of various pathologies associated with temperature changes, making it the technique of choice for many authors [6]. The extreme sensitivity of IRT permits the detection of temperature variations

CONTACT José Ríos-Díaz jrios@nebrija.es Centro de CC de la Salud San Rafael, Universidad Antonio de Nebrija, Pº de La Habana, 70 bis, Madrid 28036, Spain

This article has been republished with minor changes. These changes do not impact the academic content of the article
Supplemental data for this article can be accessed here.

generated by metabolic changes in situations such as the regeneration of injured tissue [7], alterations of the sympathetic nervous system [8], inflammatory processes [9], infections [10], vascular disorders [11] or hormonal disorders [12].

Although some authors have reported good reproducibility [13], a comprehensive methodology and protocol is required to accurately determine temperature [14]. The study of factors that may influence thermal capture has allowed a protocol for obtaining thermographs to be normalised [15,16]. In this sense, the IRT of structures or areas determined on the body through the selection of regions of interest (ROI) can be considered as the most reliable method in static situations, whereas other methods are needed when the exploration is carried out in dynamic processes, involving the use averages of areas around hot spots within the area explored [17].

Unlike the protocol for IRT, there is no clear consensus for the determination of ROI [18]. Thus, some authors delimit the ROI by means of markers on the skin [9,19–21], with the disadvantage that manipulation of the area during positioning can alter the temperature of the ROI [22]. Other authors delimit the ROI on already captured thermographs [23,24], although accurately interpreting anatomical references in this way is difficult [25]. Additionally, the software is being developed that allows the automatic positioning of ROI [26]. Recently, a protocol has been developed by consensus to improve the acquisition of thermographic images [27]. However, the process of placing reference markers on the skin may introduce bias into the recorded temperature.

We propose an alternative method to select the ROI while avoiding any modification of the original thermogram. The aim of this study was to assess the reliability and reproducibility of this IRT method to select ROIs by means of markers on the skin without manipulation of the region, which might alter the interpretation of the thermogram.

2. Material and methods

2.1. Study subjects

A total of 17 participants (34 bilateral images) (7 women and 10 men) between 18 and 62 years old (mean: 32.2 years; S.D:10.9 years) were voluntarily recruited from a private Physical Therapy Centre (Murcia, Spain) in July and August 2018. All participants were informed and signed the informed consent document. The study was approved by the Ethical Committee of the Catholic University of Murcia (CE111803). As it is a study that compares the size, location and average temperature of the thermograms, the intrinsic influence factors of the subjects were not considered.

2.2. Sample size determination

The sample size was calculated by the data proposed by Walter et al. [28]. For an expected intraclass correlation coefficient of 0.9 and a minimum acceptable value of 0.7, and two measurements per image, the minimum required sample size is 19 participants with alpha = 0.05 and beta = 0.2.

2.3. IRT imaging

All images were recorded following the same standard protocol. The participant was acclimatised in an isolated room at a mean temperature of (22.7 ± 0.5ºC) and a relative humidity of (43.4 ± 4%) for 20 min without clothing on the lower limbs.

The participant was seated on a hydraulic stretcher with his/her feet on a step-in order to isolate contact with the ground. Then, a point was marked bilaterally on the dorsal face of the metatarsophalangeal joint of the second toe and a vertical line on the Achilles tendon that was moved to the heel [29]. These two references were used to position the feet on two parallel lines (25 cm apart) drawn on the step. The knees were positioned at 90 degrees of flexion which allows a right angle of radiation while the skin that covers the patellar tendon a greater part of the patellar tendon [30], than in the standing position [4,9]. In addition, the sitting position improves perfusion and skin circulation by reducing the circulatory collapse of the area caused by gravity while standing, and also the influence on skin temperature [31].

The IRT images were recorded with an OPTRIS PI 450 IRT camera coupled to Optris PI Connect Software (Germany). The IRT camera has a Noise Equivalent Temperature Difference <40 mK with 38º x 29º FOV, a wide range of temperature from −20°C to +100°C, spectrum range of 7.5–13 µm, focal plane array sensor size of 382 × 288 pixels, emissivity set at 0.98 and a measurement uncertainty of ± 2% of the overall temperature reading. The size of the capture frame was 55.4 × 40.63 cm (1.5 mm/px).

The most mid-cranial part of the patella was marked with metallic ink using a 0.7 mm marker so that it could be easily observed on the thermogram (reference points) and placed outside the ROI. The camera was positioned 80 cm from the knees and aligned on the three axes by means of a self-levelling laser with respect to the knee and step reference points [32] (Figure 1(a,b)). In this position a first thermogram (T1) was recorded without manipulation or modification (raw thermogram) (Figure1(c)).

In order to delimit the area of skin corresponding to the patellar tendon, metallic adhesives (Figure2(a)) were fixed on the skin with the following references: (1) midpoint: proximal-distal midpoint of the patella; (2) lateral point: 1 cm lateral to the most lateral point of the patella [33], p.3) medial point: over the most medial point of the patella; and (4) distal point: 5 cm distal to the external femoro-tibial articular interline [30]. Contralateral knee ROI was symmetrically adjusted [34].

A second thermogram (T2) was saved and ROI boxes were adjusted to the metal adhesives (Figure 2(b,c)). The size and position of ROI boxes on the pixel matrix (X- and Y-axis) of the image provided by the software were calculated. On the second thermogram (T2), the pixel distance between the ROI boxes and the reference points was calculated (Figure 2(c)). The ROI boxes from the second thermogram (T2) to the first (T1) (Figure 2(d)) were transferred considering the size of the boxes and their distance (pixels) to the reference points (Figures 1(c) and 2(b)). Thermogram 1 (T1) was re-recorded with the transferred of the ROI boxes of thermogram 2 (T2) and the average temperature, position and size data were extracted (Figure 2(d)).

The same first thermogram (T1) was used for both examiners as a reference image. The reference points and ROI (T2) were located by the two examiners independently and blinded (interexaminer analysis) at two different times (1 week) (intraexaminer analysis). The images were coded, and the order of analysis was random. The flowchart with the analysis phases is shown in Figure 3.

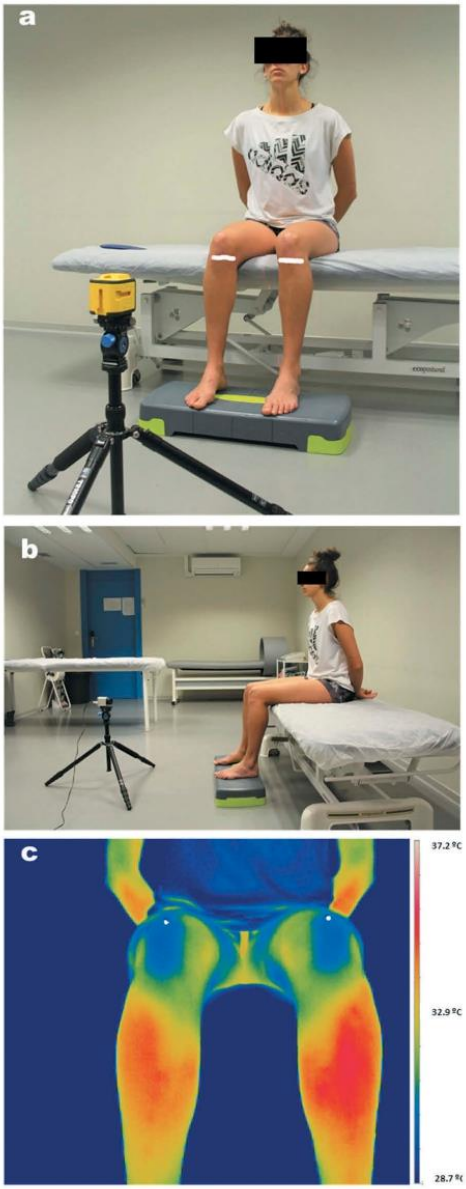

Figure 1. Participant and camera positioning (a,b) and the first thermogram with reference points(c).

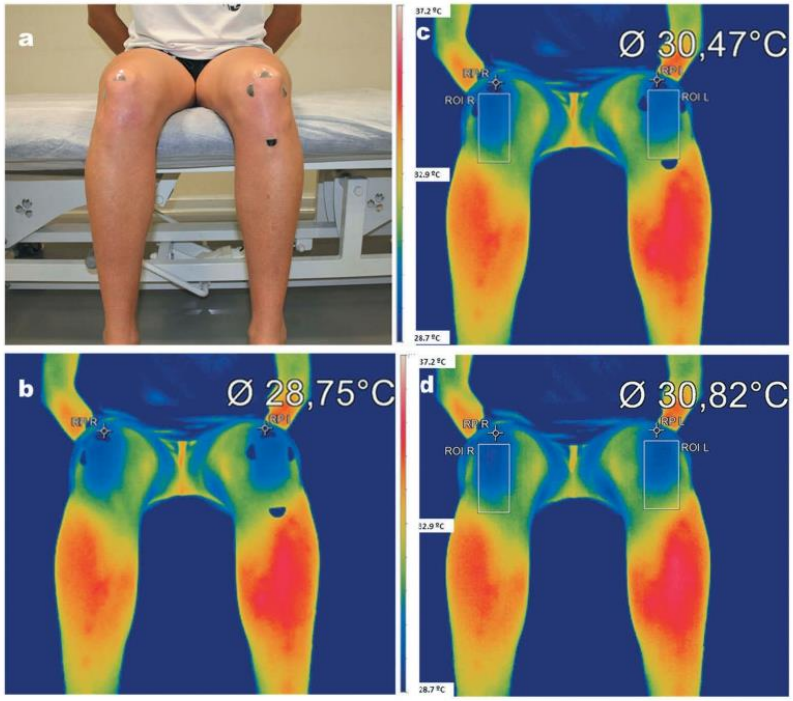

Figure 2. Metallic markers (a), thermogram with reference points (b), ROI boxes on the second thermogram (c) and superimposed over first thermogram (d).

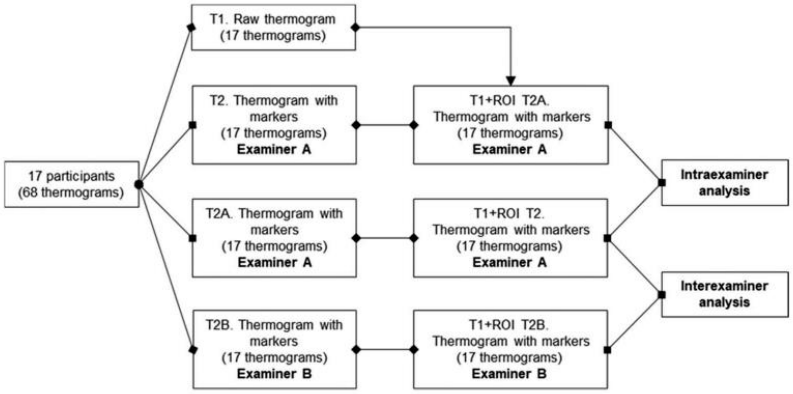

Figure 3. Flowchart of the analysis method.

The main outcome was mean temperature of ROI (ºC) but the box size (width and height in pixels) and the position on the X and Y axis were also analysed.

2.4. Statistical analysis

Descriptive statistics were calculated for ROI dimension variables: width, height, position on x-axis and y-axis, and mean temperature of the boxes in both knees corresponding to the different thermographs obtained by both observers. Although the sample size (n = 34) allows the assumption of normality, it was checked with the coefficients of asymmetry, kurtosis, the Q-Q normality plots and the Kolmogorov–Smirnov test. Parametric tests were applied to all variables. Descriptive statistics were used (mean, standard deviation, range and quartiles) to summarise the data for each examiner's assessment.

The intraclass correlation coefficient (ICC) was calculated in total agreement with a two-factor alpha model and mixed effects ($ICC_{2,1}$) for each of the variables of interest [35,36]. This coefficient offers values of between 0 and 1, where 0 would be a lack of agreement and 1 would be total agreement. Although the interpretation of these cut-off points is, to a certain extent, arbitrary, very good (ICC>0.8), good (ICC = 0.61–0.80), moderate (0.41 to 0.6), low (0.21 to 0.4) and poor (<0.21) reproducibility will be considered [37].

Measurement precision [38,39] was evaluated using the standard error of measurement (SEm) [$SEm = SD \cdot \sqrt{(1\text{-}ICC)}$] and its relative value with respect to the average of all measurements and the smallest real difference (SRD). SRD is useful for determining whether a change in the parameter is due to a real change or lies within the limits of error of the measuring method [$SRD = 1.96 \cdot SEm \cdot \sqrt{2}$].

The limits of agreement (LOA) were calculated according to the method described by Bland and Altman [40] and the presence of summative or multiplicative biases with Passing-Bablock's linear regression method [41].

For a direct clinical interpretation, the graphical method proposed by Luiz et al. [42], based on the Kaplan-Meier estimate representing the probability of survival as a function of the degree of disagreement, was applied.

Statistical analysis was performed using IBM SPSS Statistics 19.0 (SPSS Inc. IBM Company, 2010) and the *jmv package* (version 0.9) [43] for R (version 3.5.0; 2018) . P-values of <0.05 were considered to indicate statistical significance.

3. Results

A total of 68 thermograms were recorded from 17 participants. Table 1 shows the descriptive data. The width-box variable showed no statistical differences in the intra-examiner ($F_{1,33}$ = 1.47; p = 0.233) or inter-examiner ($F_{1,33}$ = 0.454; p = 0.505) analysis. The intra-examiner differences in height-box were not significant ($F_{1,33}$ = 0.815; p = 0.373) but statistical differences in the means were found for inter-examiner data ($F_{1,33}$ = 4.40; p = 0.044). The X-axis did not show intra-examiner ($F_{1,33}$ = 0.045; p = 0.833) or inter-examiner ($F_{1,33} \approx 0$; $p \approx 1.0$) differences. The means of the Y-axis were similar intra-examiner ($F_{1,33}$ = 2.65; p = 0.133) but not inter-examiner ($F_{1,33}$ = 42.3; p = 0.001). Finally, the skin temperature was similar to intra-examiner ($F_{1,33}$ = 0.488; p = 0.490) and inter-examiner ($F_{1,33}$ = 0.011; p = 0.917).

Table 1. Descriptive values for intra- and inter-observer analysis.

Parameter	Mean (SD)	C.I. 95%	Minimum	Median (IQR)	Maximum
Width box A	34.1 (3.28)	33 to 35	26	34 (32 to 36)	40
Width box A2	33.9 (3.11)	33 to 35	26	35 (32 to 36)	40
Width box B	33.9 (3.64)	33 to 35	25	35 (31 to 36.3)	40
Height box A	56.6 (4.61)	55 to 58	47	56 (53.8 to 61)	63
Height box A2	56.3 (4.85)	55 to 50	47	57 (54 to 61)	61
Height box B	57.2 (4.45)	56 to 59	49	58 (54 to 61)	64
X-axis location A	192.5 (82.01)	164 to 221	106	193 (112 to 272)	279
X-axis location A2	192.4 (81.47)	164 to 221	107	194 (112 to 273)	278
X-axis location B	192.5 (80.99)	164 to 221	109	192 (112 to 272)	278
Y-axis location A	122.3 (7.99)	120 to 125	102	123 (119 to 124)	152
Y-axis location A2	121.7 (8.27)	119 to 125	98	122 (119 to 125)	147
Y-axis location B	120.3 (7.98)	118 to 123	98	121 (118 to 123)	147
Temperature A	32.9 (0.85)	32.6 to 33.2	31.2	32.9 (32.4 to 33.6)	34.6
Temperature A2	32.9 (0.85)	32.6 to 33.2	31.2	32.9 (32.4 to 33.6)	34.6
Temperature B	32.9 (0.84)	32.6 to 33.2	31.2	32.9 (32.5 to 33.6)	34.6

Box parameters units are pixels. Temperature in degrees Celsius. A: first evaluation for examiner A. A2: second evaluation for examiner A. B: evaluation for examiner B.

The reliability results are shown in Table 2 and Figures 4 and 5. Excellent reliability was observed both intra and inter-examiner in all parameters. No bias was found for the parameters analysed. Only, as expected, in the X-axis parameter was a systematic bias detected, although it did not affect reproducibility.

For skin temperature, the difference between intra-examiner measurements was 0.006ºC (LOA: −0.10 to 0.10), and the differences between examiners were 0.001ºC (LOA: −0.13 to 0.13).

Further information is provided in the supplementary material (Suppl 1 and Suppl 2).

Table 2. Reliability for both intra- and inter-observer analysis.

Parameter	ICC (95% CI)	Agreement	Mean difference (95% LOA)	% Change	SEm	SEm %	SRD (95% CI)	SRD %
Width box intra-observer	0.937 (0.878 to 0.968)	Excellent	−0.235 (−2.45 to 1.98)	−0.6	0.80	2.3%	2.21 (−1.5 to 2.92)	6.5%
Width box inter-observer	0.904 (0.818 to 0.951)	Excellent	−0.176 (−3.17 to 2.82)	−0.5	1.07	3.1%	2.96 (−1.72 to 4.19)	8.7%
Height box intra-observer	0.92 (0.846 to 0.959)	Excellent	−0.294 (−4.02 to 3.43)	−0.5	1.33	2.4%	3.68 (−2.80 to 4.56)	6.5%
Height box inter-observer	0.92 (0.846 to 0.959)	Excellent	0.588 (−2.62 to 3.79)	1.1	1.41	2.5%	3.91 (−2.50 to 5.32)	6.9%
X-axis location intra-observer	1 (1 to 1)	Excellent	−0.059 (−3.22 to 3.10)	0.1	0.00	0.00%	0 (-)	0.0%
X-axis location inter-observer	1 (0.999 to 1)	Excellent	0.00 (−4.97 to 4.97)	0.3	0.00	0.00%	0 (-)	0.0%
Y-axis location intra-observer	0.968 (0.937 to 0.984)	Excellent	−0.559 (−4.48 to 3.37)	−0.5	1.44	1.2%	4 (−2.56 to 5.45)	3.3%
Y-axis location inter-observer	0.946 (0.544 to 0.984)	Excellent	−2.0 (−5.51 to 1.51)	−1.6	1.43	1.2%	3.96 (−1.78 to 6.14)	3.3%
Temperature intra-observer	0.998 (0.997 to 0.999)	Excellent	0.0059 (−0.090 to 0.10)	0.0	-	-	-	-
Temperature inter-observer	0.997 (0.994 to 0.999)	Excellent	0.0012 (−0.127 to 0.129)	0.0	-	-	-	-

Box parameters units are pixels. Temperature in degrees Celsius. ICC: intraclass correlation coefficient. LOA: limits of agreement. %Change: mean difference respect total average of measures. SEm: standard error of measurement. SRD: smallest real difference. SEM and CRD for temperature are not shown because it is an interval variable.

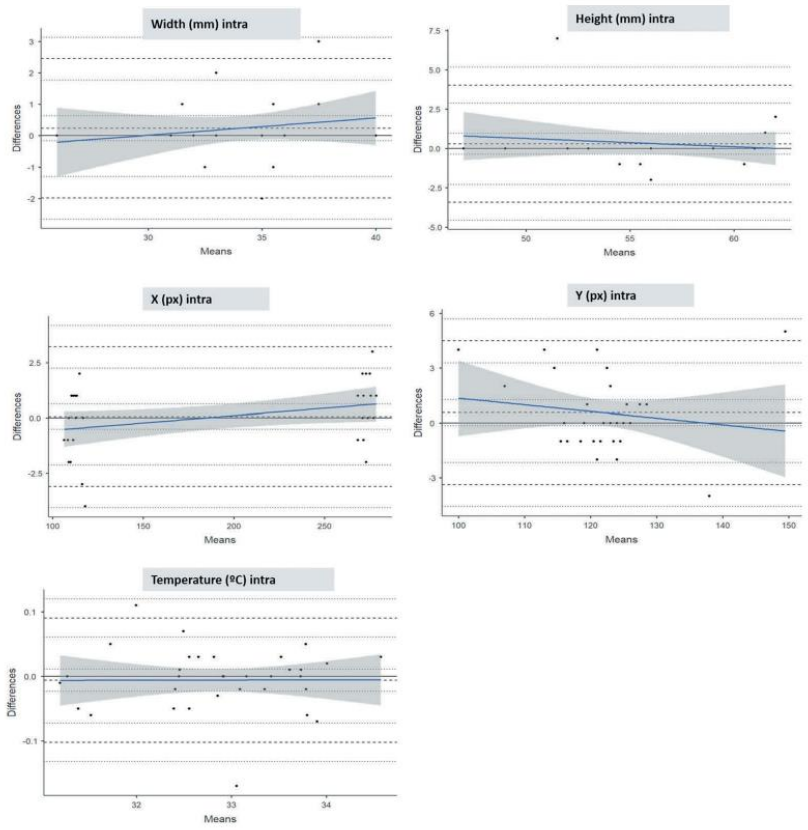

Figure 4. Intra-examiner reliability Bland–Altman's plots. Each pair of measurements is represented by a point determined by the mean value (x-axis) and by the difference between them (y-axis). Dotted lines represent the limits of agreement with the confidence intervals. Dark zone and blue line represent the proportional bias line with confidence intervals. The Width and Height are in millimetres (mm), X and Y are coordinates in pixels and Temperature is in Celsius grades (ºC).

4. Discussion

In this study, we analysed the intra- and inter-observer reliability of a method of ROI determination for thermographic analysis that does not modify the original thermogram positioning through the positioning of markers.

The lower limits of the ICC confidence interval showed very close agreement for all variables (>0.85, except for Y-axis inter-examiner) and specifically superiors 0.99 for the intra- and inter-examiner temperature values. This finding may be due to several factors that are decisive for which extreme precautions were taken, such as the choice of easily locatable anatomical

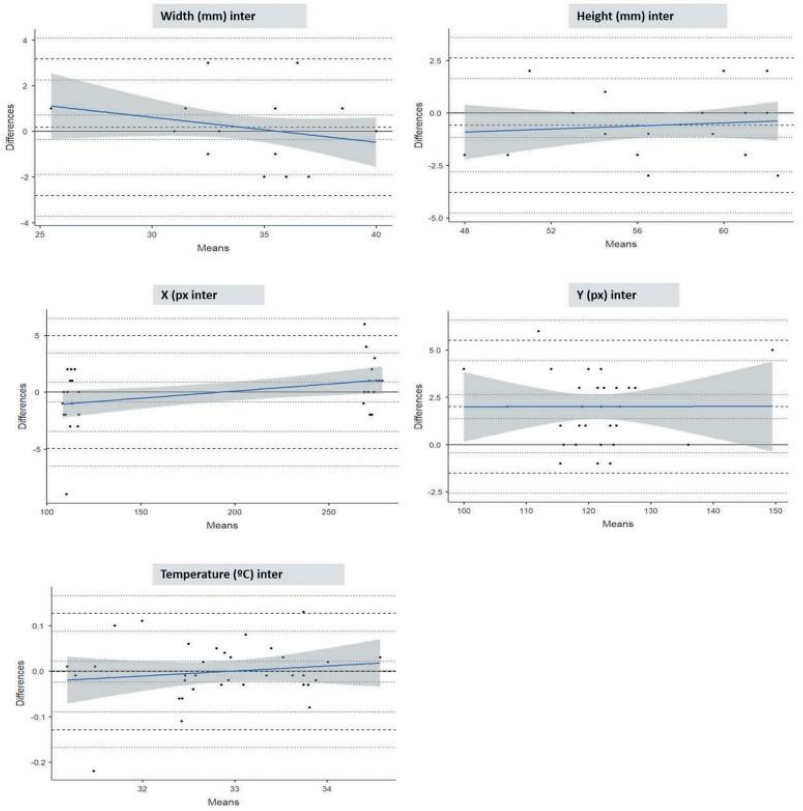

Figure 5. Inter-examiner reliability Bland–Altman's plots. Each pair of measurements is represented by a point determined by the mean value (x-axis) and by the difference between them (y-axis). Dotted lines represent the limits of agreement with the confidence intervals. Dark zone and blue line represent the proportional bias line with confidence intervals. The Width and Height are in millimetres (mm), X and Y are coordinates in pixels and Temperature is in Celsius grades (ºC).

references, prior consensus by the observers and the meticulous positioning of the camera and the participant, which left little room for subjectivity on the part of the technicians.

Also facilitating the high degree of agreement in the size variables of the ROI was the use of symmetrical ROI boxes for both knees, which is an important factor when analysing thermal differences on both sides of the body [34]. It should also be mentioned that the boxes are rectangular, which facilitates their positioning in relation to skin markers, whose inner edge is also rectilinear (Figure 2).

From a practical point of view, mean differences were between 0 and 2 pixels, with $R^2 >$ 82%, with a maximum relative SEm of 2.5% and a maximum relative SRD of 8.7%. All the differences were less than 10 px (Figures 4 and 5.)

As regards the temperature, the reliability was even higher, with mean differences in the order of the tenth degree, both in the intra-examiner and inter-examiner analysis. The total differences were below 0.20ºC.

It is possible that the close agreement found would be lower if, rather than using the same thermogram to determine the size, position and mean temperature of the ROI, different primary thermograms were used for each measurement and examiner. In this study, it was decided to use a single primary thermogram to minimise the influence of both extrinsic and intrinsic factors that may affect the uptake of infrared radiation and thus analyse only the factors that influence the creation and positioning of ROI.

Inter-observer reliability has also been investigated in other studies with good results. Selfe et al. [19] observed ICC values between 0.82 and 0.97 in patients with knee pathologies. Similar results were obtained by Spalding et al. [44] in patients with arthritis of the hands, by Costa et al. in cervical and facial musculature [21] with very good agreement (ICC between 0.852 and 0.998). By contrast, Mustacchi et al. [45] found poor reliability in breast thermograms.

With regard to intra-examiner reliability, the good results of Varju et al. [23] (ICC = 0.899) in hand measurements and Costa et al. [21] (ICC = 0.879 to 0.998) in measurements of the cervical and facial musculature should be highlighted. On the other hand, Denoble et al. [9] obtained a much lower ICC (0.5 to 0.72) in the knee. Zaproudina et al. [13] suggested that the relatively poor intra and inter-observer results obtained for ICC is because the selection of the ROI is essentially based on a manual procedure and therefore the skill of the technician to select the ROI.

In order to eliminate this subjective factor, different softwares have been developed to automate the ROI selection process [46]. Fernandez et al. used a software with which they obtained very good results (inter-examiner ICC = 0.989 and intra-examiner = 0.997) [26]. However, it should be borne in mind that ROI obtained automatically by software include more general location regions and do not allow measurements to be focused on specific structures because they cannot recognise determining anatomical references.

In recent years the technology and methodology of thermographic recordings have improved and different authors have analysed the asymmetries in body temperature of different body regions to discriminate preventively areas susceptible to injury in football players [46] and in different pathologies [8,17,22] so that it could become an imaging technique for preventive use and control of the evolution of both injuries and pathologies.

4.1. Limitations

The most important limitation of this study is that we located the ROI over only one raw thermogram for each participant. However, as discussed above, the objective was to determine the reproducibility of the reference points to locate ROI, without the influence of other sources of variability.

The main strength of our study is the description of the method of anatomical localisation of reference points without modifying skin temperature and the statistical analysis of the reliability from different perspectives and not only based on the ICC, which has several limitations [36,38–40].

5. Conclusion

The results obtained confirm that the method used has a very good reliability and reproducibility, while any influence on the detected temperature is negligible.

In this sense, it will be of interest to extend the study in order to ascertain the reliability between different thermal cameras and software, which could increase the strength of the method.

Disclosure statement

No potential conflict of interest was reported by the authors.

Notes on contributors

Javier Molina-Payá (PhD, MSc, BiolS, PT): PhD in Health Sciences, Master in Research Methodology and Statistics, Biologist and Degree in Physical Therapy with 20 years of research in image processing and analysis applied in Health Sciences.

José Ríos-Díaz (PhD student, MSc, PT): Degree in Physical Therapy, Master Degree in Manual Therapy and Osteopathy and PhD Student in Health Sciences with 20 years of clinical experience and specialist in musculoskeletal ultrasonography and thermography.

Jacinto Martínez-Payá (PhD, MSc, PT): PhD in Health Sciences, Kinesiology Degree and Physical Therapy Degree wint 20 years of research in ultrasonography applied to musculoskeletal system and physiotherapy.

ORCID

Javier Molina-Payá http://orcid.org/0000-0002-2343-3613
José Ríos-Díaz http://orcid.org/0000-0002-4786-3351
Jacinto Martínez-Payá http://orcid.org/0000-0002-9214-812X

References

[1] Charkoudian N. Skin blood flow in adult human thermoregulation: how it works, when it does not, and why. Mayo Clin Proc. 2003;78(5):603–612.
[2] Kellog D, Pérgola P. Skin responses to exercise and training. In: Garrett WE, Kirkendall DT, editors. Exerc and Sport Sci. London: Lippincott Williams & Wilkins; 2000. p. 239–250.
[3] Vardasca R. Symmetry of temperature distribution in the upper and lower extremities. Thermol Int. 2008;18:154–155.
[4] Selfe J, Whitaker J. A narrative literature review identifying the minimum clinically important difference for skin temperature asymmetry at the knee. Thermol Int. 2008;18:51–54.
[5] Vardasca R, Ring F, Plassmann P, et al. Thermal symmetry of the upper and lower extremities in healthy subjects. Thermol Int. 2012;22:53–60.
[6] Ring EFJ, Ammer K. Infrared thermal imaging in medicine. Physiol Meas. 2012;33:R33.
[7] Mangine RE, Siqueland KA, Noyes FR. The use of thermography for the diagnosis and management of patellar tendinitis. J Orthop Sports Phys Ther. 1987;9:132–140.
[8] Schuhfried O, Vacariu G, Lang T, et al. Thermographic parameters in the diagnosis of secondary Raynaud's phenomenon. Arch Phys Med Rehabil. 2000;81:495–499.
[9] Denoble AE, Hall N, Pieper CF, et al. Patellar skin surface temperature by thermography reflects knee osteoarthritis severity. Clin Med Insights Arthritis Musculoskelet Disord. 2010;3:69–75.

[10] Romanò CL, D'Anchise R, Calamita M, et al. Value of digital telethermography for the diagnosis of septic knee prosthesis: a prospective cohort study. BMC Musculoskelet Disord. 2013;14:7.
[11] Huang C-L, Wu Y-W, Hwang C-L, et al. The application of infrared thermography in evaluation of patients at high risk for lower extremity peripheral arterial disease. J Vasc Surg. 2011;54:1074–1080.
[12] Costa APC, Maia JM, Brioschi ML, et al. Thermography evaluation in patients with hypothyroidism and fibromyalgia by analyzing the temperatures of the palms of hands. In: Lhotska L, Sukupova L, Lacković I, et al. editors. World congr med phys biomed eng 2018. [Internet]. Singapore: Springer Singapore; 2019 [citado 2019 de octubre de 10]. p. 15–19. Available from: http://link.springer.com/10.1007/978-981-10-9035-6_3
[13] Zaproudina N, Varmavuo V, Airaksinen O, et al. Reproducibility of infrared thermography measurements in healthy individuals. Physiol Meas. 2008;29:515–524.
[14] Costello JT, Stewart IB. Use of thermal imaging in sports medicine research: A short report. Int Sportmed J. 2013;14:94–98.
[15] IACT. Standards and protocols in clinical thermography imaging. Thermology Guidelines Electronic Version Internet; 2002 [cited 2019 Apr 15]. Available from: http://www.iact-org.org/professionals/thermog-guidelines.html
[16] Ammer K. The Glamorgan protocol for recording and evaluation of thermal images of the human body. Thermol Int. 2008;18:125–129.
[17] Ludwig N, Formenti D, Gargano M, et al. Skin temperature evaluation by infrared thermography: comparison of image analysis methods. Infrared Phys Technol. 2014;62:1–6.
[18] Choi E, Lee P-B, Nahm FS. Interexaminer reliability of infrared thermography for the diagnosis of complex regional pain syndrome. Skin Res Technol Off J Int Soc Bioeng Skin ISBS Int Soc Digit Imaging Skin ISDIS Int Soc Skin Imaging ISSI. 2013;19:189–193.
[19] Selfe J, Hardaker N, Thewlis D, et al. An accurate and reliable method of thermal data analysis in thermal imaging of the anterior knee for use in cryotherapy research. Arch Phys Med Rehabil. 2006;87:1630–1635.
[20] Selfe J, Sutton C, Hardaker NJ, et al. Anterior knee pain and cold knees: a possible association in women. Knee. 2010;17:319–323.
[21] Costa ACS, Dibai Filho AV, Packer AC, et al. Intra and inter-rater reliability of infrared image analysis of masticatory and upper trapezius muscles in women with and without temporomandibular disorder. Braz J Phys Ther. 2013;17:24–31.
[22] Ferreira JJA, Mendonça LCS, Nunes LAO, et al. Exercise-associated thermographic changes in young and elderly subjects. Ann Biomed Eng. 2008;36:1420–1427.
[23] Varjú G, Pieper CF, Renner JB, et al. Assessment of hand osteoarthritis: correlation between thermographic and radiographic methods. Rheumatol Oxf Engl. 2004;43:915–919.
[24] George J, Bensafi A, Schmitt AM, et al. Validation of a non-contact technique for local skin temperature measurements. Skin Res Technol Off J Int Soc Bioeng Skin ISBS Int Soc Digit Imaging Skin ISDIS Int Soc Skin Imaging ISSI. 2008;14:381–384.
[25] Herry CL, Frize M. Quantitative assessment of pain-related thermal dysfunction through clinical digital infrared thermal imaging. Biomed Eng OnLine. 2004;3:19.
[26] Fernández-Cuevas I, Marins JC, Carmona PG, et al. Reliability and reproducibility of skin temperature of overweight subjects by an infrared thermography software designed for human beings. Thermol Int. 2012;22:130–137.
[27] Moreira DG, Costello JT, Brito CJ, et al. Thermographic imaging in sports and exercise medicine: A Delphi study and consensus statement on the measurement of human skin temperature. J Therm Biol. 2017;69:155–162.
[28] Walter SD, Eliasziw M, Donner A. Sample size and optimal designs for reliability studies. Stat Med. 1998;17:101–110.
[29] Ribeiro AP, Trombini-Souza F, Tessutti V, et al. Rearfoot alignment and medial longitudinal arch configurations of runners with symptoms and histories of plantar fasciitis. Clinics. 2011;66:1027–1033.

[30] Zooker C, Pandarinath R, Kraeutler MJ, et al. Clinical measurement of patellar tendon: accuracy and relationship to surgical tendon dimensions. Am J Orthop Belle Mead NJ. 2013;42:317–320.
[31] Ratovoson D, Jourdan F, Huon V. Influence of gravity on the skin thermal behavior: experimental study using dynamic infrared thermography. Skin Res Technol Off J Int Soc Bioeng Skin ISBS Int Soc Digit Imaging Skin ISDIS Int Soc Skin Imaging ISSI. 2013;19:e397–408.
[32] Tká M, Hudák R, Foffová P, et al. An importance of camera subject distance and angle in musculoskeletal applications of medical thermography. Acta Electrotech Inf. 2010;10:57–60.
[33] Veeramani R. Gender differences in the mediolateral placement of the patella and tibial tuberosity: a geometric analysis. Anat Int J Exp Clin Anat. 2010;4:45–50.
[34] Nahm FS. Infrared thermography in pain medicine. Korean J Pain. 2013;26:219–222.
[35] McGraw KO, Wong SP. Forming inferences about some intraclass correlation coefficients. Psychol Methods. 1996;1:30–46.
[36] Weir JP. Quantifying test-retest reliability using the intraclass correlation coefficient and the SEM. J Strength Cond Res. 2005;19:231–240.
[37] Shrout PE, Fleiss JL. Intraclass correlations: uses in assessing rater reliability. Psychol Bull. 1979;86:420–428.
[38] Lexell JE, Downham DY. How to assess the reliability of measurements in rehabilitation. Am J Phys Med Rehabil. 2005;84:719–723.
[39] Atkinson G, Nevill AM. Statistical methods for assessing measurement error (reliability) in variables relevant to sports medicine. Sports Med. 1998;26:217–238.
[40] Atkinson G, Nevill A. Measures of reliability in sports medicine and science: correspondence. Sports Med. 2000;30:375–381.
[41] Bablok W, Passing H. Application of statistical procedures in analytical instrument testing. J Autom Chem. 1985;7:74–79.
[42] Luiz RR, Costa AJL, Kale PL, et al. Assessment of agreement of a quantitative variable: a new graphical approach. J Clin Epidemiol. 2003;56:963–967.
[43] Love J, Dropmann D, Selker R. Jamovi project; 2018. [Internet]. [cited 2019 Dec 08] Available from: https://www.jamovi.org
[44] Spalding SJ, Kwoh CK, Boudreau R, et al. Three-dimensional and thermal surface imaging produces reliable measures of joint shape and temperature: a potential tool for quantifying arthritis. Arthritis Res Ther. 2008;10:R10.
[45] Mustacchi G, Milani S, Ciatto S, et al. Observer variation in mammary thermography: results of a teaching file test carried out in four different centers. Tumori. 1990;76:29–31.
[46] Plassmann PMP. CTHERM for standardised thermography. 9thEuropean Congress of Medical Thermology, Krakow (Poland); 2003.

11.5. ANEXO 5. ARTÍCULO II

ARTICLE IN PRESS

Ultrasound in Med. & Biol., Vol. 00, No. 00, pp. 1–10, 2021

0301-5629/$ - see front matter

https://doi.org/10.1016/j.ultrasmedbio.2021.08.010

● *Original Contribution*

RELIABILITY OF A NEW SEMI-AUTOMATIC IMAGE ANALYSIS METHOD FOR EVALUATING THE DOPPLER SIGNAL AND INTRATENDINOUS VASCULAR RESISTANCE IN PATELLAR TENDINOPATHY

FRANCISCO J. MOLINA-PAYÁ,* JOSÉ RÍOS-DÍAZ,† FRANCISCO CARRASCO-MARTÍNEZ,‡ and JACINTO J. MARTÍNEZ-PAYÁ§

* Doctoral Program in Health Sciences, Universidad Católica de Murcia, Murcia, Spain; † Fundación San Juan de Dios. Centro de Ciencias de la Salud San Rafael, Universidad Nebrija, Madrid, Spain; ‡ Private Practice, Clínica de fisioterapia F&C, Huelma, Spain; and § Physiotherapy Department, Facultad de Medicina, Universidad de Murcia, Murcia, Spain

(*Received* 12 *February* 2021; *revised* 9 *August* 2021; *in final form* 14 *August* 2021)

Abstract—The aim of this study was to determine the intra- and inter-rater reliability of a new semi-automatic image analysis method for quantification of the shape of the Doppler signal and the intratendinous vascular resistance in patellar tendinopathy. Thirty athletes (27.4 y, standard deviation = 8.57 y) with patellar intratendinous vascularity were included in a cross-sectional study (42 tendons analyzed). The intratendinous blood flow was assessed with power Doppler and ImageJ (Version 1.50b, National Institutes of Health, Bethesda, MD, USA) quantification software over a manually selected region of interest. Two blinded observers performed the analysis of the Doppler signal (vascular resistance) and shape descriptors (number of signals, pixel intensity, area, perimeter, major diameter, minor diameter, circularity and solidity). The intraclass correlation coefficient (ICC) was calculated, and the Bland–Altman mean of differences (MoD) and 95% limits of agreement (LoA) were determined. Also, small real differences (SRDs) and the standard error of measurement (SEM) were calculated. Intra-rater reliability was at a maximum for area (ICC = 0.999, 95% confidence interval [CI] = 0.998–0.999) and at a minimum for solidity (ICC = 0.782, 95% CI: 0.682–0.853). The MoD and 95% LoA were very low, and the relative SRD and SEM were below 5.3% and 2%, respectively. The inter-rater reliability was the maximum for area (ICC = 0.993, 95% CI = 0.989–0.996) and the minimum for circularity (ICC = 0.73; 95% CI=0.611–0.817). The MoD and 95% LoA were low, with the SRD and SEM below 6% and 2.2%. The proposed quantitative method for studying the intratendinous Doppler signal in the patellar tendon is reliable and reproducible. (E-mail: jrios@nebrija.es)

Key Words: **Doppler ultrasonography, Tendinopathy, Image processing, Computer-assisted, Vascular resistance, Blood flow velocity.**

INTRODUCTION

The use of Doppler ultrasound is especially interesting in the evaluation of tendinopathies (de Vos et al. 2007; De Jonge et al. 2014) because it enables areas with increased blood flow to be observed, and even quantified (Roth et al. 2019; Vlist et al. 2020). Power Doppler facilitates visualization of low-velocity blood flow in very small vessels, representing an effective imaging modality for evaluation of intratendinous vascularization (de Vos et al. 2007; Quack et al. 2020).

It is widely accepted that the presence of an intratendinous Doppler signal (DS) can be considered a sign of abnormality in the tendon (Alfredson and Ohberg 2005; Richards et al. 2005), while the absence of such a signal is a sign of healthy tendons (Ohberg et al. 2001; Alfredson et al. 2003). However, these findings contrast with those of other studies that suggest that intratendinous flow is not always a sign of a pathological disorder, but rather a part of an adaptive response to a normal physiological load (Malliaras et al. 2008; Boesen et al. 2012; Tol et al. 2012). Such variability can lead to the conclusion that the study of intratendinous vascularization is unreliable.

In any case, to quantify a DS, semiquantitative procedures are frequently used, based mainly on counting

Address correspondence to: José Ríos-Díaz, Centro de Ciencias de las Salud San Rafel, Fundación San Juan de Dios, Universidad de Nebrija, Paseo de la Habana 70 bis, Madrid, Spain. E-mail: jrios@nebrija.es

Francisco J. Molina-Payá and José Ríos-Díaz contributed equally to this work.

scales to grade the degree of DS presence (Vlist et al. 2020; Simon et al. 2021); these procedures have limited usefulness because only qualitative data can be obtained. By contrast, quantitative procedures involve mainly color pixel measurements (Terslev et al. 2003b; Koenig et al. 2007b; Boesen et al. 2012), vessel length (Cook et al. 2005) or, in the case of the resistance index (RI), automatic ultrasound measurements (Koenig et al. 2007b; Albrecht et al. 2008; Karzis et al. 2017). In addition, the procedures permit the measurement of vascular resistance (VR), which could be useful in assessing the state of the tissue.

In this way it is possible to express numerically tissue resistance to the flow originated by the microvascular bed distal to the measurement site by reference to the RI (Léandre Pourcelot Société parisienne d'expansion chimique 1982), defined as (peak systolic flow − end diastolic flow)/peak systolic velocity. A low RI is associated with low peripheral resistance and high perfusion of the distal bed and, therefore, an inflammation situation (Terslev et al. 2003b; Bjordal et al. 2006; Koenig et al. 2007a; Torp-Pedersen et al. 2008; Terabayashi et al. 2014). The measurement of RI in intratendinous vessels is complicated because the DSs that appear can be very small and numerous, making it difficult or impossible to use the traditional measurement methodology (Terslev et al. 2003a; Koenig et al. 2007a, 2007b).

Therefore, in the present study, our objective was to study the intra- and inter-rater reliability of a new semi-automatic image analysis method for quantification of the shape of the DS and the intratendinous VR, obtained from pixel intensities (Delorme et al. 1995) that allows quantification on regions of interest (ROIs) with numerous and small Doppler signals.

METHODS

Study design and participants

A total of 30 athletes (8 women and 22 men) with patellar intratendinous vascularity were included in this cross-sectional observational study (42 tendons analyzed). Age ranged between 18 and 50 years (mean = 27.4 y, standard deviation [SD] = 8.57 y), and the participants were voluntarily recruited from a private physical therapy center (Clinica F&C Fisioterapia Avanzada y Neuro-Rehabilitación, Huelma, Spain) in July and August 2018. All participants were informed of the study's aims and signed an informed consent. The study was approved by the ethics committee of the Catholic University of Murcia, Murcia, Spain (30/11/2018 CE111803).

Power Doppler parameters and scan method

The examination was performed with a Telemed SmartUS ultrasound system (Vilnius, Lithuania) and a 7-15 MHz linear probe (L15-7L40H-5). The intratendinous blood flow was assessed by Power Doppler set at a Doppler frequency of 6.7 MHz and a pulse repetition frequency of 0.7 kHz. The lowest wall filter and gain standardized to just below the level that produced random noise was applied. The adjustment parameters were the same for all patients, and pressure on the tendon from the probe was minimized to prevent vessel compression by placing the transducer on the skin without pressure.

The patient was positioned in a supine position with the knees extended to avoid occlusion of the vessels caused by the tension of the fibers of the patellar tendon (Koenig et al. 2007b); both knees were evaluated. The patellar tendon was scanned in power Doppler mode in the longitudinal plane at the location of maximum intratendinous Doppler activity, and a 4-s video was recorded for further analysis. All scans were performed by the same ultrasonographer with more than 20 y of experience in musculoskeletal ultrasonography.

Quantification of intratendinous DS shapes

Processing and analysis of the videos and images was carried out using ImageJ software (Version 1.50b, National Institutes of Health, Bethesda, MD, USA). After scaling the image, two observers manually selected and extracted the ROIs on the images with the highest and lowest signal corresponding to the systolic peak and the end of diastole for each patient. The image data were coded, anonymized and randomized thereafter to avoid possible bias or recall effects.

The observers, who were blinded to the patient's data, analyzed the set of images at two different times with at least a 15-d delay.

Because the DS appears in color on a gray-scale background, it is easy to segment and isolate the region for quantification. We used the color threshold plugin, which allows the cutoff point to be adjusted manually with slider bars.

To quantify the DS, the saved frame with the highest DS from each video was selected, and the area of color pixels was calculated. In addition, the number of signals, pixel intensity, area, perimeter, major diameter, minor diameter, circularity and solidity were automatically calculated on the frames with the highest DS of each recording (Fig. 1). Circularity and solidity are dimensionless parameters included in the so-called shape descriptors that evaluate the shape of a contour. When circularity is about 1, the contour is like a circle, and when is about 0, it is like a line.

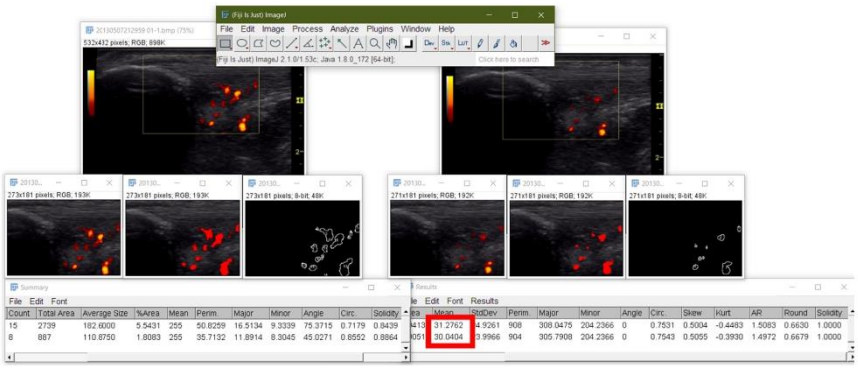

Fig. 1. Quantification of intratendinous Doppler signals and color pixel quantization. Left frame: Peak systolic flow. Right frame Diastolic flow. The analysis method reveals the number of Doppler signals and their morphology. The intensity of signals allows the vascular resistance to be obtained.

The solidity is a ratio that indicates the relationship between the area of the shape and the convex area (theoretical maximum = 1).

Quantification of intratendinous vascular resistance

The flow pattern was evaluated by calculating the mean pixel color of the DS for each image. The pixel color mean of the image with the highest signal was considered the maximum systolic velocity, and that with the lowest signal, as the final diastolic velocity. These data were transferred to the RI formula, giving a value associated with the intratendinous VR (Fig. 1).

In the images in which a DS was not detected, or did not present an intratendinous DS in diastole, the VR was considered 1, which represents normality in the musculoskeletal tissue (Terslev et al. 2003c; Koenig et al. 2007a).

Statistical analysis

As the sample size allowed a normal distribution to be assumed, parametric tests were applied for all variables, and the descriptive statistics used to summarize the data for each of the evaluators were mean, SD, range and quartiles. The analyses were conducted for the number of DSs, intensity of color, total area (mm^2) of active vessels, total perimeter (mm) of active vessels, major diameter, minor diameter, circularity (index between 0 and 1), solidity and VR.

The intraclass correlation coefficient (ICC) was calculated based on a total agreement and two-factor random-effects model (ICC2,1) for each of the variables of interest (McGraw and Wong 1996; Weir 2005). This coefficient offers values of between 0 and 1, where 0 would be a lack of agreement and 1 would be total agreement. Although the interpretation of these cutoff points is, to a certain extent, arbitrary, in our context an ICC >0.90 was considered excellent, between 0.90 and 0.75 good, between 0.75 and 0.50 moderate and <0.50 poor (Portney and Watkins 2009).

Measurement precision (Atkinson and Nevill 1998; Lexell and Downham 2005) was evaluated using the standard error of measurement (SEM) (SEM = SD•√[1 ICC]) and its relative value with respect to the average of all measurements and the smallest real difference (SRD). SRD is useful for determining whether a change in the parameter is owing to a real change or lies within the limits of error of the measuring method (SRD = 1.96·SEM·√2) (Schuck and Zwingmann 2003).

The limits of agreement (LoA) were calculated according to the method described by Bland and Altman (1986; Hopkins 2000), and the presence of summative or multiplicative biases was determined with the Passing–Bablock linear regression method (Passing and Bablok 1983; Bablok et al. 1988). For a direct clinical interpretation, the graphical method proposed by Luiz et al. (2003), based on the Kaplan–Meier estimate representing the probability of survival as a function of the degree of disagreement, was applied.

The analyses were conducted using IBM SPSS Statistics 19.0 (2010; IBM, Armonk, NY, USA) and the jmv package (Version 0.9) for R (Version 3.5.0; 2018).

Table 1. Baseline characteristics (n = 30)

Variable	Mean (SD)	Minimum	Q1	Median	Q3	Maximum
Age	27.4 (8.57)	18	21	23	35.5	50
Time of evolution (mo)	21 (26.34)	0	0	12	36	120
VisaP	75.2 (22.18)	29	56.75	75.5	100	100
Tendinopathy, n (%)	22 (73%) Yes					
Side lesion, n (%)	12 (40%) Right	10 (33%) Left				
Sex, n (%)	22 (73%) Male	8 (27%) Female				
Sport practice, n (%)	22 (73%) Yes	8 (27%) No				

SD = standard deviation. VisaP = Victorian Institute of Sport Assessment—Patella.

RESULTS

Patient characteristics

Thirty participants aged between 18 and 50 y (mean = 27.4 y, SD = 8.57 y) took part in the study. All of them presented with intratendinous vascularity: 22 (73%) symptomatic and 8 (27%) asymptomatic. Twelve participants presented with bilateral and 18 with unilateral intratendinous vascularization, meaning that a total of 42 tendons were analyzed. In addition, each image was analyzed at maximum systolic speed and minimum diastolic speed so that finally all the parameters were calculated by both observers for a total of 84 images (Table 1).

Reliability

Overall, both intra- and inter-rater reliability was very good, and no additive or multiplicative biases were detected (Supplementary Figs. S1 and S2, online only).

More specifically, the intra-rater ICC was maximum for area (ICC = 0.999; 95% confidence interval [CI]: 0.998–0.999) and minimum for solidity (ICC = 0.782, 95% CI: 0.682–0.853). The mean of differences (MoD) and 5% limits of agreement (95% LoA) (Table 2 and Fig. 2) were very low with respect to the magnitude of the measurement (at least one order), and the relatively SRDs were below 5.3%, and the relative SEM (%), below 2% (for VR). Supplementary Figure S3 (online only) contains the plot obtained with the Kaplan–Meier method. Although it cannot be taken as an indicator of reproducibility, no differences were found in *t*-tests for mean differences.

The agreement was also very good for inter-rater reliability, although, as expected, slightly lower than that for intra-rater reliability (Table 3 and Fig. 3). Similarly, the maximum ICC was for area (ICC = 0.993; 95% CI: 0.989–0.996) and the minimum for circularity (ICC = 0.73, 95% CI: 0.611–0.817). The MoD and 95% LoA remained at least one order below the measurement, with a relative SEM (%) below of 2.2% and a relative SRD (%) below of 6% in the number of signals. Supplementary Figure S4 (online only) is a practical interpretation of the magnitude of the differences.

DISCUSSION

Our results revealed very good intra- and inter-observer reliability both for measurements of the DS and for the calculation of intra-tendon VR. These good results are probably owing to the semi-automatic nature of the measurement procedure, in which the dependence of the operator is involved only in selection of the location of the intratendinous ROI, in adjustment of the parameters of the computer program for the selection of the signal Doppler and in detection of images with higher and lower Doppler signal.

In comparing our results with those of other studies, we can only focus on the quantification of the DS area because VR can only be quantified using the RI. This is because the quantification methods that have been used were based mainly on the number of colored pixels (Strunk et al. 2007; Ellegaard et al. 2008) or on semi-quantitative scales corresponding to the count of the number of DSs (D'Agostino et al. 2009; Sunding et al. 2016; Risch et al. 2018), while RI measurements are made automatically through the ultrasound scanner (Qvistgaard et al. 2001; Terslev et al. 2003b; Albrecht et al. 2008).

The intra-rater and inter-rater reliability results for the remaining morphological and pixel intensity variables of the DS studied here were good, although we have not found studies that have examined the reliability of these variables, making it impossible to compare results.

In patients with rheumatoid arthritis (Qvistgaard et al. 2001), the area of the DS in the synovium has been quantified to determine the degree of joint inflammation of the fingers, the methodology used having excellent intra-rater (ICC = 0.82–0.97, $p < 0.0001$) and good inter-rater (ICC = 0.81, $p < 0.0001$) reliability. In the study of tumor vascularization in patients with gestational trophoblastic neoplasia, intra-rater reliability was also excellent (ICC = 0.94) (Li et al. 2018). These good results coincide with our study, in which quantification of the area revealed excellent agreement for intra-rater and inter-rater reliability. Such good results are possible because it is a semi-automatic procedure whereby the influence of the operator is minimal.

Table 2. Intra-observer reproducibility and reliability

Parameter (n = 84)	Mean (SD) 1	Mean (SD) 2	*t* Value	*p* Value	Effect (Cohen's *d*)	MoD (95% LoA)	ICC (95% CI)	SEM	SEM%	SRD	SRD%
No. of signals	3.17 (2.281)	3.01 (2.209)	1.78	0.080	0.19	0.16 (−0.02 to 0.33)	0.935 (0.901−0.958)	0.028	0.90%	0.08	2.50%
Pixel intensity (0−255)	18.98 (5.449)	18.71 (5.806)	1.20	0.235	0.13	0.28 (−0.19 to 0.74)	0.928 (0.891−0.952)	0.053	0.28%	0.15	0.78%
Area (mm^2)	2.05 (2.041)	2.04 (2.043)	1.71	0.090	0.19	0.02 (0−0.04)	0.999 (0.998−0.999)	0.000	0.02%	0.00	0.05%
Perimeter (mm)	3.04 (1.986)	3.09 (2.165)	−0.61	0.542	0.07	−0.05 (−0.21 to 0.11)	0.937 (0.904−0.958)	0.009	0.29%	0.02	0.80%
Major diameter (mm)	0.918 (0.8263)	0.916 (0.8524)	0.06	0.954	0.01	0 (−0.05 to 0.05)	0.966 (0.948−0.978)	0.000	0.02%	0.00	0.06%
Minor diameter (mm)	0.35 (0.2821)	0.354 (0.2892)	−0.48	0.633	0.05	0 (−0.02 to 0.01)	0.963 (0.944−0.976)	0.001	0.16%	0.00	0.44%
Circularity (0−1)	0.678 (0.2154)	0.665 (0.2393)	0.81	0.419	0.09	0.01 (−0.02 to 0.04)	0.803 (0.712−0.867)	0.004	0.59%	0.01	1.65%
Solidity (0−1)	0.836 (0.2154)	0.808 (0.2493)	1.64	0.105	0.18	0.03 (−0.01 to 0.06)	0.782 (0.682−0.853)	0.009	1.10%	0.03	3.04%
Vascular resistance (n = 42)	0.198 (0.3362)	0.218 (0.3582)	−0.95	0.350	0.15	−0.02 (−0.06 to 0.02)	0.921 (0.859−0.957)	0.004	1.92%	0.01	5.31%

SD = standard deviation; MoD (95% LoA) = mean of differences (95% limits of agreement); ICC (95% CI) = intraclass correlation coefficient (95% confidence interval); SEM = standard error of mean; SRD = smallest real difference.

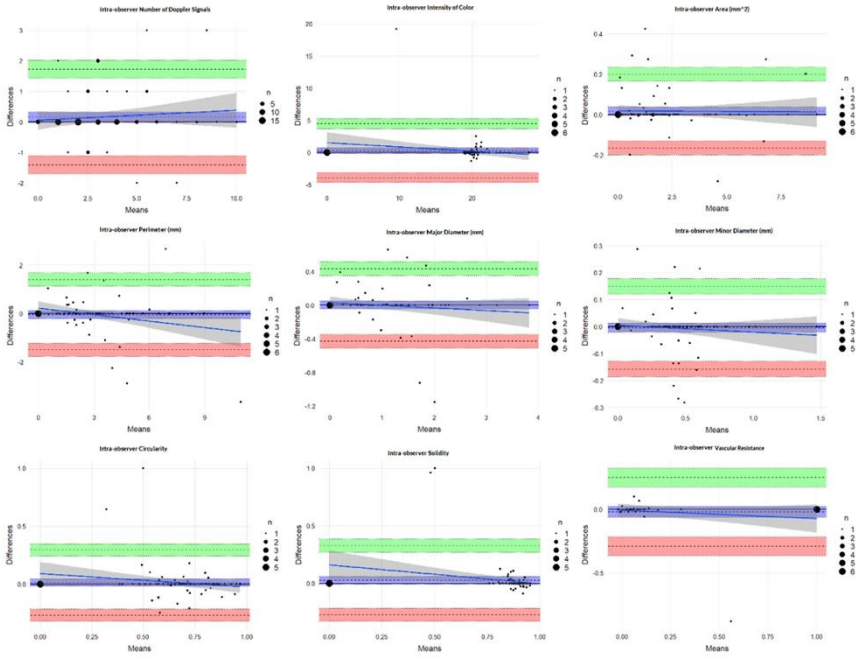

Fig. 2. Bland–Altman plots for intra-observer (A1–A2) agreement. In order are the number of signals, pixel intensity mean, area, perimeter, major and minor diameter, circularity, solidity and vascular resistance.

Counting of the intratendinous DSs by the investigator is essential for the different evaluation scales of the DS to be applied. Its use in the presence of abnormalities in the quadriceps tendon, patellar and Achilles tendons and plantar fascia (Bandinelli et al. 2011) led to excellent results for intra-rater (ICC = 0.97, 95% CI: 0.90–1) and inter-rater (ICC = 0.95; 95% CI: 0.89–1) reliability, using the classification of D'Agostino et al. (2009). Poltawski et al. (2012) evaluated reliability to quantify hyperemia in the common extensor tendon in tennis elbow. To evaluate the DS, they used a PD scale that assigned five grades based on a subjective estimation of the extent of visible blood vessels. Inter-rater reliability was good (ICC = 0.89, 95% CI: 0.79–0.95) for DS graduation. Sunding et al. (2016) analyzed the intra and inter-rater reliability of evaluating Achilles and patellar tendon neovascularization by means of color Doppler using a modified Öhberg score. The intra-rater reliability results were good for neovascularization measured with this qualitative scale in the patellar tendon (κ coefficient = 0.79–0.86) and the Achilles tendon (κ coefficient = 0.64–0.78). However, the inter-rater reliability results were moderate for neovascularization in the patellar tendon (κ coefficient = 0.45–0.76) and the Achilles tendon (κ coefficient = 0.59–0.87).

Although in our method the intratendinous ROI must be selected manually to determine the number of DSs, this is more sensitive than a visual inspection for detecting the signals, and both intra-rater and inter-rater reliability scores are good and clearly better than what can be achieved using qualitative methods. Qualitative methodology seems sensitive to slight changes in the number of vessels when complex vascularization is scored (Risch et al. 2018). However, this scoring procedure allows easy, immediate and absolute quantification of the intratendinous vessels and, therefore, may be suitable for application in clinical practice.

Another method used to quantify vascularization of the patellar tendon is that proposed by Cook et al. (2005), who used color Doppler and measured the length of the

Table 3. Inter-observer reproducibility and reliability

Parameter (n = 84)	Mean (SD) 1	Mean (SD) 2	*t* Value	*p* Value	Effect (Cohen's *d*)	MoD (95% LoA)	ICC (95% CI)	SEM	SEM%	SRD	SRD%
Number of signals	3.17 (2.281)	2.9 (2.408)	2.05	0.044	0.22	0.26 (0.01−0.52)	0.871 (0.806−0.915)	0.067	2.19%	0.18	6.08%
Pixel intensity (0-255)	18.98 (5.449)	18.69 (5.799)	1.27	0.208	0.14	0.02 (−0.08 to 0.11)	0.927 (0.889−0.952)	0.057	0.30%	0.16	0.84%
Area (mm^2)	2.05 (2.041)	1.99 (2.056)	2.81	0.006	0.31	0.05 (0−0.1)	0.993 (0.989−0.996)	0.004	0.20%	0.01	0.54%
Perimeter (mm)	3.04 (1.986)	3.22 (2.203)	−1.50	0.138	0.16	−0.14 (−0.39 to 0.11)	0.85 (0.777−0.9)	0.051	1.64%	0.14	4.54%
Major diameter (mm)	0.918 (0.8263)	0.97 (0.9077)	−1.32	0.190	0.14	−0.05 (−0.13 to 0.03)	0.912 (0.868−0.942)	0.011	1.16%	0.03	3.21%
Minor diameter (mm)	0.35 (0.2821)	0.362 (0.2898)	−0.81	0.422	0.09	−0.01 (−0.04 to 0.02)	0.895 (0.843−0.931)	0.003	0.74%	0.01	2.06%
Circularity (0−1)	0.678 (0.2154)	0.642 (0.2454)	1.97	0.053	0.21	0.04 (0−0.07)	0.73 (0.611−0.817)	0.013	2.00%	0.04	5.55%
Solidity (0−1)	0.836 (0.2154)	0.803 (0.2491)	1.91	0.060	0.21	0.03 (0−0.07)	0.772 (0.667−0.846)	0.011	1.34%	0.03	3.70%
Vascular resistance (n = 42)	0.198 (0.3362)	0.217 (0.3593)	−0.88	0.386	0.14	−0.02 (−0.06 to 0.02)	0.921 (0.859−0.957)	0.004	1.78%	0.01	4.95%

SD = standard deviation; MoD (95% LoA) = mean of differences (95% limits of agreement); ICC (95% CI) = intraclass correlation coefficient (95% confidence interval); SEM = standard error of mean; SRD = smallest real difference.

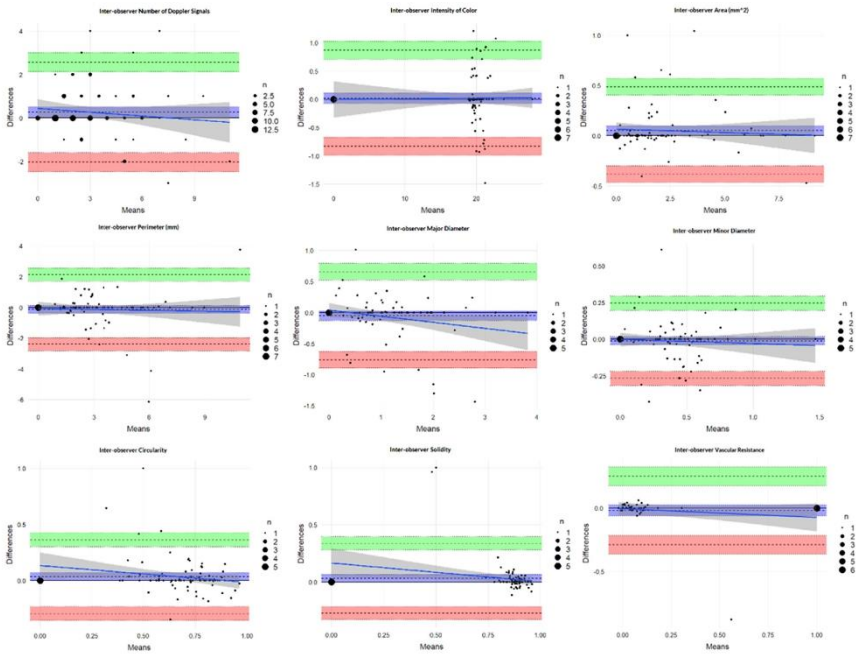

Fig. 3. Bland–Altman plots for inter-observer (A1–A2) agreement. In order are the number of signals, pixel intensity mean, area, perimeter, major and minor diameter, circularity, solidity and vascular resistance.

vessels. The test–retest reliability of the measured vessel length was excellent (ICC = 0.94; 95% CI: 0.88–0.97), with good raters (ICC = 0.84, 95% CI: 0.51–0.94). However, unlike our quantification system, this classification system does not provide information on vascular diameter, and it remains debatable whether evaluation of the total vessel length is relevant to clinical practice (Cook et al. 2005; Risch et al. 2016).

In the few studies that have measured intratendinous VR, the most commonly used methods are based on the automatic measurement of RI using the pulsed Doppler mode, either as an average of three vessels (Koenig et al. 2007a, 2007b) or for a single vessel (Karzis et al. 2017). We have found no studies that have tested the reliability of intratendinous RI measurements, probably because many author believe it does not depend on the experience of the researcher, but on the ultrasound machine itself (Terslev et al. 2003b). However, the reliability of RI measurements has been tested in other tissues by measuring the RI of a single vessel. Albrecht et al. (2008) evaluated the inter-rater reliability of RI (ICC = 0.60) in hand and wrist arthritis during anti-inflammatory treatment. Strunk et al. (2007) conducted a similar study, evaluating only the wrist; they found a weak correlation between observers (Pearson's $r = 0.53$).

The test–retest reliability of assessments of clitoral blood flow in healthy women using color Doppler in a pelvic floor muscle contraction task had moderate to good intra-rater reliability for the RI at rest (ICC = 0.67, 95% CI: 0.08–0.88, $p = 0.018$) and excellent reliability after a pelvic floor muscle contraction task (ICC = 0.81, 95% CI: 0.51–0.92, $p < 0.001$) (Mercier et al. 2018). These RI reliability results are poorer than the intratendon VR measurements used in our study (ICC = 0.921, 95% CI = 0.859–0.957), which may be due not only to the operator or the technical equipment, both of which influence the acquisition and interpretation of the images (Albrecht et al. 2007; Patil and Dasgupta 2012), but also to the difficult localization of the same intra-articular blood vessel (which can be very small) during the examinations, whereas our study used the mean of all SDs found in the ROI.

In the studies analyzed, the reliability results for the RI are worse than those obtained for quantification of the area of DS, perhaps because the results shown for the RI include those obtained during the exploration process of each researcher, and also because the RI is a relationship that depends on several measurements at different times. Intuitively, parameters that depend on several measurements are more likely to have lower reliability, compounded by the imperfect reliability of the individual measurements included in their equations (Mercier et al. 2018). This difference contrasts with our results, in which the VR had excellent intra- and inter-rater reliability, and coincides with the results of most of the Doppler area quantification variables, probably because of the semi-automatic nature of the quantification procedure in both cases.

The main limitation of this study is that, although the reliability of the method is good, the analysis must be performed offline the ultrasound device and requires extra time for video export, image extraction and image analysis; therefore, its clinical application is not immediate. However, it can be considered a valid method for use in the investigation and quantification of tendon vascularization in this context.

The other limitation is related to the determination of RI, which, although it could be obtained from spectral analysis, in this study we calculated it indirectly from the pixel intensity in systole and diastole. The advantage of this approach is that the intensity values are obtained using the same procedure used for other morphological parameters, thus saving time. However, it would be interesting in a future study to test the correlation between the RI obtained in this way and that obtained by spectral analysis.

In future studies, it would also be interesting to analyze the color Doppler mode, which is currently gaining momentum for evaluation of intratendon vascularization because of the improved sensitivity of ultrasound scanners (Torp-Pedersen et al. 2015).

Furthermore, including an examination of patients could give results more typical of clinical practice. Finally, the shape variables of the DS and the VR could be correlated with the symptoms of the patient, and their prognostic and monitoring capacity could be analyzed.

This quantification methodology exhibits very good reliability and reproducibility and is capable of combining the quantification of the number of signals, the magnitude and the VR of the tissue, which would allow a more precise evaluation of the state of the tissue, the improved monitoring of changes over time and the establishment of a threshold between pathological and physiological blood flow.

CONCLUSIONS

The results obtained confirm that the proposed method has very good reliability and reproducibility, while any influence on the detected DSs is negligible. In this sense, it will be of interest to extend the study to ascertain the reliability between different ultrasound scanners and software, which could increase the robustness of the method.

Conflict of interest disclosure—The authors of this manuscript declare no relationships with any companies, whose products or services may be related to the subject matter of the article and declare no conflict of interest.

SUPPLEMENTARY MATERIALS

Supplementary material associated with this article can be found in the online version at doi:10.1016/j.ultrasmedbio.2021.08.010.

REFERENCES

Albrecht K, Müller-Ladner U, Strunk J. Quantification of the synovial perfusion in rheumatoid arthritis using Doppler ultrasonography. Clin Exp Rheumatol 2007;25:630–638.

Albrecht K, Grob K, Lange U, Müller-Ladner U, Strunk J. Reliability of different Doppler ultrasound quantification methods and devices in the assessment of therapeutic response in arthritis. Rheumatology (Oxford) 2008;47:1521–1526.

Alfredson H, Ohberg L. Sclerosing injections to areas of neo-vascularisation reduce pain in chronic Achilles tendinopathy: A double-blind randomised controlled trial. Knee Surg Sports Traumatol Arthrosc 2005;13:338–344.

Alfredson H, Ohberg L, Forsgren S. Is vasculo-neural ingrowth the cause of pain in chronic Achilles tendinosis? An investigation using ultrasonography and colour Doppler, immunohistochemistry, and diagnostic injections. Knee Surg Sports Traumatol Arthrosc 2003;11:334–338.

Atkinson G, Nevill AM. Statistical methods for assessing measurement error (reliability) in variables relevant to sports medicine. Sports Med 1998;26:217–238.

Bablok W, Passing H, Bender R, Schneider B. A general regression procedure for method transformation: Application of linear regression procedures for method comparison studies in clinical chemistry, Part III. J Clin Chem Clin Biochem 1988;26:783–790.

Bandinelli F, Milla M, Genise S, Giovannini L, Bagnoli S, Candelieri A, Collaku L, Biagini S, Cerinic MM. Ultrasound discloses entheseal involvement in inactive and low active inflammatory bowel disease without clinical signs and symptoms of spondyloarthropathy. Rheumatology (Oxford) 2011;50:1275–1279.

Bjordal JM, Lopes-Martins RAB, Iversen VV. A randomised, placebo controlled trial of low level laser therapy for activated Achilles tendinitis with microdialysis measurement of peritendinous prostaglandin E2 concentrations. Br J Sports Med 2006;40:76–80.

Bland JM, Altman DG. Statistical methods for assessing agreement between two methods of clinical measurement. Lancet 1986;1:307–310.

Boesen AP, Boesen MI, Torp-Pedersen S, Christensen R, Boesen L, Hölmich P, Nielsen MB, Koenig MJ, Hartkopp A, Ellegaard K, Bliddal H, Langberg H. Associations between abnormal ultrasound color Doppler measures and tendon pain symptoms in badminton players during a season: A prospective cohort study. Am J Sports Med 2012;40:548–555.

Cook JL, Ptazsnik R, Kiss ZS, Malliaras P, Morris ME, De Luca J. High reproducibility of patellar tendon vascularity assessed by colour Doppler ultrasonography: A reliable measurement tool for quantifying tendon pathology. Br J Sports Med 2005;39:700–703.

D'Agostino MA, Aegerter P, Jousse-Joulin S, Chary-Valckenaere I, Lecoq B, Gaudin P, Brault I, Schmitz J, Dehaut FX, Le Parc JM, Breban M, Landais P. How to evaluate and improve the reliability of power Doppler ultrasonography for assessing enthesitis in spondylarthritis. Arthritis Rheum 2009;61:61–69.

De Jonge S, Warnaars JLF, De Vos RJ, Weir A, van Schie HTM, Bierma-Zeinstra SMA, Verhaar JAN, Tol JL. Relationship between

neovascularization and clinical severity in Achilles tendinopathy in 556 paired measurements. Scand J Med Sci Sports 2014;24:773–778.
de Vos RJ, Weir A, Cobben LPJ, Tol JL. The value of power Doppler ultrasonography in Achilles tendinopathy: A prospective study. Am J Sports Med 2007;35:1696–1701.
Delorme S, Weisser G, Zuna I, Fein M, Lorenz A, van Kaick G. Quantitative characterization of color Doppler images: Reproducibility, accuracy, and limitations. J Clin Ultrasound 1995;23:537–550.
Ellegaard K, Torp-Pedersen S, Lund H, Henriksen M, Terslev L, Jensen PS, Danneskiold-Samsøe B, Bliddal H. Quantification of colour Doppler activity in the wrist in patients with rheumatoid arthritis—The reliability of different methods for image selection and evaluation. Ultraschall Med 2008;29:393–398.
Hopkins WG. Measures of reliability in sports medicine and science. Sports Med 2000;30:1–15.
Karzis K, Kalogeris M, Mandalidis D, Geladas N, Karteroliotis K, Athanasopoulos S. The effect of foot overpronation on Achilles tendon blood supply in healthy male subjects. Scand J Med Sci Sports 2017;27:1114–1121.
Koenig MJ, Torp-Pedersen S, Holmich P, Terslev L, Nielsen MB, Boesen M, Bliddal H. Ultrasound Doppler of the Achilles tendon before and after injection of an ultrasound contrast agent—Findings in asymptomatic subjects. Ultraschall Med 2007a;28:52–56.
Koenig MJ, Torp-Pedersen ST, Christensen R, Boesen MI, Terslev L, Hartkopp A, Bliddal H. Effect of knee position on ultrasound Doppler findings in patients with patellar tendon hyperaemia (jumper's knee). Ultraschall Med 2007b;28:479–483.
Léandre Pourcelot Société parisienne d'expansion chimique. Application de l'examen Doppler à l'étude de la circulation périphérique. Paris: Specia; 1982.
Lexell JE, Downham DY. How to assess the reliability of measurements in rehabilitation. Am J Phys Med Rehabil 2005;84:719–723.
Li Y, Tang MX, Agarwal R, Patel D, Eckersley RJ, Barrois G, Roddie ME, Dayal L, Savage PM, Seckl MJ, Lim A. Power Doppler quantification in assessing gestational trophoblastic neoplasia. Ultraschall Med 2018;39:206–212.
Luiz RR, Costa AJL, Kale PL, Werneck GL. Assessment of agreement of a quantitative variable: A new graphical approach. J Clin Epidemiol 2003;56:963–967.
Malliaras P, Richards PJ, Garau G, Maffulli N. Achilles tendon Doppler flow may be associated with mechanical loading among active athletes. Am J Sports Med 2008;36:2210–2215.
McGraw KO, Wong SP. Forming inferences about some intraclass correlation coefficients. Psychol Methods 1996;1:30–46.
Mercier J, Tang A, Morin M, Khalifé S, Lemieux MC, Reichetzer B, rest Dumoulin CTest–retest reliability of clitoral blood flow measurements using color Doppler ultrasonography at, women after a pelvic floor contraction task in healthy adult. Neurourol Urodyn 2018;37:2249–2256.
Ohberg L, Lorentzon R, Alfredson H. Neovascularisation in Achilles tendons with painful tendinosis but not in normal tendons: An ultrasonographic investigation. Knee Surg Sports Traumatol Arthrosc 2001;9:233–238.
Passing H, Bablok. A new biometrical procedure for testing the equality of measurements from two different analytical methods: Application of linear regression procedures for method comparison studies in clinical chemistry, Part I. J Clin Chem Clin Biochem 1983;21:709–720.
Patil P, Dasgupta B. Role of diagnostic ultrasound in the assessment of musculoskeletal diseases. Ther Adv Musculoskelet Dis 2012;4:341–355.
Poltawski L, Ali S, Jayaram V, Watson T. Reliability of sonographic assessment of tendinopathy in tennis elbow. Skeletal Radiol 2012;41:83–89.
Portney LG, Watkins MP. Foundations of clinical research: Applications to practice. : Pearson/Prentice-Hall; 2009.
Quack V, Betsch M, Hellmann J, Eschweiler J, Schrading S, Gatz M, Rath B, Tingart M, Laubach M, Kuhl CK, Dirrichs T. Evaluation of postoperative changes in patellar and quadriceps tendons after total knee arthroplasty—A comprehensive analysis by shear wave elastography, power Doppler and B-mode ultrasound. Acad Radiol 2020;27:e148–e157.
Qvistgaard E, Røgind H, Torp-Pedersen S, Terslev L, Danneskiold-Samsøe B, Bliddal H. Quantitative ultrasonography in rheumatoid arthritis: Evaluation of inflammation by Doppler technique. Ann Rheum Dis 2001;60:690–693.
Richards PJ, Win T, Jones PW. The distribution of microvascular response in Achilles tendonopathy assessed by colour and power Doppler. Skeletal Radiol 2005;34:336–342.
Risch L, Cassel M, Messerschmidt J, Intziegianni K, Fröhlich K, Kopinski S, Mayer F. Is sonographic assessment of intratendinous blood flow in Achilles tendinopathy patients reliable?. Ultrasound Int Open 2016;2:E13–E18.
Risch L, Wochatz M, Messerschmidt J, Engel T, Mayer F, Cassel M. Reliability of evaluating Achilles tendon vascularization assessed with doppler ultrasound advanced dynamic flow. J Ultrasound Med 2018;37:737–744.
Roth J, Stinson SE, Chan J, Barrowman N, Di Geso L. Differential pattern of Doppler signals at lower-extremity entheses of healthy children. Pediatr Radiol 2019;49:1335–1343.
Schuck P, Zwingmann C. The "smallest real difference" as a measure of sensitivity to change: A critical analysis. Int J Rehabil Res 2003;26:85–91.
Simon D, Kleyer A, Bayat S, Knitza J, Valor-Mendez L, Schweiger M, Schett G, Tascilar K, Hueber AJ. Biomechanical stress in the context of competitive sports training triggers enthesitis. Arthritis Res Ther 2021;23:172.
Strunk J, Strube K, Rumbaur C, Lange U, Müller-Ladner U. Interobserver agreement in two- and three-dimensional power Doppler sonographic assessment of synovial vascularity during anti-inflammatory treatment in patients with rheumatoid arthritis. Ultraschall Med 2007;28:409–415.
Sunding K, Fahlström M, Werner S, Forssblad M, Willberg L. Evaluation of Achilles and patellar tendinopathy with greyscale ultrasound and colour Doppler: Using a four-grade scale. Knee Surg Sports Traumatol Arthrosc 2016;24:1988–1996.
Terabayashi N, Watanabe T, Matsumoto K, Takigami I, Ito Y, Fukuta M, Akiyama H, Shimizu K. Increased blood flow in the anterior humeral circumflex artery correlates with night pain in patients with rotator cuff tear. J Orthop Sci 2014;19:744–749.
Terslev L, Torp-Pedersen S, Qvistgaard E, Bliddal H. Spectral Doppler and resistive index: A promising tool in ultrasonographic evaluation of inflammation in rheumatoid arthritis. Acta Radiol 2003a;44:645–652.
Terslev L, Torp-Pedersen S, Qvistgaard E, Danneskiold-Samsoe B, Bliddal H. Estimation of inflammation by Doppler ultrasound: quantitative changes after intra-articular treatment in rheumatoid arthritis. Ann Rheum Dis 2003b;62:1049–1053.
Terslev L, Torp-Pedersen S, Qvistgaard E, Kristoffersen H, Røgind H, Danneskiold-Samsøe B, Bliddal H. Effects of treatment with etanercept (Enbrel, TNRF:Fc) on rheumatoid arthritis evaluated by Doppler ultrasonography. Ann Rheum Dis 2003c;62:178–181.
Tol JL, Spiezia F, Maffulli N. Neovascularization in Achilles tendinopathy: Have we been chasing a red herring?. Knee Surg Sports Traumatol Arthrosc 2012;20:1891–1894.
Torp-Pedersen TE, Torp-Pedersen ST, Qvistgaard E, Bliddal H. Effect of glucocorticosteroid injections in tennis elbow verified on colour Doppler ultrasonography: Evidence of inflammation. Br J Sports Med 2008;42:978–982.
Torp-Pedersen S, Christensen R, Szkudlarek M, Ellegaard K, D'Agostino MA, Iagnocco A, Naredo E, Balint P, Wakefield RJ, Torp-Pedersen A, Terslev L. Power and color Doppler ultrasound settings for inflammatory flow: Impact on scoring of disease activity in patients with rheumatoid arthritis. Arthritis Rheumatol 2015;67:386–395.
Vlist AC, Veen JM, Oosterom RF, Veldhoven PLJ, Verhaar JAN, Vos R. Ultrasound Doppler flow in patients with chronic midportion Achilles tendinopathy: Is surface area quantification a reliable method?. J Ultrasound Med 2020;39:731–739.
Weir JP. Quantifying test-retest reliability using the intraclass correlation coefficient and the SEM. J Strength Cond Res 2005;19:231–240.